LEIBNIZ-INSTITUT
FÜR ARBEITSFORSCHUNG
AN DER TU DORTMUND

Leibniz
Gemeinschaft

A role of glycerophosphodiesterase EDI3 in glycogen metabolism

Dissertation

zur Erlangung des akademischen Grades des Doktors der Naturwissenschaften (Dr. rer. nat.) an der Fakultät für Chemie und Chemische Biologie der Technischen Universität Dortmund vorgelegt

vorgelegt von

Gregor M. Leonhardt (M.Sc.)

Dortmund 2020

Für Lukas, für Paul

&Fortuna

Index

I Table of content

Index

Index

II Table of tables

III Table of Figures

IV Abbreviations

%	Percent
°C	Degrees in Celsius
AA	Amino acid
Adj	Adjusted
APS	Ammonium persulphate
ATP	Adenosine triphosphate
BCA	Bicinchoninic acidBisTris Bis-(2-hydroxy-ethyl)-amino-tris(hydroxymethyl)-
BMI	Body mass index
BSA	Bovine serum albumin
CaCl2	Calcium chloride
cAMP	Cyclic adenosine monophosphate
CAZy	Carbohydrate-Active enZyme
CBM	carbohydrate-binding module
cDNA	Complementary DNA
CREB	cAMP response element binding protein
pCREB	At serine 133 phosphorylated cAMP response element binding protein
Da	Dalton
DAB	3, 3'-Diaminobenzidine
DAPI	4',6-diamidino-2-phenylindole
DEPC	Diethyl pyrocarbonate
DMEM	Dulbecco'smodified Eagles'medium
DMSO	Dimethylsulfoxid
DNA/RNA	Deoxyribonucleic acid/Ribonucleic acid
DTT	Dithiothreitol
EDTA	Ethylenediaminetetraacetic acid
EDI3	Endometrial carcinoma Differential 3
EM	Electron microscopy
Eif2a	Eukaryotic translation initiation factor 2A
e.g.	For example
Et al.	And others
FM	Full media

Index

g/mg/µg	gram/milligram/microgram
G1P	Glucose-1-phosphatase
G3P	Glycerol-3-phosphate
G6P	Glucose-6-phosphatase
GABARAPL1	GABA type A receptor associated protein like 1
GAPDH	Glyceraldehyde 3-phosphate dehydrogenase
GBE	Glycogen branching enzyme
GDE	Glycerophosphodiester phosphodiesterases
GN	Glycogenin
GPAM	Glycerol-3-phosphate acyltransferase
GPC	Glycerophophocholine
GPCPD1	glycerophosphocholine phosphodiesterase 1
GYS1	Glycogen synthase 1
h/min/sec	hours/minutes/seconds
HRP	Horseradish peroxidase
HEPES	4-(2-hydroxyethyl)-1-piperazineethanesulfonic acid
IfADo	Leibniz-Institut für Arbeitsforschung an der TU Dortmund
IHC	Immunohistochemistry
IP	Immunoprecipitations
Kb	Kilobase pair
LB	Lysogeny broth
l/ml/µl	Litre/millilitre/microliter
LD	Lafora disease
LC-MS/MS	Liquid chromatography-mass spectrometry/mass spectrometry
LPA	lipid lysophosphatidic acid
M/mM/µM/nM	Molar/millimolar/micromolar/nanomolar
MHC	Myosin heavy chain
N	Number of biological replicates
Nm	Nanometre
NMJ	Neuromuscular junction
NP-40	Nonidet P-40 substitute
ON	Over night

Index

PAGE	Polyacrylamide gel electrophoresis
PAS-D	Periodic Acid-Schiff (-diastase)
PBS	Phosphate-buffered saline
PCK1	Phosphoenolpyruvate carboxykinase 1
PEI	Polyethylenimine
PFA	Paraformaldehyde
PHH	Primary human hepatocytes
PMH	Primary mouse hepatocytes
PI3K	Phosphoinositid-3-Kinase
PKA	Protein kinase A
PVDF	Polyvinylidene fluoride
qRT-PCR	Quantitative real-time polymerase chain reaction
RFU	Relative fluorescence units
Rpm	Rounds per minute
ROS	Reactive oxygen species
RT	Room temperature
SBD	starch-binding domain
SDS	Sodium dodecyl sulphate
siRNA	Small interfering RNA
SOC	Super Optimal Broth cum glucose
STBD1	Starch- binding domain- containing protein 1
TAE	Tris-Acetate-EDTA
TBS-T	Tris-buffered saline
TEMED	Tetramethylethylenediamine
T_m	Meting temperature
T-tubules	transverse tubules
Tris	Tris(hydroxymethyl)aminomethane
U	Enzymatic unit
UMP/UDP-glucose	Uridine-mono/diphosphate-glucose
v/v; w/v	Volume per volume, weight per volume
xg	Standard gravity

Abstract

The glycerophosphodiesterase EDI3 (endometrial differential 3) is a key enzyme in various metabolic signalling pathways because it cross-links the triglyceride and choline signalling pathway by hydrolysing glycerophosphocholine (GPC) to glycerol-3-phosphate (G3P) and choline. The enzyme has two functional domains - the GDE domain, where the active site of the protein is located, and the carbohydrate binding domain (CBM), whose function is completely unknown. EDI3 is part of the evolutionary conserved GDE protein family, whose members have different functions. In previous work, high EDI3 expression in primary toumors of ovarian and endometrial carcinomas was associated with increased metastasis, increased cell migration and poorer survival. In this work the role of the CBM20 domain was investigated on a large scale and a possible new role for EDI3 was found.

The present work confirms previous research on other CBM20 proteins (Laforin and STBD1) that showed that the CBM domain is essential for protein stability. The deletion of the entire CBM20 domain (ΔCBM20) and mutations of a conserved amino acid within the CBM20 (W32A) significantly reduced protein stability. As a consequence of these mutations, the enzymatic activity of the protein was decreased (W32A) or completely eliminated (ΔCBM20) and the phenotypic migration effect was reduced. Furthermore, this work could show that EDI3 forms dimers or oligomers and the CBM20 domain is required for this process.

A characteristic of CBM20 is the interaction with plant starch. For laforin and STBD1, an interaction with glycogen via the CBM20 domain was additionally demonstrated. In this work EDI3 could be associated for the first time with glycogen in vitro and with glycogen-associated proteins of the human skeletal and cardiac muscle. While no binding of EDI3 and glycogen could be detected in human liver, glucagon regulation was observed in primary mouse hepatocytes, potentially linking EDI3 to a role during gluconeogenesis. In skeletal muscle, EDI3 was associated with Type II skeletal muscle cells and the T-tubules, where it co-localizes with ryanodine receptor 1, suggesting a role of EDI3 in calcium signalling

Zusammenfassung

Die Glycerophosphodiesterase EDI3 (Endometrial differential 3) ist ein Schlüsselenzym in unterschiedlichen metabolischen Signalwegen, da es durch die Hydrolyse von Glycerolphosphocholin (GPC) zu Glycerol-3-Phospohat (G3P) und Cholin den Triglycerid und den Cholin Signalweg vernetzt. Das Enzym hat zwei funktionelle Domänen – die GDE Domäne, in welcher das aktive Zentrum des Proteins lokalisiert ist und die Kohlenhydrat-Bindungsdomäne (CBM), dessen Funktion bisher komplett unbekannt ist. EDI3 ist Teil der evolutionär konservierten GDE Protein Familie, deren Mitglieder unterschiedliche Funktionen haben. In früheren Arbeiten konnte eine hohe EDI3 Expression in primären Tumoren von ovarial und endometrial Karzinomen mit erhöhter Metastasenbildung, erhöhter Zellmigration und schlechteren Überlebenschancen verknüpft werden. Im Rahmen dieser Arbeit wurde die Rolle der CBM20-Domäne in großem Umfang untersucht und eine mögliche neue Rolle für EDI3 gefunden.

Die vorliegende Arbeit bestätigt bisherige Forschung und anderen CBM20 Proteinen (Laforin und STBD1) die bereits zeigte, dass die CBM Domäne unerlässlich für die Protein Stabilität ist. Die Deletion der gesamten CBM20-Domäne (ΔCBM20) und die Mutationen einer konservierten Aminosäure innerhalb der CBM20 (W32A) verringerten die Proteinstabilität signifikant. Als Folge dieser Mutationen war die enzymatische Aktivität des Proteins vermindert (W32A) oder vollständig ausgeschaltet (ΔCBM20) und der phänotypische Migrationseffekt wurde reduziert. Darüber hinaus konnte diese Arbeit zeigen, dass EDI3 Dimere oder Oligomere bildet und die CBM20-Domäne für diesen Prozess benötigt wird.

Ein Charakteristikum der CBM20 die Interaktion mit pflanzlicher Stärke. Bei laforin und STBD1 wurde zusätzlich eine Wechselwirkung mit Glykogen über die CBM20 Domäne nachgewiesen. In dieser Arbeit konnte EDI3 zum ersten Mal mit dem Glykogen in vitro und mit Glykogen assoziierten Proteinen des menschlichen Skelett- und Herzmuskels in Verbindung gebracht werden. Während in menschlicher Leber keine Bindung von EDI3 und Glykogen detektiert werden konnte, wurde in primären Maus Hepatozyten eine Regulation durch Glukagon beobachtet, die EDI3 potentiell mit einer Rolle während der Gluconeogenese in Verbindung bringt. Im Skelettmuskel konnte EDI3 mit Typ II Skelettmuskelzellen und den T-Tubuli assoziiert werden, wo es mit dem Ryanodin-Rezeptor 1 ko-lokalisiert, was auf eine Rolle von EDI3 bei der Calciumsignalisierung hindeutet.

1. Introduction

1.1 Glycogen

1.1.1 Glycogen structure

Glycogen is one of the many types of polysaccharides found in nature. At the molecular level, polysaccharides consist of covalently-linked monosaccharides - the simplest form of sugar, such as glucose - bound together by glycosidic linkages (Figure 1.1). Polymers of glucose, also known as polyglucans, form glycogen in animals, and amylopectin and amylose in plants (Figure 1.1). Both glycogen and amylopectin are connected by α-1,4 glycosidic linkages and the branch points by α-1,6 glycosidic linkages (DiNuzzo and Schousboe 2019). At the centre of each glycogen particle is a dimeric glycogenin molecule that is covalently connected to a single glucose polymer chain, which gives rise to all subsequent chains at the branching points (Roach et al. 2012). Each linear chain yields two new branches and each new subset of branches is defined as a tier (Figure 1.2) (ILLINGWORTH et al. 1952). In a theoretical model, it was suggested that glycogen could not exceed 12 tiers, around 55000 glucose molecules, since higher tiers would become inaccessible to enzymes, since the surface is too large (Meléndez-Hevia et al. 1993). The outermost tier would harbour around one-third of the total glucose molecules which fits with experimental data (LARNER et al. 1952; Meléndez et al. 1997). Via branching, glycogen avoids the formation of double helices which would lead to its insolubility and lower binding affinity to glycogen-depleting proteins, thus resulting in pathological consequences (EMANUELLE et al. 2016).

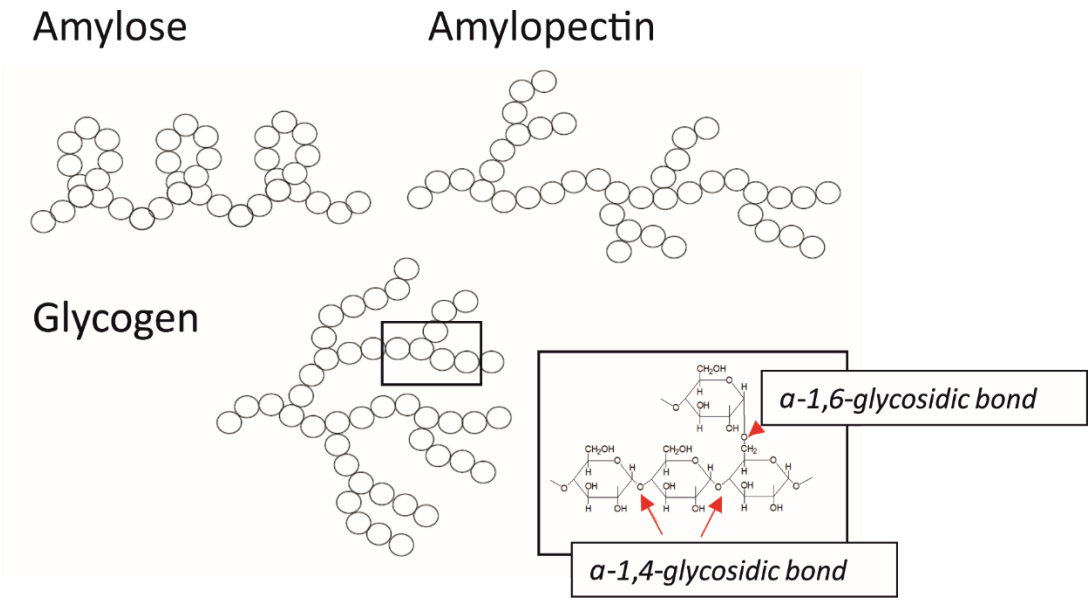

Figure 1.1 **Forms and bonds of glucose polymers**

Glycogen constitutes up to 400 g or 8% volume of the liver, up to 100 g or 2% of muscle and 1.5 g or 0.1% of the brain (Prats et al. 2018). Liver glycogen is usually located in the cytoplasm, but closely associated with the smooth endoplasmic reticulum (Cardell and Cardell 1990). In skeletal muscle, glycogen is found in close proximity to the sarcoplasmic reticulum and transverse tubules (See also section 1.4.3), and is localized throughout the brain with high levels in astrocytes (Prats et al. 2018). Glycogen is also found in skin, retina, adipose tissue, leukocytes, thymus and kidney (DiNuzzo and Schousboe 2019).

On a macromolecular level, three different structures have been identified by electron microscopy (EM), termed α- and β-granules and γ-particles (Drochmans 1962). The biggest glycogen structure (10^8 Dalton) appears to be the α-granules, which is mostly found in liver. They consist of a several β-granules, possibly linked via glycogenin, and arranged in a 'cauliflower-like' manner (Tan et al. 2018). The β-granules (10^6-10^7 Dalton) usually contains around 7-9 tiers on average and increases in number rather than size (Graham et al. 2010; DiNuzzo and Schousboe 2019). The β-granules include several γ-particles, 3 nm protein-rich compartments with a high electron density (Prats et al. 2018).

1.1.2 Glycogen associated proteins

To date, several proteins have been identified that can bind glycogen, which are necessary for anabolism, catabolism, and size maintenance (table 1.1). The majority of proteins are directly related to catabolism or anabolism of the polyglucan; however, a few proteins are needed glycogen homeostasis. For example, glycogenin is the core protein of each glycogen molecule. It is an auto-glycosylating protein that catalyses and initiates the formation of a short glucose polymer. This polymer is elongated by glycogen synthase (GS) via α-1, 4 glycosidic linkages until a length of at least 11 glucose molecules is reached. The glycogen branching enzyme changes the position of seven α-1,4 glycosidic-linked glucose molecules from the donor chain, and fuses it to the acceptor chain via α-1,6 glycosidic linkage. With regard to catabolism, glycogen catalyses the transfer of glucose moieties from the glycogen molecule to inorganic phosphate, releasing the product glucose-1-phospate (G1P). Phosphoglucomutase then metabolises intermediate G1P to glucose-6-phosphate (G6P), which feeds into glycolysis or other pathways. An additional glycogen-debranching enzyme is necessary to linearize glycogen, which has two enzymatic functions. The first, with its 4-α-glucanotransferase activity, it can elongate a neighbouring chain with three polymerized glucose molecules. The

last glucose molecule of the degraded chain is hydrolysed and released by glycogen-debranching enzymes second enzymatic function, the amylo-α-1,6-glucosidase activity (Roach et al. 2012; Zois et al. 2014; Zois and Harris 2016).

Table 1.1: **Glycogen associated proteins**

Gene name	Protein	Function on glycogen
GN1	Glycogenin 1	Initiation, core protein
GN2	Glycogenin 2	Initiation, liver, , core protein
TRIM7, GNIP	Tripartite motif-containing protein	Regulation
GS1	Glycogen synthase 1	Synthesis
GS2	Glycogen synthase 2	Synthesis, liver
GBE1	Glycogen branching enzyme	Synthesis
GP, PYGM	Glycogen Phosphorylase muscle	Degradation, releases G1P
GP, PYGL	Glycogen Phosphorylase liver	Degradation, releases G1P
GP, PYGB	Glycogen Phosphorylase brain	Degradation, releases G1P
GDE, AGL	Glycogen debranching enzyme	Degradation, releases G1P
STBD1	Starch binding domain 1	Homeostasis, Autophagy
Malin	E3 ubiquitin-protein ligase NHLRC1	Homeostasis
EPM2A	Laforin glucan phosphatase	Homeostasis
PHKA1	Phosphorylase Kinase 1	Degradation, muscle
PHKA2	Phosphorylase kinase 2	Degradation, liver
AMPK	5'AMP-activated protein kinase	Regulation
PP1	Proteinphosphatase 1 and targeting subunits	Regulation
PPP1R3A, PPP1R3B, PPP1R3C, PPP1R3D, PPP2CA, PPP1CA, PPP2R1B		

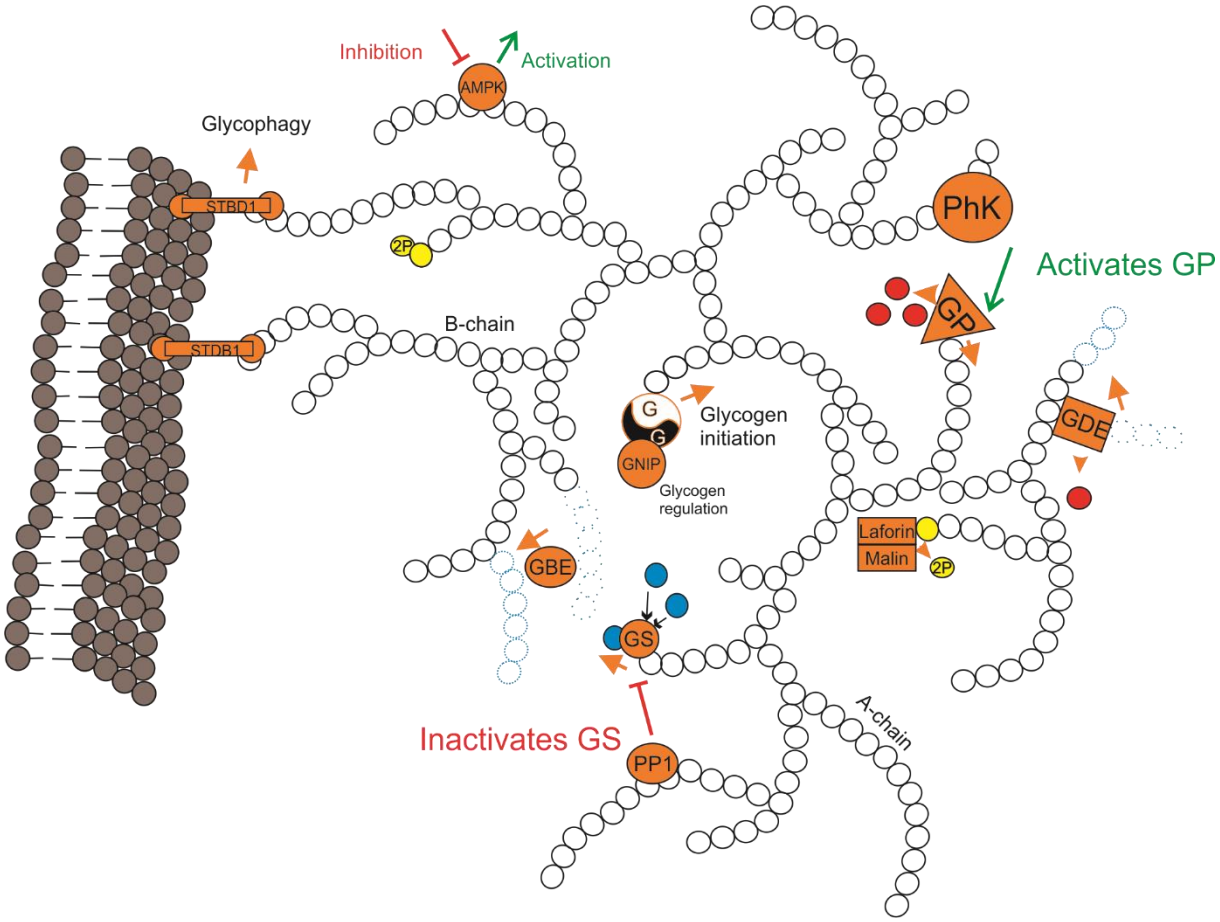

Figure 1.2 **Glycogen associated proteins and their functions.** Glucose molecules are indicated as white circles, hyperphosphorylated glucose is shown in yellow. Released glucose units are highlighted as red circles, newly linked glucose moieties are highlighted with blue circles, dotted blue circles indicate a shift of glucose. Proteins are highlighted in orange, protein function on glycogen is shown with an orange arrow, protein inhibition with red lines and protein activation with a green arrow. The A-chain represents an unbranched and the B-chain a branched chain. The cellular is highlighted in brown. Protein abbreviation can be found in table 1.1.

The functions of glycogen associated proteins are illustrated in Figure 1.2. While the glycogen associated proteins are the 'executive power' they are controlled by the regulatory and counter-regulatory hormones, glucagon and insulin in order to maintain euglycemia.

1.1.3 Glycogen regulation via insulin and glucagon

The main function of glycogen is to store energy in the form of glucose. During hypoglycaemia, due to for example, starvation or physical activity, the liver alters the levels of hepatic glucose release through controlling the processes of glycogen breakdown (glycogenolysis) or de novo glucose production (gluconeogenesis) to maintain blood sugar levels (Nordlie et al. 1999). After a meal, during hyperglycaemia, the liver increases its glucose uptake and stores glucose as glycogen (glycogenesis). These processes are regulated by two hormones with antagonizing function, insulin and glucagon (Figure 1.3) (ELRICK et al. 1958).

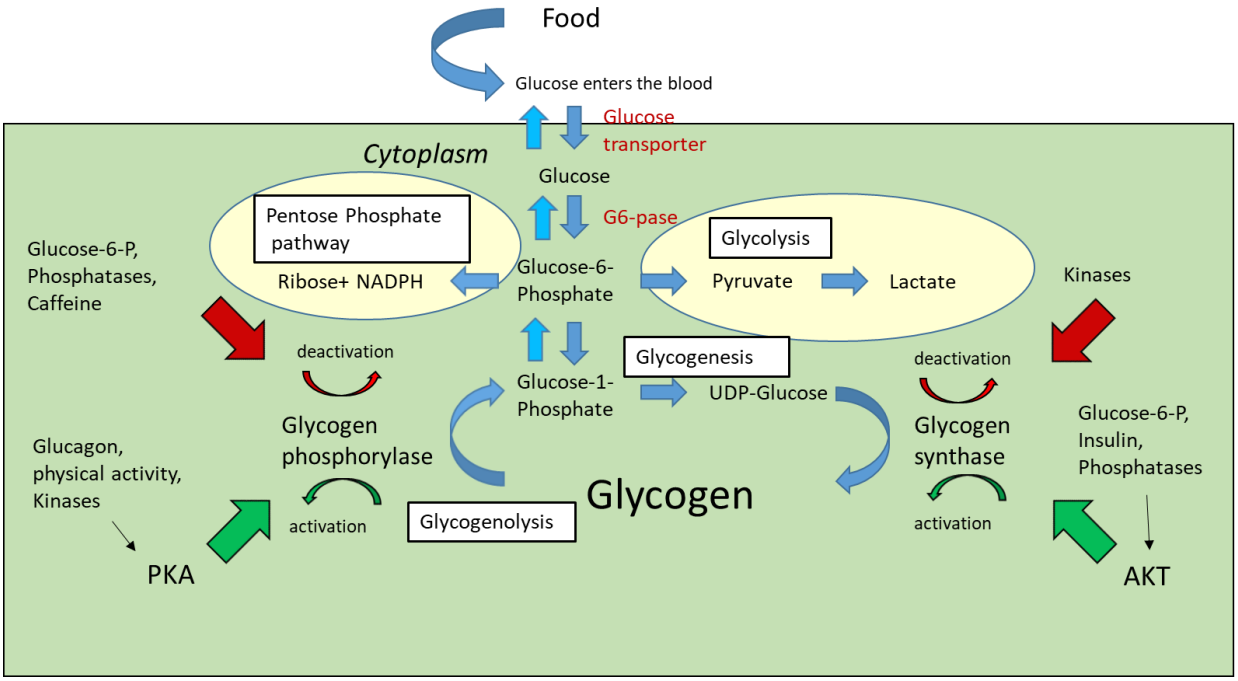

Figure 1.3 **A simplistic view on the regulation of glycogen metabolism by glycogen synthase and glycogen phosphorylase**. Food is digested and glucose is taken up by the cells via glucose transporters and is immediately phosphorylated the glucose-6-phosphate (G-6-P). G-6-P can be rapidly used in glycolysis or other pathways like the pentose phosphate way or stored as part of glycogen. Therefore it is entering the glycogenesis pathway and G-6-P is isomerized to glucose-1-phosphate (G-1-P). This process is supported by insulin which activates the glycogen synthase by activating the AKT pathway and thus inhibiting the glycogen synthase kinase. If energy is needed due to starvation (glucagon) or physical activity (adrenaline) the process of glycogenolysis is activated. Via the PKA pathway glycogen synthase is deactivated via conformational change and glycogen phosphorylase is activated. (Zois and Harris 2016).

Human insulin is a 51 amino acid long protein with a molecular mass of 5808 Da. It is a heterodimer of an A- and a B-chain, which are bound together via disulfide bonds, and is formed in the beta cells in the islets of Langerhans (Giacometti 1969). In 1929 it was found that insulin could increase glucose uptake in rats, giving rise to newly formed glycogen in liver (Cori and Cori, 1929). Much later, in1980, the insulin receptor was discovered (Massague et al. 1980) and the PI3K-Akt pathway was identified as a key regulator of insulin signalling. The underlying mechanism of glucose regulation via this pathway has since been a major topic of research (Brazil and Hemmings 2001). The PI3K-Akt signalling cascade is highly conserved and its activation is tightly regulated. Insulin stimulates the insulin receptor and causes autophosphorylation at a number of tyrosine residues within the tyrosine kinase catalytic domain which next leads to the recruitment and phosphorylation of insulin receptor substrates (IRS) proteins. These events result in the attachment of the lipid kinase phosphoinositide-3-kinase (PI3K) to the plasma membrane, where it phosphorylates phosphatidylinositol (3,4)-bisphosphate (PIP2) to phosphatidylinositol (3,4,5)-trisphosphate (PIP3), a second messenger that stimulates insulin-dependent processes, such as increasing the activity of 3-phosphatidylinositol-dependent kinase-1 (PDK1) (Brazil and Hemmings 2001). PDK1

phosphorylates the serine/threonine protein kinase AKT (from **AK**R mouse **T**hymoma) at residues S473 and T308 which activates the kinase and starts inducing a series of events, including the phosphorylation and therefore inactivation of glycogen synthase kinase-3 (GSK3) (Brazil and Hemmings 2001; Hemmings and Restuccia 2012). One key substrate of GSK3 is glycogen synthase (GYS) and phosphorylation of GYS leads to the inactivity of this protein. The inactivation of GSK3 by AKT results in the dephosphorylation and thus activation of GYS, which initiates glycogen synthesis (Lizcano and Alessi 2002; FRAME and COHEN 2001). Insulin is also a major regulator of hepatic glucose output. In healthy human beings, physiological hyperinsulinemia suppresses glycogenolysis completely and gluconeogenesis by 20% (Gastaldelli et al. 2001; Hatting et al. 2018).

Glucagon (GLUCose-AGONist) was discovered in an early preparation of insulin and first classified as an impurity and described as toxic, since it increases blood sugar levels even until death (Fisher 1923). Today, it is known that the 29 amino acids long protein is released during hypoglycaemia and induces glycogenolysis, followed by gluconeogenesis, which both leads to the release of glucose (Schade et al. 1979; Scott and Bloom 2018). During periods of starvation, glycogen is degraded within the first 12 hours, and as a result the maintenance of euglycemia becomes increasingly dependent upon gluconeogenesis, which starts with a slow onset after 3 hours and reaches a peak at two days (Cahill 2006; Petersen et al. 2017). Gluconeogenesis is the formation of glucose from pyruvate or other 3- or 4-carbon compounds. The main sources in humans are lactate, glycerol, alanine, and glutamine, which accounts for 90% of gluconeogenic substrates. Nevertheless, circling intermediates from the Krebs cycle, glycerol-related pathways and fatty acids can also serve as substrates for gluconeogenesis (Garrett and Grisham 2002; Gerich et al. 2001). Mechanistically, glucagon interacts with the glucagon- or β-adrenergic receptor, which is a G protein-coupled receptor (GPCR) on the plasma membrane. The interaction with glucagon leads to a conformational switch within the receptor which in turn activates G-coupled proteins (Ramnanan et al. 2011). Adenylate cyclase is stimulated and consequently increases cyclic adenosine monophosphate (cAMP) levels, which in turn induces activation of protein kinase A (PKA) and the cAMP response element-binding (CREB) protein (Habegger et al. 2010). On the one hand, CREB enters the nucleus and induces the transcription of glucose 6-phosphatase and phosphoenolpyruvate carboxykinase (PEPCK or PCK1), which increase gluconeogenesis. On the other hand, PKA induces glycogenolysis. It activates phosphorylase kinase, which in turn

activates glycogen phosphorylase and the conversion of glycogen to glucose-1-phosphate (G1P) is increased. Phosphoglucomutase can convert G1P to Glucose-6-phosphate and be further metabolised in other pathways (Figure 1.4). Furthermore, glycogen synthase is inhibited, which overall lowers glycogen levels and results in hepatic glucose release (Petersen et al. 2017; Janah et al. 2019).

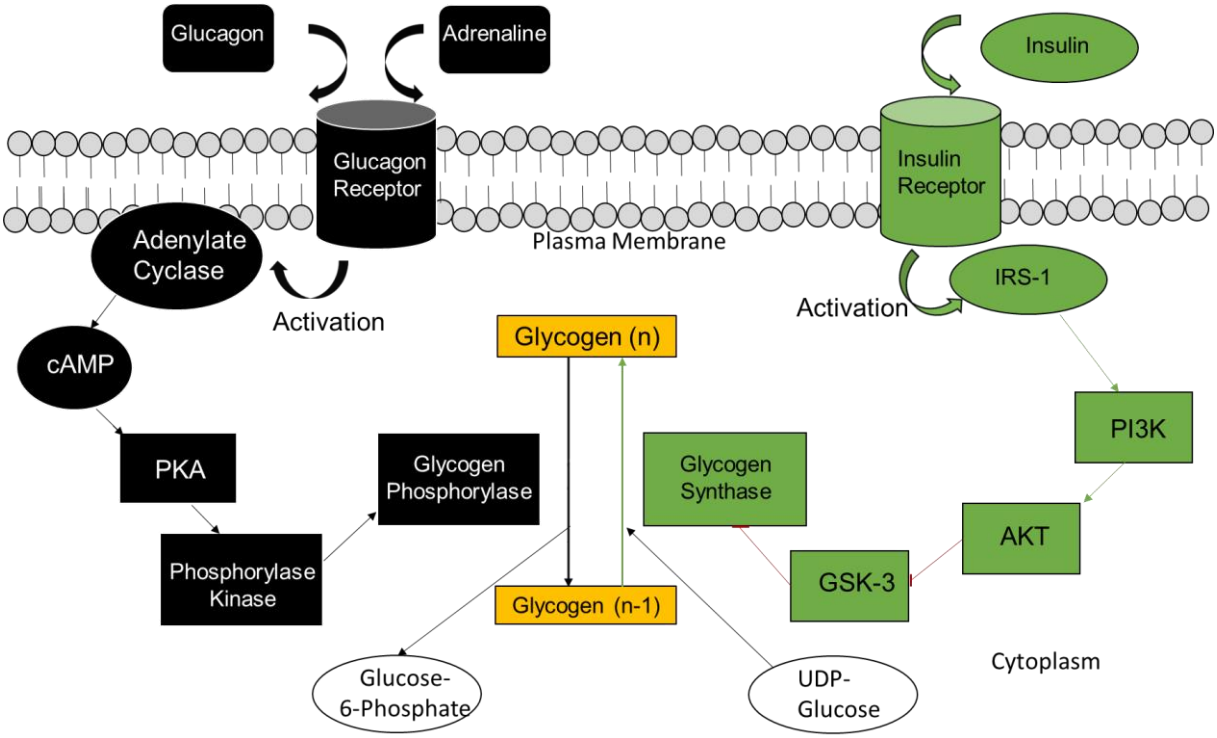

Figure 1.4 **Simplistic view of the PKA and AKT pathway in glycogen metabolism.** During periods of physical activity glucagon and epinephrine activate the PKA pathway. Due to the activation of glycogen phosphorylase, glucose-6-phosphate is released and glycogenesis is inhibited. Conversely, feeding enhances insulin-mediated signalling in the liver, leading to the activation of AKT, thus promoting glycogen synthesis and glucose uptake from the blood (Han et al. 2016).

While glycogenolysis gives a detectable biological response within minutes (due to rapid phosphorylation cascades), gluconeogenesis relies on gene transcription and physiological effects do not result until hours after glucagon secretion (Marliss et al. 1970). Nevertheless, the influence of glucagon on hepatic glucose production with exhausted glycogen stores is rather small (ELRICK et al. 1958; Brand et al. 1994; Brand et al. 1995; Cryer 2012).

Glucagon and insulin strongly regulates proteins which are associated with the catabolism and anabolism of glycogen. The glycosome (glycogen + proteins), with a median size of 10^6-10^7 Dalton, is a fragile organelle which must be ready to release glucose residues rapidly. To ensure efficient catabolism, several proteins are responsible for maintaining the form and structure of the glycogen granule. Common to these proteins is a carbohydrate binding module, in more detail the CBM20.

1.2 The CBM20

1.2.1 CBM alignments

A carbohydrate-binding module (CBM) is a domain within a protein that gives the protein the ability to bind onto raw, thermally untreated, granular starch. This domain, which can be found in either pro- or eukaryotic organisms, is a structurally and functionally independent unit which allows proteins to bind and interact with carbohydrates. In many cases proteins which exhibit a CBM domain also contain an enzymatic domain and while the CBM domain connects the protein and carbohydrate, the enzymatic domain can process it (Gilbert 1999; Boraston et al. 2004).

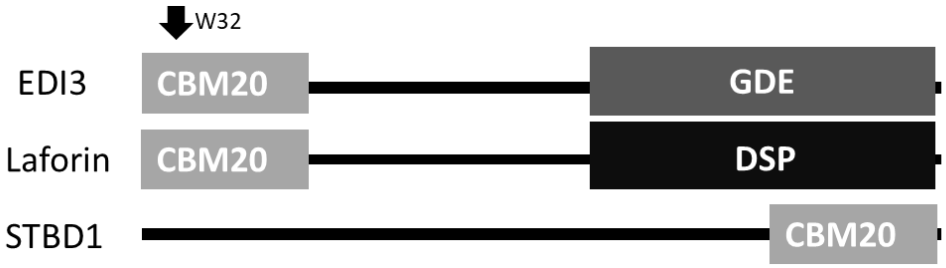

Figure 1.5 **Schematic overview of CBM20-containing proteins in humans.** *Abbreviations:* GDE, Glycerophosphodiesterase; DSP, Dual specificity Phosphatase, CBM20 Carbohydrate-binding module 20

Among the species, the CBMs differ broadly but similarities based on sequence and folding can be detected. In 1999 the CAZy (Carbohydrate-Active enZyme) database was originated as a classification system of all CBM containing enzymes that form, degrade and/or modify saccharides (Gilbert 1999; Cantarel et al. 2008; Lombard et al. 2014). The CBMs could be sorted due to their form and function and according to the latest review, 85 different CBM domains, also known as CBM families are established in the database (Janeček et al. 2019). The CBM20 is one of the best characterized CBM family's and is usually found in glucosylhydrolases and glucotransferases from bacteria, fungi, and plants (Janecek and Sevcík 1999; Janeček et al. 2011). In humans, there are only three proteins which contain a CBM20 (Figure 1.5), laforin, Starch binding domain containing protein 1 (STBD1) and Endometrial carcinoma DIfferential 3 (EDI3, aka: GPCPD1, GDE5, Kiaa1434) (www.cazy.org). Among the CBM20 themselves, the CBM20 of EDI3 is structurally most similar the CBM20 of laforin (Emanuelle et al. 2016).

1.2.2 Lessons from the CBM20 structural analysis

The three-dimensional structures of the different CBM20s in pro- and eukaryotic organisms – either in its free form or complexed with glucans – provide detailed insights into the binding of carbohydrates and polypeptides. For several CBM20 containing proteins its structure was already solved via NMR or X-ray (Christiansen et al. 2009a). Recently the full laforin protein (Raththagala et al. 2014) could be crystallized as the first human CBM20 protein.

In general, the CBM20 domains, independent form the origin organism, consists of approximately 90-120 amino acids, and its secondary structure is formed by two antiparallel β-sheets that adopt a β-sandwich fold with the two starch binding sites (SBD1 and SBD2) (Penninga et al. 1996; Mikami et al. 1999; Sankhala et al. 2015). In maximum, three carbohydrate can be bound to one CBM20 protein, one to each SBD and furthermore a third carbohydrate can be bound to a potential active centre. For glycosyltransferase of *Bacillus circulans strain 251* the simultaneous binding of three carbohydrates was experimentally proven (Lawson et al. 1994).

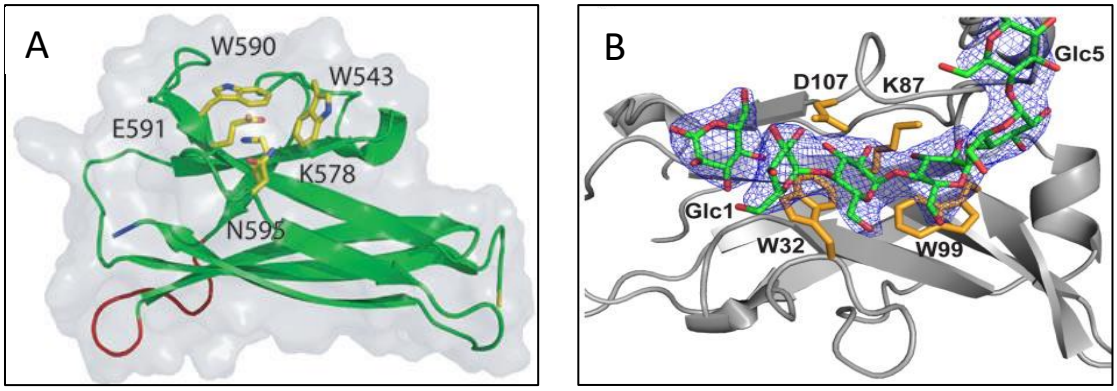

Figure 1.6 **Carbohydrate binding domain 20 within different species**. **A,** Conserved amino acids within the protein structure of the conserved binding site 1 of *Aspergillus niger*. The N-terminus and the C-terminus are highlighted in yellow and blue. Conformational change upon ligand binding in red. Ligand-binding residues implicated in ligand interactions are shown as sticks in yellow (Christiansen et al. 2009a). **B,** Crystal structure of the conserved binding site 1 of laforin showing the conserved amino acids in orange the substrate in green and the secondary structure of laforin in grey (Raththagala et al. 2014).

In NMR studies for the CBM20 of the GH15 glucoamylase from *Aspergillus niger* it was shown that the SBD1 differ in their structure from SBD2. Binding site 1, consisting of W543, K578, W590, E591 and N595 is conserved (Figure 1.6). The indole rings of residues 543 and 590 are essential to carbohydrate binding. Upon interaction, the solvent exposed binding site undergoes very little structural change and is characterized by a small ligand contact area. Conversely, the binding site 2, has a higher structural plasticity and shows conformational changes in complex with β-cyclodextrin (Sorimachi et al. 1997).

The crystal structure of laforin was solved in a complex with the maltohexaose and in contrast to former studies, the CBM20 of laforin, despite the two SBDs, binds to only one maltohexaose chain per CBM20. Here, the SBD1 and the same conserved residues W32, K87 and W99 (*Homo sapiens* laforin numbering) as mentioned for *Aspergillus niger* W543, K578 and W590 (*Aspergillus niger* GH15 glucoamylase numbering) are involved (Raththagala et al. 2014; Kuchtová et al. 2018). Additional, another independent maltohexanose chain is bound to the catalytic domain of laforin which would suggest that laforin prefers to bind at branching points of polysaccharides (Raththagala et al. 2014). For the other human CBM20 proteins no crystal structure is available but similarities to laforin's CBM20 are likely.

1.2.3 Stability and dimerization of CBM20 proteins

The mutation of the mentioned conserved residues W32, K87 and W99 in laforin, leads to a complete loss of glycogen binding for W32G and a weaker binding for K87A and W99A. Furthermore, the enzymatic activity for all three laforin mutants is decreased. Additional, the W32 residue also seems to be very important for protein stability, since the determination of melting point (T_m) in the W32G mutant is 5°C lower compared to wild type laforin (Raththagala et al. 2014). For STBD1, the CBM20 is also necessary for its protein stability, studies with truncated CBM20 showed a protein half-life of less than 3 h (Zhu et al. 2014). For EDI3 no knowledge is available at this time point.

Several studies have proposed that the CBM20 domain is important for dimerization; however, the current data are not conclusive. The first researchers who addressed this issue focused on the laforin protein, showing that it could forms dimers *in vitro*, and that point mutations within the CBM20, therefore outside of the enzymatic domain, decreased enzymatic function. Thus, the authors concluded that the dimerization of laforin is essential for full enzymatic efficiency and the CBM20, as a mediator, might be involved in this process (Liu et al. 2006). Another group however, showed that both the laforin -monomer and -dimer have equal phosphatase activity, and that the protein predominantly exists as a monomer with a small fraction existing as a dimer *in vitro* and *in vivo* (Dukhande et al. 2011). Subsequent work by the same group solved the crystal structure of laforin, indicating that it exists as an antiparallel dimer mediated by the enzymatic domain but not the CBM20 (Raththagala et al. 2014). In the case of STBD1, a yeast two hybrid system was performed, showing binding of full length STBD1 to an STBD1 mutant containing primarily the CBM20, which supported the

dimerization of STBD1 formed by interactions between the CBM20 domains (Jiang et al. 2010). For EDI3, only theoretical models are available. Information in the protein databank (pdb) suggests an asymmetric hexameric unit of EDI3's CBM20 referring to an unpublished and not further described manuscript (Saijo et al. 2008). Furthermore, EDI3 related enzymes, such as the glycerophosphodiester phosphodiesterase (GDPD) in *Agrobacterium tumefaciens*, also form hexameric structures (Shi et al. 2008). Taken all the data together, the data suggests that all human CBM20 proteins form dimers but the exact role of the CBM20 domain in this dimerization still remains to be elucidated.

1.3 Function of CBM20 Proteins

1.3.1 Laforin, a protein with many functions

Laforin is the most investigated of all the CBM20 proteins, with over 190 publications found on PubMed in November 2020. It is encoded by a 130 Kb gene, *EPM2A*, on chromosome 6q24 of the human genome. It is ubiquitously expressed in all tissues, although brain, skeletal muscle, heart and liver have the highest levels of expression in humans (Serratosa et al. 1999). Laforin which encloses two functional domains - the CBM20 and the dual-specificity protein phosphatase (DSP) domain which contains the enzymatic active centre - is known to have two independent functions.

One the one hand laforin can serve as in a protein complex with the E3 ubiquitin ligase, malin, which is encoded by *EMP2B* (Fernández-Sánchez et al. 2003). Upon interaction, laforin recruits enzymes involved in glycogen synthesis, which are then ubiquitinated by malin and degraded, thus resulting in decreased glycogen size (Vilchez et al. 2007; Solaz-Fuster et al. 2008; Worby et al. 2008). The laforin-malin complex is also involved in thermal stress (Sengupta et al. 2011), ER stress reduction (Vernia et al. 2009), cytotoxicity (Garyali et al. 2009) and autophagy (Sanchez-Martin et al. 2020).

On the other hand, laforin by its DSP is an catalytically active enzyme, which dephosphorylates amino acids (Ganesh et al. 2000; Wang et al. 2002) and carbohydrates (Worby et al. 2006; Tagliabracci et al. 2007). The mechanism of glycogen dephosphorylation was first described in 2007 by Tagliabracci et al. and assign laforin as a proofreading protein for glycogen synthase (GYS) (Figure 1.7).

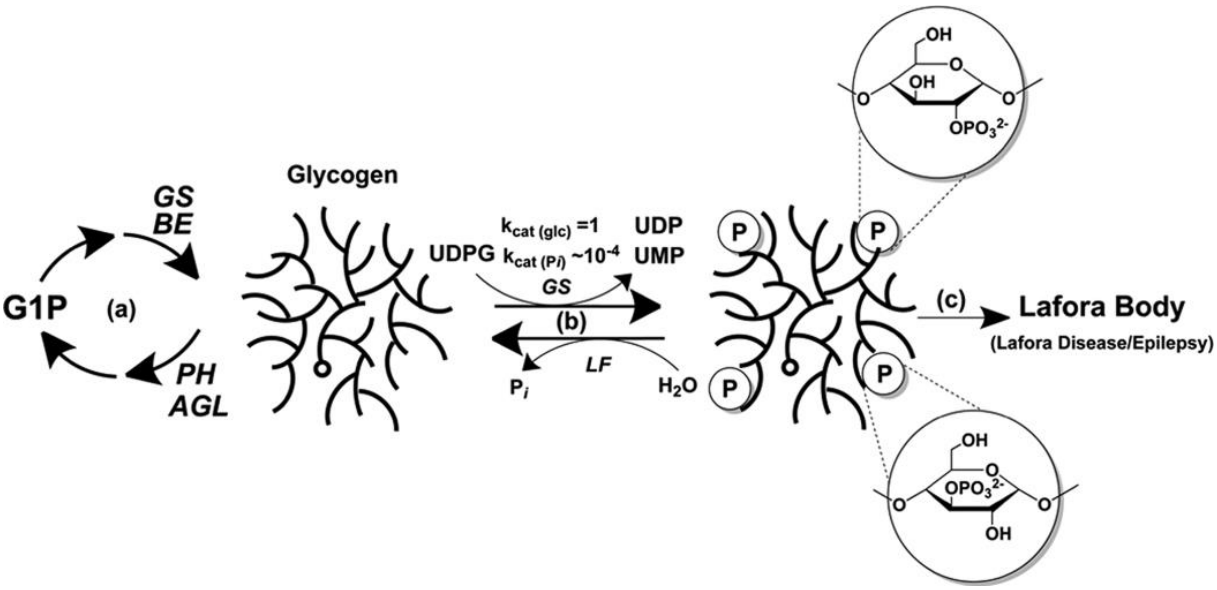

Figure 1.7 **Lafora body formation and how laforin prevents it. A,** Glucose in the cell is phosphorylated to Glucose-1-Phosphate (G1P) and if not needed linked via glycogen synthase (GS) and Glycogen branching Enzyme (BE) to glycogen. If Glucose is needed in the cell, glycogen is degraded via glycogen phosphorylase and glycogen debranching enzyme (AGL). G1P is released. **B,** G1P is linked to glycogen via converting it to the reactive form uridine-diphosphate-glucose (UDPG) yielding glycogen (n+1) and UDP but in one of ten thousand cases, this reaction yields Glycogen (n+1+phosphate) and uridine-monophosphate (UMP). In this case the glycogen gets hyperphosphorylated at C2 or C3 carbons. This reaction can be reversed via laforin, which can dephosphorylate glycogen in a hydrolysis reaction. **C** The constant hyperphosphorylation of glycogen leads to lafora bodies which can cause epilepsy (Tagliabracci et al. 2007).

During glycogen synthesis GYS elongates the glycogen branch with UMP-glucose (uridine-monophosphate-glucose). In this process, glycogen is also phosphorylated; however, at a rate of 1 phosphate/10,000 glucose moieties, GSY incorporates the β-phosphate of UDP-glucose (uridine-diphosphate-glucose) as C2- or C3-linked monoesters, resulting in the hyperphosphorylation and misbranching of glycogen. The CBM20 of laforin is able to bind to the misbranched glycogen, the DSP dephosphorylates it and the initial glycogen is restored. If the *EMP2A* is mutated and thus the CBM20 or the DSP domain are not fully functional, glycogen stays hyperphosphorylated, becomes water insoluble and appears as so called lafora body (LB) (Tagliabracci et al. 2011). Over the years, these LBs accumulate in most but especially glycogen rich tissue (Turnbull et al. 2011) and were shown to possess 2–3 fold higher amounts of phosphate compared to glycogen (Yokoi et al. 1967). A pathological outcome of the enrichment of LBs is lafora disease (LD) (Lafora 1911; Lafora and Glueck 1911) a severe form of progressive myoclonus epilepsies (PMEs), which unlike other forms is difficult to treat, and patients usually die within ten years of diagnosis (Berkovic et al. 1991; GENTRY et al. 2009). The origin of this genetic disease can be traced to at least 86% percent of the known cases to mutations in the *EMP2A* and *EMP2B* genes (Minassian et al. 1998; Serratosa et al. 1999; Chan et al. 2004) and underlines the importance of the CBM20 as functional domain.

1.3.3 STBD1: linking glycogen to autophagy

The starch- binding domain- containing protein 1 (STBD1; genethonin) was identified as GENX-3414, chromosomally localized at position 4q24-q25, as a novel human gene transcript that is highly expressed in skeletal muscle, liver, heart and placenta (Bouju et al. 1998). In cells, STBD1 is localized to the endoplasmic reticulum (Zhu et al. 2014) and mitochondria (Demetriadou et al. 2017). Unlike the other two human CBM20 domain-containing proteins, the CBM20 domain of STBD1 is located to the C-terminus and the protein itself does not have an enzymatic domain (Figure 1.5) (Janecek 2002; Machovic and Janecek 2006). The first experimental proof that STBD1 binds to glycogen was shown in a proteomic analysis, where glycogen particles from mouse and rat liver were isolated, treated with trypsin and analysed on a mass spectrometer. Here, the authors could describe STBD1 as one of the proteins binding glycogen in liver (Stapleton et al. 2010). Jiang and colleagues further showed a strong binding of STBD1 to amylopectin and weak binding to glycogen *in vitro*. Moreover, *GYS1* overexpressing COS9 cells (Jiang et al. 2010), HeLa, C2C12 cells (Demetriadou et al. 2017) and Rat-1 fibroblasts (Skurat et al. 2017) were used to confirm the interaction of STBD1 and glycogen in living cells. Truncations of critical residues in the CBM20 of STBD1 (ΔW293) impaired this binding. Furthermore, the 24 N-terminal hydrophobic residues of STBD1 allows the protein and with it the C-terminally bound glycogen to anchor at cell membranes and organelles. (Jiang et al. 2010).

The interaction of STBD1 with GABA type A receptor associated protein like 1 (GABARAPL1) connected STBD1 to a function in autophagy (Jiang et al. 2010). In a follow-up study by the same authors, this link could be strengthened and STBD1 residues W203 and V206 were determined as essential for its interaction with GABARAPL1 (Jiang et al. 2011). On a functional level the authors proposed that STBD1 can recognize pathological glycogen (like lafora bodies) since it preferentially binds to amylopectin, which conversely is less branched or misfolded glycogen. Upon binding to STBD1, the pathological glycogen is anchored to the cellular membrane and next, GABARAPL1 and other autophagy proteins (LAMP1, GABARAPL2) are recruited to STBD1 where they facilitate the forming of autophagosomes (Figure 1.8). Glycogen is transported to lysosomes where it is directly hydrolysed to glucose by a lysosomal α-glucosidase, a process termed the autophagy of glycogen or “glycophagy”, which now is an accepted expression in the field (Jiang et al. 2010; Jiang et al. 2011; Zhao et al. 2018; Delbridge et al. 2015).

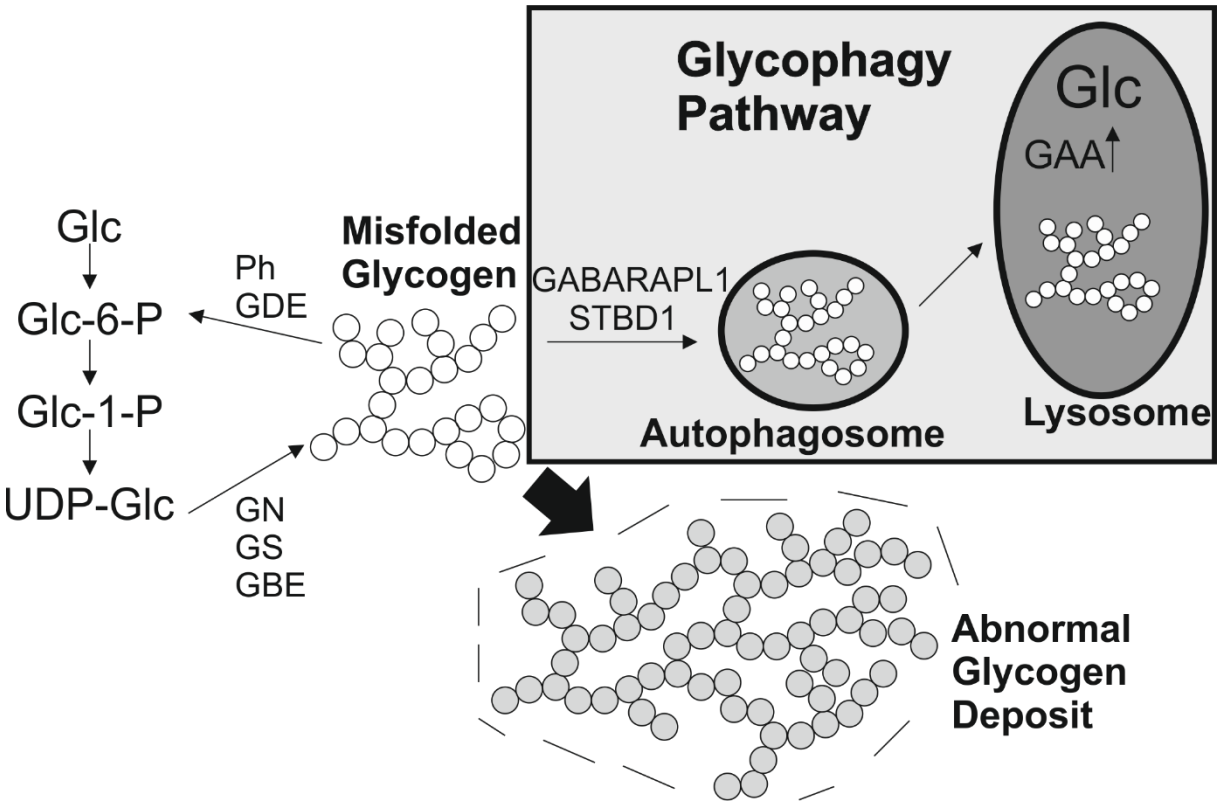

Figure 1.8 **A possible role for Stbd1 participation in glycogen metabolism.** Glucose is stored as glucose-1-phosphate (Glc-1-P) in Glycogen. Its transition via the glucosyl donor UDP-glucose (UDP-Glc) is accompanied by glycogenin (GN), glycogen synthase (GS) and glycogen branching enzyme (GBE). Vice versa, glycogen degradation via glycogen phosphorylase (Ph) and debranching enzyme (GDE) yields Glc-1-P. Misfolded glycogen can lead to abnormal glycogen deposits in the cell or be detected be STBD1 and be degraded via the glycophagy pathway. STBD1 recruits autophagy proteins like GABARAPL1 which guides the glycogen to the lysosomes where it is hydrolysed to glucose by lysosomal α-glycosidase (GAA). (Inspired by Jiang et al. 2010)

Taken together, existing data suggest that STBD1 is not directly involved in the metabolism but in the homeostasis of glycogen. The main function seems to involve controlling the branching of glycogen and if needed assisting as a scaffold protein on the glycogen molecule to recruit autophagy proteins, which transport the polysaccharide to the lysosomes or even other compartments.

1.3.4 EDI3: a so-far uncharacterised CBM20 protein

The third human CBM20-containing protein is Endometrial differential 3 (EDI3, KIAA1434, PREI4, GDE5). In mice, the gene was initially identified as preimplantation protein 4 (PREI 4, U01136), and hypothesized to be important during embryogenesis, showing high mRNA expression in oocytes, especially in the one-cell state 3 h after fertilization (Temeles et al. 1994; Temeles and Schultz 1997). In humans, EDI3 was first listed as KIAA1434 in a cDNA sequencing project carried out at the Kazusa DNA Research Institute, Japan (Ohara et al. 1997; Nagase et al. 2000). The corresponding gene, glycerophosphocholine phosphodiesterase 1 (*EDI3*, *GPCPD1*) is localized on chromosome 20p12.3, encodes a protein that is 672 amino

acids (AA) long with a mass of 76.035 Dalton (Da), which contains two functional domains: the CBM20 at the N-terminus ,AA 1-115, and an enzymatic glycerophosphodiesterase (GDE) domain at the C-terminus ,AA 318-618 (Figure 1.4)(uniport.org). A phylogenetic analysis of the GDE domain identified EDI3 as GDE5, and categorized it into the family of glycerophosphodiester phosphodiesterases (GDE) (Zheng et al. 2003). Unlike the other GDE members, EDI3 does not have a transmembrane region and was thus placed into a different subgroup (Zheng et al. 2003). In independent studies, two research groups could identify the enzymatic function of EDI3 as a hydrolysis reaction, cleaving L-1-glycero-3-phosphocholine (GPC) to glycerol-3-phosphate (G3P) and choline (Stewart et al. 2012; Okazaki et al. 2010), indicating that EDI3 could be relevant in several metabolic pathways (Figure 1.9)

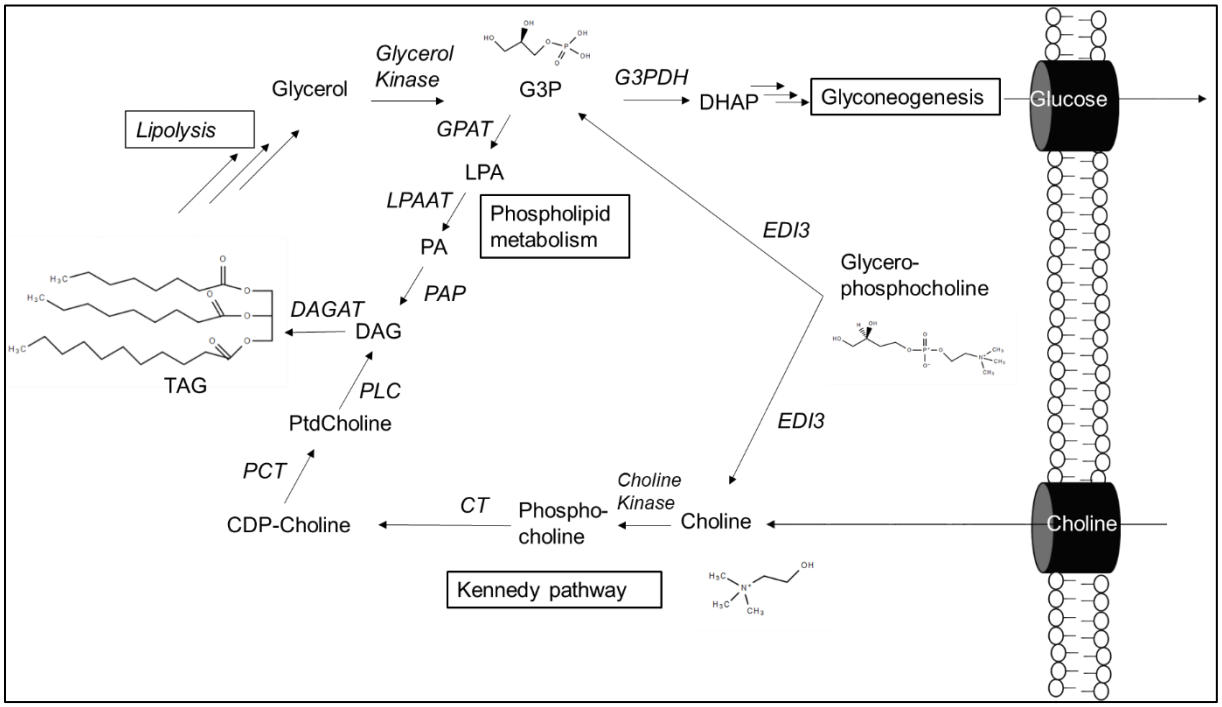

Figure 1.9 **The role of EDI3 in different metabolic pathway**. EDI3 cleaves GPC to choline and Glycerol-3-phosphate (G3P), linking the choline, glycerophospholipid, and triglyceride metabolism. EDI3 may be involved in gluconeogenesis due to the conversion of G3P to dihydroxyacetone phosphate (DHAP) via G3P-dehydrogenase (G3PDH), and in signalling pathways activated by the lipiphosphatidic acid (PA), and diacylglycerol (DAG). Furthermore EDI3 can participate in the choline metabolism. *Abbreviations:* CDP-Choline, cytidine 5′-diphosphocholine; CT, phosphocholine cytidyltransferase; DAGK, DAGAT, DAG acyltransferase; GPAT, G3P acyltransferase; LPAAT, LPA acyltransferase; PAP, PA phosphatase; PCT, diacylglycerol choline phosphotransferase; PLC, phospholipase C; PtdCholine, phosphatidylcholine; TAG, triacylglycerol

Our group first identified EDI3 in a screening study using differential display analysis to analyse RNA expression in metastasizing versus non-metastasizing endometrial cancer (Stewart, 2012). The average gene expression of *EDI3* (*GPCPD1)* in metastatic tumours was 6.4 times higher than in non-metastatic tumours. Kaplan-Meier and multivariate analyses could show a

correlation between high *EDI3* gene expression and worst prognosis and shorter survival time in endometrial and ovarian cancer (Stewart et al. 2012).

In vitro characterization of EDI3 in different cancer cells lines where EDI3 was silenced or overexpressed revealed a role for EDI3 in cancer-related phenotypes, such as migration and adhesion (Lesjak et al. 2014). Furthermore, inhibition of the enzymatic activity of EDI3 with the general phosphodiesterase inhibitor, dipyridamole, also decreased the migration in different cell culture models (Stewart et al. 2012). To identify the link between EDI3's role in migration and its metabolic function, the group investigated the pathways downstream of EDI3 and showed that glycerol-3-phosphate acyltransferase (GPAM), which metabolizes G3P and the signalling lipid which is produced, lysophosphatidic acid (LPA) are important for EDI3's role in migration (Marchan et al. 2017). Thus, it appears that the enzymatic function of EDI3, and the resulting metabolic changes are important for EDI3's role in cancer-related phenotypes. The CBM20 of EDI3 however, is not characterized. Only one older review on the GDE family suggested that due to the CBM20, EDI3 may bind glycogen and be involved in glucose metabolism and/or utilization in skeletal muscle (Yanaka 2007).

1.4 Skeletal muscle

1.4.1 General structure of the skeletal muscle

The skeletal muscle is a well-organized organ that is structured in layers. The muscle cell (myofibril) is the smallest unit and its basic cellular compartment is called the sarcomere. Bundles of muscle cells form the fascicles and bundles of fascicles form the muscle tissue. Each tier is encapsulated by extracellular matrix and supported by cytoskeletal networks. The whole muscle is innervated, and due to its need for glucose and other metabolites highly vascularized. In order to guarantee sufficient energy production, the muscle is equipped with components of the metabolic and regulatory machinery (Mukund and Subramaniam 2020).

1.4.2 Muscle fibre classification

Muscle fibres, which are composed of myofibrils, are quite heterogeneous. The muscle structure encompasses tens to hundreds of motor units, each with its specific role adjusted to specific needs within the body and the environment, in more detail, some cells are specialized for long distance running other cells for weight lifting (Schiaffino and Reggiani 2011). One of the oldest ways to characterize different muscle cells is by colour. Skeletal muscle type I cells are highly vascularized, saturated with mitochondria and myoglobin, and therefore identified

by its red colour and aptly named red muscle cells. In contrast, skeletal muscle type II cells are less oxygenated (and less red), and are named white muscle cells (Needham 1926). Over time, more distinct methods were developed to distinguish the different muscle fibres, including histochemical and physiological studies of the individual motor units (Close 1967), determination of oxidative and glycolytic enzymes (Edström and Kugelberg 1968), differentiation of myosin ATPase (Guth and Samaha 1969; Peter et al. 1972), and analysing the intracellular Z-disc and the mitochondrial content of skeletal muscle fibres via electron microscopy (Schiaffino et al. 1970; Sjöström et al. 1982). Most of these differentiation methods are linked to the metabolic profile of the cells, which in turn is closely associated with its cellular function and its resistance to fatigue, the disability to generate force (table. 1.2).

Table 1.2 **Properties of different skeletal muscle fibre types**

	Type I fibre	**Type II A fibre**	**Type II X fibre**
Contraction time	Slow	Moderately fast	Fast
Resistance to fatigue	High	Fairly high	Low
Activity used for	Aerobic activities	Long anaerobic activities	Short term anaerobic activities
Maximum duration	Hours	Less than 30 min	Less than 5 min
Produced power	Low	Medium	High
mitochondrial density	Very high	High	Low
capillary density	High	Intermediate	Low
Oxidative capacity	High	High	Low
Major storage metabolite	Triglycerides	Creatine phosphate, Glycogen	Creatine phosphate, Glycogen

Phenotypically, Type I muscle cells (slow-twitch) are resistant to fatigue, contract slowly and for long periods with little force generated. They use constantly high amounts of energy and are needed for endurance sport, posture and to generate heat. They primarily run on oxidative phosphorylation. Conversely, type II muscle cells (fast-twitch) are able to generate strong force for a short period of time, they contract fast, and fatigue much easier then type I cells. Since these cells need energy fast, which is difficult to predict at times, they rely on anaerobic glycolysis. Type II cells have a high glycolytic capacity ensuring efficient ATP generation to compensate for the accelerated rate of ATP hydrolysis (Mukund and Subramaniam 2020). Three different isoforms of type II cells have been identified: IIA, IIB and IIX; However, type IIB is not present in humans. The distinction among the cell types mainly relies on the protein abundance of different myosin heavy chain isoforms (MHC), depending on skeletal fibre muscle type (Schiaffino et al. 1988; Schiaffino et al. 1989). Another way to differentiate between the skeletal muscle fiber is the source of substrates used for energy production. The

triglyceride concentration in skeletal muscle type I cells is reported to be up to 7 mM; while type II cells have only 4.2 mM (Gollnick et al. 1981). Additionally, the lipid droplet volume within white muscle fiber (IIX) is >0.1%, and thus lower than the 0.5% measured in red muscle cells (Howald et al. 1985). The opposite is found for the glycogen content.

1.4.3 Glycogen in muscle

While the highest amount of glycogen is found in the liver with 30.2-43.1 mg/g tissue (Khandelwal et al. 1979; Vissing et al. 1989; Kusunoki et al. 2002), the second highest levels are found in skeletal muscle with 5.8-7.1 mg/g tissue (Garetto et al. 1984; Vissing et al. 1989; Baker et al. 2005), followed by the heart with 4.1-4.5 mg/g tissue (Conlee et al. 1989; Vissing et al. 1989). These three tissues represent the major sites for maintaining energy homeostasis in animals (Mukund and Subramaniam 2020). In skeletal muscle itself, glycogen levels are higher in the fast compared to slow fibres, with fast fibres having 16% (Vøllestad et al. 1984) to 31% (Greenhaff et al. 1993) more glycogen than slow fibers. Nevertheless, during exercise, glycogen decreases first in type I, second in type IIA and then in type IIX fibers (Gollnick et al. 1974), which is due to the motor unit recruitment sequence. During muscle contraction, the type I cells are activated first, followed by the type IIA cells, and finally the type IIX fibers (Schiaffino and Reggiani 2011). Among the muscle fibre types, it has been reported that there is a pronounced difference in glycogen breakdown rate during maximal contractions: 0.35 (slow) and 0.52 (fast) mM/s, which indicates that the breakdown in fast fibres is 32% faster (Vøllestad et al. 1992). Finally, after intense exercise, glycogen resynthesis can take up to 24 h with the initial rate (first 3–5 h) faster in type I fibres (Terjung et al. 1974; Castillo et al. 2009).

Studies using electron microscopy could identify three (two minor and one major) distinct subcellular localizations of glycogen within the human skeletal muscle cells. First, 5% of the cellular glycogen is intramyofibrillar glycogen, which is harboured in the myofibrils, interspersed within the contractile filaments, and often associated with the sarcomere. Second, there is the subsarcolemmal glycogen, which is found near to the surface membrane in close vicinity of mitochondria, lipids and nuclei, and which makes up the final 15% of muscle glycogen. Third, there is intermyofibrillar glycogen, which is located between the myofibrils in close proximity of the sarcoplasmic reticulum (SR), the transverse tubules (t-tubules) and mitochondria. This store makes up 75% of the cellular glycogen (Nielsen and Ørtenblad 2013).

Between the SR and the t-tubules, the glycogen rich triad junction is located which is studded with and is highly metabolic active proteins (Hong and Shaw 2017). The triad is mostly known for their role in muscle contraction. Here, the action potential generated at the neuromuscular junction (NMJ) is transmitted to the muscle fibre, initiating muscle to contract via calcium signalling (Figure 1.10.A) (Mukund and Subramaniam 2020).

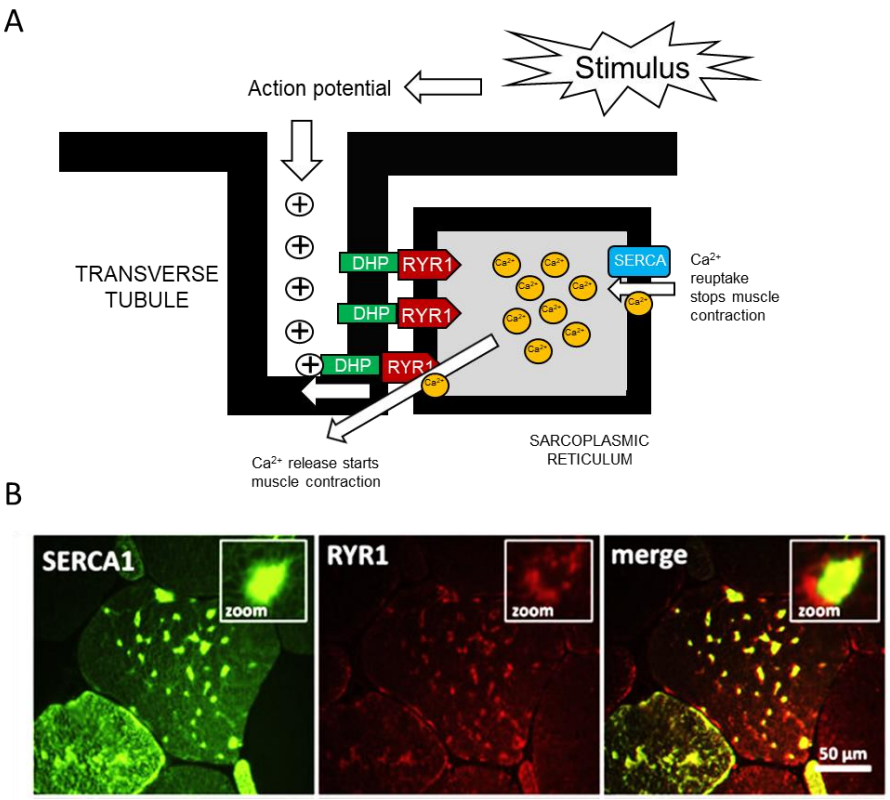

Figure 1.10 Localization of RyR1 and SERCA in the skeletal muscle. A, The role of the T-tubules in the muscular transmission of stimuli is shown in simplified form. A neural stimulus is converted into an action potential and processed in the T-tubules. (DHP) is altered and controls the opening of RYR1 through direct molecular interactions. Calcium is released from the SR and starts the muscle contraction. After relaxation SERCA pumps calcium back into the SR. *Abbreviations:* RYR1, Ryanodine receptor 1; SERCA, sarcoplasmic/endoplasmic reticulum Ca2+ ATPase; DHP, Dihydropyridine receptor; SR, sarcoplasmic reticulum **B,** Immunohistochemical staining in human skeletal muscle showing the localization of RYR1 and SERCA1 (Böhm et al. 2013)

In very short, in skeletal muscle, the action potential depolarizes the dihydropyridine receptor (DHPR) in the t-tubules, which leads to the opening of Ryanodine receptor 1 (RYR1) through direct molecular interactions. As a consequence, the intracellular release of Ca^{2+} from the sarcoplasmic reticulum (SR) initiates muscle contraction. Muscle relaxation, thus removal of cytosolic Ca^{2+} is performed by sarcoplasmic/endoplasmic reticulum Ca^{2+} ATPase (SERCA) (Mukund and Subramaniam 2020). Also glycogen is involved in the Ca^{2+} signalling. In a number of studies it could be shown, that the regeneration of glycogen between different fatigue runs

is needed to keep the calcium signalling on a constant high level (Chin et al. 1997; Kabbara et al. 2000; Helander et al. 2002; Ørtenblad et al. 2013).

1.4.4 EDI3 in mouse skeletal muscle

Although there is still a lot that is not known about the physiological function of EDI3, two publications have described a role for EDI3 in skeletal muscle development (Okazaki et al. 2010; Hashimoto et al. 2016). The authors reported high *Edi3* gene expression in skeletal muscle (Quadriceps, gastrocnemius), heart muscle, brain and intermediate expression in mouse liver. Age, immobilization and removal of the sciatic nerve led to decreased *Edi3* gene expression which could also be observed in a diabetic mouse model. Silencing *Edi3* with siRNA in C2C12 cells, an immortalized mouse myoblast cell line, resulted in increased expression of myogenin, a muscle-specific transcription factor, which coordinates muscle development and repair (Hasty et al. 1993). In addition, silencing *Edi3* resulted in an increase in the number of myotubes - cells that develop into muscle fibres formed by the fusion of multiple myoblasts. Overexpression of full length Edi3, in addition to a truncated version, Edi3Δ471 that lacks the enzymatic function of the protein, decreased the number of forming myotubes. The research group also created a transgenic mouse model that overexpressed mouse *Edi3Δ471* gene specifically in the quadriceps and gastrocnemius via the human α-actin promotor. The transgenic mice showed a significant decrease in skeletal muscle weight and size compared to the control mice. Furthermore, skeletal muscle type I remained unchanged, but the number skeletal muscle type II cells was highly reduced in the transgenic mice. In a subsequent study investigating the mouse model carrying the truncated Edi3 (*Edi3Δ471)* gene (Hashimoto et al. 2016), the authors reported alterations in the neuromuscular junction (NMJ) 4 weeks after birth compared to control mice. The neuromuscular junction is defined as the chemical synapse that connects the motor neuron with the muscle fiber. In the 4 week old EDI3Δ471 mice, increased mRNA levels of acetylcholine esterase, α- and ε- subunits, but not the γ-subunit was observed. Morphological changes of the NMJ was not reported (Hashimoto et al. 2016).

In summary, EDI3 is needed for the development of skeletal muscle and regulated *MYOG* levels and impaired locomotion decreased EDI3 levels. According to mRNA data a role of EDI3 in neuromuscular transmission is possible.

1.5 Aim of the study

Our research group identified EDI3 as a gene associated with worst prognosis in endometrial or ovarian cancer. EDI3 is categorized as a glycerophosphodiesterase (GDE) because of the GDE domain at its C-terminus, and our group showed that it hydrolyses glycerophosphocholine (GPC) to glycerol-3-phosphate (G3P) and choline. Among the GDE proteins, EDI3 is unique because it is cytoplasmic, and contains a CBM20 domain at its N-terminus, which remains uncharacterized. **This domain-characterization will be the first major goal of this thesis.** Based on sequence alignment and published knowledge of the other CBM20 proteins, laforin and STBD1, in a first step, mutation of a key conserved residue within the CBM20 and complete CBM20 deletion will be created and analysed for characteristics, such as protein stability, enzymatic activity, dimerization and phenotypic effects.

The CBM20 is known to be important for binding amylopectin and glycogen, as described for STBD1 and laforin. Since the role of EDI3 in carbohydrate binding remains unknown, **a second major goal is to investigate whether EDI3 binds amylopectin and glycogen.** First experiments will include glycan precipitation experiments where polysaccharides, amylopectin and glycogen will be mixed with cell lysate from EDI3 –overexpressing cells. In a second step, binding of EDI3 to glycogen in cells and organs will be tested. Furthermore, a role in glycogen degradation will be investigated. For the latter, immunohistochemical analyses will be performed in human liver and muscle, organs associated with high glycogen content.

The binding of EDI3 to glycogen, if observed should underlie a purpose and also be regulated. Thus, t**he third goal of this thesis is to investigate the role of EDI3 in glycogen metabolism.** Here, EDI3 RNA and protein levels will be investigated upon manipulating glycogen levels under fed and starved conditions, and under the influence of glycogen-associated hormones, glucagon and insulin in glycogen rich cells.

According to literature, EDI3 is associated with skeletal muscle development in mice and potentially with stimulus conduction. Muscle, both skeletal and cardiac, harbours high amounts of glycogen. Therefore, the **last aim of the study is to characterize the role of EDI3 in human skeletal and cardiac muscle** using immunohistochemical analyses of key muscle and glycogen metabolism proteins to identify a potential link between EDI3, glycogen and neuromuscular transmission.

2. Materials and Methods

2.1 Material

2.1.1 Technical equipment

Table 2.1: **Equipment**

Equipment	**Company**
Adapter for 1 thick-walled tubes 3 ml	Laborgeräte Beranek
Autoclave VX-150	Systec
Autosampler MPS-2	Gerstel
Axio Scan.Z1	Zeiss
Balance	EW, Kern
Brady Printer BBP 33	Brady
Blot imager Vilber Fusion Fx7	Vilber Lourmat
Box VX5	Vilber Lourmat
Casy cell Counter	Roche
Centrifuge, Avant JNX-26	Beckmann Coulter
Centrifuge with cooling function	Biofuge Fresco, Heraeus
Centrifuge with cooling function 5424R	Eppendorf
Centrifuge MiniSpin plus	Eppendorf
Concentrator Plus	Eppendorf
Confocal microscope (LSM), FV1000	Olympus
CO_2 Incubator	Binder
Electrophoresis unit Mini-PROTEAN®	Bio-Rad
Electrophoresis unit SE260	Höfer
EVOQ™ Elite Triple Quadrupole	Bruker
Fume hood	Waldner
HM 450 Sliding Microtome	Thermo
Live Insect Forceps, Narrow Sharp, 10 cm	F.S.T.
Magnetic stirrer IKAMAG RCT	Ikamag
Microscope BX41	Olympus
Microscope eclipse T5100	Nikon
Microscope Primo Vert	Zeiss, Software ZEN from Zeiss
Microwave oven	Bosch
Milli-Q	Millipore
Modular tissue embedding center	Thermo Fisher Scientific
NanoDrop ND-2000	Thermo Fisher Scientific
QTrap4000	Shimadzu
pH meter	Schott
Pipets (10 µL, 2 µL, 100 µL, 200 µL, 1 ml, 5 ml)	Eppendorf
Pipet boy	Integra
Plate reader infinite M200 Pro	Tecan
Power pack HC	Bio-Rad
Power pack P25T	Biometra
Precision balance EW150-3M	Kern
Precision balance ME235P	Sartorius
Polycarbonat tubes 3,0 / 3,5 ml (FA / SW), 13x51 mm, thick-walled	Laborgeräte Beranek
qPCR system ABI 7500	Applied Biosystems
Rotating Wheel	VWR

Equipment	Company
Rotor, JLA-16.250	Beckman Coulter
Rotor, Ja-25.50	Beckman Coulter
Rotor, T-880	Sorvall
Rocking Platform	VWR
Shaker KS 260 basic	IKA
Slide drying oven TDO Sahara	Medite
Sliding Microtome HM 450	Microm
Sonicator sonoplus mini	Bandelin
Spin Tissue Processor STP 120	Thermo Fisher Scientific
Sterile hood	Hereaus
Thermo cycler T Gradient	Biometra
Thermomixer	Eppendorf
Thermo shaker PHMT Grant-bio	Keison
Thermo shaker	peqlab
Transfer chamber fast blot B44	Biometra
Transfer chamber Trans-Blot SD	Bio-Rad
UFLC system	Shimadzu
Ultracentrifuge, Discovery 90 SE	Sorvall
Vacuum pump	Vacuubrand
Vent Filter 12FC	Millipore
FV-1000 viewer software	Olympus
Vortex-Genie2	Bender & Hobein
Water bath	Labortechnik
Zen software	Zeiss

2.1.2 Consumables

Table 2.2: **Consumables**

Consumables	Company
Blade N35HR (for Microtome)	Thermo
Blot Filter Paper, 7 x 8.4 cm	Bio-Rad
CASY cups	OLS Omni Life Sciences
CASY ton	OLS Omni Life Sciences
Cell culture Microplate 96 well, PS, F-Bottom, Black	Greiner bio-one
Cell scraper (25 mm)	Sarstedt
Cell culture Inserts 24 well 8.0 µm pore	Falcon
Cover slips	VWR
Cover glasses, Ø 14 mm	Nordic biolabs
Cryogenic Vials	Sarstedt
Cover slices 18x18 0,13-0,16 mm	Menzel
Cuvettes (Black)	Sarstedt
Embedding cassettes	Carl Roth
Fat pen	Dako
Freezing container (Mr. Frosty)	Thermo Fisher Scientific
Glass Pasteur Pipettes	BRAND GmbH + Co
Humid chamber	Custom made
MicroAmp® Optical Adhesive Film	Thermo Fisher Scientific
MicroAmp® Optical 96-Well Reaction Plate	Thermo Fisher Scientific
Microscope slide SuperFrost Plus	Thermo Fisher Scientific

Consumables	Company
Minisart® syringe filters (0.45 µM)	Sartorius
Pestle and Microtube	VWR
Pipets	Eppendorf
Pipet tips (filtered/not filtered)	Sarstedt
PVDF Membrane	Perkin Elmer
RNase-free Microfuge Tubes 1.5 ml	Thermo Fisher Scientific
RNaseZap™ RNase Decontamination Solution	ThermoFisher Scientific
Reaction tubes (0.5 - 50 ml)	Sarstedt
Serological pipettes 5, 10, 25 ml	Sarstedt
Tissue culture flask 25, 75, 175 cm^2	Sarstedt
Tissue Culture plates 6-, 24-, 96- well (colourless)	Sarstedt

2.1.3 Chemicals and dyes

Table 2.3: **Chemicals**

Chemicals/dyes	Company
Acetic acid	Carl Roth
Acetic acid glacial	Carl Roth
Ammonium persulfate	Sigma-Aldrich
Ampicillin sodium salt	Sigma-Aldrich
β-Mercaptoethanol	Carl Roth
Bis-(2-hydroxyethyl)imino-tris-(hydroxymethyl)-methane (Bis-Tris)	Carl Roth
Bodipy (493/503)	Thermo Fisher Scientific
Bovine serum albumin (BSA)	Carl Roth
Bovine serum albumin (BSA), fatty acid free	Sigma-Aldrich
Bromphenol blue	Carl Roth
Chloroform	Carl Roth
Citric acid monohydrate	Carl Roth
Collagenase from Clostridium hystolyticum	Sigma-Aldrich
p-Coumaric acid	Sigma-Aldrich
Creatinine hydrochloride	Sigma-Aldrich
4',6-diamidino-2-phenylindole (DAPI)	Thermo Fisher Scientific
Dimethyl sulfoxide (DMSO)	Sigma-Aldrich
Dithiothreitol (DTT)	Sigma-Aldrich
Ethylene glycol diamine tetraacetic acid (EGTA)	Carl Roth
Entellan®	Merck
Ethanol, absolute	Carl Roth
Ethylenediaminetetraacetic acid (EDTA)	Carl Roth
Fetal Calf serum (FCS) Sera Plus	Pan-Biotech
Glucose	Carl Roth
L-Glutamine	Sigma-Aldrich
Glycerol	Carl Roth
Glycine	Carl Roth
HEPES	Carl Roth

Chemicals/dyes	Company
Hydrochloric acid 32%	Carl Roth
Hydrogen peroxide 30%	Merck
Kanamycin sulfate	Roche
Luminol	Sigma-Aldrich
Magnesium chloride	Carl Roth
Methanol, HPLC grade	Carl Roth
Methyl-tert-butyl ether (MTBE)	Merck
Nonidet P-40 substitute (NP-40)	Roche
Oleic acid	Sigma-Aldrich
Paraformaldehyde 4% (PFA)	Carl Roth
Periodic acid	Carl Roth
Potassium chloride	Carl Roth
Potassium dihydrogen phosphate	Carl Roth
2-Propanol	Carl Roth
Rotihistol®	Carl Roth
Tetracycline	Sigma-Aldrich
Schiff's reagent	Carl Roth
SDS pellets	Carl Roth
Sodium chloride	Carl Roth
Sodium deoxycholate	Carl Roth
Sodium glycolate	Thermo Fisher Scientific
Sodium glyoxylate monohydrate	Sigma-Aldrich
Sodium hydrogen phosphate	Carl Roth
Sodium hydroxide pellets	Carl Roth
Tetramethylethylenediamine (TEMED)	Carl Roth
Tris	Carl Roth
Tris-HCl	Carl Roth
TritonX-100	Sigma-Aldrich
Tween20	Sigma-Aldrich
Tween80	Sigma-Aldrich

2.1.4. Commercial buffers and reagents

Table 2.4: **Reagents**

Buffer/reagent	Company
Acrylamide (30% (v/v))	Carl Roth
Amino acid solution	PAN-Biotech
Anode-/Cathode-buffer concentrate A & K	Carl Roth
Diethylpyrocarbonate treated (DEPC) water	Thermo Fisher Scientific
DAKO EnVision +System HRP (DAB)	Dako
DMEM 10x 1g/l Glucose	PAN biotech
Fluoroshield™ mounting medium	Sigma-Aldrich
Fluoroshield™ with DAPI histology mounting medium	Sigma-Aldrich
MG-132	Selleckchem
Lipofectamine 3000	Life Technologies
Lipofectamine RNAiMAX	Life Technologies
Mayer’s haemalaum solution	Merck

Buffer/reagent	Company
NuPAGE® MES SDS Running Buffer (20X)	Thermo Fisher Scientific
OptiMEM	Life Technologies
Phosphatase-Inhibitor-Cocktail II&III	Sigma-Aldrich
Precision Plus Protein Dual Colour standards	Bio-Rad
Protease-Inhibitor-Cocktail	Sigma-Aldrich
RNase-Free DNase Set	Qiagen
RNeasy Mini Kit	Qiagen
Substrate Chromogen	Dako
QIAzol Lysis-Reagent	Qiagen
Venor® GeM Classic	Minerva Biolabs
Taqman Universal PCR Master Mix	Thermo Fisher Scientific

2.1.5 Commercial assays and kits

Table 2.5: **Assays and kits**

Commercial assays and kits	Company
Amplex Red GPC Assay (adapted from Amplex Red PLD Assay kit)	Thermo Fisher Scientific
BCA Protein assay	Thermo Fisher Scientific
Glycogen Assay Kit	Sigma-Aldrich
Gibson Assembly® Master Mix	NEB
High-Capacity cDNA Reverse Transcription Kit	Thermo Fisher Scientific
Pierce™ Protein A/G Magnetic Beads	Thermo Fisher Scientific
Quantifast SYBR Green RT-PCR kit	Qiagen
Q5 Site-Directed Mutagenesis Kit	NEB
RNase-Free-DNase kit	Qiagen

2.1.6 Enzymes and small molecules

Table 2.6: **Enzymes and small molecules**

Enzymes and small molecules	Company
alpha-Amylase (Diastase)	Roche
Collagen rat tail lyophilised	Roche
Glycerophosphocholine (GPC)	Sigma-Aldrich
GPCPD1 (EDI3) recombinant protein	Origene
PrimeSTAR GXL DNA Polymerase	Takara
Restriction Enzymes	NEB/ Thermo Fisher Scientific
Trypsin 0.05% EDTA	Pan Biotech

2.1.7 Prepared buffers and reagents

Table 2.7: **Prepared buffers and reagents for molecular biological methods**

	Compounds	**Concentration**
Lysogeny broth (LB-Media)	Bacto-trypton yeast extract NaCl (+ Agar) pH 7.5	1% (w/v) 0.5% (w/v) 1% (+2% (w/v))
Tris-Acetate-EDTA (TAE) Buffer (1x)	Tris Acetic acid EDTA in ultrapure water	40 mM 20 mM 1 mM
Tris-Acetate-EDTA (TAE) Buffer (50x)	Tris Acetic acid EDTA in ultrapure water	2 M 1 M 50 mM

Table 2.8 **Prepared buffers and reagents for protein analysis**

	Compounds	**Concentration**
Anode buffer	Buffer concentrate A Methanol in ultrapure water	10% 20%
APS solution	Ammonium persulfate in ultrapure water	10% (w/v)
Cathode buffer	Buffer concentrate K Methanol in ultrapure water	10% 20%
Enhanced Chemiluminescent solution	Luminol p-Coumaric acid in 0.1 M Tris	2.5 mM 0.2 mM
EDI3 Activity Assay Buffer (5x)	Tris-HCl NaCl $MgCl_2$ in ultrapure water, pH 7.4	250 mM 700 mM 10 mM
Glycan binding buffer	Tris-HCl, pH 7.5, NaCl, β-Mercaptoethanol Triton X-100	50 mM 150 mM 0.1% 0.1%
IP Lysis buffer	Tris-HCl pH 7.4 NaCl EDTA NP-40 Glycerin	25 mM T 150 mM 1 mM 1 % 5 %
Lämmli-buffer (5x)	Bromophenol blue DTT Glycerol SDS Tris-HCl	0.05% (w/v) 0.25 M 50% (w/v) 5% (w/v) 0.225 M

PBS (10x)	KCl KH_2PO_4 Na_2HPO_4 NaCl in ultrapure water	27 mM 18 mM 100 mM 1.37 M
RIPA buffer	NaCl NP-40 Tris-HCl (pH 7,4) Sodium deoxycholate SDS Protease-/Phosphatase-Inhibitor-Cocktail	25 mM 1% 150mM 1% 0.1% 1%
Running buffer (10x)	Glycine SDS Tris in ultrapure water, pH 8.3	1.92 M 1% (w/v) 0.25 M
SDS solution	SDS in ultrapure water	10% (w/v)
Separation buffer	Tris in ultrapure water, pH 8.8	3 M
Stacking buffer	Tris in ultrapure water, pH 6.8	0.47 M
Stripping buffer	Glycine SDS Tween 20 in ultrapure water, pH 2.2	0.2 M 0.1% (w/v) 1% (v/v)
TBS (10x)	NaCl Tris in ultrapure water, pH 7.4	1.5 M 0.5 M
TBS-T	TBS (10x) Tween20	10% (v/v) 0.1% (v/v)

Table 2.9: **Prepared buffers for Immunocytochemistry**

Buffer	**Compounds**	**Concentration**
Blocking solution	BSA Tween 20 in ultrapure water	3% 0.3%
Staining solution	BSA Tween 20 in ultrapure water	0.3% 3%

Table 2.10: **Prepared buffers for Immunohistochemistry**

Buffer	**Compounds**	**Concentration**
Blocking solution	BSA Tween 80 in ultrapure water	3% 3%
Citrate buffer	Citric acid monohydrate in ultrapure water, pH adjusted to 6	0.01 M

Buffer	Compounds	Concentration
Haematoxylin	Mayer's haemalaun in ultrapure water	20% (v/v)
Staining solution	BSA Tween 80 in ultrapure water	0.3% 3%
TBS (1x)	TBS (10x) In Ultrapure water	10% 90%

Table 2.11: **Prepared buffers for perfusion**

Buffer	Compounds	Amount
Collagenase buffer	Amino acid solution CaCl2 solution (19 g/l CaCl2* 2 H2O) Collagenase Type 1 Glucose solution (9 g/l) Glutamine (7 g/ml) HEPES (60 g/l) (pH 8.5) KH buffer	30 ml 10 ml 100 mg 155 ml 2.5 ml 25 ml 25 ml
EGTA buffer	Amino acid solution EGTA solution (47.5 g/l) Glucose solution (9 g/l) Glutamine (7 g/l) HEPES (60 g/l) (pH 8.5) KH Buffer	60 ml 1.6 ml 248 ml 4 ml 30 ml 30 ml
KH buffer	KCl KH_2PO_4 NaCl Filled to 1 l with ultrapure water Adjusted pH to 7.4	1.75 g 1.6 g 60 g
Suspension buffer	Albumin Fraction V Amino acid solution CaCl2 solution (19 g/l CaCl2* 2 H2O) Glucose solution (9 g/l) Glutamine (7 g/ml) HEPES (60 g/l) (pH 7.6) KH buffer MgSO4 solution (24.6 g/l MgSO4 * 7 H_2O)	400 mg 30 ml 1.6ml 124 ml 2 ml 20 ml 20 ml 0.8 ml

Table 2.12: **Prepared buffers for cell culture assays**

Buffer	Compounds	Concentration
Crystal violet solution	Methanol/Ultrapure water Crystal violet	80%/20% 0.5%

2.1.8 Plasmids

For additional information, the sequence of all custom designed or In house modified plasmids is listed in the supplementary data (Section 6.1). All plasmids were sequenced by Seqlab (Göttingen).

Table 2.13: **Custom designed plasmids**

Custom designed plasmids		
Plasmids	**Promotor**	**Company**
EDI3-turboRFP [amp/kan]	CAG	Vector builder
EDI3-3xHA [amp]	CMV	Vector builder
STBD1-3xFLAG-GFP [amp]	CMV	Vector builder
EDI3-GFP [amp]	CMV	AMSbio
CMV-Neo (empty vector) [amp]	CMV	

Table 2.14**: In house modified plasmids**

Plasmids	**Backbone**	**Oligonucleotides**
EDI3-W32A-3xHA	EDI3-3xHA	Infusion 46/57
EDI3- ΔCBM20-3xHA	EDI3-3xHA	KLD1/KLD2

2.1.9 Small interfering RNA (siRNA)

Table 2.15: **Small interfering RNA using the Stealth siRNA Transfections-Kit**

Target	**Assay ID**	**Company**
EDI3 Oligo B	HSS125510	Thermo Fisher Scientific
EDI3 Oligo C	HSS183474	Thermo Fisher Scientific
siRNA Negative Control for Lo GC	#12935-200	Thermo Fisher Scientific

2.1.10 Oligonucleotides

All oligonucleotides for cloning were ordered from Sigma-Aldrich.

Table 2.16: **Oligonucleotides for cloning**

Name	**Sequence**
Infusion 46	GTTTCCCAAAGCATCACA
Infusion 57	TGTGATGCTTTGGGAAACGCGAATCCTCAAAATGCT
KLD1	AGGTGTCATGGTGGCAGC
KLD2	ACATGTCAGACTGAAATAAGATTACGTTTG

All Taqman assays were purchased from Thermo Fisher Scientific.

Table 2.17: **Taqman gene expression assays**

Target gene	**Mouse**	**Human**
GPCPD1	Mm01333971_m1	Hs00325631_m1
GAPDH	4352932E	4352934E
EIF2A	Mm01289723	Hs00201903_m1
PCK1	Mm01247058_m1	Hs00159918_m1

All used QuantiTect Primer Assays were purchased from Qiagen.

Table 2.18: **QuantiTect Primer Assays**

Target gene	QT code	Target species
GPCPD1	QT00066598	Human
GAPDH	QT01192646	Human
ACTB	QT00095431	Human

2.1.11 Bacteria

Table 2.19: **Bacteria**

NEB 5-alpha Competent *E. coli*	Strain of bacteria used to amplify plasmids; Genotype: *fhuA2 Δ(argF-lacZ)U169 phoA glnV44 Φ80 Δ(lacZ)M15 gyrA96 recA1 relA1 endA1 thi-1 hsdR17* Source: New England BioLabs GmbH, Frankfurt am Main, Germany

2.1.12 Secondary cell lines

Table 2.20: **Secondary cell lines**

BT-474	The BT-474 line was isolated from a solid, invasive ductal carcinoma of the breast from a 60 years adult Caucasian female (Lasfargues et al. 1978).
HCC1954	HCC1954 was derived from a primary stage IIA, grade 3 invasive ductal carcinoma with no lymph node metastases originating in a 61-year-old East Indian woman (Gazdar et al. 1998). These cells were used as a second cell line with high EDI3 expression.
HEK293T	Human embryonic kidney 293 cells derived from human embryonic kidney cells grown in tissue culture that expresses a mutant version of the SV40 large T antigen (DuBridge et al. 1987). It is mainly used for protein expression and generation of recombinant retroviruses.
MCF-7	The slowly metastasizing MCF7 cell line is the most studied human breast cancer cell line worldwide and was derived from the pleural effusion of a 69 year old nun suffering from a breast adenocarcinoma. It was named after the Michigan Cancer Foundation (MCF) (Soule et al. 1973).
SkBr3	This cell line was isolated by scientists at the Memorial Sloan–Kettering Cancer Center in 1970 and was derived from a pleural effusion of an adenocarcinoma originating in a 43-year-old Caucasian female (Fogh et al. 1977). It is often used if HER2 signalling needs to be targeted.
T47D	This cell line was isolated from a pleural effusion obtained from a 54 year old female patient with an infiltrating ductal carcinoma of the breast (Horwitz et al. 1982). It is commonly used as an alternative to MCF7 cells.
Cell lines created in the Leibniz Research Centre for Working Environment (IfADo)	
HCC1954_ shEDI3	A HCC1954_Luciferase positive cell line, with tetracycline–inducible silencing of *EDI3.* Addition of doxycycline leads to generation of EDI3 hairpin sequence, as well as the transcription of RFP. Created by *Annika Glotzbach*
HeLa_EDI3	Hela cell line that stably overexpresses human EDI3. Created by *Michaela Lesjak* and *Moritz Anft*

Cell lines used were authenticated by the Leibniz institute DSMZ-German Collection of Microorganisms and Cell Cultures.

2.1.13 Cell culture reagents

Table 2.21: **Cell culture reagents**

Primary cell culture		
Cells/cell lines	**Medium**	**Company**
Primary mouse hepatocytes/ Primary human hepatocytes	500 ml Williams E +20 µl Dexamethasone (0.04%) (Glucocorticoid, anti-inflammatory) +0.5 ml Gentamicin (0.1%) (antibiotic) +5 ml L-Glutamine (1%) (Nutrition enhancer) +5 ml Pen/Strep (1%) (antibiotic) (+50 ml Sera plus (10%) for attaching)	PAN Biotech Sigma Aldrich PAN Biotech PAN Biotech PAN Biotech PAN Biotech
Secondary cell culture		
Cells/cell lines	**Medium**	**Company**
BT474	500 ml DMEM/ F12 +50 ml Sera plus (10%)	PAN Biotech PAN Biotech
HCC1954	500 ml RPMI +50 ml Fetal Bovine Serum (10%) +5 ml Sodium Pyruvate (1%)	PAN Biotech
HEK293T	500 ml DMEM +50 ml Sera plus (10%)	PAN Biotech PAN Biotech
MCF7	500 ml DMEM +0.5 µl Insulin (If not stated otherwise) +0.5 ml Non-essential Amino acids (0,1%) +50 ml Sera plus (10%) +5 ml Sodium Pyruvate (1%)	PAN Biotech Sigma-Aldrich PAN Biotech PAN Biotech PAN Biotech
SkBr3	500 ml DMEM +50 ml Fetal Bovine Serum (10%)	PAN Biotech Gibco
T47D	500 ml DMEM/ F12 +50 ml Sera plus (10%)	PAN Biotech PAN Biotech

2.1.14 Antibodies

Table 2.22: **Antibodies**

Primary Antibodies			
Antibody	**Host**	**Application**	**Company/ Cat#**
Anti β-actin	Mouse	WB	Sigma Aldrich, A5316
Anti-EDI3 Clone 3B8G3	Mouse	WB, IHC	AMSBio, Custom made
Anti EDI3 #28	Rabbit	WB	Pineda, custom made
Anti-HA-Tag	Mouse	IP, WB	Abcam, ab18181
Anti-AKT	Rabbit	WB	CST, #9272
Anti-pAKT (S473)	Rabbit	WB	CST #9271
Anti CREB	Rabbit	WB	CST #4820
Anti-pCREB	Rabbit	WB	Abcam, ab32096
Anti-ERK 1 /2	Rabbit	WB	CST #9102
Anti Glycogen-Snythase 1	Rabbit	WB, IHC	Abcam, ab40810
Anti-FLAG tag	Mouse	WB, IP	Sigma Aldrich, F3165
Anti Myosin II	Mouse	IHC	Proteintech, 66212-1-Ig
Anti-Myosin VII	Mouse	IHC	Sigma-Aldrich, M8421
Anti-RYR1	Rabbit	IHC	Thermo Fisher PA5-84288
Anti-STBD1	Rabbit	IHC	Thermo Fisher, PA5-52884

Secondary Antibodies			
Antibody	**Host**	**Application**	**Company/ Cat#**
Anti-mouse HRP linked	Horse	WB	CST, #7076
Anti-rabbit HRP linked	Goat	WB	CST, #7074
Alexa Fluor® 488 AffiniPure Donkey IgG (H+L)	Rabbit	IHC	Jackson Immuno Research
Alexa Fluor® 647 AffiniPure Donkey IgG (H+L)	Mouse	IHC	Jackson Immuno Research

2.2 Methods

Molecular biological methods

2.2.1.1 Bacterial Transformation

Large quantities of DNA were initially prepared for each available plasmid. Competent cells (NEB 5-alpha Competent E. coli), normally stored at -80°C, were slowly thawed on ice. Agar plates, containing the appropriate antibiotic needed for the respective plasmid were pre-warmed to 37°C before usage in an incubator. 100-200 ng plasmid DNA were added to one vial (50 µl) of NEB 5-alpha competent E. coli and gently mixed by flicking the tube, and the resulting cell/DNA mixture was incubated on ice for 30 min. In this thesis, the heat shock method was used for transformation. Therefore, the cell/DNA mixture was heated for 45 sec at 42°C on a heat block and then directly placed on ice for 2 min. 950 µl Super Optimal Broth cum glucose (SOC) media (without antibiotic) was then added to the transformed bacteria, and the vial was incubated in a 37°C shaking incubator for 45 min. Next, 200 µl of the transformed cells containing SOC media was added to the agar plate, distributed with a cell spreader and incubated overnight at 37°C. The plates were observed the next day for the presence of single colonies.

2.2.1.2 Creating Bacterial Glycerol Stocks

Glycerol stocks of bacterial liquid cultures were prepared for long term storage of plasmids. After overnight incubation, 0.5 ml liquid bacterial cultures were combined with 0.25 ml glycerol (100%) in 2 ml screw-cap tubes, which were inverted 5 times, and stored at -80°C.

2.2.1.3 Plasmid purification (Miniprep Scale)

Lysogeny broth (LB)-media (2 ml), containing antibiotic (dependent on plasmid), was inoculated with single-bacterial colonies from LB-agar plates, and incubated overnight at 37°C in a shaking incubator at 200 round per minute (rpm). Isolation of plasmid DNA was performed using Qiagen's Plasmid Mini Kit, according to the manufacturers' instructions. In short, after overnight incubation bacterial-cells were pelleted via centrifugation, resuspended, lysed, and then neutralized. The lysate was passed through a column, to which the DNA bound. The

column was then washed, and the DNA eluted in DNase/RNase free H_2O. The concentration of the obtained plasmid was measured using a Nano Drop 2000 (Thermo Scientific).

2.2.1.4 Plasmid purification (Maxiprep Scale)

To generate larger quantity of plasmid DNA, the NucleoBond® Xtra Maxi kit (Machery-Nagel) was used. A "pre-culture" was established by inoculating 2 ml LB-media, containing an appropriate antibiotic with single-bacteria colonies from LB-agar plates or with 30 µl bacterial glycerol stock (2.2.1.2) and incubated at 37°C for 6-8 h at 200 rpm. For the "main culture", 250 ml LB-media with an appropriate amount of antibiotic were inoculated with 300 µl of the pre-culture and incubated overnight at 37°C at 180 rpm.isolation was conducted according to manufacturers' instructions. The concentration of the plasmid was measured using a Nano Drop 2000 (Thermo Scientific).

2.2.1.5 Agarose gel electrophoresis

DNA was separated using agarose gel electrophoresis, with gel concentrations ranging from 1%-2% agarose (w/v) according to DNA fragment size to be detected. To prepare the gel, agarose was dissolved in 100 ml TAE (1x) and heated for 4 min to a gentle boil. Ethidium bromide (0.01%) was then added under a chemical hood once the agarose stopped boiling and the agarose temperature decreased to approximately 55^{o}C. Next, the agarose solution was added to a prepared gel casting tray and left to polymerize. The DNA samples were mixed with double distilled H_2O and DNA Gel Loading Dye (6X) (New England Biolabs), prior to being loaded onto the gel, which was immersed in the running chamber in 1xTAE buffer. 3 µl of the GeneRuler 1 kb Plus DNA Ladder was also loaded onto the gel, which was run at a constantly applied current of 120 mA for 30 min. The bands were visualized using UV-light with the Box VX5 imager (Vilber).

2.2.1.6 PCR and DNA amplification

For the PCR-reaction, template DNA (1-10 ng) was added to a master mix containing 0, 25 µl (0,31 Units) PrimeSTAR GXL DNA Polymerase (Takara), 1 µl (50 µM) nucleotides (dNTPs) and 1 µL (0.3 µM) from each oligonucleotides (custom designed and ordered from Sigma) added to a volume of 10 µL with double distilled H_2O.

The PCR-Reaction was performed in a thermocycler (Biometra) using the following protocol for 30-40 times:

(I) Denaturation step at 98°C were the hydrogen bonds between the DNA-bases are melting

(II) Annealing step at 55-60°C (according to the primer set), were the primers bind to the single nucleotide template strand

(III) Extension step at 68-72°C, where the polymerase binds to the DNA single strand and synthesizes the new DNA strand.

2.2.1.7 Gibson Assembly® Method

After the successful amplification of the desired DNA-fragment, an enzymatic digest was performed using 5 Units (U) of DpnI (New England Biolabs) in the recommended buffer for 1-3 h. DpnI only digests methylated DNA; therefore, only the template DNA, and not the PCR product is rendered useless. After the digest, the Gibson Assembly® Master Mix (2.5 µl) was used to ligate the different fragments. For this reaction, the concentration of the inserted fragment (100-200 ng) should be two- or three times higher than the backbone fragment (50-100 ng). The ligation mixture was then diluted with DEPC-treated water to a total volume of 5 µl, and the samples left to ligate for 15-60 min at 50°C. During the ligation reaction, NEB 5-alpha Competent *E. coli* bacteria were thawed on ice, and after the 15-60 min incubation period, 2 µl of the ligated plasmid were added to the bacteria. The plasmid-containing bacteria mixture was stored on ice for 30 min, followed by a heat shock reaction, where the bacterial cells were incubated at 42°C for 0.5 min and then immediately placed on ice for 2 min. After the heat shock, 950 µl SOC media was added and the cells incubated in a heat block for 1 h at 37°C. After the incubation period, 200 µl of the cells were transferred to agar plates containing the appropriate antibiotic and incubated at 37°C overnight.

2.2.1.8 DNA digestion by restriction enzymes

The restriction enzyme digest was performed to evaluate the success of the cloning strategy. After plasmid purification (2.2.1.3), the isolated DNA was cleaved using of specific restriction endonucleases. The restriction sites were chosen so that the cleavage pattern from the desired plasmid differs from that of the input plasmid. For the restriction reaction, 200 ng of DNA and 5 U of matching restriction enzymes and corresponding buffer were diluted in DEPC-treated water to a total volume of 10 µl. The mixture was incubated at 37°C for 1-2 h. Once the incubation period was over, DNA Gel Loading Dye (3 µl) was added to all samples, which were then separated by agarose gel electrophoresis (2.2.1.5), and the DNA cleavage products visualized using UV-light with the Box VX5 imager (Vilber). If the size of the DNA bands reflected the correct cleavage pattern, the plasmid DNA was sequenced (Seqlab) as a further validation step.

Cell biological methods

2.2.2 Primary cell culture

Primary cells differ from secondary cell cultures because they are isolated directly from tissue. In this work primary mouse hepatocytes were used.

2.2.2.1 Isolation of Mouse hepatocytes

The method for the isolation of primary hepatocytes from a mouse liver was based on a two-step perfusion (Seglen 1976).

2.2.2.2 Human hepatocytes

Primary human hepatocytes were ordered from Lonza and stored at -196°C until they were used for experiments. Details of the specific donors are included in the supplementary data.

2.2.2.3 Cultivation of primary hepatocytes

Primary hepatocytes from male C57BL6 mice were cultured under sterile conditions and maintained in a humidified incubator at 37°C and 5% CO_2. For the following experiments, two different types of collagen coating were used. For the first so-called 'sandwich culture', collagen was added to the well of a 6 well plate to produce a thin later and left to air dry overnight or at 37 degrees for 1 h. Once dried, hepatocytes were seeded followed by the addition of a top layer of collagen which formed a thick layer on top of the cells (bilayer). In the second 'monolayer' culture, plates were only coated with the thin collagen layer on the bottom, but the thick layer on top was omitted (monolayer). To produce the collagen for the bilayer, 10 mg rat tail collagen was dissolved in 40 ml 0.2% acetic acid for the coating or in 9 ml for the thick layer at 4°C overnight to generate a 250 µg/ml and 1.1 mg/ml collagen solution, respectively. Ideally, the cell culture dishes that are needed for the experiment were rinsed with 250 µg/ml collagen solution and left to dry overnight in the lamina flow, otherwise the cell culture dishes can be rinsed with the same solution and incubate in the incubator for 1 h. Before cells were pipetted, the monolayer was washed three times with William's E medium without supplements to adjust the pH and remove loose collagen.

The cells were diluted in William's E medium containing all supplements and 10% sera plus FBS (table 2.21). The cells were evenly distributed by gently shaking the plate, which was then placed in the incubator for 3 h to attach to the well plate. After the incubation period, the thick collagen layer was prepared on ice by mixing 1 ml (10%) of 10x DMEM (PAN) to 9 ml 1.1 mg/ml collagen solution for a concentration of 1 mg/ml collagen. The neutralisation of the

solution was done by adding 400 µl 1 M NaOH, which was detected via a colour change from yellow to fuchsia. The attached hepatocytes were carefully washed with warm William's E medium to remove dead and non-attached cells before being covered with the thick collagen layer. The second layer was added according to table 2.23 and polymerised within 45 min. After successful polymerisation, William's E medium with supplements was added to the cells. In case of monolayer preparation, the hepatocytes were handled as described above but after the attachment time, the cells were washed and then incubated in William's E medium with supplements overnight.

Table 2.23: **Conditions for primary hepatocytes cultivation**

Well size	**Cell number**	**1 mg/ml collagen**	**William's E medium & supplements**
6-well plate	950000 cells/well	350 µl	2 ml
12-well plate	400000 cells/well	200 µl	1 ml
24-well plate	200000 cells/well	100 µl	0.5 ml

2.2.3 Secondary cell culture

2.2.3.1 Freezing of secondary cell lines

Cell lines can be stored for longer periods in liquid nitrogen since they remain dormant under these conditions (Lindl and Gstraunthaler 2008). For storage, medium was removed from cells with a confluency of around 70%, rinsed once with 1x PBS prior to the addition of 0.05% trypsin with 1 mM EDTA (Pan Biotech). After 5-10 min incubation at 37°C, cells were transferred into 10 ml fresh medium and cells were pelleted at 800x g. Next, the supernatant was removed and the cell pellet was resuspended in an appropriate volume of sera plus containing media and counted. In total 1-2 million cells were diluted in 900 µl media and 5-10% DMSO was added to avoid ice crystal formation. Next, 1 ml aliquots were filled into cryo-vials, placed in a freezing container and stored at -80 °C overnight in a freezing container filled with 2-propanol (such as Mr. Frosty (VWR)), which facilitates a consistent cooling rate. Cells are then placed in the gaseous phase of the liquid nitrogen storage tank on the following day.

2.2.3.2 Maintenance of secondary cell culture

All cell lines were cultured in an incubator at 37°C, 5% CO_2 in an aqueous saturated vapour. All conducted work was performed under a sterile hood using aseptic reagents and technique. No antibiotic was used in the cell culture media.

Cells were sub-cultivated once they reached a confluency of 80% with media changes every two to three days. Cells were rinsed once with 1x PBS prior to addition of 0.05% trypsin/1 mM EDTA (Pan Biotech). After 5-10 min incubation at 37°C, cells were transferred into 10 ml fresh medium and pelleted at 800 g. The cell pellet was re-suspended in fresh medium, cell number was determined using a CASY counter and cells were added to a new cell culture dish or flask at the desired density.

2.2.3.3 Downregulation of gene expression in secondary cell lines

One way to study protein function in a wide range of cell types is to knock down gene expression using RNA interference using 21-mer oligonucleotides short/small interfering RNAs (siRNAs), which transiently decrease the expression of a specific target genes. Complementary binding of siRNA to its target messenger RNA (mRNA), results in degradation of the mRNA, thus preventing translation of the mRNA and finally protein production.

The following protocol was adapted from: "Invitrogen's Stealth/siRNA Transfection Protocol" The gene expression of *EDI3* was downregulated using specific validated siRNAs (table 2.15) in the cells of interest using the reverse transfection method. 500 µl OptiMEM was added per well of a six well dish, to which 20 nmol siRNA was added, followed by 5 µl Lipofectamine RNAiMAX to form transfection complexes. After 20 min incubation time, the cells (for MCF7 400,000 cells) were added to each well, the contents gently mixed by tilting the plate back and forth, and the plate incubated at 37 °C and 5% CO_2 for three days. Gene knockdown efficiency was verified at the RNA and protein level using quantitative real time PCR and western blotting, respectively. In the case of the HCC1954_ shEDI3 cells, the shRNA sequence targeting *EDI3* was already integrated in the cells. The gene knockdown regulation was induced three days before treatment by the addition of 0.5 µg Tetracycline to the medium.

2.2.3.4 Transient transfection of cells via PEI transfection reagent

Cells were transfected with plasmid DNA using two different methods. In the first method, DNA is introduced into the host cell using polyethylenimine (PEI), a cationic polymer. PEI condenses DNA into positively charged particles that bind to the anionic cell surface, and this DNA-PEI complex is endocytosed by the cells and the DNA eventually released into the cytoplasm. For transfection, cells were plated one or two days before the transfection at a density which resulted in at least 60% confluency on transfection day (table 2.24). At first OptiMEM was pipetted into reaction tubes, then DNA and PEI were added in a ratio 1:6 (DNA: PEI). The tube was then vortexed to mix contents, and incubated at room temperature for

17-20 minutes. The plated cells were washed with 1x PBS and the DNA-PEI mixture was added dropwise onto the cells. The cells were incubated for 4 h at 37°C with 5% CO_2. After incubation, the DNA-PEI mix was removed and replaced by the respective amount (table 2.24) of appropriate medium. After 16-72 h, transfection efficiency was observed under a microscope for fluorescence (if a fluorophore was present in the plasmid), or the protein extracted for western blot analysis.

Table 2.24: **Conditions for PEI transfection**

Cell Culture Plate	Cellular Density	DNA/PEI conc.	+ /- DMEM/+/+DMEM
10 cm	3* 10^6	12 µg/72 µg	3 ml/10ml
6-well plate	4* 10^5	4 µg/24 µg	1 ml/3 ml
24-well plate	1* 10^4	1 µg/6 µg	0,.3 ml/1 ml

2.2.3.5 Transient transfection via Lipofectamine 3000

In addition to the PEI transfection method, commercially available transfection reagent, Lipofectamine 3000 (Thermo Scientific) was used according to manufacturers' recommendation. For a six-well dish, OptiMEM (125 µl) was combined with DNA (2.5 µg) and a P3000 reagent, (5 µl), which increases the transfection efficiency and incubated for 5 min in the first tube. In a separate tube, Lipofectamine 3000 (10-15 µl) was diluted in 125 µl OptiMEM. After the 5 min the two fractions were combined and vortexed, and incubated at room temperature for 10 min to form the DNA-Lipofectamine complexes. Finally the mixture was added to cells that were around 70% confluent, and left in the incubator overnight. Media was changed the next day.

2.2.4 Gene expression analysis

2.2.4.1 RNA isolation via QIAzol Lysis-Reagent

RNA from hepatocytes were isolated via QIAzol reagent (Qiagen). QIAzol consists of guanidinium thiocyanate and phenol, which lyses cells and inhibits RNases (Chomczynski and Sacchi 1987). For RNA extraction, culture dishes were placed on ice, then the cells wash once in William's E medium, the supernatant was aspirated, and the cells lysed in QIAzol (1 ml QIAzol per 6-well, 0.5 ml QIAzol per 12-well). After scraping, the cell lysates were transferred to RNAse free-reaction tubes and sonicated on ice (50% power, 30 s, 5 s pulse, 2 s break). Samples were then either stored at -80°C or the RNA-extraction procedure performed. For extraction, 200 µL chloroform were added to each reaction tube. The samples were shaken

thoroughly for 1 min, then, to improve the phase separation, incubated for 5 min at RT and subsequently centrifuged at 12000 g and 4°C for 15 min. The upper aqueous RNA containing phase was transferred to a reaction tube containing 500 µL 2-propanol to precipitate the RNA. After 10 min incubation at RT, a 15 min centrifugation step at 12000 g and 4°C followed. The RNA pellet was washed thrice with each time 850 µL: first, 100%, second with 80% and third with 70% ethanol. After each washing step, the samples were centrifuged for 5 min at 4°C and 10000 g to sediment the RNA. The supernatant was completely removed and the RNA pellet was air-dried for 5 min. The RNA pellet was dissolved in 15-30 µL DEPC-treated water. The yield of the RNA was photometric determined with the Nanodrop2000 (Thermo Fisher Scientific). RNA samples were stored at – 80 °C until further analysis.

2.2.4.2 RNA isolation via RNeasy-Kit

Another method used to collect and isolate RNA was with the RNeasy kit (Qiagen). Briefly, 600 µl RLT lysis buffer was added to the well of a 6 well plate, cells scraped and added to 1.5 ml tubes. Cell suspensions were vortexed for 30 sec and either stored at -80 degrees or placed in a column and centrifuged for two minutes at 13,000 g. Total RNA from homogenized cell lysates was precipitated with 70% ethanol, isolated and purified using RNeasy mini kit and RNase-Free-DNase kit (Qiagen), following manufacturer's instructions.

2.2.4.3 cDNA Synthesis

Since the isolated RNA is analysed in a two-step real-time polymerase chain reaction (RT-PCR) for gene expression, it is beneficial to generate cyclic DNA (cDNA), which is less fragile than RNA. The conversion to cDNA was conducted using the high capacity cDNA reverse transcription kit (Applied Biosystems) following manufacturer's instructions. RNA concentration was equalized to 2 µg with DEPC water and mixed with appropriate volumes of 10x RT-Buffer, 10x random primers, 25x dNTP mix and reverse transcriptase. The total volume of this reaction mix was adjusted to 20 µL with DEPC water. Following the recommended program in the Thermo cycler (Biometra) was used (table 2.25).

Table 2.25: **Conditions for cDNA synthesis**

Converting step	**Temperature**	**Time**
Incubation	25 °C	10 min
Reverse transcription	37 °C	120 min
Inactivation	85 °C	5 min
4 °C	Pause	

After the PCR reaction, the samples were diluted to a final concentration of 10 ng/µl (1:10) in DEPC-treated water.

2.2.4.4 Real-time PCR

Quantitative real time PCR is a technique used to detect and quantify expression of a target gene. The roots of this method are based in the conventional PCR as described in 2.2.1.6, but the amplified PCR product is continuously (in real-time) measured via certain fluorescent signals whose intensity correlates the produced DNA (Higuchi et al. 1993; Navarro et al. 2015).

In this thesis, two fluorescence indicators, a DNA intercalating dye SYBR green (QuantiFast® SYBR Green PCR Kit from Qiagen) and TaqMan primers (Thermo Fisher Scientific) were used. SYBR green binds all newly synthesized DNA complexes and fluoresces. The fluorescence accumulates as the cycles of the PCR continues and is measured after each PCR cycle. The intensity of fluorescence above a threshold value (CT) is measured and used to quantify the newly generated double stranded DNA. In the TaqMan assay, the fluorescence signal is harboured in the applied primer pair, which carries a fluorescent reporter on the 5'-end and a quencher on the 3'-end. Kept in close proximity, the quencher suppresses the fluorescent signal due to fluorescence resonance energy transfer (FRET). During the PCR reaction, the fluorescent reporter and quencher are spatially separated and thus the fluorescent signal can be detected which is proportional to the amplified DNA concentration, and the intensity above the threshold level (CT) can be used to quantify the newly synthesized DNA.

To observe the expression of different genes, a 7500 Real-Time PCR System (Applied Biosystems) was used and all measurements, including a negative control were water was used instead of cDNA, were at least performed in technical duplicates. For a TaqMan approach (table 2.26) 50 ng cDNA was mixed with 2x universal mastermix and 20x specific TaqMan probe. For SYBR green (table 2.27) 50 ng cDNA, 12.5 µl QuantiFast® SYBR Green and 2.5 µl primermix were added. The total volume per reaction in both approaches was adjusted to 25 µL with DEPC water.

Table 2.26**: Program for TaqMan Assays**

Standard amplification Setup	**Temperature**	**Time [min]**	**Cycles/Repetitions**
Activation of DNA polymerase	50°C	2:00	1
	95°C	10:00	1
DNA denaturation	95°C	0:15	40
Annealing and Elongation	60°C	1:00	

Table 2.27: **Program for SYBR Green Assays**

Standard amplification Setup	**Temperature**	**Time [min]**	**Cycles/Repetitions**
Activation of DNA polymerase	50°C	2:00	1
	95°C	5:00	1
DNA denaturation	94°C	0:10	40
Annealing and Elongation	60°C	0:30	

To determine relative expression change, the "$2^{(-\Delta\Delta CT)}$ method" based on the publication from Livak and Schmittgen was used (Livak and Schmittgen 2001). In this method, the CT values for the gene of interest (GOI) were subtracted from a housekeeping gene (HKG), which are endogenous control genes whose expression is stable, that is, remains unaltered with treatment. In this project, *GAPDH*, *EIF2A* and *ACTB* were used as housekeeping genes ($\Delta Ct = Ct_{(GOI)} - Ct_{(HKG)}$). To calculate the ΔΔCT values, the ΔCT for the GOI is normalized, to an untreated sample (FM or vector control). In order to see the differences between the samples, the calculation $2^{-\Delta\Delta CT}$ was applied. Values greater than 1 show a gen upregulation, values smaller than 1 indicate a downregulation.

$$\Delta CT = CT_{(GOI)} - CT_{(HKG)}$$

$$\Delta\Delta CT = \Delta CT_{(treated)} - \Delta CT_{(untreated)}$$

$$\text{Relative Expression} = 2^{(-\Delta\Delta CT)}$$

2.2.5 Protein Analysis

2.2.5.1 Lysis of eukaryotic cells

Cells were washed once with ice-cold 1x PBS and then lysed with ice cold RIPA-buffer (table 2.28) containing protease and phosphatase inhibitors and incubated for 5 min.

Table 2.28: **Conditions for cell lysis with RIPA buffer**

Dish	**12-well**	**6-well**	**10 cm**
RIPA buffer [ml]	0.1	0.1	0.1

With a cell scraper, cells were detached from the plate and then transferred to a precooled 1.5 ml tube. Next, the cells were vortexed constantly for 1 min. Cell debris were pelleted by centrifugation at 20,000 g and 4°C for 15 min and the supernatant was transferred to a fresh 1.5 ml tube. Until further usage, lysates were stored at -80°C.

2.2.5.2 Determination of protein concentration

The pierce bicinchoninic acid (BCA) Protein Assay Kit from Thermo Fisher Scientific was used to estimate the protein content of the lysates in two steps. The first involved the reduction of Cu^{2+} to Cu^{+} by peptide bonds under alkaline conditions and for the second, the sensitive colorimetric detection of Cu^{+} with BCA was used. The Cu^{+}-molecule (complexed with the protein) chelates with two BCA molecules and leads to increased absorbance at 562 nm that is proportional to the protein concentration.

A standard of bovine serum albumin (BSA), ranging from 0 µg/ml to 2000 µg/ml, was prepared in triplicate. Protein lysates were also pipetted in triplicates into 96-well plates and diluted 1:5 in H_2O. Next, 196 µL BCA working reagent, consisting of 49 parts of solution A and 1 part of solution B were added to each well. The plate was incubated for 30 min at 37 °C before the absorbance at 562 nm was measured in a plate reader (Infinite M200 Pro, Tecan). The protein concentrations of the samples were calculated based on the standard curve.

2.2.5.3 SDS polyacrylamide gel electrophoresis

Proteins were resolved according to their molecular weight via SDS polyacrylamide gel electrophoresis (SDS-PAGE; Miniprotean; Bio-Rad). Therefore, equal amounts of protein samples were diluted in 5x Lämmli-buffer, denatured at 95°C for 5 min, briefly centrifuged and loaded onto a prepared gel, including the separation gel (8-14%, Tris, pH 8.8) and a stacking gel (5%, Tris, pH 6,8) in a chamber filled with 1xTris/Glycin/SDS Buffer (Bio-Rad). To monitor the gel electrophoresis, 3 µl of Precision Plus Protein™ Dual Colour Standards (Bio-Rad) was

added in one lane of the SDS-PAGE. Proteins were separated by applying a constant electric field at 25 mA per Gel.

2.2.5.4 Protein transfer to nitrocellulose membrane

Semi-dry transfer was performed using the Trans-Blot® SD Semi-Dry Transfer Cell® (Bio-Rad). Subsequent to the SDS-PAGE, gels were removed from the glass plates and equilibrated in cathode buffer. Whatman™ paper were cut into 8.5 X 6 cm pieces (16 in total) and soaked in anode buffer (12 pieces) or cathode buffer (4 pieces). The PVDF membrane was permeabilized in methanol and then placed in anode buffer. For the transfer, a sandwich was prepared as follows: 12x Whatman™Paper (from anode buffer), PVDF membrane, gel, and 4x Whatman™Paper (cathode buffer). An electric field of 0.23 A per gel (5 mA/cm²) was generated leading to migration of the negatively charged proteins towards the membrane where they were bound.

To identify the success rate of transfer, membranes were stained with Ponceau red solution for 30 sec and then extensively washed in water until the protein bands were well defined. TBS-T was used to completely destain the membrane again prior to the blotting steps described below.

2.2.5.5 Immunoblot

Proteins of interest were identified by specific antibodies via an indirect enzymatic reaction. Since all proteins from the cell lysate bind the PVDF-membrane, the membrane was incubated in blocking solution, either 5% milk-powder (w/v) or 5% BSA (w/v) in TBS-T for 2 h at room temperature on a benchtop shaker to prevent unspecific background binding. The membrane was rinsed with TBS-T prior to incubation with primary antibodies, which were diluted in blocking solution according to manufacturers' recommendation (table 2.29). Membranes were incubated over night with shaking at 4°C. Thereafter, the membrane was washed three times in TBS-T while agitating, 5 minutes per wash, to remove residual primary antibody. Incubation with an appropriate secondary antibody followed for one hour at room temperature. All secondary antibodies were conjugated to horseradish peroxidase, thus allowing protein detection via bioluminescence with the Vilber Fusion Fx7 (Vilber, Lourmat). For this purpose, the membrane was covered with enhanced chemiluminescence solution (ECL) plus 0.06% H_2O_2. Densitometric analysis was performed using the software ImageJ. In case further protein detection was needed on the same membrane (for loading control), the antibodies were removed from the membrane by incubating the membranes with a stripping

buffer for 45 min and subsequent washing in TBS-T, blocking and incubation with the primary antibody.

Table 2.29 **Parameters for antibody incubation (Western blotting),** *Abbreviations*: ON, overnight; RT room temperature

Primary antibody	Secondary antibody	Dilution	Incubation
Anti β-actin	Mouse	1:1000/1:5000 BSA	ON 4°C/ 1.5 h RT
Anti-EDI3 Clone 3B8G3	Mouse	1:1000/1:5000 milk	ON 4°C/ 1.5 h RT
Anti EDI3 #28	Rabbit	1:1000/1:5000 milk	ON 4°C/ 1.5 h RT
Anti-HA-Tag	Mouse	1:1000/1:5000 milk	ON 4°C/ 1.5 h RT
Anti-AKT	Rabbit	1:1000/1:5000 BSA	ON 4°C/ 1.5 h RT
Anti-pAKT (S473)	Rabbit	1:1000/1:5000 BSA	ON 4°C/ 1.5 h RT
Anti CREB	Rabbit	1:1000/1:5000 BSA	ON 4°C/ 1.5 h RT
Anti-pCREB	Rabbit	1:1000/1:5000 BSA	ON 4°C/ 1.5 h RT
Anti-ERK 1 /2	Rabbit	1:1000/1:5000 BSA	ON 4°C/ 1.5 h RT

2.2.5.6 EDI3 Activity Assay

This enzymatic activity, which was adapted from the Amplex® Red phospholipase D Assay Kit (Invitrogen), is used to indirectly measure the enzymatic activity of EDI3 more specifically for this study, to observe if mutation of EDI3 affect activity. EDI3 cleaves glycerophosphocholine and generates choline and glycerol-3-phosphate. Choline is further metabolised to betaine with H_2O_2 forming as a by-product. Horseradish peroxidase (HRP) oxidizes Amplex Red to resorufin, which reduces H_2O_2. The emission of resorufin can be detected with a spectrophotometer at 590 nm and is an indirect indicator of EDI3 activity (Stewart et al. 2012).

To investigate the effect of mutating conserved residues of EDI3 on activity, HEK293T cells were chosen due to their high transfection efficiency. These cells were transfected with EDI3-3XHA or mutants via PEI method (2.2.3.4). After 48 h, cells were harvested and protein concentration was determined (2.2.5.1-2.2.5.2). A master mix containing 1x reaction buffer, 2 U/ml HRP, 0.2 U/ml choline oxidase, 0.5 mM GPC (Sigma Aldrich) and 100 µM Amplex® Red reagent were prepared. A similar master mix, but without GPC was also generated to measure background choline.

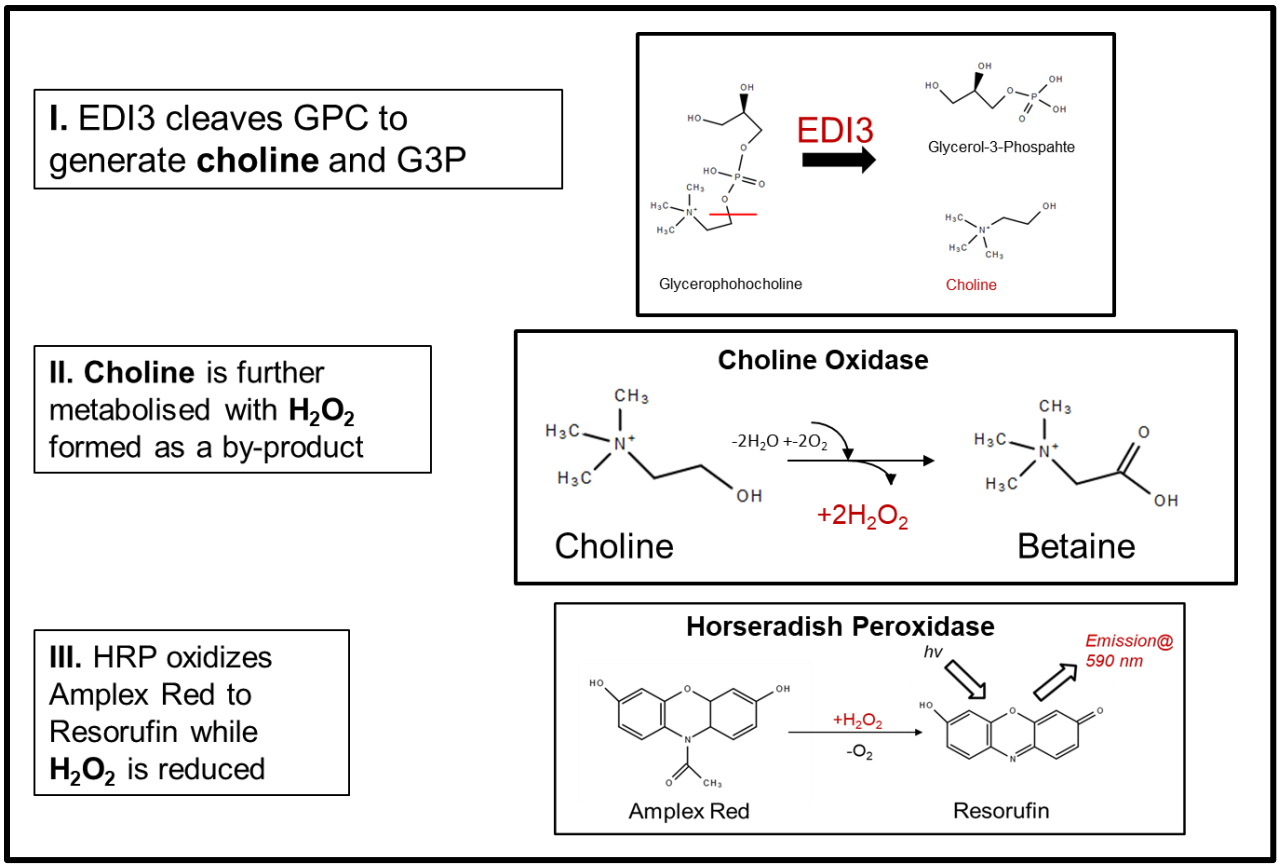

Figure 2.1 **Schematic layout of the EDI3 activity assay.**

50 µg cell lysate was diluted in a total volume of 100 µl 1x EDI3 Activity Assay Buffer (2.1.7.1) and pipetted into the well of a black 96 well microplate (Greiner), followed by 100 µl of the master mix with or without GPC (all samples prepared in technical replicates). Reaction buffer (1x) without cell lysate was used as a negative control. Fluorescence (Excitation 540 nm, Emission 590 nm) was measured at 0 min and every 10 min for 2 hours at 37°C using a microplate reader (Tecan). To define the enzymatic activity of the protein at each time point, values derived from sample without GPC were subtracted from values derived from sample with GPC and background fluorescence was corrected by subtracting the values derived from the buffer-control.

2.2.5.7 Immunoprecipitation

With this assay, potential interaction partners of EDI3 could be identified. HEK293T cells were seeded in a 10 cm culture dish and on the next day transfected with plasmids of interest using the PEI Method (2.2.3.4). After 48 h, cells were lysed in ice-cold IP lysis buffer (table 2.8) and protein concentration was determined with the BCA assay (2.2.5.2). IPs were performed using 800 µg of protein sample incubated with the appropriate antibody coupled to Pierce™ Protein A/G Magnetic Beads (Thermo) according to manufacturer's instructions. The bead-, protein-

antibody-solution was allowed to rotate overnight at 4°C. On the next day, immunocomplexes were purified with a magnet and washed 3 × with IP Lysis-buffer and once with DEPC-treated water. Proteins were eluted by incubating at 95°C for 10 min in 25 µl 1× lämmli buffer. Proteins were separated with a magnet, and supernatants subsequently analysed via immunoblotting (2.2.5.3-2.2.5.5). The antibodies that were used for immunoprecipitation are listed in table 2.18.

2.2.5.8 Polysaccharide Binding Assay

The polysaccharide-binding assay was adapted and modified from Jiang et al (Jiang et al. 2010). The aim of this assay is to find a potential glycan-binding partner by separating intracellularly located or exogenously supplied glycogen or amylopectin from the cell homogenate. To apply this method, the molecular weight and the low water solubility of these molecules were utilized. Polysaccharides are heavy molecules which stay in solution at low centrifugation speed but precipitate at higher speed. Therefore, proteins that bind to the glycans also sediment, and consequently comparing the proteins located in the supernatant to those in the sediment could help identify potential glycan-binding partners.

Cells stably overexpressing *GPCPD1* (Hela_EDI3) were plated and lysed as described in 2.2.5.1, and protein concentration was determined (2.2.5.2). Cell lysates (400 µg/ml) and 2 mg of amylopectin (Sigma Aldrich) or glycogen from rabbit liver (Sigma Aldrich) were added in a total volume of 2 ml glycan binding-buffer and incubated for 1.5 h at 4°C with rotation (table 2.8). For the polysaccharide binding assay in mouse organs, glycogen-containing organs, such as muscle and liver were collected, weighed, homogenized and diluted in 3 x the weighted volume in water and centrifuged at 10,000 × g for 20 min at 4°C. The supernatants were transferred to polycarbonate tubes and diluted in a total volume of 2 ml binding buffer, followed by ultracentrifugation (Ultracentrifuge, Discovery 90 SE, Sorvall) at 100,000 × g at 4°C for 90 min. The pellets were washed and centrifuged again at 100,000 × g at 4°C for 60 min, and re-suspended by sonication. The supernatants were concentrated with a Milli-Q-Filter (Millipore). Proteins from both fractions were eluted in 1x Lämmli buffer solution at 95°C for 10 min by breaking the glycan protein binding. Proteins from the supernatant and pellet were subsequently analysed via immunoblotting (2.2.5.3-5). As further control, Hela_EDI3 full cell lysate or for the oran pulldown primary mouse hepatocytes were used.

2.2.5.9 Glycogen quantification

The purpose of the glycogen assay from Sigma Aldrich was to determine the concentration of glycogen within cells. Glucoamylase hydrolyses glycogen to glucose, which is oxidized by glucose oxidase to D-gluconic acid and H_2O_2. The H_2O_2 itself reacts with OxiRed which yields a colorimetric product that can be detected using a plate reader, where the absorbance at 570 nm is proportional to the glucose level in the cells. To calculate the true cellular glycogen content, the free glucose needs to be subtracted from the glycogen value (Figure 2.2).

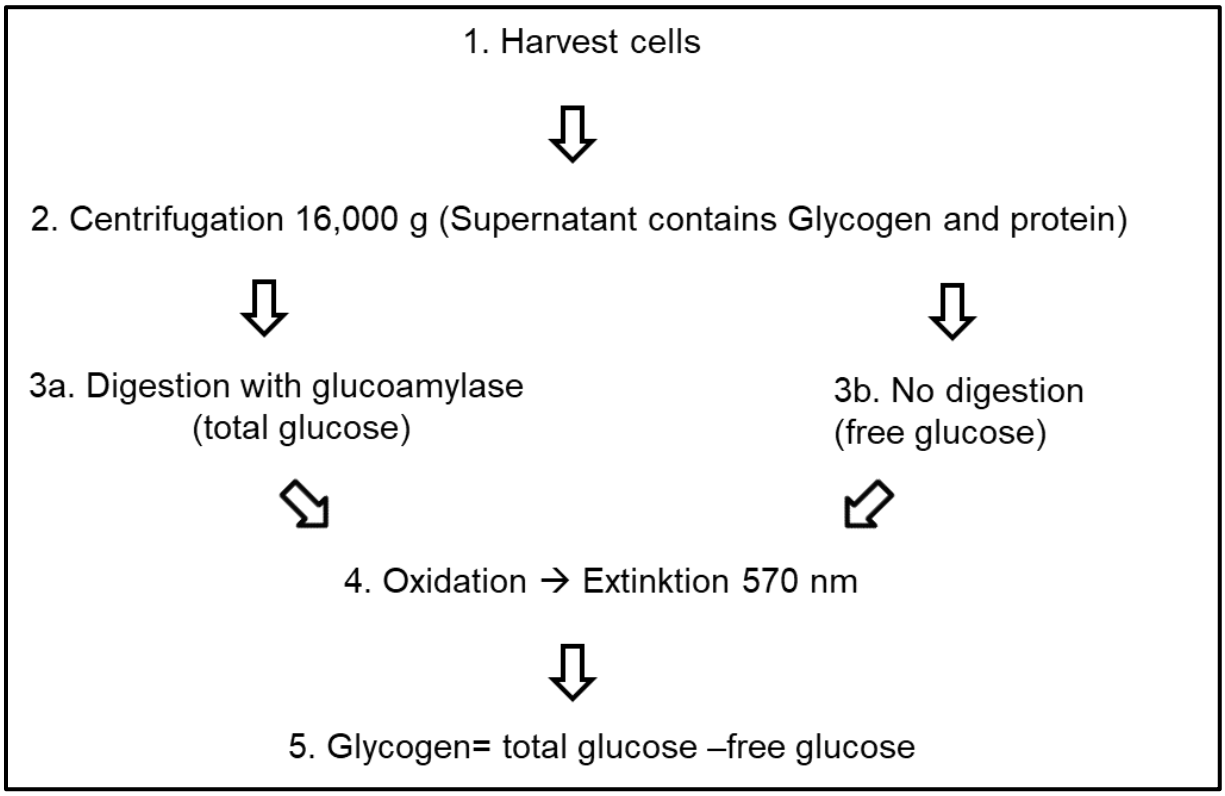

Figure 2.2 **Workflow for the Glycogen Assay.**

For the assay, 10^6 cells were washed in PBS to remove any glucose residue from the media, and cells were harvested from a six well plate using a cell scraper in an appropriate amount of water (100 µl for six well plates). Then, 20 µl of lysate was later used for protein quantification via BCA (2.2.5.2). The remaining cells were incubated at 95°C to inactivate glycogen-depleting proteins and centrifuged at 13000 rpm for 5 min to remove cell debris. The supernatant was transferred into a new tube and three times 20 µl of each sample were pipetted into three wells of a 96-well plate. A standard curve of glycogen, ranging from 0 µg/ml to 10 µg/ml, was prepared. The standard curve and two of the three of the sample wells were treated with 2 µl glucoamylase (reagents were provided in the glycogen assay kit) for 30 min. Next, a mixture containing glucose oxidase, OxiRed and assay buffer were added to the wells, which were thoroughly mixed by pipetting. After 30 min incubation, the absorbance was measured at

570 nm using a plate reader (Infinite M200 Pro, Tecan), which yielded the amount of glucose in the wells. The glycogen concentrations in the samples were calculated based on the standard curve and by subtracting the value of the undigested sample.

2.2.5.10 Challenge primary hepatocytes with glucagon and insulin

Two major regulators of glycogen amount within hepatocytes are insulin and glucagon. The aim of this experiment was to investigate if the two hormones have impact on the *EDI3* gene expression on RNA and protein level. To generate a 20 µmol stock solution, 1 mg glucagon powder (Sigma-Aldrich) was freshly dissolved in 10 ml 50 mM acidic acid, since the acid environment increased the solubility of glucagon in aqueous solutions. Insulin was provided as 10 mg/ml stock solution (Sigma-Aldrich). Glucagon and Insulin were diluted to a 10 nmol- or 100 nmol working solution in William's E medium with supplements. Hepatocytes, cultivated a day before (2.2.2.3), were wash twice with pure William's E medium and then the glucagon and insulin containing solution were added to the cells. After 1 h, 3 h, 6 h and 24 h RNA (2.2.4.1, 2.2.4.3-4) and protein (2.2.5.1-2.2.5.5) was collected and analysed.

2.2.5.11 Transwell Assay

The aim of this assay was to determine the migration rate of cancer cells. In this study, a modified version of the Boyden Chamber assay is used to detect migration. A plastic insert with a porous membrane (24-well plate insert, pore size, 8.0 µm, Falcon) is placed into a well of a companion plate (24-well plate, Flacon) which contains medium and/or chemoattractants. Cells of interest, cultivated in deprivation (normally serum-free) media, are plated into the insert and migrate through the pores, to the underside of the membrane into the nutrition rich media. Migratory cells are then stained and counted.

HEK293T cells were transfected via PEI method and cultivated for 48 h. Cells were detached, counted and 100,000 cells were suspended in 500 µl serum free media (DMEM, 4.5 g/l Glucose) and pipetted into the insert which was positioned in the 24-well companion plate. 600 µl of serum-containing media (DMEM, 4.5 g/l Glucose+10% FBS) was added into the well of the 24 well plate. After 24 h of incubation, cells in the upper chamber were removed with a cotton swab and cells which migrated through the pores were fixed and stained with a solution containing crystal violet and methanol (table 2.12) and dried overnight. Images of migrated cells were taken with a phase contrast Eclipse T5100 microscope (Nikon).

2.2.6 Metabolite analysis

2.2.6.1 Metabolite collection for LC-MS/MS

The aim of this analysis was to identify how EDI3 related metabolites are altered in response to glucagon treatment in primary mouse hepatocytes. For this purpose, the addressed metabolites, the EDI3 educt GPC, the products choline and glycerol-3-phosphate plus further metabolised phosphocholine and betaine were analysed.

The primary mouse hepatocytes were isolated and cultured as described in 2.2.2.1 and 2.2.2.3. On the next day, glucagon was added to the cells as described in 2.2.5.11 and the intracellular metabolites were collected after 1 h, 3 h and 6 h to characterize the change in EDI3- relevant metabolites induced by a glucagon challenge. Each time point was collected in five technical replicates. The six-well plates were washed three times with ice-cold 1xPBS. After the last washing step, PBS was removed and the plate briefly incubated in liquid nitrogen to rupture the cellular membrane. Next, 500 µl ice-cold methanol, spiked with 50 nmol/L d9-choline; 50 nmol/L d9-glycerophosphocholine; 500 nmol/L d9-phosphocholine (Sigma Aldrich), was added to each plate and incubated for 15 min at 4°C while shaking. The supernatant was collected and stored at -80°C until the measurement. The cell membranes on the plate were completely lysed with 200 µl RIPA buffer containing all protease and phosphatase inhibitors as described in 2.2.5.1 and protein concentration determined using the BCA (2.2.5.2).

2.2.6.2 LC-MS/MS-based analysis of metabolites

The samples for metabolite determination were centrifuged for 3 min at room temperature with 21,100 g and 20 µL of the supernatant was transferred to a sample vial for LC-MS/MS measurement. Calibration curves using internal standards were generated from 5-100 nmol/L for choline and glycerophosphocholine and from 50-1,000 nmol/L for phosphocholine.

LC-MS/MS-analysis was carried out on a QTrap4000 triple quad mass spectrometer (Sciex, Darmstadt) coupled to a Shimadzu UFLC system (Shimadzu, Duisburg). 2 µL of sample were injected into a 150 mm long, 3 mm I.D. Nucleoshell HILIC column with 2.7 µm particle diameter and separated isocratically using 50% solvent B (solvent A: acetonitrile; solvent B 50% methanol, 5 mM ammonium formate) at a flow rate of 500 µL/min within 10 min. The mass spectrometer was operated in positive mode using selected-reaction-monitoring with the parameters stated in table 2.30. Data was interpreted using the Skyline Daily software (PMID: 31984744).

Table 2.30: **Transition data for selected reaction monitoring**

Analyte	Q1 mass [Da]	Q3 mass [Da]	dwell time [ms]	collision energy [V]
choline	104.1	60.0	250	23
d9-choline	113.1	69.0	250	23
phosphocholine 1	184.0	86.0	250	27
phosphocholine 2	184.0	125.0	250	27
d9-phosphocholine 1	193.0	95.0	250	27
d9-phosphocholine 2	193.0	125.0	250	27

Cellular and histological stainings

2.2.7 Cellular stainings

2.2.7.1 Fixing of transfected cells

With this method it was possible to determine the intracellular location of the proteins of interest within the cells which were transfected with fusion proteins (2.2.2.4-2.2.2.5).

48 h after transfection, cells were carefully washed with 1x PBS, and fixed with 4% paraformaldehyde (PFA) for 20 min at RT under a chemical hood. Next, the cells were washed three times with 1x PBS to remove residual PFA, and cover slips with ultrapure water to remove residual salt. The cover slips were fixed onto object slides using Fluoroshield™ with DAPI histology mounting medium (Sigma-Aldrich) and dried overnight. On the next day, the cells were observed on a confocal microscope (FV1000, Olympus).

Table 2.31**: Florescent vectors transfected into different cell lines**

Protein	Fluorophore
EDI3	Turbo red fluorescent protein (RFP)
STBD1	Green florescent protein (GFP)

2.2.8 Histological Staining

2.2.8.1 Cutting of paraffin embedding of tissue

Blocks of paraffin-embedded liver or muscle tissue were cut into 5 µm sections with a feather blade type N35HR in a HM 450 Sliding Microtome (Thermo Fisher Scientific). The tissue sections were heated for 15 min at 60 °C to mount the slides onto the slide holder. The tissue slides were stored at 4°C. In this study, only human paraffin embedded skeletal muscle tissue was used.

2.2.8.2 Chromogenic immunohistochemical staining

The aim of this method is to locate EDI3 and other glycogen binding proteins in high glycogen containing tissues (liver and heart).

Rehydrating: With this step the histological section gets accessible for further treatment. Paraffin embedded (serial) sections of 5 µm thickness were incubated three times in Rotihistol (Roth) for tissue deparaffinization. Later, the tissue on the slides were rehydrated in an ethanol gradient (95%, 90%, 80%, 70%,50%, 30%) for 5 min each, followed by washing in distilled water for 5 min.

Antigen retrieval: Antigen retrieval is used to break methylene bridges formed as a result of formaldehyde cross linking in order to expose antigenic sites. In this study the heat induced epitope retrieval (HIER) was used. First, the citrate-buffer (10 mM, pH6) was heated in a pressure cooker to 96°C. The tissue slides were then incubated for 15 min at 96°C in the buffer and then slowly cooled for 20 min. The slides were washed in TBS-T to remove the citrate buffer.

Blocking: A pap pen (Dako) was used to draw a barrier around the tissue sample on the slide to ensure that all solutions added remained on the tissue itself. At first, the peroxidase block solution (Dako) was applied to the tissue slides for 5 min to block potential endogenous peroxidase. After washing with TBS-T (1x), the sections were incubated in the blocking solution (2.10) for 1 h to cover unspecific epitopes.

Antibody application: The primary antibody was diluted in staining solution (2.10) according to the manufacturer's recommendations or as established beforehand (table 2.32). The tissue sections were incubated over night at 4°C. The peroxidase labelled polymer (Dako) is linked to horseradish peroxidase (HRP) on the secondary antibody, which was chosen depending on the host species of the primary antibody. After overnight incubation, the slides were thoroughly washed in TBS-T, then incubated in an appropriate peroxidase-labelled polymer for 30 min and washed again before the 3, 3'-Diaminobenzidine (DAB) treatment.

Chromogenic detection: 3, 3'-Diaminobenzidine (DAB) is a derivative of benzene. It is oxidized by hydrogen peroxide in a reaction catalysed by HRP to form a brown precipitate at the location of the HRP, which later can be visualized using microscopy. The DAB solution (20 µl liquid DAB + 1 ml Chromogen, DAKO) was added to the carefully cleaned tissue sample. The

detection time is determined by the emergence of the brown colour, recorded and the reaction is stopped by returning the tissue to TBS-T.

Haematoxylin stain: The cell nuclei are stained with haematoxylin. The tissue slides were incubated in Mayer´s Hemalum solution (1:5 diluted with sterile-filtered DEPC water) for 5 min. Subsequently, the slides were washed for 7 min under running tap water.

Dehydrating and mounting: Slides were washed in distilled water for 30 sec and dehydrated in ethanol gradient for 15 sec (30%, 50%), 3 min in (70%) 15 sec (80%, 90%) and 3 min in 100% ethanol, followed by 2 x 3 min incubation in Rotihistol. Subsequently, the stained tissue was preserved with Entellan (Merck) and covered (Cover slices, Menzel), and allowed to dry overnight before analysis on the next day with the Axio Scan (Zeiss) using the Zen software (Zeiss).

2.2.8.3 Fluorescent immunohistochemical staining

The aim of this fluorescent immunohistochemical staining (IF-IHC) was to investigate whether EDI3 co-localized with other proteins in human skeletal muscle tissue. The advantage of this method in comparison to chromogenic staining is that it allows for the simultaneous detection of more than one protein, and microscopic structures are more easily detected with fluorescent microscopy.

Rehydration and antigen retrieval in paraffin embedded skeletal muscle tissue (5 µm) was conducted as described in 2.3.8.5 and the tissue was circled with the DAKO Pap pen. The blocking solution (table 2.10) was added for 1 h and then primary antibody, in case of a co-staining both antibodies simultaneously, was/were applied in an appropriate dilution (table 2.32) in staining solution (table 2.10) overnight at 4°C. On the next day, the slides were washed 3x in 1x PBS for 5 min and then incubated with secondary antibody for 1.5 h. In case of a co-staining, both secondary antibodies were applied at the same time. Later, slides were washed 3x with 1x PBS and 1x in DEPC treated water for 5 min. The tissue slides were preserved with DAPI histology mounting medium (Sigma-Aldrich) and covered (Cover slices, Menzel) and dried overnight at 4°C protected from light. Images were taken on a confocal microscope (FV1000, Olympus).

Table 2.32: **Dilution of antibodies in staining procedures**

Primary Antibodies		
Antibody	**Host**	**Dilution IHC**
Anti-EDI3 Clone 3B8G3	Mouse	1:1500
Anti Glycogen-Snythase 1	Rabbit	1:1000
Anti Myosin II	Mouse	1:150
Anti-Myosin VII	Mouse	1:2000
Anti-RYR1	Rabbit	1:50
Anti-STBD1	Rabbit	1:500
Secondary Antibodies		
Antibody	**Host**	**Dilution IHC**
Alexa Fluor® 488 AffiniPure Donkey IgG (H+L)	Rabbit	1:100
Alexa Fluor® 647 AffiniPure Donkey IgG (H+L)	Mouse	1:100

2.2.8.4 Periodic acid–Schif stainings

The Periodic Acid-Schiff (PAS) reaction and Periodic Acid-Schiff reaction with diastase (PAS-D) are two special staining procedures used to detect glycogen in tissue. Periodic acid oxidizes the vicinal diols, creating a pair of aldehydes which reacts further with the Schiff reagent. This reaction leads to the staining of glycogen but also other carbohydrates, such as polysaccharides, glycoproteins, and mucins in purple. PAS-D is a very sensitive histochemical method for the examination of glycogen. Diastase, which is also referred to as α-amylase, acts on glycogen and depolymerizes it into smaller sugar units (maltose and glucose), which are then washed out of the tissue section. Performing the PAS and the PAS-D staining in parallel allows for the differentiation between glycogen and other PAS positive staining, since only glycogen disappears due to the α-amylase treatment.

Serial sections from human liver and skeletal muscle were rehydrated (2.2.8.4) and treated with α-amylase (Merck) (PAS-D) or DEPC treated water (PAS) for 1 h at 37°C. Slides were washed in water to remove the α-amylase. Next, both slides were incubated in 0.5% periodic acid for 10 min. After another washing step, slides were placed in Schiff's reagent (Roth) for 15 min. Thereafter, slides were washed in lukewarm tap water for 5–10 min in order for the tissue to develop a pink colour. To stain the nuclei, a haematoxylin stain was performed. Slides were dehydrated, mounted (2.2.8.2) and hardened overnight. A successful PAS-D staining shows less pink colour then the PAS staining.

2.3 Statistical data analysis

All experiments were performed with three or more biological replicates if not mentioned otherwise. The numeric numbers were represented as mean values with standard deviation. To evaluate whether a difference between conditions was significant, the unpaired T-test *in vitro* samples was applied. For mouse samples, the unpaired T-test was performed, if not mentioned otherwise. P-values below 0.05 were accepted as significant. GraphPad PRISM 7.05 was used for these analyses.

3. Results

3.1 Characterization of the EDI3-CBM20

The first aim of this project was a basic characterization of the the carbohydrate-binding module 20 (CBM20) of EDI3 itself. Since to date, there are no reports on EDI3's CBM20 domain, similar experiments were performed as previously conducted for the well-characterized CBM20-containing proteins, laforin and STBD1 (ref) to gain insight into the role of EDI3 and its CBM20 domain.

3.1.1 EDI3-CBM20 shows high sequence homology to other CBM20 proteins

In order to identify whether the conserved CBM20 residues present in the already characterized CBM20 proteins - laforin and STBD1 – are present in EDI3, the sequences of all three proteins were aligned. Additionally, the Edi3 sequence from mouse, zebrafish and *Xenopus* laevis were also included to find out if the residues are also conserved among species (Figure 3.1). Four conserved amino acids were found in the sequence alignment of all CBMs investigated: G24, L29, G30 and W32 (Homo sapiens EDI3 numbering).

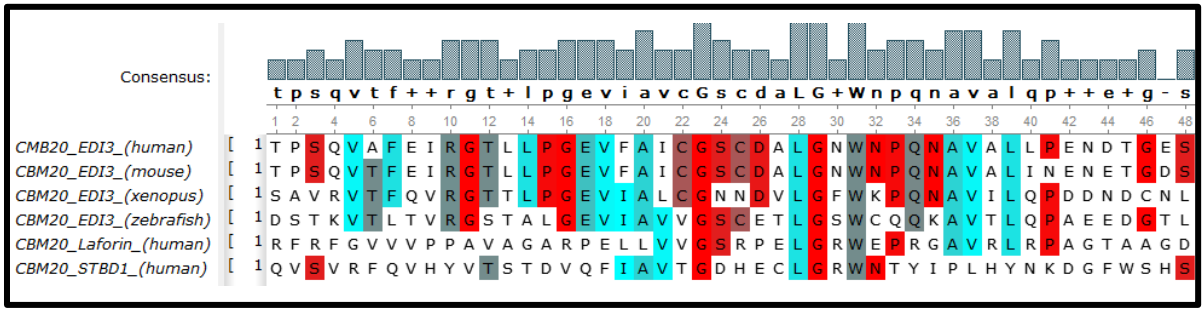

Figure 3.1 **Sequence alignment of the CBM20 of several family members**. Shaded letters indicate the level of conservation within the amino acids of the EDI3 family across species, and the two CBM20 family in humans. The different colours represent the different properties of residues.

In a second approach, the sequence homology of EDI3 was compared to the other CBM20-containing proteins using the Smith-Waterman algorithm, which performs local sequence alignments, like protein domains (Needleman and Wunsch 1970; Smith and Waterman 1981). In addition to aligning the entire protein sequence, the CBM20 domain alone was analysed. This algorithm was used to align the CBM20 sequences of the different proteins (EDI3, laforin, STBD1) with one another, as well as the entire proteins with one another thus revealing potentially unknown homology-rich regions within the proteins. As a positive control, EDI3 from mouse was included in the algorithm, as well as AMPK beta 1, a CBM21-containing protein, which is phylogenetically closely related to the CBM20 domain

(Machovic et al. 2005), and was shown to interact with both STBD1 (Ducommun et al. 2019) and laforin (Romá-Mateo et al. 2011).

A	Sequence alignment (full Protein)	Aligned	Identity [%]	Similarity [%]	Gaps [%]	Score
EDI3 human (672 AA)	vs. EDI3_mouse (675 Amino Acids)	675	92	97	0,4	3332
	vs. Laforin_human (331 Amino Acids)	380	21	31	36	74
	vs. STBD1_human (358 Amino Acids)	84	25	38	23	59
	vs. AMPK-beta-1 human (270 Amino Acids)	155	21	33	28	39

B	Sequence alignment (CBM domain)	Aligned	Identity [%]	Similarity [%]	Gaps [%]	Score
EDI3 human (115 AA)	vs. EDI3_mouse (115 Amino Acids)	115	90	96	0	562
	vs. Laforin_human (124 Amino Acids)	131	24	35	32	63
	vs. STBD1_human (100 Amino Acids)	84	25	38	23	58
	vs. AMPK-beta-1 human (96 Amino Acids)	62	26	36	30	31

Figure 3.2 **Determination of local alignments within the human CBM20 proteins using the Smith-Waterman algorithm. A,** Full Human EDI3 protein was aligned with the CBM20 proteins laforin and STBD1, the CBM21-containing protein AMPK-beta-1, and full mouse EDI3 protein as a positive control. **B**, The corresponding CBM20/21 of the aforementioned proteins were aligned. In both cases, the Smith-Waterman algorithm from EMBL-EBI was used (https://www.ebi.ac.uk/Tools/psa/emboss_water/).

Using the algorithm, an alignment score is calculated which reflects the homology of the compared proteins. A high score signifies a high - and a low score low homology. As an example, two aligned human EDI3 proteins (672 amino acids) would show an identity and similarity of 100% and a score of 3537, identical, larger proteins (>672 amino acids) would obtain a higher score, since the score increases with a higher number of aligned amino acids. Proteins with no homology would produce a score of 0. The alignment of human to mouse EDI3 yielded a sequence identity of 92% (Figure 3.2A) for the whole protein, and 90% for the CBM20 alone (Figure 3.2.B). The generated score from the CBM20 alone 562 (Figure 3.2.B) to the whole protein 3332 (Figure 3.2.A) increased almost six-fold, indicating high homology within the whole protein. Conversely, the alignment of full length EDI3 to the other CBM20

proteins show similar scores for the whole protein (59, STBD1) (Figure 3.2 A) and the CBM20 (58) (Figure 3.2 B) alignment, revealing the sequence homology between these proteins is almost exclusive to the CBM20.

Altogether, the sequence homology between human and mouse EDI3 is very high, while laforin and STBD1 only show homology with EDI3's CBM20 domain, but not other parts of the proteins. For AMPK beta 1, the same trend could be identified, although the sequence homology between EDI3 CBM20 and the chosen CBM21 is half of that observed among the CBM20s.

3.1.2 Generation of altered EDI3 constructs

According to the sequence alignment analysis, the CBM20 domain is conserved among the CBM20 proteins. Therefore, to investigate the role of EDI3's CBM20, the conserved W32 was mutated to alanine (W32A), and the entire CBM20 domain was deleted to generate a ΔCBM20 mutant (Figure 3.3) from pRP-CMV-EDI3. Finally, a triple HA tag (3xHA) was inserted into all designed EDI3 constructs at the C-terminus, and as a result the plasmid could be used for subsequent immunoprecipitation experiments.

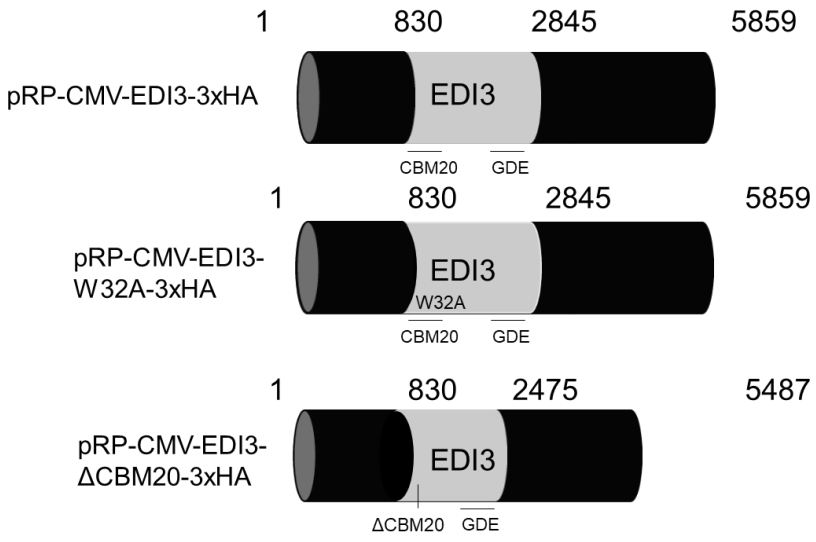

Figure 3.3 **EDI3-mutants used in this project.** Schematic plasmids illustrated as a tube. The EDI3 sequence is highlighted in grey. Numbers above the plasmids indicate the nucleotide site, pRP-CMV-EDI3-3xHA is shown at the top, pRP-CMV-EDI3-W32A-3xHA in the middle and pRP-CMV-EDI3- ΔCBM20-3xHA is shown at the bottom.

3.1.3 The CBM20 of EDI3 is important for protein stability

To determine if these mutants affect the stability of EDI3, the plasmids pRP-CMV-EDI3-3xHA, pRP-CMV-EDI3-W32A-3xHA, pRP-CMV-EDI3-ΔCBM20-3xHA, pRP-CMV-EDI3-turboRFP and an empty vector were transfected into HEK293T cells using the stable cationic polymer,

polyethylenimine (PEI). The transfected cells were lysed and EDI3 protein expression analysed by western blot. Despite loading similar amounts of total protein, the band obtained for the EDI3 W32A mutant was approximately 20% less than the wild type EDI3, while the ΔCBM20-mutant was 30% less (Figure 3.4.A and B). These results suggest that mutating the conserved W32 residue and removing the CBM20 domain affects protein stability, agreeing with previous reports for the other CBM20 containing proteins that the CBM20 domain is needed for protein stability (Zhu et al. 2014; Raththagala et al. 2014). To estimate the transfection efficiency during the experiment, pRP-CAG-EDI3-turboRFP was transfected into HEK 293T cells and florescence was observed after 48 h. In all experiments, over 85% of the transfected cells were fluorescent (Figure 3.4.C).

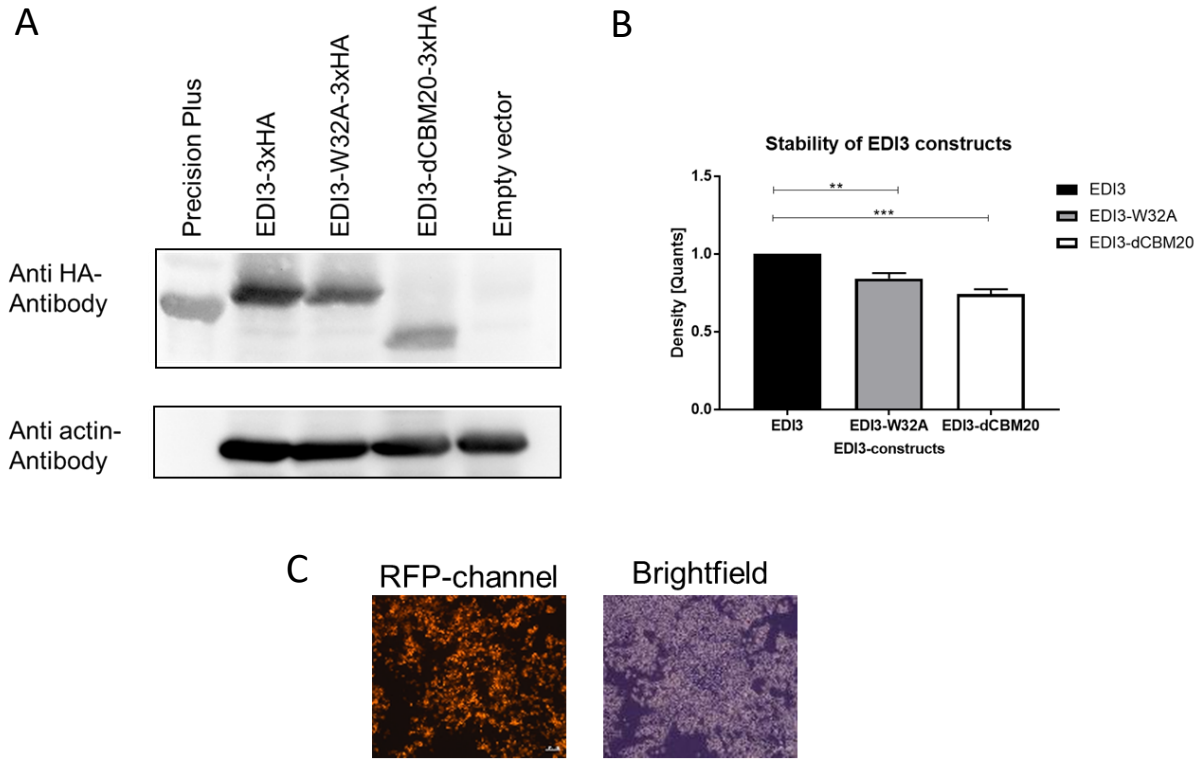

Figure 3.4 **Altering the CBM20 of EDI3 leads to destabilization of the protein. A,** Representative Western blot of EDI3 and mutant structures**.** HEK293T cells were transfected with pRP-CMV-EDI3-3xHA, EDI3-W32A-3xHA, EDI3-ΔCBM20-3xHA or an empty vector. Cells were lysed after 48 h and proteins were analysed via western blot. To identify the transfected proteins, an anti HA antibody was used; β-Actin was used as a loading control. **B,** Densitometry analysis of the detected EDI3-3xHA, EDI3-W32A-3xHA and EDI3 ΔCBM20-3xHA luminescence signal normalized to the β-Actin signal **C,** Representative image of HEK293T cells 48 h after transfection with pRP CAG EDI3 turboRFP to observe the transfection efficiency. (N=3), ** indicates $p < 0.01$. *** indicates $p < 0.001$.

3.1.4 EDI3 is a dimer with only minor impact of the CBM20

A feature of the CBM20 proteins, which is described for STBD1 and Laforin, is their ability to form homodimers (Liu et al. 2006; Jiang et al. 2010). The solved crystal structure for laforin indicates that the protein is an antiparallel dimer; however, the CBM20 domain was not

reported to be involved (Raththagala et al. 2014). One publication thus far has however reported that the CBM20 of STBD1 is needed for dimerization. To date, no experimental data are available regarding EDI3's dimerization ability.

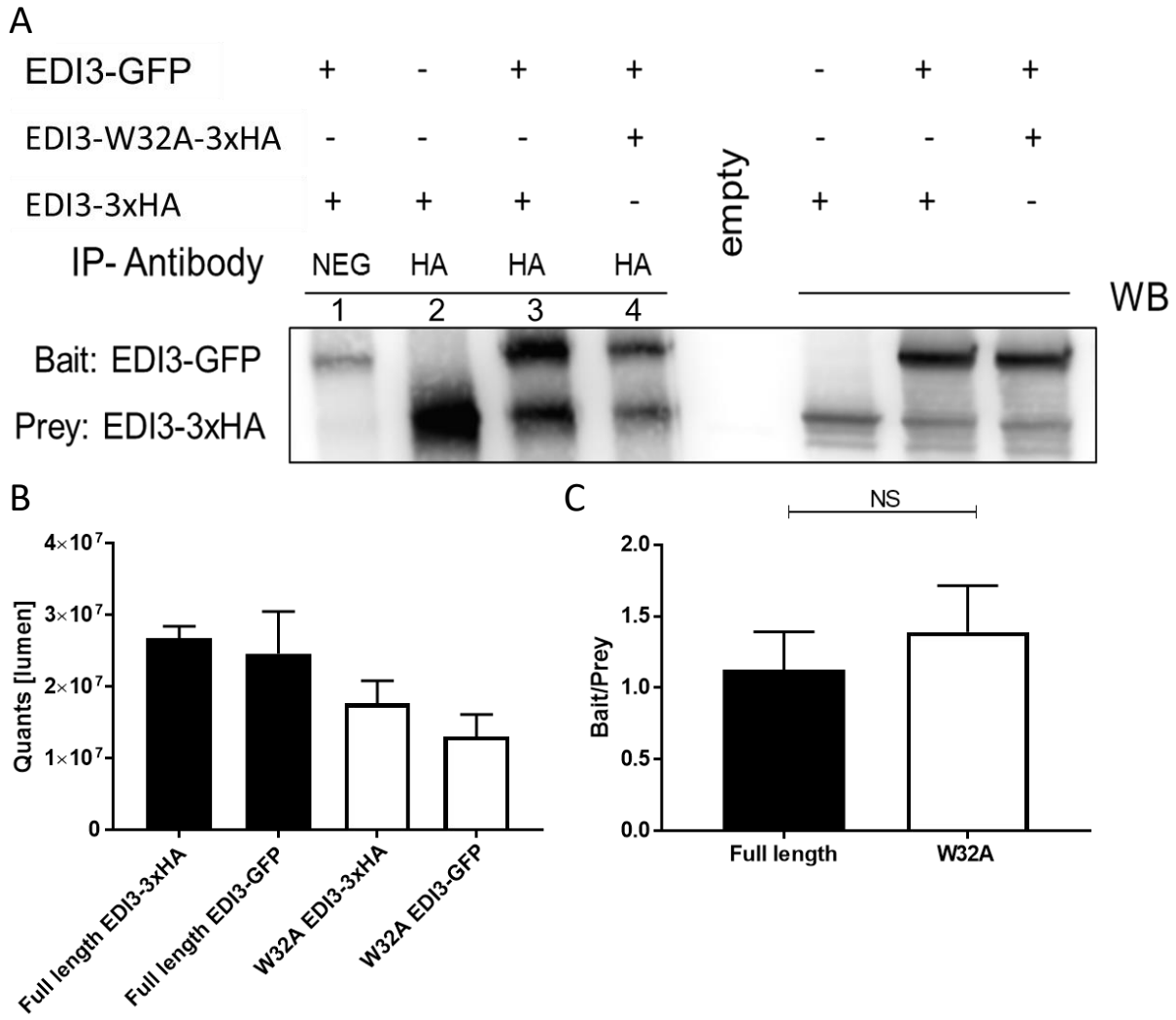

Figure 3.5 **EDI3 forms dimers which is not influenced by the W32A mutation. A,** Representative western blot image of an immunoprecipitation (IP) experiment using EDI3 wild type and mutants constructs. pCMV-EDI3-GFP was either co-transfected with pRP-EDI3-3xHA or pRP-EDI3-W32A-3xHA (as indicated with + and -) in HEK293T cells. Additionally, EDI3-3xHA alone was transfected into HEK293T cells. Cells were then lysed 48 h after transfection and IP experiments performed using 800 µg cell lysate, HA antibody or an unspecific IgG mouse antibody (NEG) and magnetic beads. Beads and proteins were separated via heating (95°C). Eluted proteins (left hand side) and full cell lysates as loading control (right hand side) were analysed using western blot. **B,** Densitrometric analysis of the bands from 3 independent experiments showing full length EDI3-3xHA signal and EDI3-GFP (black bars), as well as the signal of EDI3-W32A-3xHA and the EDI3-GFP signal (white bars) **C,** Bait to prey ratio of EDI3-GFP to either EDI3-3xHA (black bar) or EDI3-W32A-3xHA (white bar) (N = 3). NS=not significant

To test if EDI3 is a dimer or oligomer and if the CBM20 is important for its dimerization, an immunoprecipitation (IP) approach with magnetic beads was performed. pCMV-EDI3-GFP was co-transfected with either pRP-CMV-EDI3-3xHA or with pRP-CMV-EDI3-W32A-3xHA in HEK293T cells and lysed after 48 h. Additionally, EDI3-3xHA was transfected alone

(no EDI3-GFP). The magnetic beads were either incubated with HA antibody, or with an unspecific anti-mouse antibody as an additional control.

Next, cell lysates from EDI3-3xHA/EDI3-GFP and the EDI3-W32A-3xHA/EDI3-GFP transfected cells were incubated with the magnetic beads, where only the HA-tagged protein were able to bind the magnetic beads. In this case, the EDI3-GFP protein acted as the prey protein. The beads were first washed, and then denaturated, and the released protein was analysed (Figure 3.5.A). The EDI3-GFP fusion protein is detected at 100 kDa while EDI3-3HA and EDI3-W32A-3xHA are detected at around 75 kDa. When expressed together in cells, EDI3-3xHA/EDI-GFP appear to form a homodimer with a band at 75 kDa and one at 100 kDa (Figure 3.5.A, lane 3). Similar results were obtained after co-immunoprecipitation with EDI3-W32A-3xHA/EDI-GFP (Figure 3.5.A, lane 4). The EDI3-3xHA immunoprecipitation-only sample revealed a band at 75 kDa (Figure 3.5.A, lane 2), and the magnetic beads loaded with the unspecific antibody show a faint band at 100 kDa (Figure 3.5.A, lane 1). Densitometric analysis of the EDI3-3xHA/EDI-GFP co-immunoprecipitation (Figure 3.5.B) indicate strong binding of either EDI3-3xHA or EDI3-GFP in a ratio of 1:1 (Figure 3.5.C), which suggests that EDI3 forms a dimer or higher oligomeric structure.

The role of the CBM20 domain in the dimerization process was investigated using the conserved W32A mutation. As described above, in addition to full length EDI3, the W32A mutant was included in the experiments and the bait to prey ratio of both co-immunoprecipitation - W32A and full length EDI3 (baits) to the EDI3-GFP (prey) - was compared. Decreased binding could be detected for the bait- (EDI3-W32A-3xHA) as well as for the prey protein (EDI3-GFP) (Figure 3.5 A, lane 4). Decreased binding could also be observed with the EDI3-W32A-3xHA/EDI3-GFP co-immunoprecipitation (Figure 3.5 B), which agrees with the previous observation that EDI3-W32A shows 20% less protein than EDI3-3xHA in the cell lysate (Figure 3.4). Furthermore, a comparison of the bait to prey ratio between the EDI3-3xHA/EDI3-GFP co-immunoprecipitation to the EDI3-W32A-3xHA/EDI3-GFP co-immunoprecipitation suggests reduced binding; however, this effect of EDI3-W32A was not significant (Figure 3.5.C).

3.1.5 Mutation or deletion of the CBM20 lowers the enzymatic activity of EDI3

Previous work has shown that mutations within the CBM20, for instance W32D of laforin led to decreased enzymatic activity (Liu et al. 2006). Whether the CBM20 domain or the

W32 mutant is important for EDI3 activity, regulated via its glycerophosphodiesterase domain (GDE) is unknown. In the present work, a kinetic assay (Stewart et al. 2012) was used to measure the enzymatic activity of pRP-EDI3-3xHA, EDI3-W32A-3xHA and EDI3-ΔCBM20-3xHA. An empty vector was used as a control. Lysates extracted from cells transfected with EDI3-3xHA showed significantly higher enzymatic activity compared to extracts from cells with EDI3-W32A-3xHA and EDI3-ΔCBM20-3xHA mutants at all time points measured (10-40 min; Figure 3.6.A). After 30 min, the EDI3-3xHA construct reached the limit of detection of the spectrophotometer at 66000 units of relative fluorescence (Figure 3.6.B); whereas, at the same time point, the EDI3-W32A-3xHA was only approximately 45% active. Importantly, removing the entire CBM20 domain (EDI3-ΔCBM20-3XHA) resulted in an almost complete loss of activity, which was comparable to the empty vector. Considering that there is 20% less protein in the EDI3-W32A-3xHA than in the EDI3-3xHA lysate (Figure 3.4), it may be estimated that mutant EDI3-W32A-3xHA is 30% less enzymatically active than full length EDI3-3xHA.

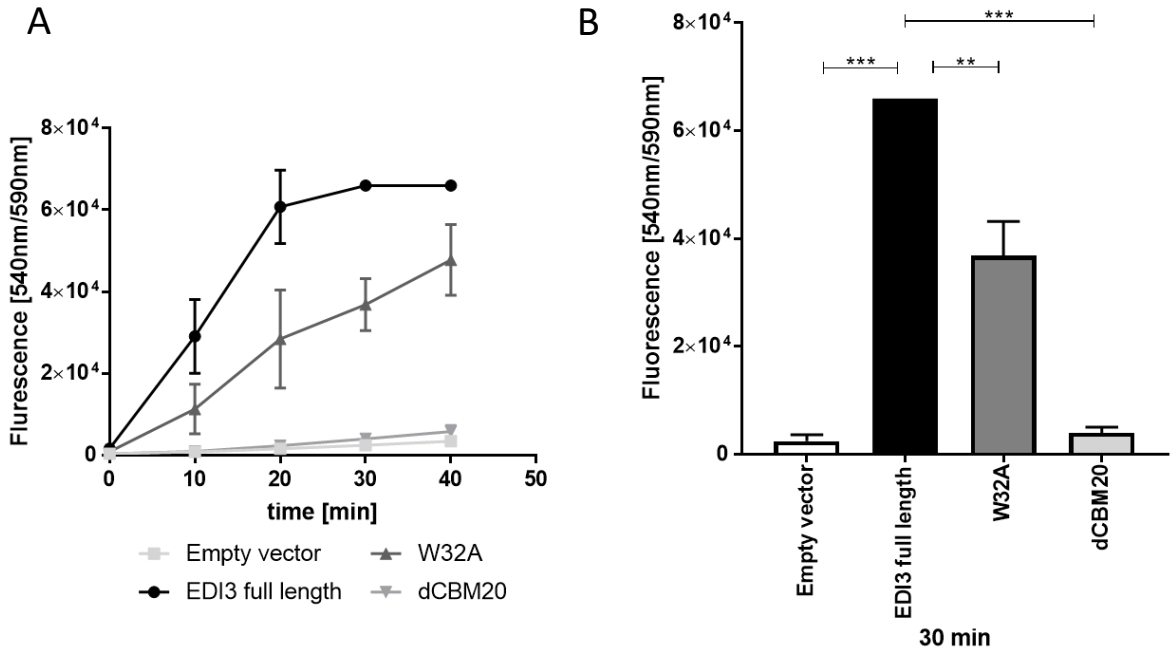

Figure 3.6 **Genetic alterations within the CBM20 of EDI3 lead to decreased enzymatic activity.** HEK293T cells were transfected with pRP-EDI3-3xHA, EDI3-W32A-3xHA and EDI3-ΔCBM20-3xHA and an empty vector for 48h. Cells were lysed, and the enzymatic activity was determined using the EDI3 activity assay as described in the materials and methods with 25 ug protein for each condition. Measurements were taken every 10 minutes up to 40 minutes. **A,** Enzymatic activity of EDI3-3xHA, EDI3-W32A-3xHA, EDI3-ΔCBM20-3xHA and an empty vector was measured over a period of 40 min time. EDI3-3-HA reached the limit of detection at 66,000 units after 30 min. **B,** Direct comparison of the 30 min time point of EDI3-3xHA, EDI3-W32A-3xHA, EDI3-ΔCBM20-3xHA and empty vector. EDI3-3xHA is significantly more active than the other constructs. All experiments were performed three independent times, and in technical duplicates. ** indicates $p < 0.01$. *** indicates $p < 0.001$.

3.1.6 EDI3 mutants -W32A and -ΔCBM20 show less migration than wildtype EDI3

In previous studies, it was shown that silencing EDI3 with siRNA, and thus decreasing its expression and activity in different cell lines, or inhibiting its enzymatic activity with the general phosphodiesterase inhibitor, dipyridamole could decrease cell migration (Stewart et al. 2012). As described above (Figure 3.6), mutations in the CBM20 of EDI3 decreases the enzymatic activity as well. Therefore, a transwell assay was performed with HEK293T cells transfected with EDI3-3xHA, EDI3-W32A-3xHA, EDI3-ΔCBM20-3xHA and an empty vector to investigate whether the altered enzymatic function of EDI3 via the CBM20 mutations would also lead to less migration.

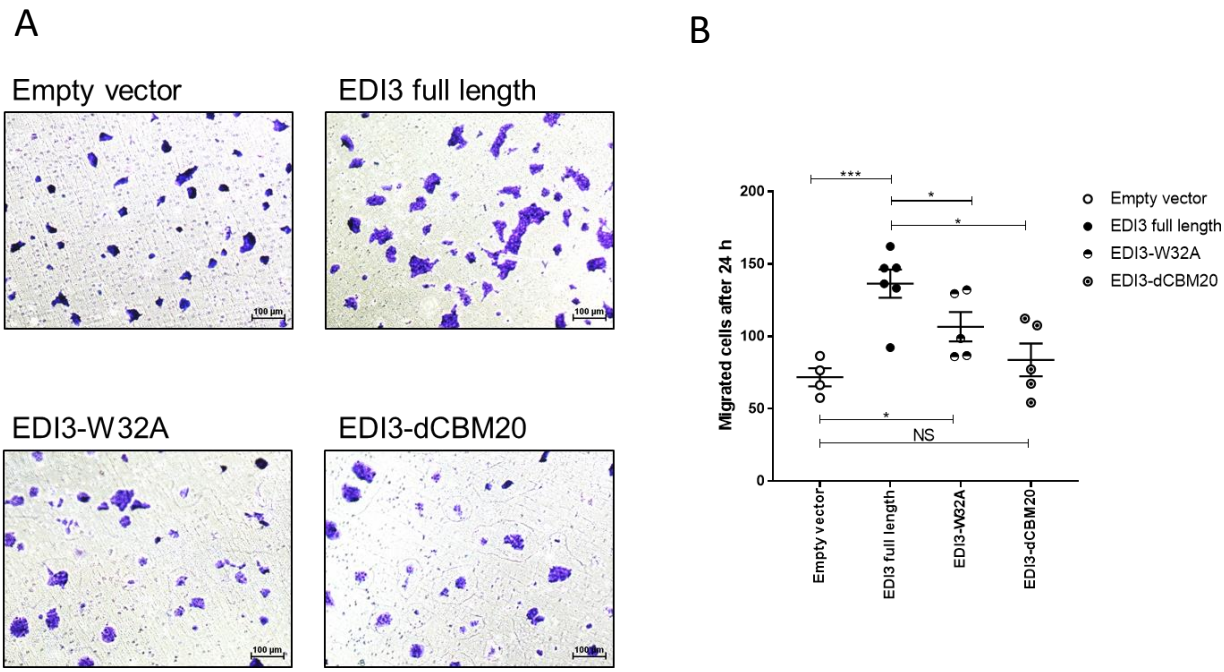

Figure 3.7 **A mutated CBM20 decreases cell migration**. **A**, Representative images of HEK293T cells, which were transfected with pRP-EDI3-3xHA (full length), EDI3-W32A-3xHA, EDI3-ΔCBM20-3xHA or an empty vector for 48 h and then seeded onto cell culture inserts. Cells that migrated to the underside of the insert were fixed and stained with crystal violet 24 h post seeding. **B,** Quantification of migrated cells. Data are mean ± SD of three independent experiments (*, P < 0.05; ***, P < 0.001). Images were taken using a 10× objective

HEK293T cells transfected with EDI3-3xHA showed significantly more migration than cells transfected with the empty vector control (Figure 3.7). Furthermore, significantly less migration was observed in cells transfected with EDI3-W32A-3xHA or EDI3-ΔCBM20-3xHA compared to cells transfected with wild-type EDI3-3xHA. No difference in migration could be detected between the empty vector and the ΔCBM20 transfection; whereas, the EDI3-W32A mutant resulted in more migration than the empty vector control. These experiments showed that mutations within the CBM20-domain of EDI3 results in decreased migration, which may be due to the loss in EDI3's enzymatic activity.

3.2 The binding of EDI3 to glycans *in vitro*

The basic characterisation of EDI3's CBM20 domain thus far indicate that like other CBM20-containing proteins, EDI3's CBM20 domain is required for protein stabilization and homodimerization. Since it could be shown that other human CBM20 proteins bind amylopectin (Worby et al. 2006; Jiang et al. 2010) and glycogen (Tagliabracci et al. 2007; Stapleton et al. 2010),, EDI3's ability to bind carbohydrates was also investigated in the present work.

3.2.1 EDI3 co-precipitates with amylopectin *in vitro*

Since carbohydrate binding is name-forming for the CBM20 domain, we tested whether EDI3 can bind in vitro to amylopectin, the plant analogue of glycogen. A similar experimental approach was used as in the study of STBD1 (Jiang et al. 2010).

Cell lysate from Hela cells stably overexpressing the *EDI3* gene (Hela_EDI3) was incubated with amylopectin for 1 h, and then a glycan pulldown was performed where ultracentrifugation was used to sediment the pellet containing amylopectin and any bound proteins (3.8.A). The supernatant was also collected as the fraction containing non-carbohydrate binding proteins. Proteins from the supernatant and the pellet were analysed with western blotting. As a control to locate the EDI3 band on the blot, Hela_EDI3 full cell lysate was used (Figure 3.8).

The data indicated that a significantly higher amount of EDI3 was found in the pellet fraction compared to the supernatant, suggesting that EDI3 binds amylopectin. Several controls were also included in the experiment, such as blotting for ERK in both the supernatant and pellet fractions. The ERK protein was mainly found in the supernatant and not in the pellet fraction, confirming that it does not bind to the glycan. A second control included the glycan pulldown with Hela_EDI3 cell lysate without amylopectin. Here, more EDI3 protein was found in the supernatant compared to the samples with amylopectin, while ERK levels remained constant. Altogether, this experiment suggests that EDI3 binds amylopectin *in vitro*.

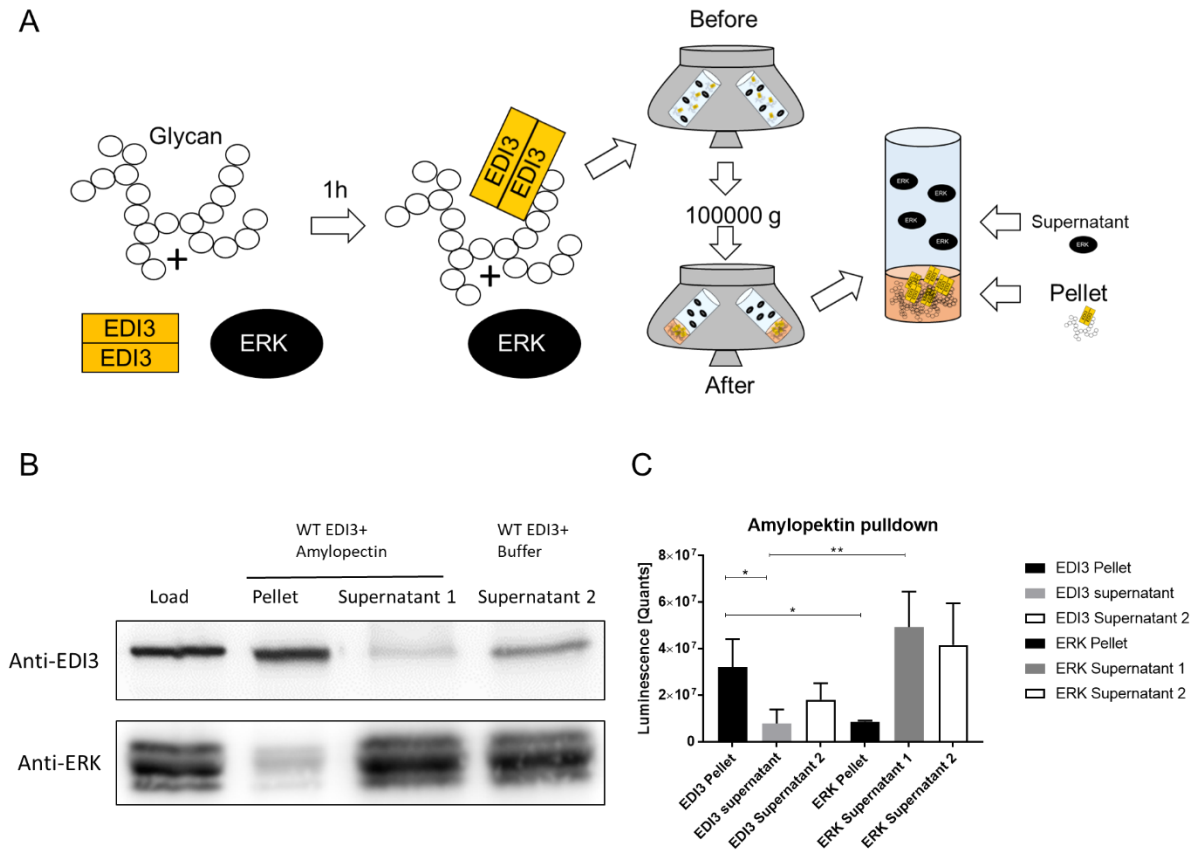

Figure 3.8 **EDI3 and amylopectin co-precipitate *in* vitro. A,** Experimental approach used to test the hypothesis that EDI3 binds glycans, here amylopectin and precipitates with it into the pellet. **B,** Representative western blot image of a performed glycan pulldown. Full cell lysate (400 µg/ml) from Hela cells stably overexpressing EDI3 was incubated with or without 2 mg amylopectin for 1 h and then centrifuged for 1.5 h at 100000 g at 4°C. Supernatant was concentrated, pellet was washed and both fractions were analysed by western blotting for EDI3, as well as ERK as a control for a protein that does not bind glycans. **C,** Densitrometric analysis of the EDI3 and the ERK luminescence signal show significant differences in the binding of ERK and EDI3 in the pellet and supernatant fractions. (n = 3) * indicates $p < 0.05$** indicates $p < 0.01$.

3.2.2 Full length EDI3 but not W32A or ΔCBM20 coprecipitates glycogen in vitro

After showing successful binding of EDI3 to amylopectin, it was next investigated whether EDI3 could also bind glycogen, and how mutations in EDI3's CBM20 domain influence this binding. Here, lysates from HEK293T cells were used, which were transiently transfected with EDI3-3xHA, EDI3-W32A-3xHA, EDI3-ΔCBM20-3xHA or an empty vector. HEK293T cell lysate was incubated with glycogen prior to the glycan pulldown assay (Figure 3.9). EDI3 could be detected in the pellet fraction in lysate from HEK293T cells transfected with EDI3-3xHA. However, EDI3-W32A-3xHA showed no binding, and EDI3-ΔCBM20-3xHA revealed a weak signal in the pellet. There was no EDI3 signal in the pellet when lysates from cells transfected with the empty vector was used. The ERK signal was only found in the supernatant for all samples.

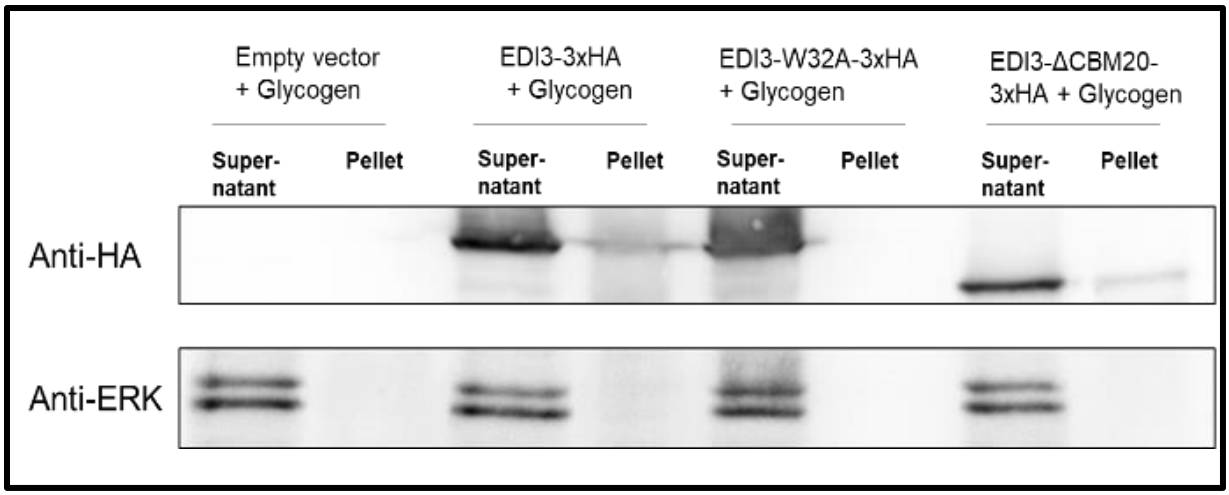

Figure 3.9 **Mutant EDI3 co-precipitates less with glycogen compared to wild type EDI3.** Representative western blot image of a glycan pulldown. Full cell lysates (400 µg/ml) of HEK293T cells transfected with pCR-CMV-EDI3-3xHA, EDI3-W32A-HA, EDI3-ΔCBM20-3xHA or empty vector were incubated with 2 mg glycogen for 1 h and then centrifuged for 1.5 h at 100000 g at 4°C. Proteins of the concentrated supernatant and the washed pellet were analysed by western blotting.

In conclusion, this experiment provides initial evidence that EDI3 also binds glycogen, and that an intact CBM20 domain is important for this binding.

3.2.3 EDI3 expression negatively correlates with glycogen levels in breast cancer cell lines

Since the initial studies suggested that EDI3 binds the carbohydrates, amylopectin and glycogen *in vitro*, the subsequent step aimed to understand the functional consequence of this binding, by first identifying suitable cell culture models.

In a first step, glycogen levels were measured in different breast cancer cell lines using a commercially-available glycogen assay. Cell lysates from MCF7, T47D, BT474, SKBR3 and HCC1954 cell lines were treated with and without amylase to metabolize all the cell's glycogen content to glucose. Free glucose was oxidized and the released H_2O_2 induced in a colour change in an added substrate which could be quantified as an indicator of glucose content. With this assay, both glycogen and free glucose could be determined.

The data show that glycogen levels vary in the different cell lines, where high glycogen levels were observed in the T47D, MCF7 and BT474 cells compared to the HCC1954 and SKBR3 cells (Figure 3.10.B). Furthermore, the ratio (Figure 3.10.C) of free glucose (data not shown) to the glycogen levels (Figure 3.10.B) show that HCC1954 and SKBR3 cells appear to be more glycolytic (values <1) compared to the other three cell lines (values >1). Interestingly, the more glycolytic cell lines (high glucose/glycogen ratio) expressed higher levels of EDI3 (Figure 3.10.A) compared to the lower glycolytic cells (T47D, MCF7, BT474).

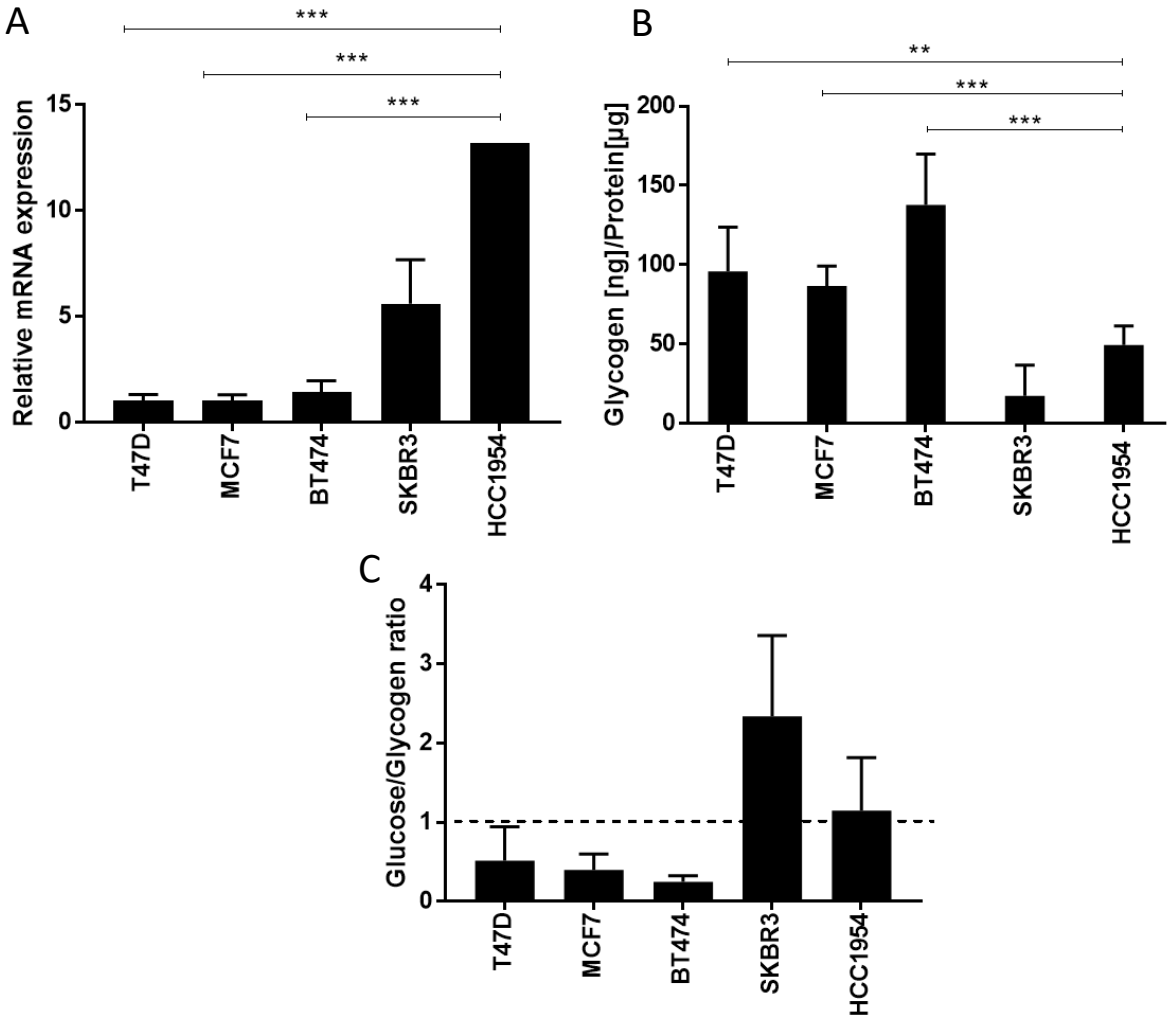

Figure 3.10 **High *EDI3* gene expression correlates with low glycogen levels**. **A,** EDI3 mRNA expression normalized to β-Actin in five breast cancer cell lines and **B,** the corresponding glycogen levels normalized to total protein content. Cells were cultivated in high glucose media, lysed and then treated with or without glucoamylase for 30 min. Via a colourmetric reaction the glucose and glycogen levels were measured in the different cell lines. Protein concentration was determined via bicinchoninic acid (BCA). **C,** Glucose to glycogen ratio calculated from the values obtained from the glycogen assay performed in **B**; the area above the line indicates a glucose ratio >1. (N=3) *** indicates $p < 0.001$.

In summary, glycogen could be detected in all investigated cell lines; however, the levels differ. Importantly, there is a negative association between EDI3 expression glycogen levels, where high *EDI3* mRNA expression is associated with low glycogen levels, suggesting that EDI3 might be needed for glycogen degradation.

3.2.4 EDI3 does not bind STBD1 in breast cancer cell lines

After identifying an inverse relationship between EDI3 expression and glycogen levels in cells *in vitro*, and verifying detectable glycogen levels in all cell lines, the next step aimed to determine whether there is an interaction between EDI3 and glycogen in cells. For further experiments, the MCF7 and the HCC1954 cell line were selected. Both cell lines express EDI3

and contain glycogen; however, as shown above, there was an inverse relationship between the two.

Since classical methods to detect glycogen, such as periodic acid schiff staining, are not suitable for cell culture (Jiang et al. 2010), an indirect approach was used by investigating the binding of EDI3 to known proteins that bind glycogen. Thus, cells were transiently transfected with plasmids containing EDI3 and STBD1, since the latter has been suggested to be a glycogen reporter protein (Skurat et al. 2017), and co-localization was investigated.

MCF7 and HCC1954 cells were co-transfected with pRP-CAG-EDI3-turboRFP and pRP-CMV-STBD1-GFP plasmids, treated with or without glucose for 6 hours prior to fixation and analysed with confocal microscopy. The images indicated that in both cell lines STBD1 localized to the perinuclear region that were enlarged to several micrometres in diameter (Figure 3.11, left panel). This pattern decreased under glucose starvation, and for example, in HCC1954 cells, smaller punctuated spots were observed throughout the cytoplasm. These staining patterns reflect what was reported in the literature suggesting that STBD1 is a good indicator of glycogen in the cell.

In contrast to the pattern seen for STBD1, EDI3 illustrated a diffuse cytosolic distribution in both cell lines (Figure 3.11, middle panel). No punctate staining could be detected, and no changes in localization could be identified upon glucose starvation, as reported for STBD1 and laforin (Singh et al. 2012). Rather, EDI3 remained cytoplasmic upon glucose starvation. Furthermore, no interaction could be visualized with STBD1-GFP (Figure 3.11, right panel). STBD1 is properly linked to a cell organelle since the EDI3 and the STBD1 staining is completely separated.

These results suggest that EDI3 is located in the cytoplasm and is not altered by glucose depravation. Furthermore, the images showed no evidence of co-localization between EDI3 and STBD1 in MCF7 and HCC1954 cells. Considering that STBD1 has been proposed as an indicator for glycogen binding, these data suggest that EDI3 does not bind glycogen in the studied cell lines.

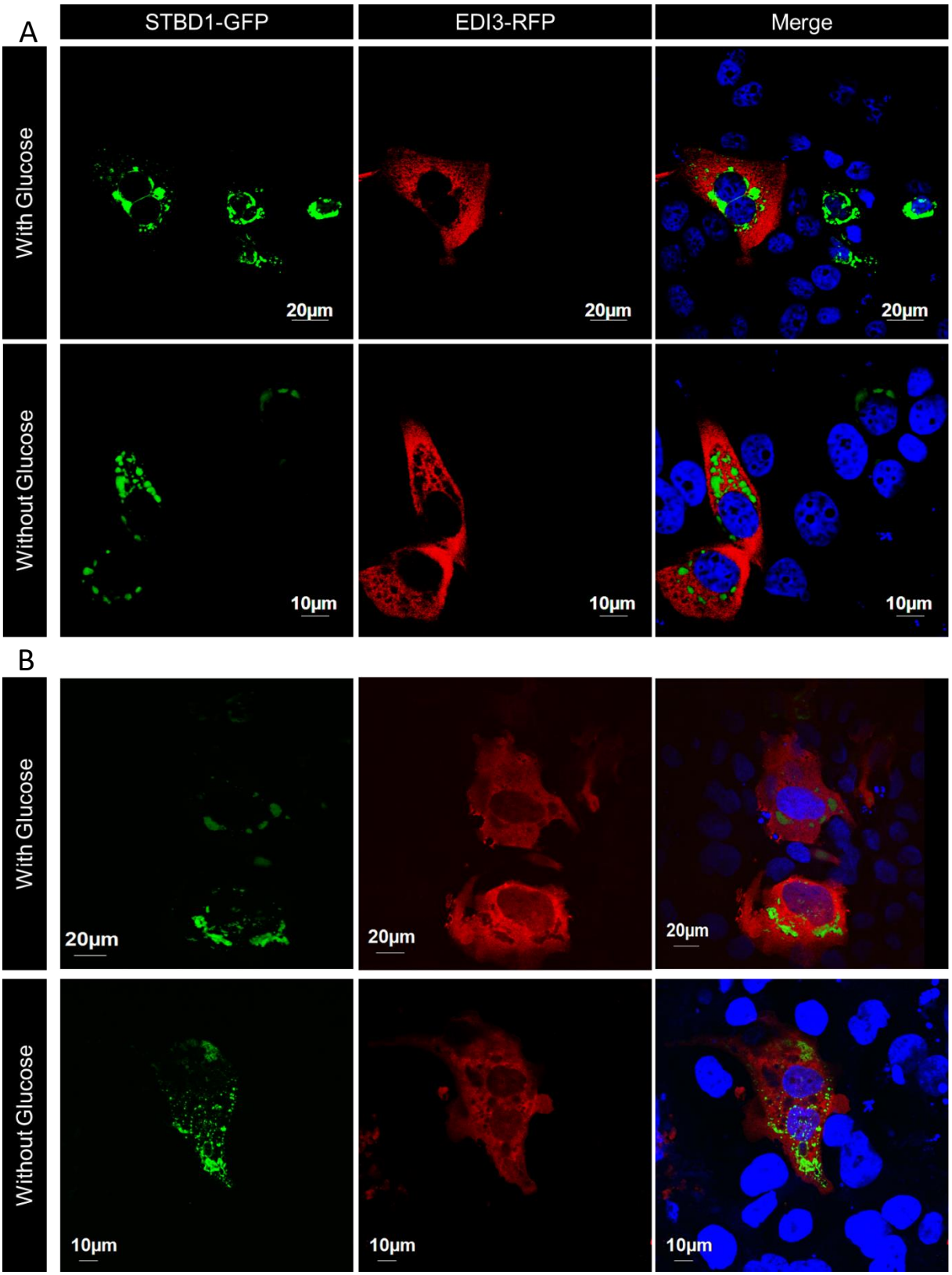

Figure 3.11 **EDI3 and STBD1 do not interact with each other in breast cancer cell lines**. **A,** MCF7 and **B,** HCC1954 cells were transfected with EDI3-turbo RFP and STBD1-GFP. After 24 h, media was changed to glucose free media, or normal glucose containing media. After 6 h cell were fixed in 4%PFA, the nuclei were stained with DAPI (blue), and the cells imaged on a confocal microscope. Representative images of 3 independent transfections

3.2.5 Glycogen levels in breast cancer cell lines are not affected by reduced *EDI3*-levels

Previous studies have suggested that both laforin and STBD1 have a potential role in glycogen degradation (Solaz-Fuster et al. 2008; Zhu et al. 2014). The transfection of the laforin-malin complex into a rat hepatoma cell line decreased glycogen levels, and STBD1 showed increased binding to glycogen-associated proteins during glycogenolysis.

To investigate its role in glycogen depletion, *EDI3* was silenced in MCF7 cells and HCC1954 (HCC1954_shEDI3) cells using siRNA oligos and an inducible shRNA vector, respectively. Three days after silencing, the cells were starved in glucose-free media for 0 h, 1 h, 3 h and 24 h, and then glycogen levels were determined (Figure 3.12.A, C). To verify the knockdown efficiency, RNA was collected from all conditions and analysed via real-time PCR and normalized to β-Actin (Figure 3.12.B, D).

In MCF7 cells, reduced levels of EDI3 using two independent oligos (Figure 3.12 A) showed no significant change in glycogen abundance compared to full media or cells transfected with non-targeting siRNA (NEG). During glycose deprivation, the glycogen levels decreased from 78 (+/- 7.2) ng glycogen to 7.5 (+/- 4) ng per µg protein after 24 h. However, the glycogen levels were not altered during the different periods of glucose starvation after EDI3 knockdown compared to the respective control (Figure 3.12 A, B). In HCC1954_ shEDI3 cells, EDI3 downregulation was controlled by the addition of doxycycline, showing a 70% decrease in RNA expression after 72h incubation (Figure 3.12.C). In contrast to the MCF7 cells, the HCC1954_ shEDI3 cells showed lower glycogen levels, which completely degrades after 1 h of glucose starvation. Later time points (3 h, 24 h) showed no recovery of glycogen levels (Figure 3.12.D).

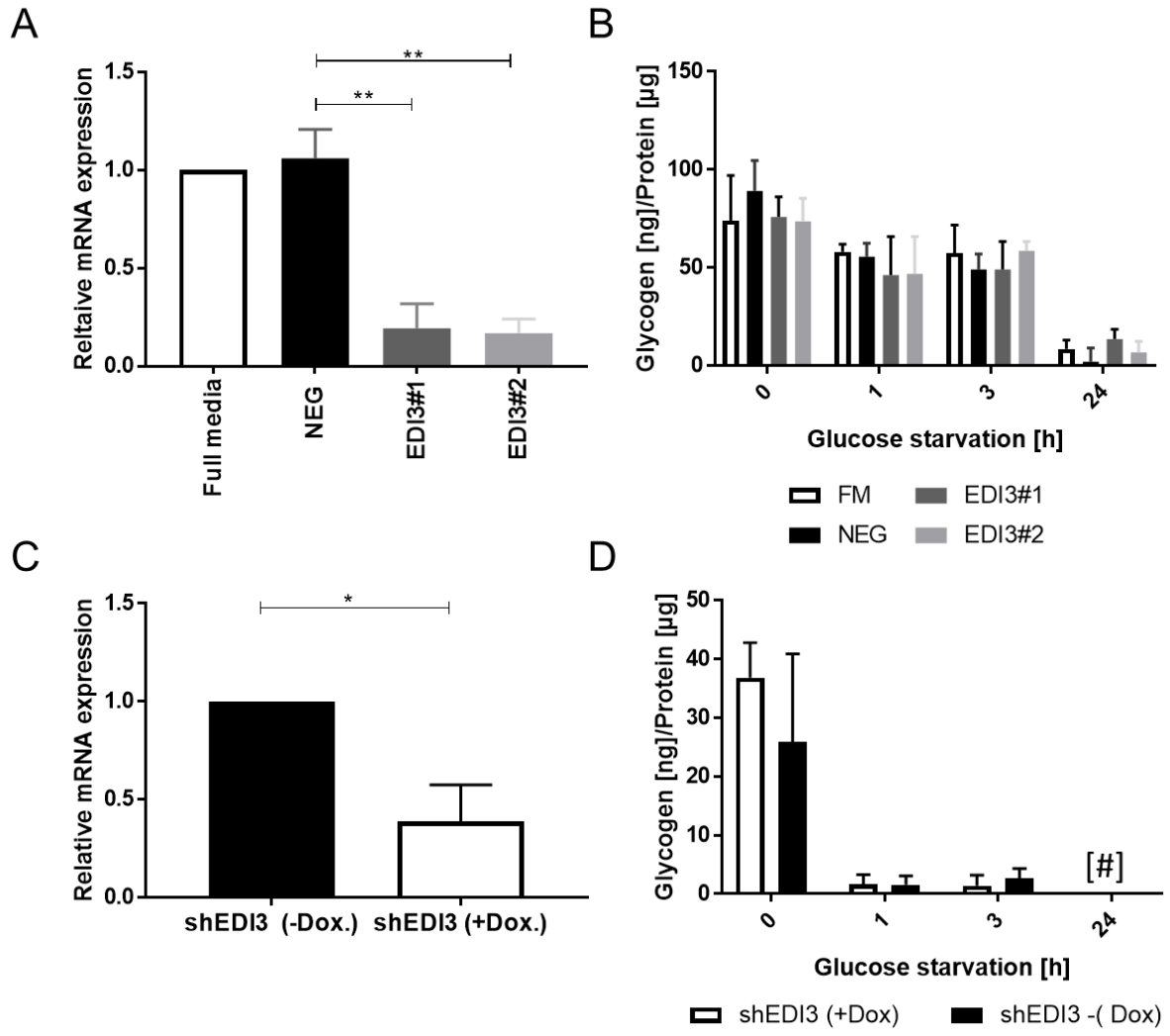

Figure 3.12 **Reducing *EDI3* gene expression does not influence glycogen levels in MCF7 or HCC1954 cell lines.** MCF7 were transfected with two different siRNA oligos (EDI3#1 or EDI3#2) or a non-targeting siRNA sequence (NEG), and HCC1954 cells were treated with 0.5 µg/ml tetracycline to induce the transient knockdown in HCC1954. After 3 d, RNA was collected and then cells were deprived of glucose for 1 h, 3 h, 6 h and 24 h. Glycogen levels were determined using the glycogen assay as described above. **A** and **C,** show RNA levels in MCF7 and HCC1954 cells respectively; **B** and **D,** Corresponding glycogen levels of MCF7 and HCC1954 cells after EDI3 reduction and glucose starvation. Corresponding EDI3 mRNA levels were collected in a separate plate, normalized to β-Actin. (N=3) * indicates $p < 0.05$, ** indicates $p < 0.01$, # under detection limit.

This set of experiments suggests that EDI3 levels have no influence on glycogen concentration in the investigated cell lines, neither in depletion nor in production, regardless of the basal levels of glycogen or endogenous expression of EDI3 in the cells.

3.3 EDI3 in liver

Since neither glycogen binding in cell culture nor an influence of EDI3 on glycogen levels in different breast cancer cell lines could be observed, it is possible that the binding affinity of EDI3 to glycogen is too low. It is plausible that a weak interaction may be observed if EDI3 and glycogen are artificially forced together in high concentrations, such as like in the glycan pulldowns shown above (3.2.1 and 3.2.2). In cancer cell lines, the glycogen levels may be endogenously too low compared to glycogen-relevant organs, such as liver, muscle and brain, making it difficult to observe binding of EDI3 to glycogen with conventional methods. Thus, in the next chapter, the role of EDI3 in glycogen metabolism in isolated hepatocytes will be investigated.

3.3.1 Glucagon influx increases *EDI3* gene expression in mouse hepatocytes

Primary mouse hepatocytes (PMH) were treated with glucagon and insulin to stimulate glycogen breakdown and production, respectively, and the effect on *Edi3* expression and protein levels is investigated. PMHs from 8 week old male C57BL/6N mice were seeded and cultivated overnight, and then treated with 10 nM, 100 nM or without glucagon for 1 h, 3 h, 6 h and 24 h. After each time point protein and RNA were collected and analysed.

In response to both 10 nM and 100 nM glucagon, *Edi3* gene expression, normalized to *Eif2α*, increased 5-fold (3 h time point) and 7-fold (6 h) compared to the samples without glucagon treatment (Figure 3.13.A). After 24 h, the mRNA expression decreased once more to the control level (Figure 3.13.A). Similar increases were seen at protein levels where 6 h after glucagon addition, Edi3 protein expression increased 2-fold compared to the untreated control normalized to the β-actin (Figure 3.13.C, D). To validate that the glucagon treatment was successful, the gene expression of *Pck1,* which encodes for the Phosphoenolpyruvate carboxykinase (Pepck1) protein, a cellular marker for gluconeogenesis, was investigated. The highest increase in *Pck1* expression was detected after 3 h, and unlike *Edi3*, did not decrease after 24 h (Figure 13.3.B). In addition, phosphorylation of cAMP response element-binding protein (Creb) at position S133 also supported the influence of glucagon on gluconeogenesis.

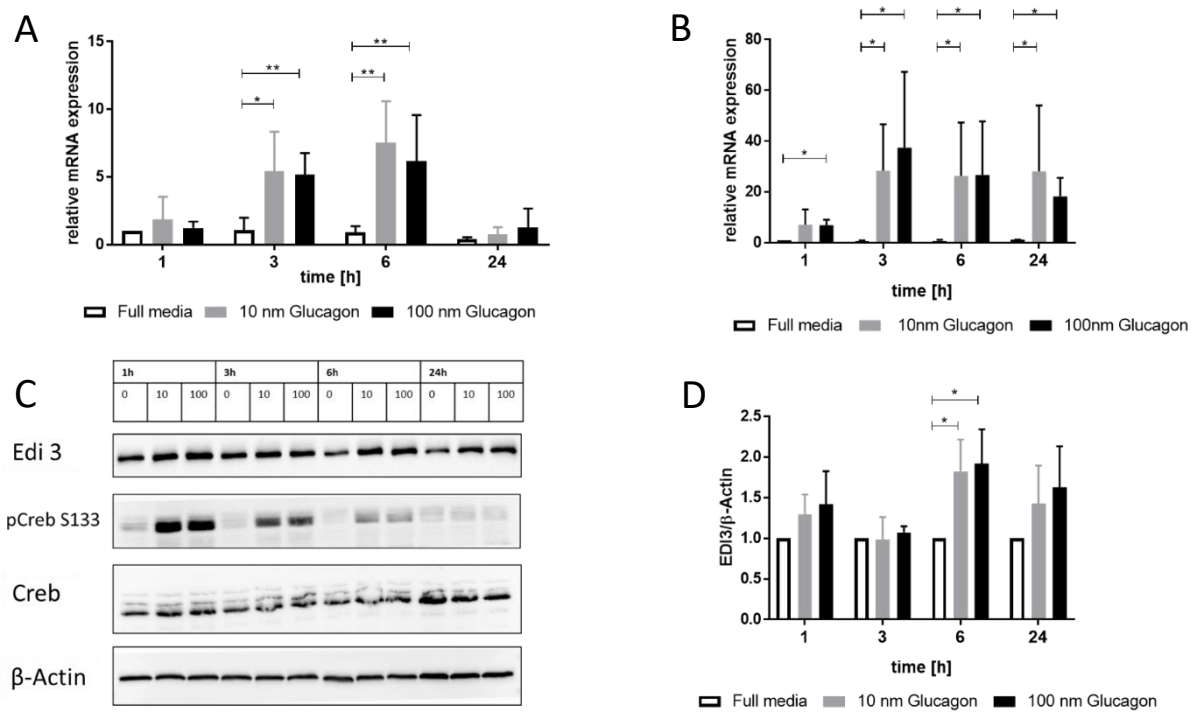

Figure 3.13 **Treating primary mouse hepatocytes (PMHs) with glucagon increases *Edi3* gene expression Edi3 protein levels significantly.** PMHs were plated in a collagen bilayer and treated with 0 nm, 10 nM or 100 nM glucagon for 1 h, 3 h, 6 h, and 24 h. After each point of time RNA and protein was collected for analysis. **A**, *Edi3* gene expression after glucagon treatment over time in PMHs normalized to the housekeeping gene, Eif2a. **B,** corresponding *Pck1* gene expression normalized to *Eif2a*. **C,** representative western blot image of proteins analysed after glucagon challenge. Analysed proteins are Edi3, β-actin, cAMP response element-binding protein (Creb) and corresponding phosphorylation at S133 over time. **D,** Densitrometric analysis of Edi3 protein expression normalized to β-actin. (N=3) * indicates $p < 0.05$, ** indicates $p < 0.01$.

In addition to investigating the effect of glycogen breakdown on *Edi3* expression, the effect of glycogen production with insulin on *Edi3* expression was further investigated by treating PMHs with 0 nM, 10 nM or 100 nM insulin. Protein and RNA were collected and analysed. Insulin had no effect on *Edi3* gene expression or Edi3 protein levels normalized to *Eif2a* (for RNA) (Figure 3.14.A) or β-actin (for protein). Phosphorylation of S473 of Akt was measured to confirm the activation of intracellular signalling by insulin (Figure 3.14.B).

Both experiments could show that glucagon, but not insulin alters the expression of Edi3 levels in primary mouse hepatocytes, suggesting a role for Edi3 in liver metabolism. Furthermore, the upregulation of *Edi3* after 3 h and the simultaneous increase of *Pck1* suggest a potential role in gluconeogenesis.

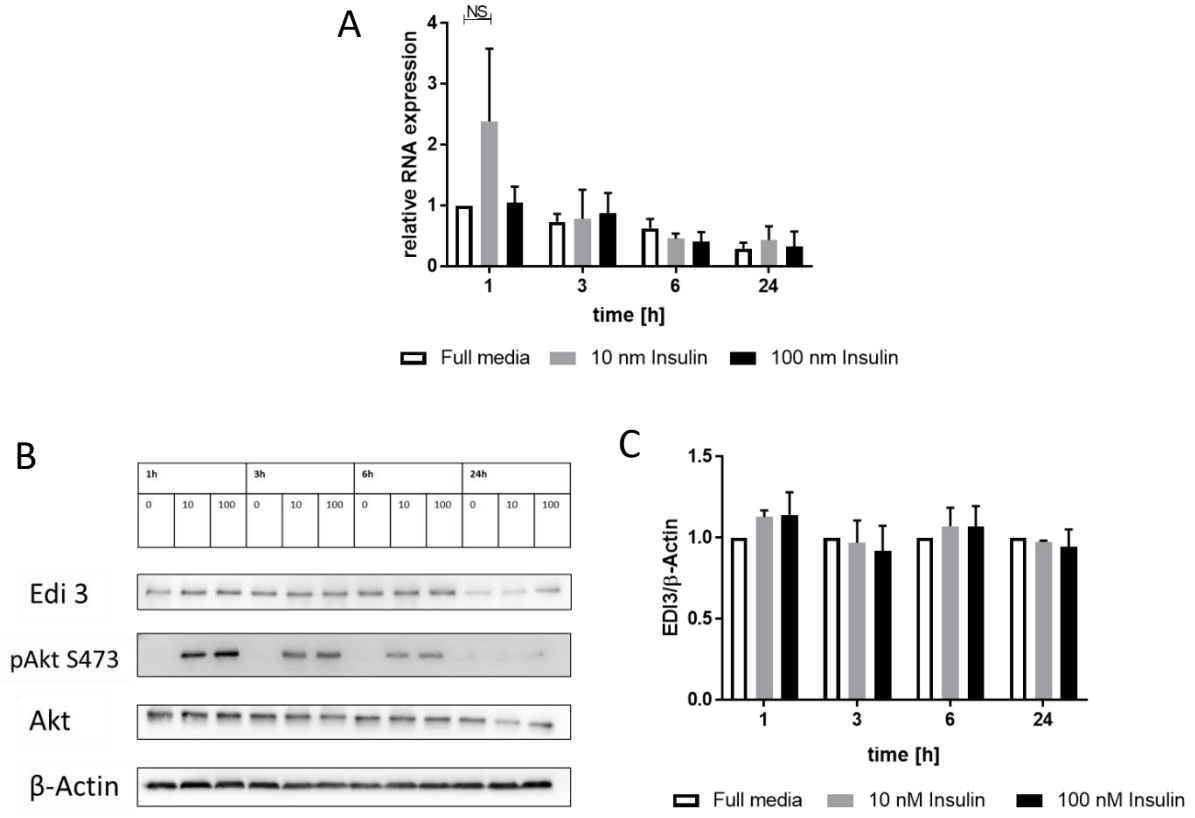

Figure 3.14 **Addition of insulin does not influence Edi3 levels.** Primary mouse hepatocytes were treated with 0 nM, 10 nM or 100 nM insulin for 1 h, 3 h, 6 h and 24 h. After each point of time RNA and protein was collected and analysed. **A,** *Edi3* gene expression over time normalized to *Eif2a*. **B,** representative western blot image of analysed proteins after insulin addition. Proteins analysed are Edi3, β-actin, protein kinase A (Akt) and corresponding phosphorylation at S476 at different points of time. **C,** Densitrometric analysis of the Edi3 normalized to β-actin. (N=3) NS= not significant

3.3.2 EDI3 associated metabolites decrease after glucagon treatment

After observing increased Edi3 levels in primary mouse hepatocytes after glucagon addition, the link between Edi3 and gluconeogenesis may be via the cleavage product of Edi3, Glycerol-3-Phosphate. Via G3P-dehydrogenase (G3PDH) G3P can be further metabolized to dihydroxyacetonphosphate (DHAP) which is a major player in gluconeogenesis. So far Edi3 is the only known protein that enzymatically cleaves intracellular GPC to Glycerol-3-phosphate (G3P) and choline (Stewart et al. 2012). The role of choline and choline associated metabolites during glucagon challenge is not well described in literature and might also be altered. To further understand the role of Edi3 in mice, the Edi3 related metabolites (GPC, choline and PCho) were analysed during glucagon challenge in PMHs via LC/MS and normalized to protein (Figure 3.15).

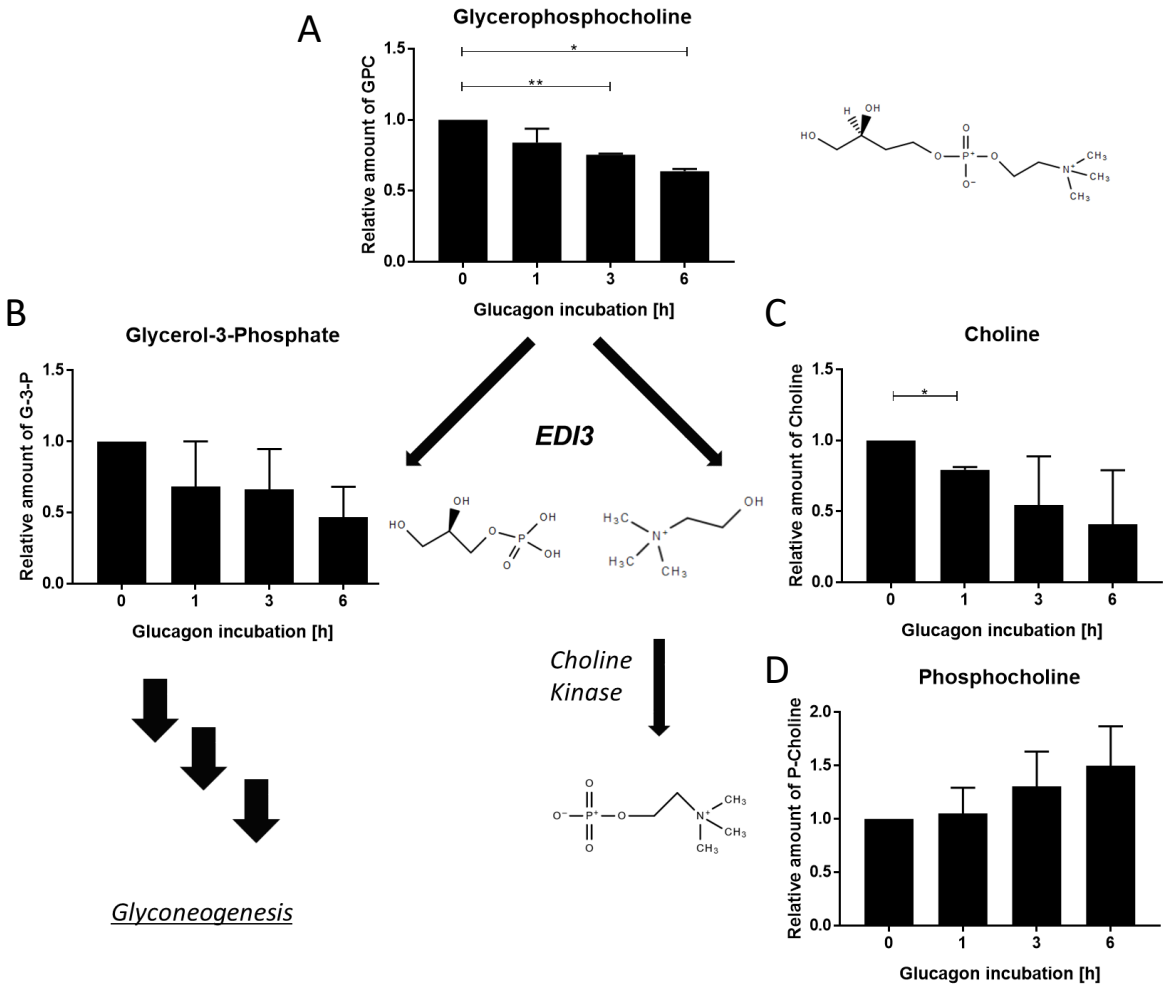

Figure 3.15 **Edi3 associated metabolites decrease after glucagon challenge.** Hepatocytes from male C57BL6 mice were isolated and incubated with 10 nM glucagon for 0 h, 1 h, 3 h and 6 h. Intracellular metabolites were collected in methanol, spiked with internal standard and measured via LC-MS/MS. **A,** Glycerophosphocholine **B,** Glycerol-3-Phosphate **C,** Choline **D,** Phosphocholine were normalized to the 0 h glucagon time point, structural formula of the metabolites are included (N=2 with 5-6 technical replicates) * indicates $p < 0.05$, ** indicates $p < 0.01$.

There was a significant reduction in GPC levels during glucagon stimulation after 3 and 6 h. Nevertheless, after 6 h around 60% of the total GPC was still present in the cells. Interestingly, the concentration of Edi3 products, G3P and choline decreased, albeit insignificantly in a time dependent manner compared to the untreated control samples. Conversely, an increase in phosphocholine was observed, with a 50% increase after 6 h glucagon stimulation compared to control.

3.3.3 Glucagon does not influence the EDI3 levels in primary human hepatocytes

In the previous experiments it could be proven, that Edi3 is influenced by glucagon on RNA and protein level, which were reflected in alterations in choline-relevant metabolites. To determine whether the changes were relevant for humans, primary human hepatocytes (PHHs) from different donors (regardless of gender and BMI status) were investigated. Further

donor information can be found in the supplementary data (6.2.1). PHHs were cultivated as described above and challenged with 10 nM glucagon. RNA and protein after 1 h, 3 h, 6 h, and 24 h were collected and further analysed.

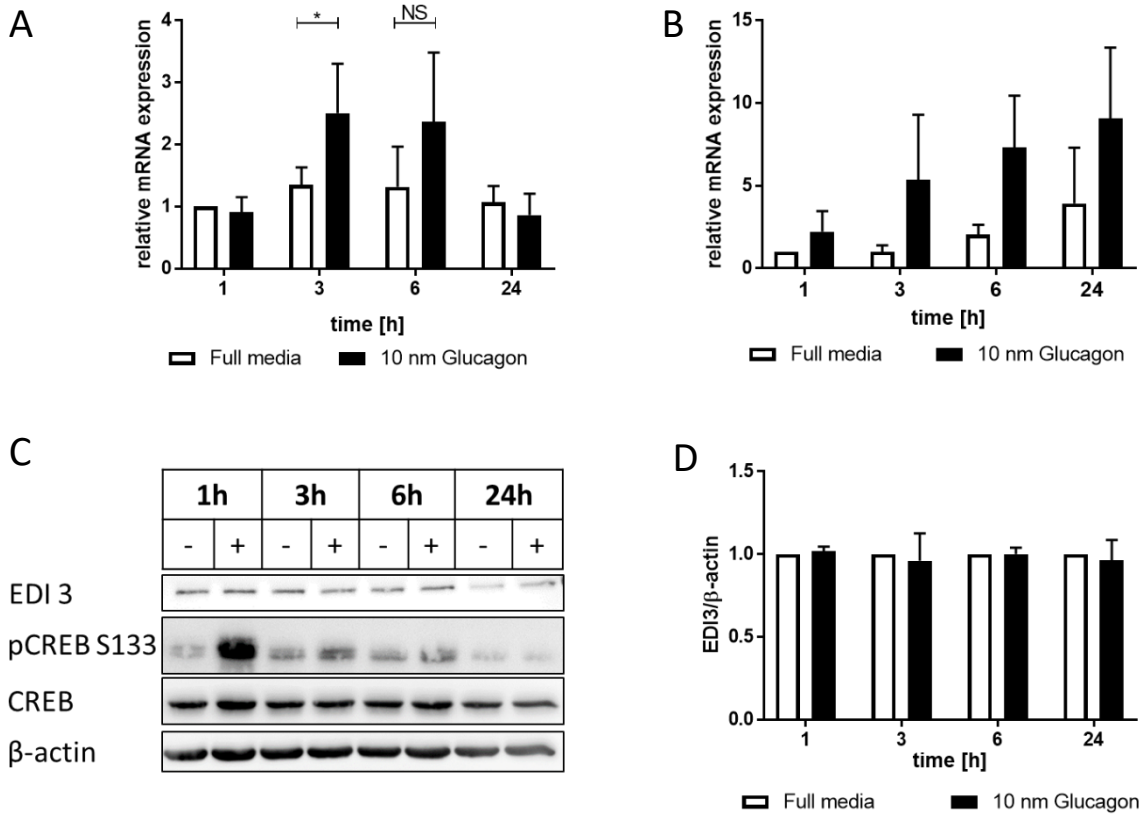

Figure 3.16 **Challenging primary human hepatocytes (PHHs) with glucagon has no effect on EDI3 expression.** PHHs were treated with 0 nm, 10 nM glucagon for 1 h, 3 h, 6 h, and 24 h. At each time point RNA and protein was collected and analysed. **A**, *EDI3* gene expression over time after glucagon addition in PMHs normalized to the housekeeping gene *EIF2A*. **B,** corresponding *PCK1* gene expression normalized to *EIF2A*. **C,** Representative western blot image of analysed proteins after glucagon challenge. Analysed proteins are EDI3, β-actin, cAMP response element-binding protein (Creb) and corresponding phosphorylation at S133 over time. (+) indicates 10 nM Glucagon (-) indicates no glucagon. **D,** Densitrometric analysis of the EDI3 protein translation normalized to β-actin. (N=4) * indicates $p < 0.05$

EDI3 gene expression in the PHHs increased two-fold compared to the unchallenged control upon glucagon treatment (Figure 3.16.A). This increase was significant at the 3 h, but not at the 6 h. EDI3 protein levels however remains unchanged after glucagon treatment (Figure 3.16.C, D). An increase in *PCK1* RNA expression (Figure 3.16.B), and phosphorylation of CREB at position S133 (pCREB) after glucagon treatment verified that PHHs were responsive to glucagon (Figure 3.16.C). The amount of CREB itself remains unchanged (Figure 3.16.C). Therefore, the addition of glucagon to primary human hepatocytes led to a small but significant increase in *EDI3* gene expression, which did not translate to higher EDI3 protein levels, indicating that EDI3 may not be relevant in glucagon-mediated glycogen breakdown in primary human hepatocytes.

3.3.4 EDI3 shows no co-localization with STBD1 in primary human hepatocytes

Although EDI3 was shown to not be directly involved in glycogen breakdown in human hepatocytes, it was nevertheless investigated whether EDI3 was able to bind glycogen and known glycogen-binding proteins in human liver.

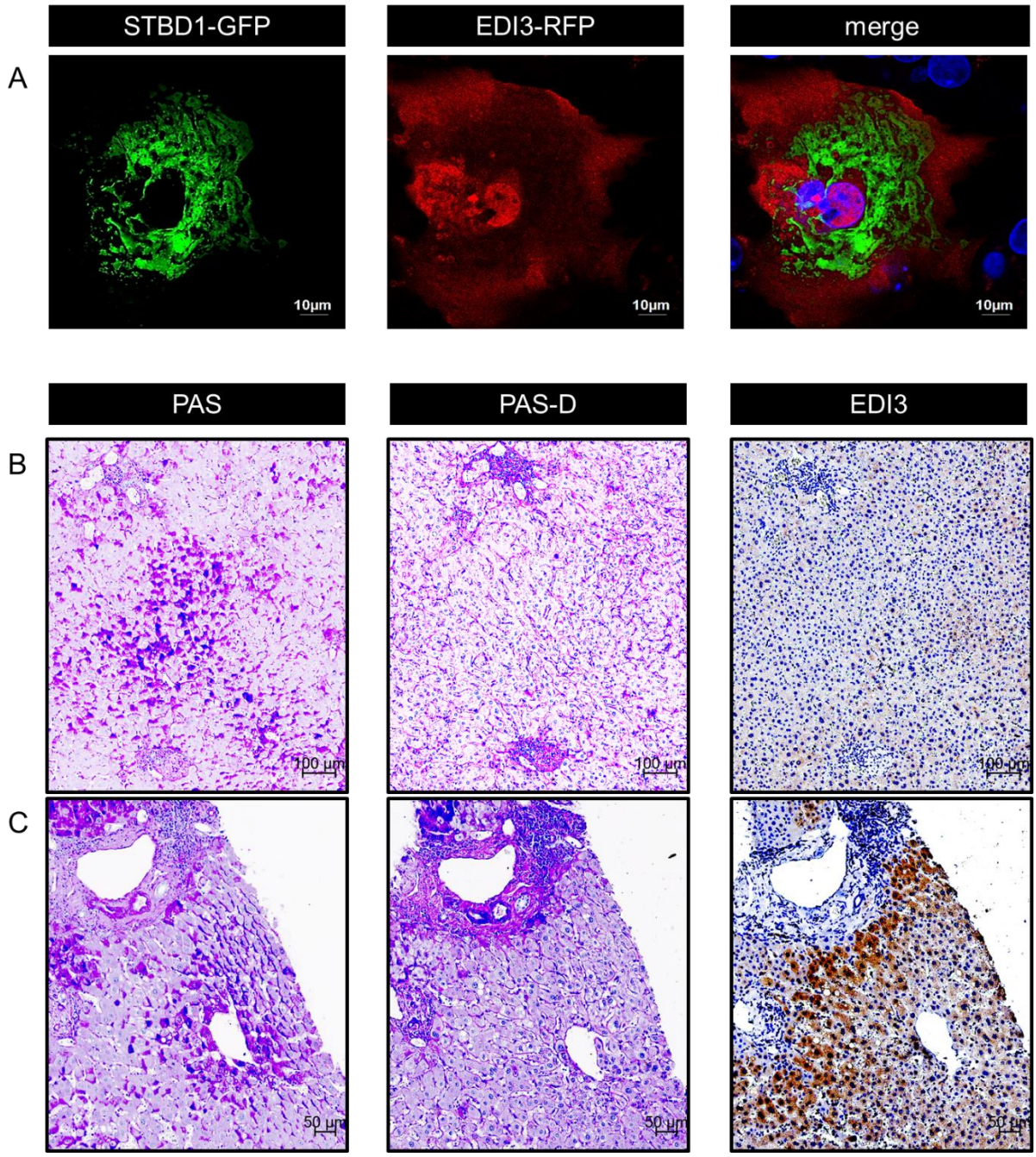

Figure 3.17 **No colocalization of EDI3 and glycogen or glycogen-associated protein in human liver A,** representative image of primary human hepatocytes transfected with pRP-CAG-EDI3-turboRFP or pRP-CMV-STBD1-GFP, showing no co-localization. Nuclei were co-stained with DAPI (N=3) **B,C** PAS staining indicating glycogen in purple (left panel), digest with diastase followed by PAS staining (PAS-D) to show specificity of PAS signal (middle panel), and immunohistological staining of EDI3, detected with 3,3'-Diaminobenzidine (DAB) indicated in brown (right panel). All images were counterstained with Mayer´s Hemalum solution to highlight the nuclei. Stainings were performed in two individual donors.

First, primary human hepatocytes were transfected with EDI3-turboRFP and STBD1-GFP for 48 h, prior to fixation with paraformaldehyde (Figure 3.17.A). No co-localization could be detected between EDI3 and STBD1. EDI3 was localized to both the cytoplasm, as well as the nucleus, whereas, STBD1 was localized to the cellular compartment, but not where EDI3 was located. However, these experiments were performed in cells; therefore to test binding in tissue, the Periodic Acid-Schiff (PAS) reaction and Periodic Acid-Schiff reaction with diastase (PAS-D) were performed in serial sections of paraffin embedded liver from human donors (6.2.2). As Illustrated in Figure 3.17.B and C, the location of glycogen in human liver could be detected with PAS staining, and verified by digesting glycogen with diastase (PAS-D). As indicated in 3.17.B, an accumulation of glycogen within the liver did not co-localize with the signal from the EDI3 antibody. Interestingly, EDI3 was abundant in regions where glycogen was not present (Figure 3.18.C), overall suggesting that EDI3 did not bind glycogen in liver.

Another attempt, how the binding of EDI3 to glycogen was investigated was using the modified glycan pulldown as described in 3.2.1 and 3.2.2. This time instead of pure glycogen, 200 mg from glycogen containing organs, liver and muscle were isolated from male C57BL6 mice. Organs were homogenized, centrifuged at high speed and the proteins from the resulting supernatants and glycogen-containing pellets were analysed by western blot. Erk was used as an example of a protein that does not bind glycogen and should thus be retained in the supernatant fraction. As a protein marker full cell lysate (load) isolated from primary mouse hepatocytes (PMH) was used.

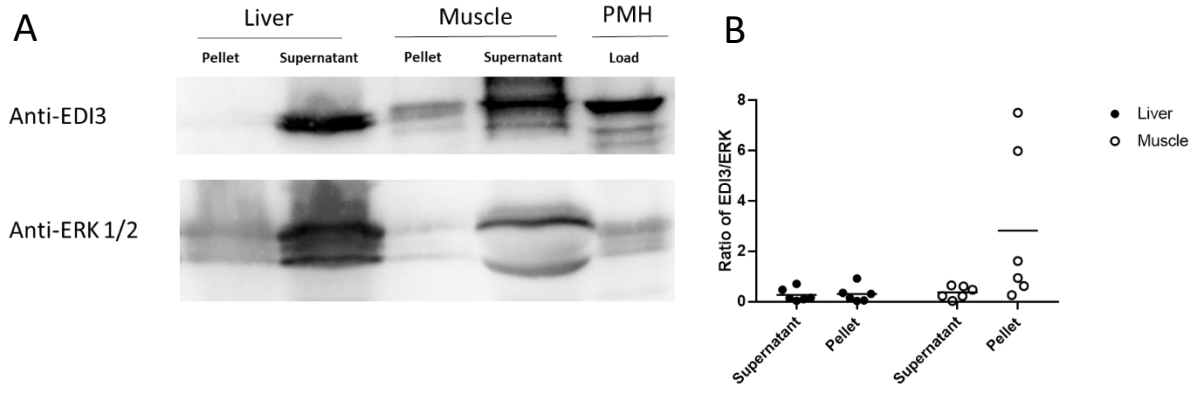

Figure 3.18 **Coprecipitation of Edi3 and glycogen in glycogen-rich mouse organs. A**, Representative image of a glycan pulldown assay performed with mouse liver and muscle. In total, 200 mg liver or muscle were homogenized, centrifuged at 100000 g, and the resulting supernatants and pellets were analysed via western blot for Edi3 and Erk. As a protein marker (load) full cell lysate from primary mouse hepatocytes (PMH) were used. **B,** Densitometric quantification of Edi3 and Erk shown here as a ratio in both the supernatant and the pellet fractions of each organ (N=6) * indicates $p < 0.05$

As demonstrated in Figure 3.18.A, there is a strong band for Edi3 and Erk in the liver supernatant fraction; whereas, no band could be observed in the pellet fraction. As already described in section 3.2.1 and 3.2.2 and also variously described in literature glycogen is sedimented after high speed centrifugation (Lazarow 1942; ORRELL and BUEDING 1964; Wang et al. 2002; Jiang et al. 2010; Díaz et al. 2011). Edi3 in the liver does not bind cell components, such as glycogen, which sediments in the pellet and thus did not precipitate. Once again Edi3 could not be associated with glycogen. Conversely, although there is a strong Edi3 signal in the supernatant fraction of the skeletal muscle, there is a distinct signal in the pellet fraction. Erk, which was used as a protein that does not bind glycogen, was found primarily in the supernatant fraction. To quantify the results, the ratio of the densitrometric Edi3 and Erk signals in the different fractions (pellet and supernatant) was determined and the ratio between the signals was calculated (Edi3/Erk, Figure 3.18.B). A high value indicated that in one fraction a higher amount of Edi3 was found (>1), a low value indicated a higher amount of Erk (<1). Equal amounts (=1) suggested equal amounts of protein in the fractions. The generated data could show that especially in the pellet fraction of skeletal muscle a high Edi3 level could be detected. This indicates that there is more Edi3 in the pellet compared to the supernatant fraction of the muscle tissue. Low or equal levels in both fractions of the liver suggesting that Edi3 is not increased in the liver pellet. Whole cell lysates from PMHs were used to identify the EDI3 protein band.

Overall, the data suggest that EDI3 does not bind glycogen in human liver, as glucagon did not increase EDI3 protein levels in PHHs, and there was no interaction between the glycogen and EDI3 in the pull down assay nor binding to STBD1, or co-localization of EDI3 and PAS-staining. In a glycan pulldown of mouse organs, a binding of Edi3 in liver could not be associated with glycogen binding. However, the pulldown assay suggests co-sedimentation of muscle Edi3 and glycogen, suggesting a possible role for Edi3 in skeletal muscle.

3.4 EDI3 in muscle

After an extensive research to identify a binding of glycogen and EDI3 in human liver and primary hepatocytes, no interaction could be detected. In set of glycan pulldowns a co-sedimentation of glycogen and muscle EDI3 could be found. According to this experiments a binding of EDI3 to glycogen in skeletal muscle is possible. In another attempt to identify a binding of EDI3 and glycogen, the last part of the project was the investigation of EDI3 in human skeletal muscle and identify a binding with glycogen.

3.4.1 EDI3 is high in skeletal muscle type II

EDI3 expression and location was investigated in skeletal muscle obtained from six different donors, both male and female, with various body mass indices (6.2.3). In order to identify the optimal antibody concentration for human skeletal muscle, an antibody titration was performed with the custom made EDI3 3B8G3 antibody (AMS Bio) in donor 1 (6.2.5). For each donor, the skeletal muscle fibre type was determined by staining for Myosin Heavy Chain 7 (MYH7) and Myosin Heavy Chain 2 (MYH2), which detects skeletal muscle type I and type II, respectively. Finally, EDI3 was stained to determine muscle type to which it localized, together with recognized glycogen-binding proteins, glycogen synthase and STBD1.

In Figure 3.19, a representative staining from one donor is illustrated. In the image, there is a clear differentiation between muscle fibers type I (MYH7) and type II (MYH2). Additionally, it could be shown that EDI3 is primarily localized to type II 3.19.A. Interestingly, EDI3 is localized to peripherally located cap-like structures that appears to sit atop or partially encircle the type I skeletal muscle cells. This caps are highlighted by the black arrowheads in 3.19.B and in Figure 3.20.A.

An association of EDI3 to skeletal muscle type II was already made in literature (Hashimoto et al. 2016). Here, the authors postulate that in mice overexpressing the *EDI3Δ471* mutant gene skeletal muscle type II fiber-rich muscle mass was reduced. The cap-like structures have not been described until that point.

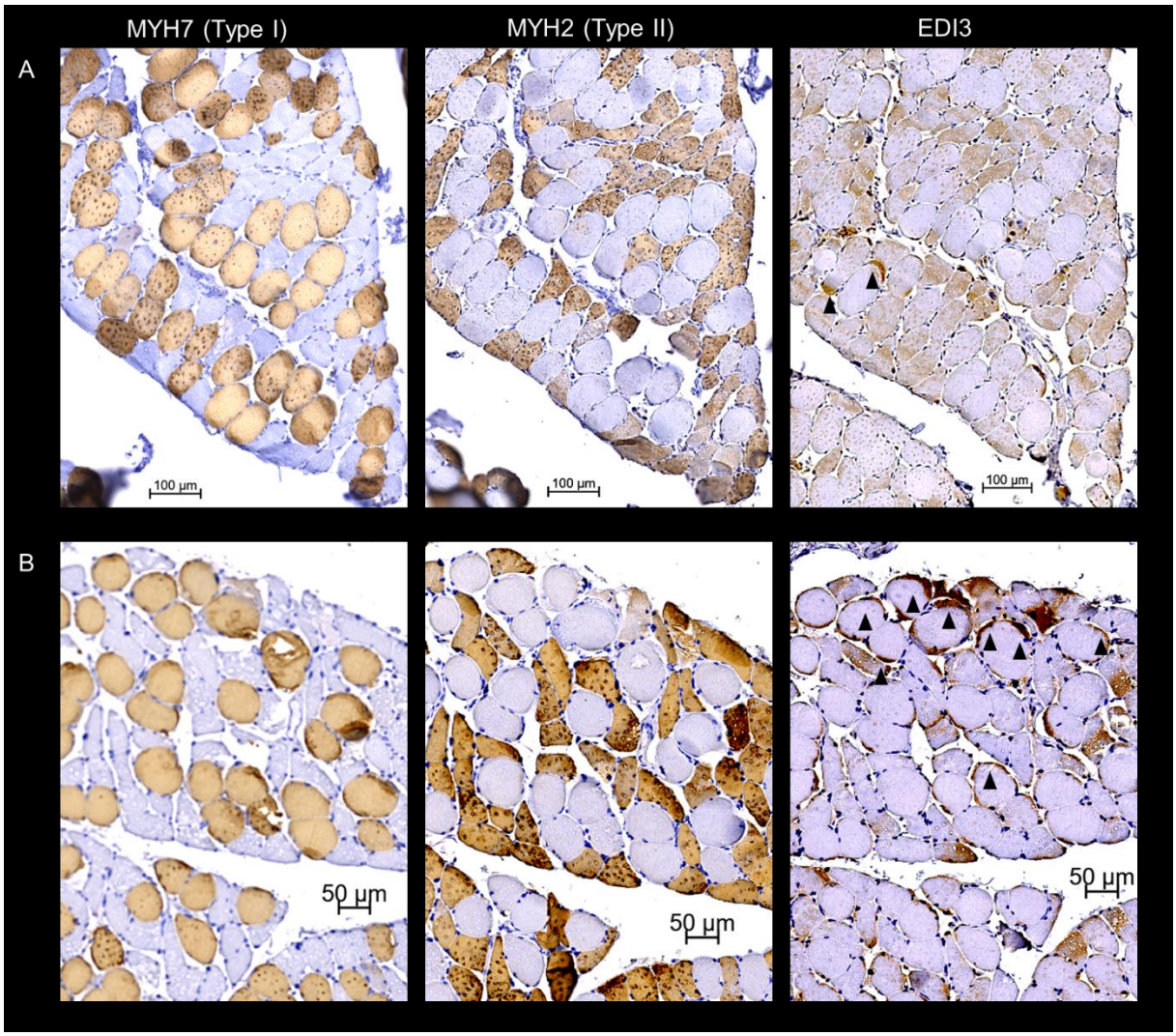

Figure 3.19 **EDI3 is predominantly located in skeletal muscle type II.** Representative immunohistochemical images of human skeletal muscle stained with Myosin Heavy Chain 7 (MYH7) to detect type I fibres, Myosin Heavy Chain 2 (MYH2) to detect type II fibres, and EDI3 antibodies and detected with 3, 3'-Diaminobenzidine (DAB). Cap-like structures, which are positive for EDI3, are indicated with black arrowheads. Stainings were performed in three different donors, two of which are shown here.

3.4.2 EDI3 interacts with glycogen associated proteins in skeletal muscle

One common characteristic of fast glycolytic skeletal muscle type II fibres which distinguishes them from oxidative skeletal muscle type I cells is the high amount of glycogen in type II cells. To find out if EDI3 binds glycogen in this cell type, immunohistochemical analysis was performed in serial sections of human skeletal muscle using antibodies against glycogen synthase 1 (GYS1) and EDI3 (Figure 3.20) and stained with DAB. The results in 3 donors, suggested that there is co-localization between GYS1 and EDI3 as exemplified in Figure 3.20 with two donors. However, although co-localization of both proteins appeared primarily in skeletal muscle type II, it was not limited to these cells.

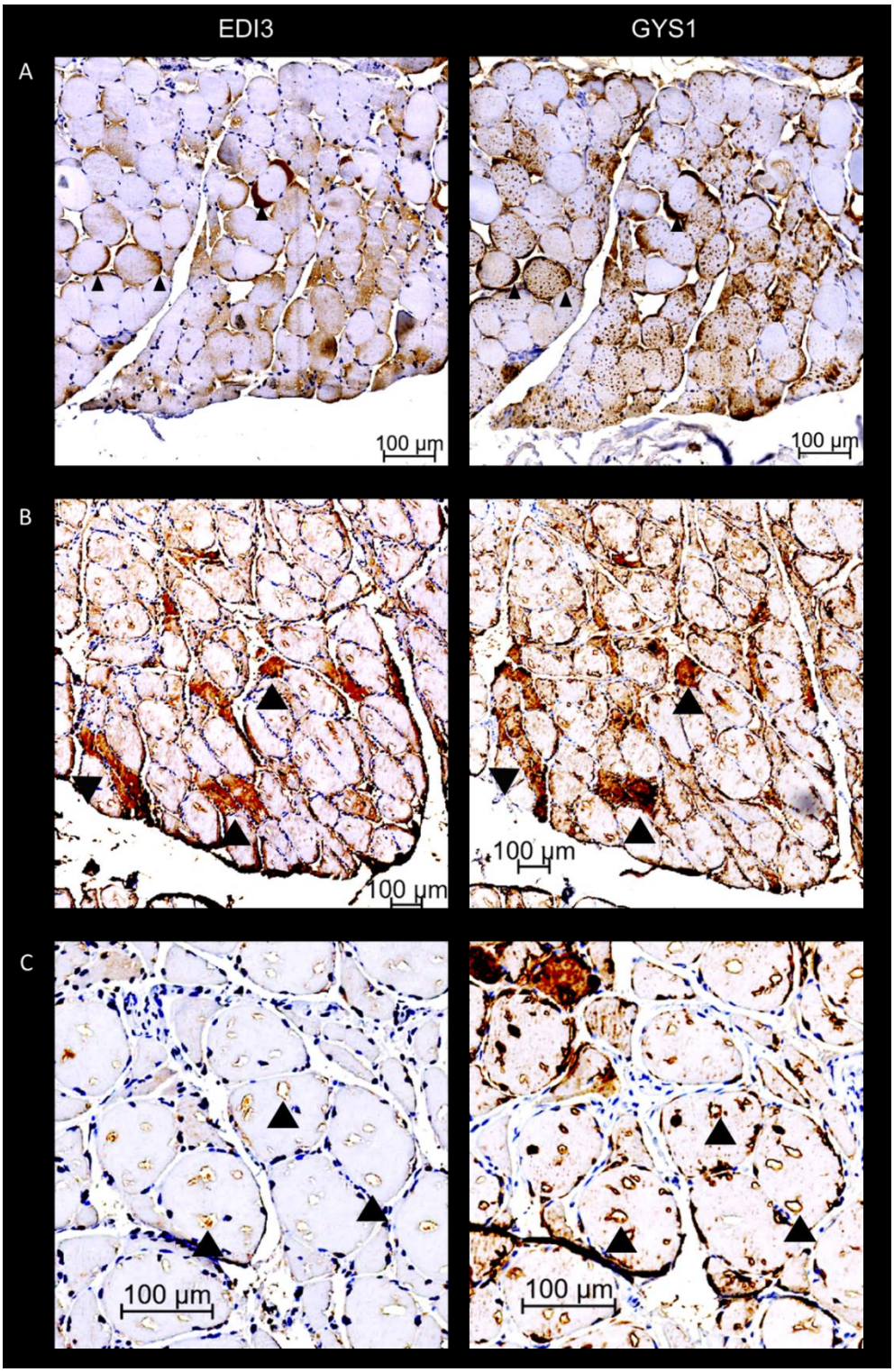

Figure 3.20 **EDI3 co-localizes with glycogen synthase in human skeletal muscle**. Human skeletal muscle serial sections were stained with antibodies against EDI3 and GYS1 and binding detected with 3, 3'-Diaminobenzidine (DAB). Nuclei were stained in blue via haematoxylin. Three patterns of co-localization are seen. **A**, Co-localization appears mainly in the cap-like structures **B**, EDI3 and GYS1 co-localizes within the whole cell **C,** EDI3 and GYS1 co-localizes around a cavity within the cell. For each region showing colocalization some examples (three arrowheads) were shown. Images from 2 donors.

In some cases, co-localization was detected primarily in the cap like-structures (Figure 3.20.A); whereas, in others co-localization was observed either throughout the entire cell (Figure 3.20.B), or in ring-like structures surrounding a cavity (Figure 3.20.C). Next, fluorescent

immunohistochemical staining (IF-IHC) were performed to validate the DAB stainings, co-staining with EDI3 (red) and GYS1 (green).

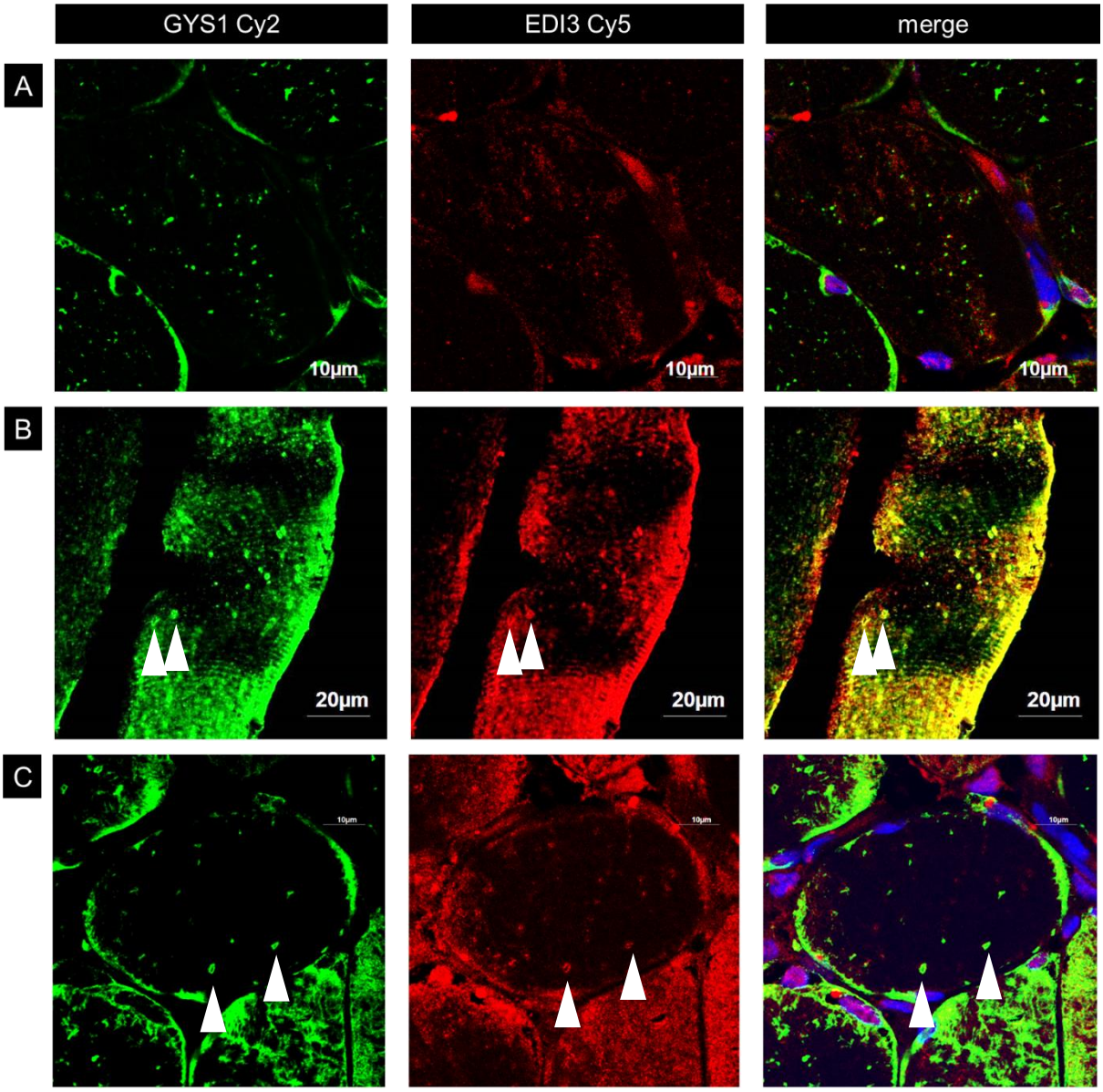

Figure 3.21 **EDI3 co-localizes with glycogen synthase in human skeletal muscle.** Representative images of human skeletal muscle, co-stained with EDI3 (red) and GYS1 (green). Nuclei were stained in blue with DAPI. Co-localization is indicated in yellow, with different patterns and signal strength observed. **A,** weak co-localization of EDI3 and GYS1 within the cell, **B,** strong co-localization throughout the cell (and along the fibers), as well as co-localization around a cavity structure (white arrowhead) and **C,** no obvious co-localization inside the cell, but co-staining around cavity structure (white arrowheads). Images from 2 donors.

Two donors were co-stained, and while they both show co-localization (Figure 2.21) the intensity of the co-localization differs. The findings already observed in the DAB stainings could be confirm, depending on the donor strong or weak co-localization could be detected. The circle round staining which surrounds the cavity could be detected in both donors (Figure 3.21.B, C).

The results thus far indicate that glycogen synthase 1 – a known glycogen binding protein - is a potential binding partner of EDI3, suggesting that EDI3 may itself bind glycogen in skeletal muscle. Therefore, to confirm that the interaction of EDI3 to glycogen synthase 1 is related to glycogen, a second glycogen-binding protein - starch binding domain containing protein 1 (STBD1) - was chosen. In addition to addressing a potential association with glycogen, an interaction of EDI3 with STBD1 would confirm possible heterodimerization/interaction among CBM20 family members. For this experiment, human skeletal muscle was co-stained with EDI3 and STBD1 antibodies, and immunoprecipitation analyses performed with EDI3-HA and STBD1-FLAG constructs.

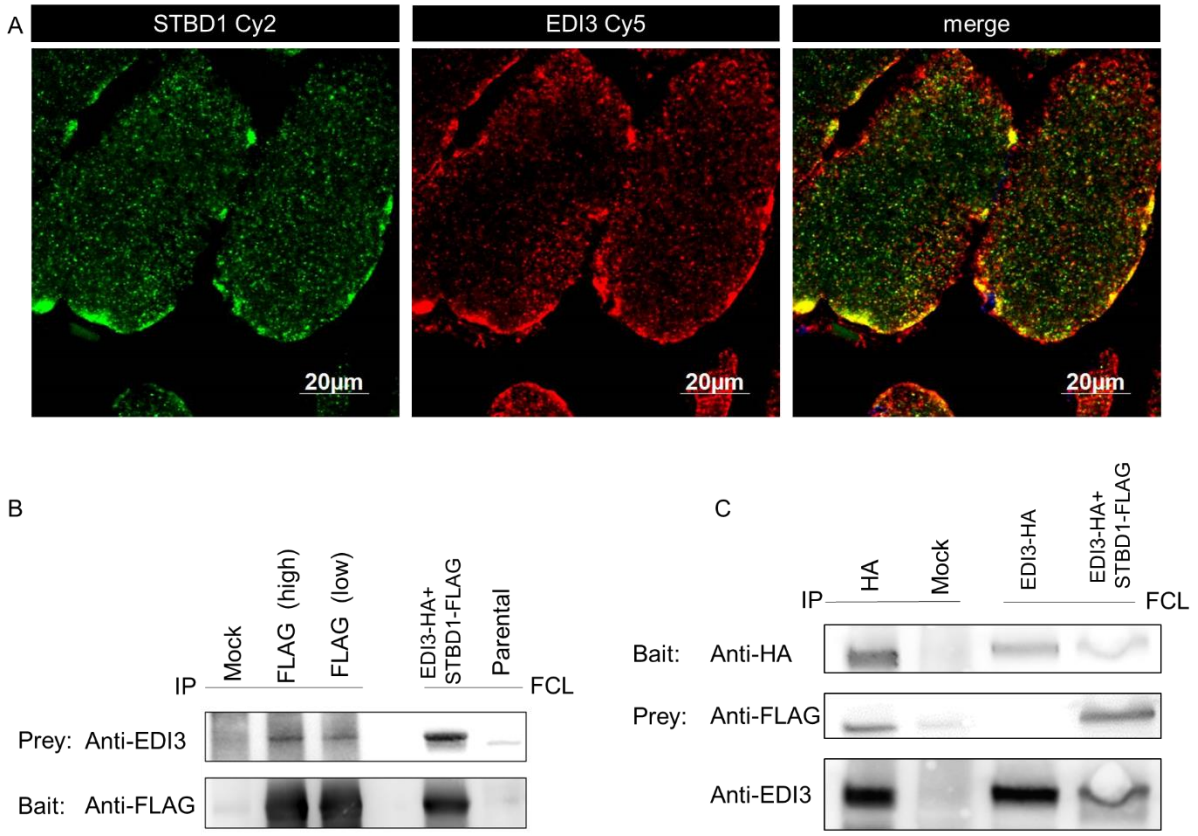

Figure 3.22 **EDI3 interacts with STBD1 in human skeletal muscle. A,** Representative image of EDI3 (red) and STBD1 (green) co-staining in human skeletal muscle. Co-localization is indicated in yellow. **B and C,** Immunoprecipitation (IP) experiments performed in HEK293T cells transfected with plasmids containing EDI3-3xHA and STBD1-3xFLAG and lysed after 48 h. **B,** Magnetic beads linked to different amounts of FLAG (low=3 µl, high=7 µl) or unspecific IgG antibody (Mock, 7 µl) were incubated with the cell lysate. Protein bound to the beads was separated at 95°C and EDI3-3xHA (bait) and STBD1-3xFLAG (prey) protein were analysed via western blot. Full cell lysates (FCL) of the transfected and parental cells are also shown. **C,** Magnetic beads were linked to HA-Antibody (5 µl) or Mock (5 µl). Bait protein is EDI3-3xHA, prey protein is STBD1-3xFLAG. Additional FCLs with EDI3-3xHA and STBD1-3XFLAG co-transfection or EDI3-3xHA alone are shown as controls. B and C (N=2)

Co-localization of EDI3 and STBD1 could be observed, especially in the sarcolemma, close to the cellular membrane (Figure 3.22.A). A weak interaction was also observed inside the cell (Figure 3.22.A), where both antibodies showed dot-like structures that were mostly red or green, indicating no co-localization, but with occasional evidence of yellow dots indicative of

co-localization. Therefore, to validate the interaction of EDI3 and STBD1, immunoprecipitation (IP) experiments were performed (Figure 3.23.B, C). For this experiment, HEK293T cells were co-transfected with EDI3-3xHA and STBD1-3xFLAG plasmids. After 48 h cells were lysed and magnetic beads were either loaded with a FLAG or a mock antibody (Figure 3.23.B) or with an HA or a mock antibody (Figure 3.23.C). The proteins are then able to bind the antibody coupled beads: FLAG antibody to the STBD1-3xFLAG protein and the HA antibody to the EDI3-3xHA antibody. Any 'prey' proteins bound to the 'baited' proteins will be associated as potential binding partner. In the FLAG IP (Figure 3.23.B) different amount of FLAG antibody (3 µl and 7 µl) was given to the magnetic beads. Western analysis for EDI3, shows stronger EDI3 signal with 'high' compared to low FLAG suggesting that EDI3 was bound to and eluted with STBD1. Binding to the mock antibody could not be detected. Additionally, loading controls of transfected full cell lysate (STBD1-3xFLAG and EDI3-3xHA) and parental HEK293T cells were shown.

The reverse IP was performed using EDI3-HA as bait to verify the interaction with STBD1-3xFLAG protein. The FLAG signal was detected with immunoblotting after EDI3-HA IP indicating binding between the two (Figure 3.23.C). While the mock band for EDI3 and HA was empty, it showed a faint signal for the FLAG antibody, indicating weak unspecific binding.

Altogether, the IHC and IP experiments suggest that EDI3 is able to bind two well-characterized glycogen binding proteins, STBD1 and glycogen synthase 1, supporting the original finding in muscle tissue that EDI3 may indeed bind glycogen in skeletal muscle.

3.4.3 EDI3 interacts with glycogen synthase in human myocardium

A type of tissue which is closely related to skeletal muscle and is also associated with high amount of glycogen is heart muscle also known as myocardium. Between the two muscle types many similar ultrastructural features can be observed. The sarcomere, and the proteins needed in muscle contraction (myosin, actin, troponin, and tropomyosin) are similar to in skeletal and cardiac muscle. Also transverse tubules can be found in cardiac muscle (Irwin and Tecklin 2004)

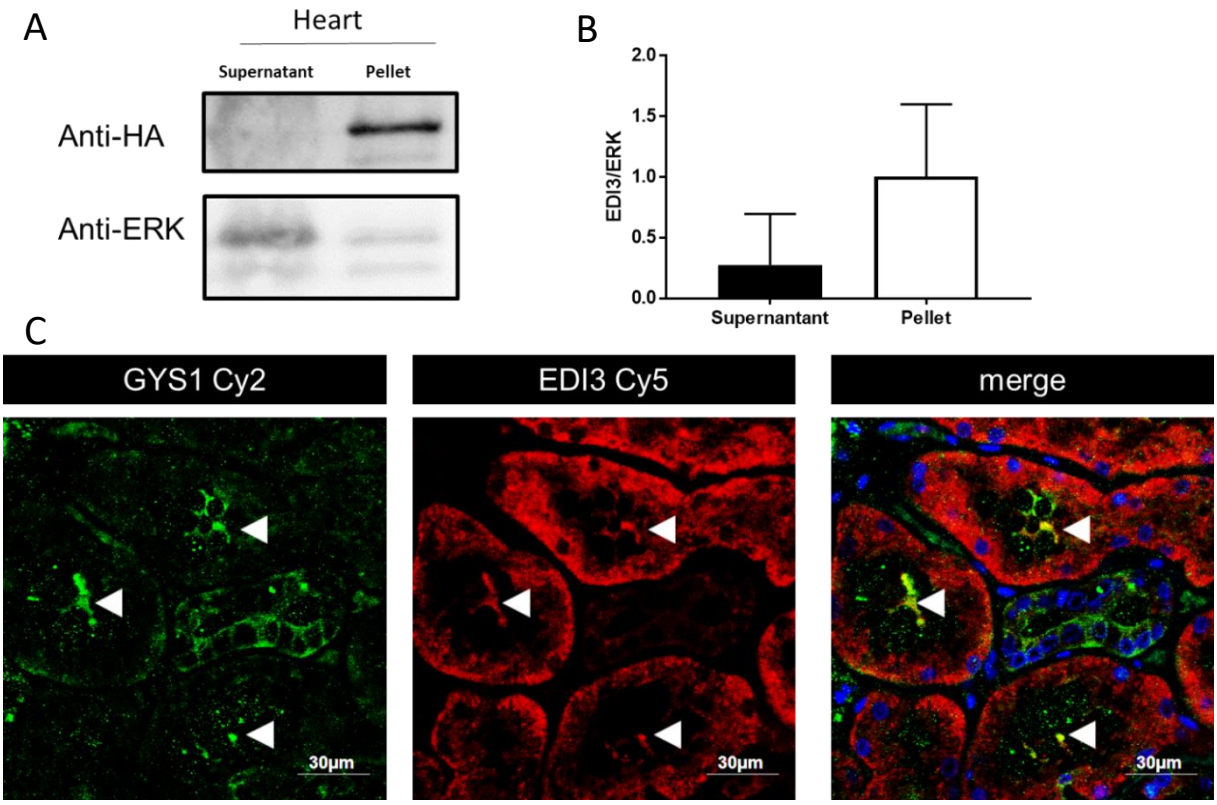

Figure 3.23 **EDI3 co-localizes with GYS1 in heart muscle. A,** Representative image of a glycogen pulldown in mouse heart, 200 mg mouse heart was homogenised and centrifuged at 100000 g. Proteins for the resulting supernatant and pellet were analysed via western blot. **B,** EDI3/ERK ratio calculated from the obtained densitrometric values (N=4) **C,** Representative image of a GYS1 (1:1500, green) and EDI3 (1:500, red) co-staining in human heart muscle. Co-localization is indicated in yellow, highlighted with the white arrowheads.

To investigate whether EDI3 binds glycogen, or glycogen-binding proteins in the heart, a glucan pull down with mouse heart muscle, as well as immunocytochemistry analyses of EDI3 and glycogen synthase in human heart muscle were explored. A glycogen pulldown in mouse heart of male BL6N mice was performed, as established before in mouse skeletal muscle and mouse liver (Figure 3.18.A). Edi3 could be detected in the pellet potentially co-precipitating with glycogen, while Erk, as a protein not associated with glycogen binding was detected in the supernatant (Figure 3.23.A). For quantification, densitometric analyses were performed, and the ratio of Edi3 to Erk signals was calculated, N=4. EDI3 was predominantly found in the pellet, suggesting a potential interaction with glycogen (Figure 3.23.B). To further strengthen the link between EDI3 and glycogen in heart muscle, human myocardium was stained with EDI3 and GYS1. The results demonstrate an interaction between both proteins (Figure 3.23.C, white arrowheads) overall supporting a link between EDI3 and glycogen in heart muscle.

3.4.4 EDI3 is located at the t-tubules

One specific structure that was visible in almost all skeletal muscle donors were ring-like formations surrounding cavities, which were also glycogen synthase 1 positive (Figure 3.21/22). Their form and location in the muscle fibre suggest that these bodies might be transverse tubules (t-tubules).

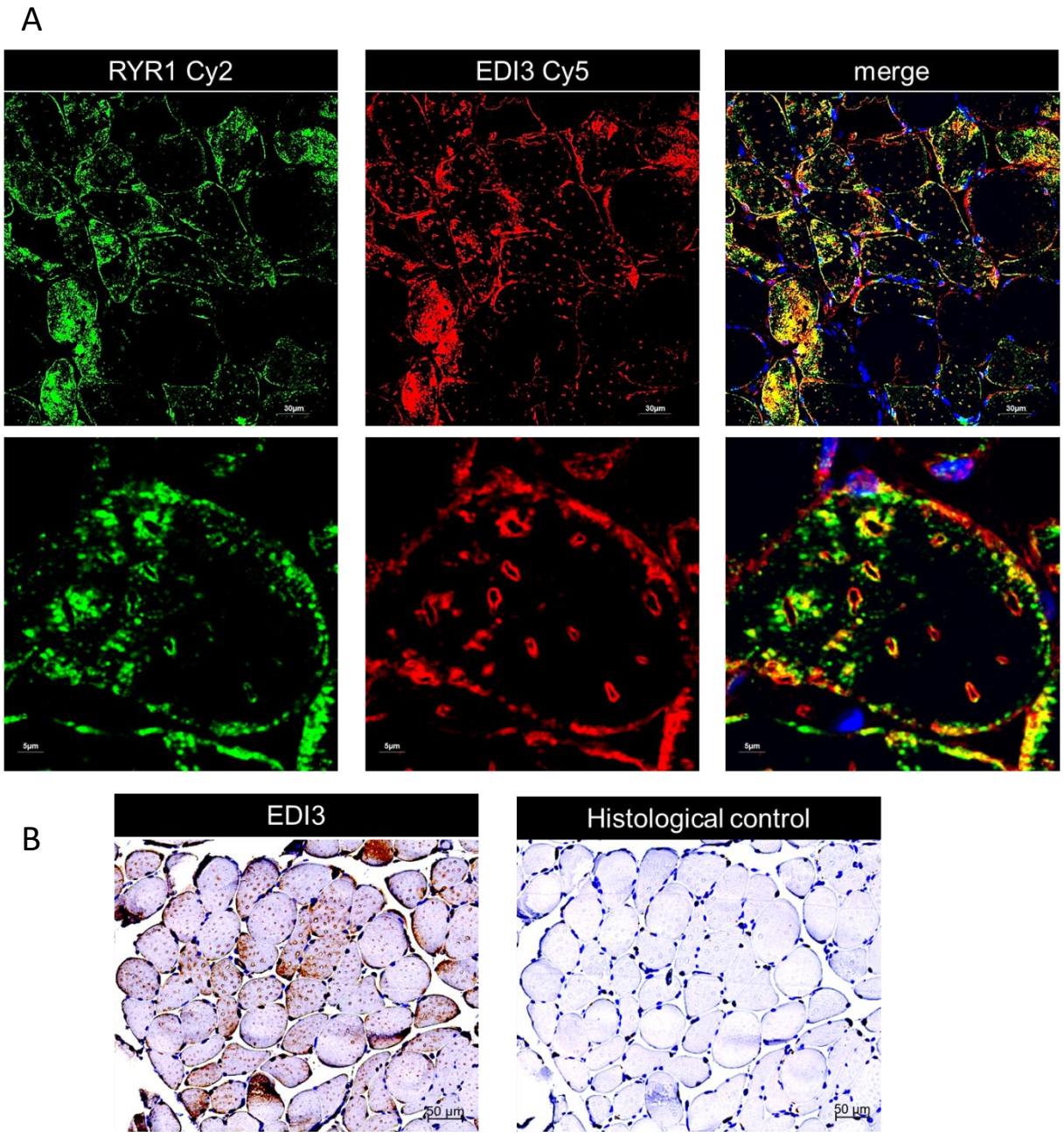

Figure 3.24 **EDI3 localizes at the t-tubules and interacts with the ryanodine receptor 1**. **A**; Representative image of IHC staining of human skeletal muscle (Donor 4) with EDI3 (red) and the ryanodine receptor 1 (RYR1) (green) in skeletal muscle. Upper panel shows an overview with more detail of a single cells shown in the middle panel. Yellow indicates co-localization of EDI3 and RYR1. **B,** Representative image of an IHC staining of EDI3 (detected with 3, 3'-Diaminobenzidine) and a histological control in human skeletal muscle.

One marker for these t-tubules is the Ryanodine receptor 1 (RYR-1). Therefore, to determine whether the structures are indeed t-tubules, and whether EDI3 binds to them, a co-staining of EDI3 (red) and the RYR1 (green) receptor was performed, which convincingly indicated co-localization of EDI3 and RYR1 in various cells as indicated in yellow (Figure 3.24.A, upper panel). While the staining suggests that EDI3 surrounds the entire t-tubule, the RYR1 receptor appears more external, to almost encircle the EDI3 protein (Figure 3.24.A, lower panel). To confirm that the EDI3 staining is specific, a single DAB staining of EDI3, and a histological control (DAB only) were performed (Figure 3.24.B).

Overall, the data suggest that EDI3 binds glycogen-associated proteins (GYS1 and STBD1) in the human skeletal and potentially cardiac muscle, which increases the probability that EDI3 may also bind to glycogen. Furthermore, EDI3 appears to be localized to the t-tubules by a co-localization with the ryanodine receptor 1, indicating a potential link to calcium signalling which will be followed up in subsequent studies.

4. Discussion

Glycogen-associated proteins are a small family of proteins found in animals; and to date, only 25 glycogen-binding proteins have been identified in humans (Prats et al. 2018). The interaction between glycogen and these glycogen-associated proteins is mediated via a conserved carbohydrate-binding module (CBM). In humans, CBMs are divided into several families, one of which is the CBM20-containing protein family which encompasses only three proteins. Of the three, only two have been characterized so far, laforin and STBD1. Although both have distinct functions, they have both been shown to bind amylopectin (Worby et al. 2006; Tagliabracci et al. 2007) and glycogen (Jiang et al. 2010; Stapleton et al. 2010). The glycerophosphodiesterase, EDI3 is the third gene containing a CBM20 domain; however, no interaction has been shown thus far between EDI3 and glycogen.

In the course of this PhD thesis, the function of EDI3's CBM20 was investigated. For this purpose, EDI3 mutants W32A and ΔCBM20 were generated. By studying and evaluating the generated mutants compared to the full length protein, the CBM20 was found to be involved in regulating protein abundance, enzymatic activity, dimerization and cell migration.

In the second part of the thesis, experiments were done to show direct interaction between EDI3 and glycogen via glycan pulldown assays, manipulation of glycogen and EDI3 levels in cells, and immunohistochemical stainings in cells and tissue. It was revealed that EDI3 interacts with glycogen associated proteins (GYS1 and STBD1), as well as with glycogen in skeletal muscle. However, the interaction could not be detected in breast cancer cell lines nor in primary liver cells. In skeletal muscle, EDI3 could be linked to the transverse tubules due to co-localization with the ryanodine receptor 1 (RYR1), which may be interpreted as a potential link of EDI3 to stimulus conduction. Finally, initial results indicate that mouse *Edi3* may be involved in gluconeogenesis.

The most important results are discussed in detail in the following sub-chapters.

4.1 Basic characterization of EDI3's CBM20

Via sequence alignment, conserved amino acids within the CBM20 domain of human EDI3 could be identified, more specifically G24, L29, G30 and W32 (Homo sapiens EDI3 numbering) (Figure 3.1). In the present work, mutating the conserved W32 to alanine, or deletion of the entire CBM20 domain of EDI3 revealed decreased protein levels indicating that the mutant protein product is less stable (Figure 3.3). In general, a protein domain is suggested to be an independent unit with respect to folding (Wetlaufer 1973), structure (Richardson 1981) and function (Bork 1991). In its folded state, bonds are usually more tightly packed in the interior of the protein compared to the exterior surface, thus generating a solid core and a 'loose' surface. Residues inside the core are often conserved; whereas, those on the surface are more variable, unless they have an enzymatic function (Zhou et al. 1999). For the CBM20 domain of human EDI3, it is therefore likely that the four aforementioned conserved amino acids are localized in the more tightly packed interior to form the core of the CBM20 domain. Indeed, it has been previously reported that mutation of core amino acids is associated with decreased stability, as shown for the other two members of the CBM20 family (Raththagala et al. 2014; Zhu et al. 2014), suggesting that the same prediction could be made for EDI3. This observation was not limited to the CBM20 family as alteration in the glycogen binding domain of glycogen debranching enzyme (GBE) also led to less protein stability (Cheng et al. 2007; Cheng et al. 2009). Thus, it appears that in addition to binding carbohydrates, carbohydrate binding domains might be important for protein stability.

In addition to stability, mutating the conserved W32 amino acid and deletion of the CBM20 domain decreased the enzymatic function of EDI3's GDE domain (Figure 3.6). The findings presented in the current thesis show that while the complete deletion of the CBM20 domain obliterated the enzymatic activity of EDI3, a "simple" point mutation was sufficient to significantly reduce the enzymatic activity. These findings suggest that there is some interaction between EDI3's CBM20 and GDE domain, and that the CBM20 of EDI3 stabilizes its GDE domain such that the enzymatic centre of the GDE domain may be hindered (W32A) or misfolded (ΔCBM20) when mutated. Furthermore, alteration in the CBM20 and the resulting decrease in enzymatic activity (Figure 3.6) caused less migration of HEK293T cells when they were transfected with the mutant (Figure 3.7) compared to cells transfected with wild type EDI3. These results support previous findings were it was shown that EDI3 is important for

migration, and inhibiting EDI3 with siRNA or decreasing its activity with the general PDE inhibitor, dipyridamole decreased migration (Stewart et al. 2012).

In the current study, EDI3 could also be identified as a dimer, albeit with only an apparent weak binding via the CBM20 domain. The reason for the dimerization of EDI3 is not yet known. It is still not fully known whether CBM20- containing proteins in general form homodimers, and whether the dimerization occurs via the CBM20 domain. Earlier studies have indicated that for both laforin and STBD1, the CMB20 domain is indeed required for homodimerization (Liu et al. 2006; Jiang et al. 2010). However, one report shows that the homodimerization of laforin is mediated via its enzymatic domain (Raththagala et al. 2014).

Crystal structures of glycogen associated proteins show that most exist as oligomeric structures in different organisms: glycogen synthase 1 was found as a dimer in *Agrobacterium tumefaciens* (Buschiazzo et al. 2004) and a tetramer in *Saccharomyces cerevisiae* (Baskaran et al. 2010), glycogen debranching enzyme as a dimer or tetramer in *Sulfolobus solfataricus* (Park et al. 2008; Song et al. 2010), glycogenin 1 was found as a decamer in rabbit muscle (Gibbons et al. 2002), glycogen phosphorylase as a catalytic active dimer and inactive tetra- or monomer (Fletterick et al. 1976; Browner and Fletterick 1992), and laforin as an antiparallel dimer (Raththagala et al. 2014). The common factor among all the proteins is the binding to glycogen via their CBM (not only the CBM20, www.cazy.org), (Janeček et al. 2019). One can speculate that in order to target a large molecule, such as glycogen, a coordinated effort is required by several proteins, and to facilitate this targeting they exist as dimers or oligomers, otherwise they would not be able to modify glycogen.

Thus, the data presented in the current thesis indicates that EDI3 is a dimeric structure, which is in agreement with current literature on other glycogen-associated proteins, and may dimerize in order to bind or be enzymatic active at the glycogen granular.

4.2 The binding of EDI3 and glycogen

The major finding in this thesis is the likely involvement of EDI3 in glycogen metabolism, in particular, it's binding to glycogen in muscle. Here, the co-localization of EDI3 with associated proteins could be demonstrated in a variety of experiments. Co-localization was shown in different muscle tissues, more specifically skeletal and heart, in several donors using two known glycogen associated proteins (GYS1 and STBD1) and two immunohistochemical staining methods (chromogenic and immunofluorescence). Additionally, in the well accepted

in vitro glycan binding pulldown assay (Wang et al. 2002; Jiang et al. 2010; Díaz et al. 2011) EDI3 co-precipitated with purified glycogen; whereas, the W32 mutation or deletions within the CBM20 domain showed decreased glycogen binding to EDI3 (Figure 3.9). Co-precipitation of mouse Edi3 was also observed in the glycogen-rich muscle and heart (Figure 3.18, 3.25). However, the results of the *in vitro* pulldown needs to be further validated (Figure 3.9). It is clear that the full length protein partially co-precipitates with glycogen, but a weak band was also seen with the dCBM20 mutant. Since the carbohydrate binding domain was removed in the dCBM20 mutant, it is very likely that the weak band is due to non-specific binding. However, the negative control ERK did not produce a signal in the precipitate, which indicates that the observed binding is specific. Nevertheless, it is possible that EDI3 and the mutant constructs, which were overexpressed in this experimental setup, are too highly concentrated and binds glycogen unspecifically. Although the results are not definitive, the experiments show a weak binding of EDI3 to glycogen. Other independent experiments suggest that EDI3 binds glycogen in skeletal and cardiac muscle, and therefore may be involved in processes associated with glycogen metabolism, which agrees with the present literature, indicating that the CBM20 in humans is weakly associated with glycogen (Tagliabracci et al. 2007; Jiang et al. 2010; Nitschke et al. 2018).

The binding of EDI3 to glycogen or glycogen associated proteins appears to be organ-specific, and not a general feature of EDI3. For example, no interaction was detected in breast cancer cell lines (Figure 3.11), primary hepatocytes or human liver (Figure 3.17). The inability of EDI3 to bind glycogen in cell culture models, liver cells and tissue is unexpected. In fact, numerous studies have previously shown binding of glycogen to the CBM20 proteins laforin and STBD1 (see also 1.3.1 and 1.3.3). In literature, similar results was reported for the CBM20 water dikinase 3 (GWD3) protein in plants (Christiansen et al. 2009b), where GWD3 showed a 50-fold lower affinity towards the starch analogue, cyclodextrin compared to the CBM20 from fungal glucoamylase. This low affinity allows a more dynamic interaction with the carbohydrate, and gives the protein a more flexible role in its metabolic regulation, it is not always bound to the carbohydrate and is allowed to participate in independent metabolic functions (Blennow and Svensson 2010). With respect to EDI3, it may be that since EDI3 has a role in lipid metabolism, as described in 1.3.4, strong binding to glycogen might hinder the necessary interaction with GPC or other lipids. Furthermore, it may be that EDI3 needs to be post-translationally modificated to bind glycogen. It is not known if EDI3 is differently modified in muscle than in

liver or cancer cells. For other CBM20 proteins, it is reported that phosphorylation events are necessary for enzymatic function (Romá-Mateo et al. 2011). Nevertheless, post-translational modifications of EDI3 have not been elucidated and the phosphorylation or glycosylation status of EDI3 needs to be investigated in future experiments.

In conclusion, it seems that the binding of EDI3 differs between organs. Under specific circumstances as shown in skeletal muscle cells a potential binding could be observed. It is not yet understood under which circumstances EDI3 can bind glycogen, but tissue-specific differences have been identified. It is possible that EDI3 was post-translationally modified in the muscle and thus enabled a binding to glycogen. One major difference between liver and cancer cells compared to heart and skeletal muscle is that the latter are excitable while the others are not.

4.3 EDI3 in the skeletal muscle

In skeletal muscle, in addition to binding to glycogen, further immunohistological stainings revealed that EDI3 is localized to the transverse tubules (t-tubules) located at the terminal cisterna also known as triad. This was determined by a potential co-localization between EDI3 and the ryanodine receptor 1 (RYR1), which is a marker for the triad, the transition zone between the t-tubules and sarcoplasmic reticulum (Figure 3.24). Additionally, co-localization was also observed between EDI3 and GYS1 in the same area (Figure 3.20, 3.21). These results may indicate that there is a relationship between EID3 and neuromuscular stimulus transmission. Supporting this hypothesis, decreased calcium blood levels were reported in EDI3 heterozygote mice by the International Mouse Phenotyping Consortium (IMPC) found (https://www.mousephenotype.org/data/genes/MGI:104898). Furthermore, the dihydropyridine receptor (DHPR), a voltage-dependent calcium channel, located in the t-tubules was altered in the brain of E16.5 EDI3 knockout embryos compared to wildtype age matched embryos as determined via RNA sequencing analyses (Manuscript in preparation).

Several reports support a potential role for EDI3 in stimulus transmission. Transgenic mice overexpressing mouse *EDI3Δ471* gene specifically in the quadriceps and gastrocnemius exhibited an upregulation of the nicotinergic receptor subunits and the acetylcholinesterase in the NMJ (Hashimoto et al. 2016). While the authors in this study linked this finding to a faster aging process in the EDI3Δ471 transgenic mice, it is also possible that the enzymatically inactive *EDI3Δ471* inhibits the enzymatic reaction of endogenous full length EDI3, and the

alterations in the NMJ are due to compensatory effects for decreased levels of G3P, choline and potentially acetylcholine.

There is increasing evidence that choline plays a previously underestimated role in muscle, and in particular at the t-tubules (Moretti et al. 2020). For example, the replacement of K^+ Ions with choline$^+$ in rabbit muscle results in a potent inhibition of sarcoplasmic/endoplasmic reticulum Ca^{2+} ATPase (SERCA) leading to decreased V_{max} of Ca^{2+} uptake into the SR (Beca et al. 2009) Furthermore, the choline derivate sphingosylphosphorylcholine (SPC) can directly bind to RYR1 (Kovacs et al. 2010; Moretti et al. 2020). Taken together, since the role of choline in muscle is only just gaining importance, no clear role can yet be assigned to EDI3, but these studies indicate that EDI3 may be involved in calcium signalling.

It is very well accepted that glycogen at the t-tubules is strongly associated with calcium signalling (Chin et al. 1997; Kabbara et al. 2000; Helander et al. 2002; Ørtenblad et al. 2013). In a number of experiments is was shown, that glycogen is needed for sufficient calcium signalling in muscle and that there is a close relationship between muscle glycogen content and fatigue resistance (Pernow and Saltin 1971; Gollnick et al. 1972; Hargreaves et al. 1995). If glycogen is depleted due to high-intensity intermittent exercise, the Ca^{2+} release is highly reduced and the muscles fibre bundles fatigue more rapidly in follow-up exercise. If the glycogen levels are restored between the exercises, the Ca^{2+} signalling is not altered (Chin et al. 1997). It is not yet known, how glycogen influences calcium signalling and how glycogen stores affect basic cell function (Ørtenblad et al. 2013). But the t-tubules, were the glycogen is located, are known for its strong metabolic activity due to a high density of ATP consuming Na/K-ATPases (Dulhunty et al. 1984; Han et al. 1992). Therefore, it is likely that glycogen acts as an energy source; however, there is evidence for a non-metabolic role of glycogen (Stephenson et al. 1999; Nielsen et al. 2009).

In this thesis, it could be shown that EDI3 may not be involved in the direct build-up or depletion of glycogen during energy metabolism, as shown in the glycogen assay experiments (3.11). It is therefore unlikely that EDI3 participates directly in glycogen metabolism at the t-tubules. These findings are in agreement with the other two CBM20 proteins that have other functions in addition to glycogen degradation (Tagliabracci et al. 2007; Jiang et al. 2010). Therefore, EDI3's CBM20 may have a role that is independent of glycogen metabolism, in that it may use the carbohydrate as a platform to localize to the t-tubules. Since it does not have a

transmembrane domain, EDI3 might anchor to glycogen in order to stay in close proximity to the triad, thus supporting this energy intensive region with metabolites, such as choline that may be required for calcium signalling (Beca et al. 2009), acetylcholine, as a neurotransmitter (Voet and Voet 2004), and G3P in gluconeogenesis or for the glycerol-3-phosphate shuttle (Ansell et al. 1997). It further can be speculated that EDI3 can no longer localize to the t-tubules in glycogen deficiency and thus cannot participate in calcium signalling anymore which could lead to more rapidly fatigue in the muscle.

Regardless of glycogen concentrations, EDI3 was fund to be highly expressed in glycolytic cells/regions, such as glycolytic breast cancer cell lines (3.10), skeletal muscle type II cells (2.19), primary mouse hepatocytes during glucagon stimulation (3.13) and t-tubules (3.24). Although a role for EDI3 in glycolysis has not yet been described, recent results in our research group could identify alterations in several glycolytic genes in E16.5 EDI3 knockout embryos compared to age-matched embryos (Manuscript in preparation). Thus, EDI3 may not directly involved in the glycogen degradation pathway, but have a role further downstream in gluconeogenesis or glycolysis (Figure 1.3, 4.1).

In conclusion, the work is this thesis suggests that EDI3 is connected to the t-tubules, where it co-localizes with RYR1, as well as glycogen synthase, indicating possible binding to glycogen. Furthermore, although no clear role could be observed for EDI3 in glycogen degradation or build-up, glycogen may act as a platform to localize EDI3 to the t-tubules were it is needed for a function potentially associated with calcium signalling or glycolysis.

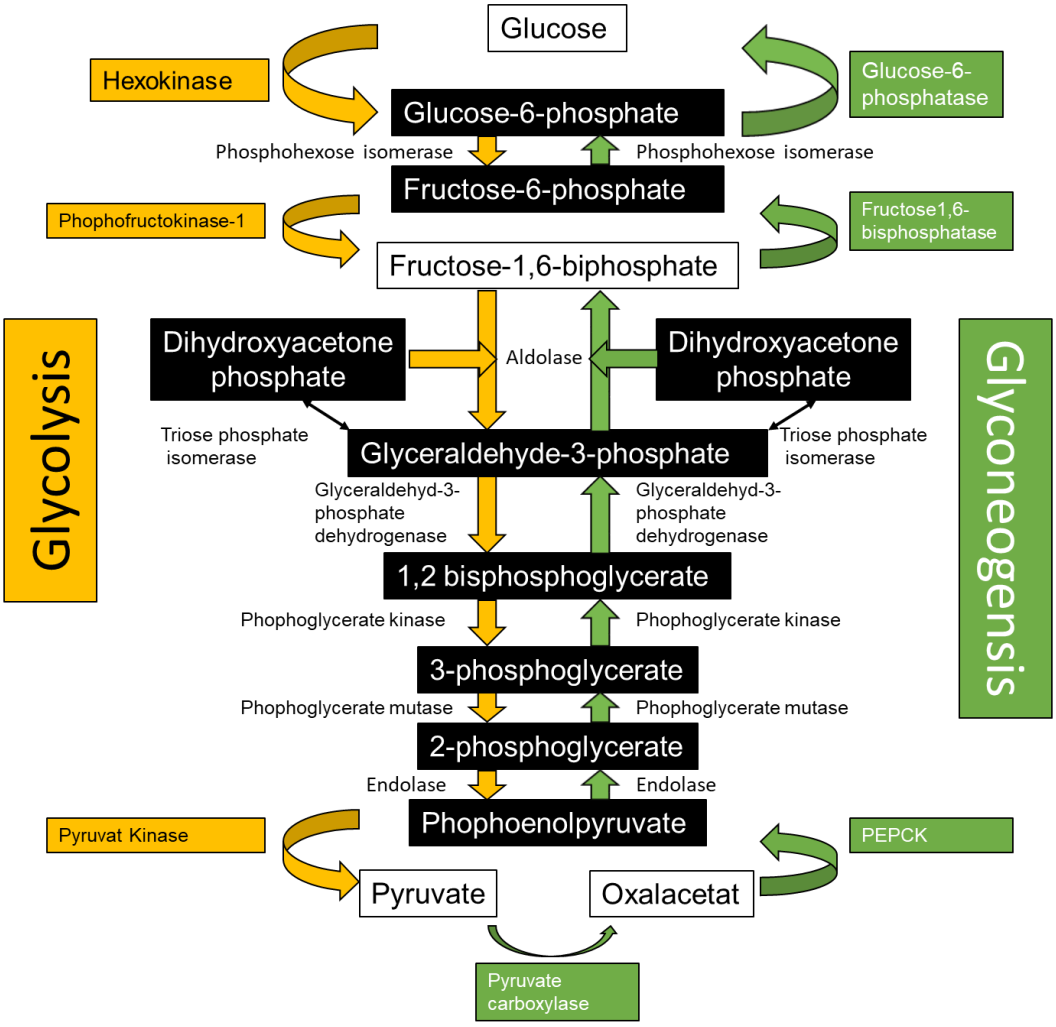

Figure 4.1 **Gluconeogenesis and glycolysis are reciprocally regulated.** In glycolysis (orange) and gluconeogenesis (green) many reactions are reversible. Irreversible reactions are highlighted in orange or green, depending on the associated pathway. PEPCK; Phosphoenolpyruvate carboxykinase (Voet and Voet 2004), modified)

4.4 *EDI3* as a potential gluconeogenetic gene in mice

During this project, the role of EDI3 in liver glycogen metabolism was investigated in depth. While it could be shown that EDI3 and glycogen do not interact in liver, an indirect link could be found between EDI3 and gluconeogenesis in mice. Gluconeogenesis is the biosynthesis of glucose from non-hexose or non-carbohydrate precursors, such as lactate, pyruvate, alanine, and glycerol.

Experiments in primary mouse hepatocytes (PMHs) which aimed to investigate the effect of glycogen degradation on EDI3 found that the addition of glucagon resulted in significantly increased *Edi3* gene expression and subsequently higher protein concentrations at three and six hours, respectively (Figure 3.13). The timing of Edi3 upregulation is of great interest since it matches that observed for genes associated with gluconeogenesis, such as *Pepck1* (Burgess et al. 2007; Lin and Accili 2011) and *Agxt* (Rowsell et al. 1969; Tsubaki and Hiraiwa 1971). On

protein level, gluconeogenesis can be determined by the phosphorylation of cAMP response element-binding protein (CREB) at position S133 (pCREB) (section 1.1.3). The physiological effects of pCREB mediated gene transcription is not detected until hours after glucagon secretion (Marliss et al. 1970), which matches the upregulated Edi3 protein levels seen after 6 h.

To determine whether EDI3 expression is altered during glycogen production, PMHs were stimulated with insulin instead of glucagon, but no effect on Edi3 expression was observed (Figure 3.14), indicating that the response is specific to glucagon treatment indicating a role in glycogenolysis and/or gluconeogenesis. It is worth noting that western blot analysis for the Edi3 protein did not reveal a shift in protein size when cells stimulated with glucagon, suggesting that there was no post-translational modification of Edi3 (Figure 3.13). This further lowers the probability of a direct role for Edi3 in glycogenolysis, which is associated with a rapid phosphorylation cascade of several proteins (Scott and Bloom 2018).

A link between Edi3 and gluconeogenesis may be via the Edi3 cleavage product, G3P which can be further metabolized to dihydroxyacetone phosphate (Figure 1.9) (Ansell et al. 1997), a metabolic intermediate of glycerol and main energy source during gluconeogenesis (Melkonian et al. 2020). Indeed, GPC decreases when PMHs are stimulated with glucagon, but the effect is not significant. Additional, the decrease of G3P is insignificant. However, a closer analysis reveals a different picture. The addition of 10-100 nmol glucagon to PMHs is above the physiological levels 20 pmol/l in plasma (Knop et al. 2007; Miyachi et al. 2017), which means that all relevant metabolic pathways are probably activated. Edi3 may be relevant in one of these signalling pathways, for example as a source of G3P for gluconeogenesis. However, the most important metabolite in gluconeogenesis is pyruvate (Garrett and Grisham 2002; Gerich et al. 2001), which is not a limiting factor in cell culture media, as observed by the consistently elevated levels of Pck1 even after 24 hours of glucagon treatment. Therefore, it may be plausible that the initial upregulation of Edi3 may be a general response of the cell to ensure energy is supplied in the event that pyruvate is a limiting factor.

Overall, Edi3 is expressed simultaneously with other well-known gluconeogenesis genes in mouse hepatocytes in response to glucagon. This supports the observation of high Edi3 in the glycolytic muscle cells. In line with glycolytic cancer cells this is another process were glycolytic/gluconeogenetic genes are involved (Figure 4.1). In support of Edi3's role in

gluconeogenesis, recent results from RNAseq analysis of liver and brain tissue isolated from E16.5 Edi3 knockout embryos revealed alterations in genes of the glycolysis/gluconeogenesis pathway when compared to wild type control mice (manuscript in preparation). It is thus likely that EDI3 is important during glycolysis/gluconeogenesis, and further work is needed to elucidate the underlying mechanism.

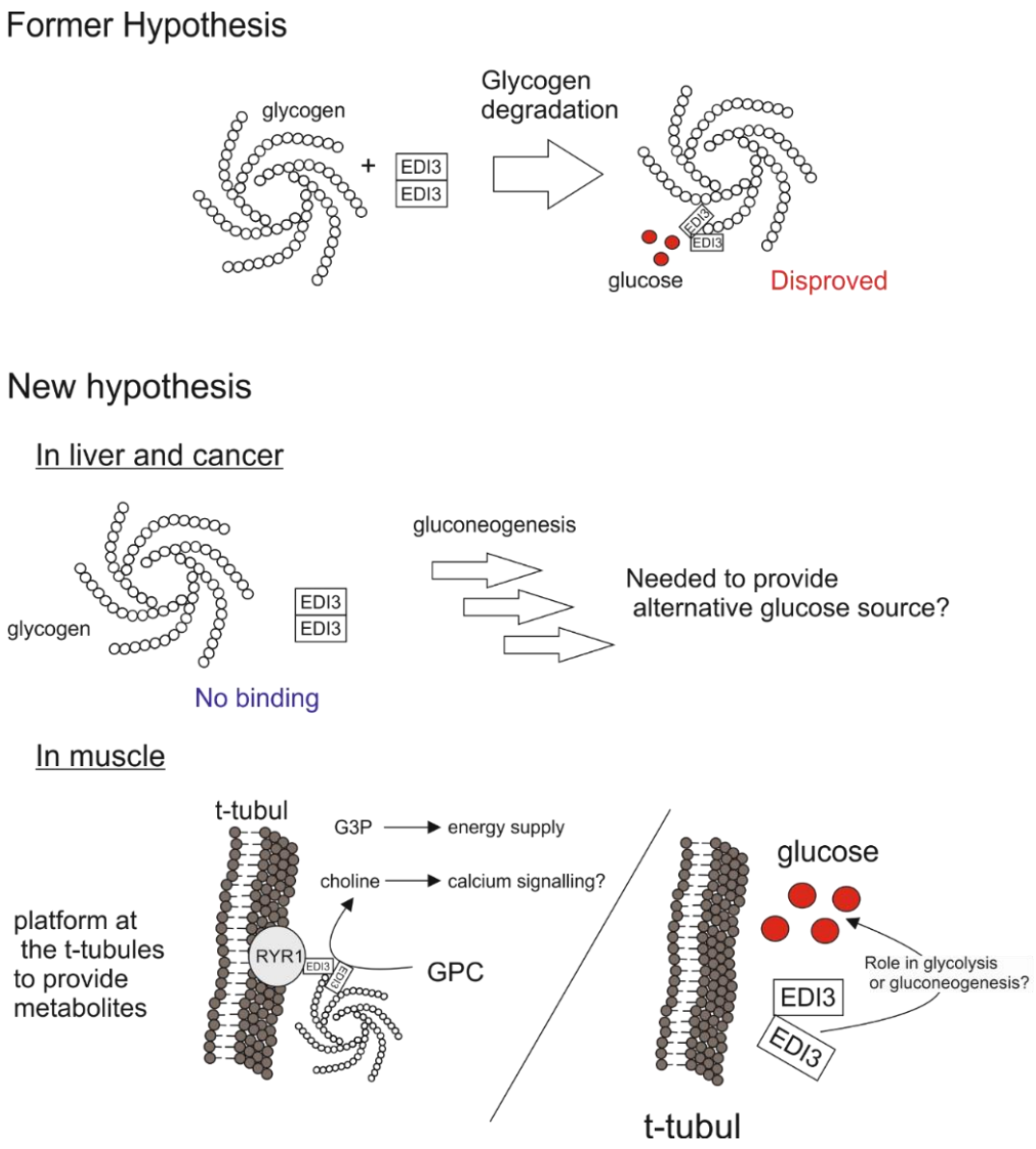

Figure 4.2 **Working Hypothesis**

4.5 Concluding remarks and outlook

In the first part of this project, it was shown that the CBM20 of EDI3 is necessary for its stability and dimerization, although it remains open which other domains of EDI3 are involved in this process. It is still unclear whether EDI3 is a dimer or a higher oligomeric structure. For further investigation, native polyacrylamide gel electrophoresis (PAGE) could be performed to see if higher oligomeric structures are detected. However, more reliable would be to elucidate the crystal structure of EDI3, which would clarify how the protein is structured, whether it forms a dimer or a higher oligomeric structure and which amino acids are involved. Ideally, EDI3 would be crystallised in complex with a carbohydrate to unequivocally demonstrate that EDI3 binds carbohydrates.

The second part of the work focused on the binding of EDI3 to glycogen (Figure 4.2). The initial hypothesis was that EDI3 binds glycogen via its CBM20 domain. However, the results suggest there is tissue and cell specificity as no binding was seen in liver and cancer cells, but instead the results support a role for EDI3 in glycogen metabolism in muscle due to interaction with glycogen and proteins associated with the t-tubules. While the initial hypothesis that EDI3 generally binds glycogen could be disproved, tissue-specific glycogen binding could be observed. For instance, in the present work in liver and cancer cells, no binding to glycogen could be found, which is remarkable due to the presence of CBM20; in muscle, indications of an interaction with glycogen and proteins associated with the t-tubules were given.

In the liver (Figure 4.2), Edi3 has been linked (at least in mice) to a possible role in gluconeogenesis. Data from the RNAseq analysis of liver and brain tissue isolated from E16.5 Edi3 knockout embryos supported this assumption (Manuscript in preparation). To investigate this role further, PMHs could be deprived of pyruvate under glucagon influence. One possible outcome is that under glucagon influence Edi3 upregulation is longer and the consumption of GPC higher. In addition, a role of CREB in regulating Edi3 expression should be investigated further using a promoter assay and the promoter region of Edi3. A very important model to understand the general role of EDI3 is an EDI3 knockout mouse model. While a constitutive knockout of Edi3 prove lethal for mice, a conditional *Edi3* knockout will soon be available to our group, which can be used to study altered gene expression and metabolites in the liver after glucagon influx or starvation *in vitro* and *in vivo*.

The interesting results showing co-localization between Edi3 and glycogen binding proteins at the t-tubules of muscle, warrants further investigation. Although there are not many skeletal cell lines available, one model which could be used is the C2C12 immortalized mouse myoblast cell line, which was previously used to show an association between Edi3 and skeletal muscle development (Okazaki et al. 2010). Using these cells, the levels of *EDI3* can be manipulated (up- or downregulated) and calcium imaging performed to understand if EDI3 is involved in the calcium signalling cascade. In addition to a potential role in calcium signalling, the cells can be used to investigate Edi3's role in glycolysis or gluconeogenesis. Thus, EDI3 levels in the C2C12 cells can be silenced or overexpressed, followed by starvation and then calcium imaging. In another set of experiments primary mouse skeletal cells can be isolated (Spinazzola and Gussoni 2017) and treated with glucagon, insulin (and additionally epinephrine), as already performed in PMHs (3.12). EDI3 expression as well as t-tubules and glycogen associated genes and proteins could be investigated. If these experiments are successful, similar experiments can be reproduced in human skeletal and cardiac muscle cells (Owens et al. 2013). Finally, to determine the biological relevance of EDI3 in muscle cells, EDI3 levels can be manipulated in the primary cells and calcium imaging performed.

The conditional *Edi3* knockout mouse is also an important model to investigate the in vivo relevance of the findings in the muscle cell lines. If EDI3 is shown to be involved in the calcium signalling or neuromuscular stimulus transmission, it is possible that knocking out Edi3 in mice leads to alterations in the skeletal and possibly heart muscle. This may especially be relevant in the skeletal muscle type II cells where EDI3 expression is high (Figure 3.20) (Okazaki et al. 2010; Hashimoto et al. 2016). Although no correlation between EDI3 and glycogen in the liver could be shown in this work, no long-term studies in vivo have been done so far. Since laforin knockout mice develop a phenotype two months after birth (Ganesh et al. 2002) glycogen levels may also change in the EDI3 knockout mice over time. The isolation of glycogen from the skeletal muscle of EDI3 knockout mice after different periods of time and subsequent glycogen analysis may show alterations, such as hyperphosphorylation or changes in size or number of glycogen molecules.

5. References

Ansell, R.; Granath, K.; Hohmann, S.; Thevelein, J. M.; Adler, L. (1997): The two isoenzymes for yeast NAD+-dependent glycerol 3-phosphate dehydrogenase encoded by GPD1 and GPD2 have distinct roles in osmoadaptation and redox regulation. In *The EMBO journal* 16 (9), pp. 2179–2187. DOI: 10.1093/emboj/16.9.2179.

Baker, David J.; Timmons, James A.; Greenhaff, Paul L. (2005): Glycogen phosphorylase inhibition in type 2 diabetes therapy: a systematic evaluation of metabolic and functional effects in rat skeletal muscle. In *Diabetes* 54 (8), pp. 2453–2459. DOI: 10.2337/diabetes.54.8.2453.

Baskaran, Sulochanadevi; Roach, Peter J.; DePaoli-Roach, Anna A.; Hurley, Thomas D. (2010): Structural basis for glucose-6-phosphate activation of glycogen synthase. In *Proceedings of the National Academy of Sciences of the United States of America* 107 (41), pp. 17563–17568. DOI: 10.1073/pnas.1006340107.

Beca, Sanja; Aschar-Sobbi, Roozbeh; Ponjevic, Dragana; Winkfein, Robert J.; Kargacin, Margaret E.; Kargacin, Gary J. (2009): Effects of monovalent cations on Ca2+ uptake by skeletal and cardiac muscle sarcoplasmic reticulum. In *Archives of biochemistry and biophysics* 490 (2), pp. 110–117. DOI: 10.1016/j.abb.2009.08.014.

Berkovic, S. F.; So, N. K.; Andermann, F. (1991): Progressive myoclonus epilepsies: clinical and neurophysiological diagnosis. In *Journal of clinical neurophysiology : official publication of the American Electroencephalographic Society* 8 (3), pp. 261–274.

Blennow, Andreas; Svensson, Birte (2010): Dynamics of starch granule biogenesis – the role of redox-regulated enzymes and low-affinity carbohydrate-binding modules. In *Biocatalysis and Biotransformation* 28 (1), pp. 3–9. DOI: 10.3109/10242420903408211.

Böhm, Johann; Chevessier, Frédéric; Maues De Paula, André; Koch, Catherine; Attarian, Shahram; Feger, Claire et al. (2013): Constitutive activation of the calcium sensor STIM1 causes tubular-aggregate myopathy. In *American journal of human genetics* 92 (2), pp. 271–278. DOI: 10.1016/j.ajhg.2012.12.007.

Boraston, A. B.; Bolam, D. N.; Gilbert, H. J.; Davies, G. J. (2004): Carbohydrate-binding modules: fine-tuning polysaccharide recognition. In *The Biochemical journal* 382 (Pt 3). DOI: 10.1042/BJ20040892.

Bork, P. (1991): Shuffled domains in extracellular proteins. In *FEBS letters* 286 (1-2), pp. 47–54. DOI: 10.1016/0014-5793(91)80937-x.

Bouju, S.; Lignon, M. F.; Piétu, G.; Le Cunff, M.; Léger, J. J.; Auffray, C.; Dechesne, C. A. (1998): Molecular cloning and functional expression of a novel human gene encoding two 41-43 kDa skeletal muscle internal membrane proteins. In *The Biochemical journal* 335 (Pt 3), pp. 549–556. DOI: 10.1042/bj3350549.

Brand, C. L.; Jørgensen, P. N.; Knigge, U.; Warberg, J.; Svendsen, I.; Kristensen, J. S.; Holst, J. J. (1995): Role of glucagon in maintenance of euglycemia in fed and fasted rats. In *American Journal of Physiology-Legacy Content* 269 (3 Pt 1), E469-77. DOI: 10.1152/ajpendo.1995.269.3.E469.

Brand, C. L.; Rolin, B.; Jørgensen, P. N.; Svendsen, I.; Kristensen, J. S.; Holst, J. J. (1994): Immunoneutralization of endogenous glucagon with monoclonal glucagon antibody normalizes hyperglycaemia in moderately streptozotocin-diabetic rats. In *Diabetologia* 37 (10), pp. 985–993. DOI: 10.1007/BF00400461.

References

Brazil, Derek P.; Hemmings, Brian A. (2001): Ten years of protein kinase B signalling: a hard Akt to follow. In *Trends in biochemical sciences* 26 (11), pp. 657–664. DOI: 10.1016/S0968-0004(01)01958-2.

Browner, Michelle F.; Fletterick, Robert J. (1992): Phosphorylase: a biological transducer. In *Trends in biochemical sciences* 17 (2), pp. 66–71. DOI: 10.1016/0968-0004(92)90504-3.

Burgess, Shawn C.; He, TianTeng; Yan, Zheng; Lindner, Jill; Sherry, A. Dean; Malloy, Craig R. et al. (2007): Cytosolic phosphoenolpyruvate carboxykinase does not solely control the rate of hepatic gluconeogenesis in the intact mouse liver. In *Cell metabolism* 5 (4), pp. 313–320. DOI: 10.1016/j.cmet.2007.03.004.

Buschiazzo, Alejandro; Ugalde, Juan E.; Guerin, Marcelo E.; Shepard, William; Ugalde, Rodolfo A.; Alzari, Pedro M. (2004): Crystal structure of glycogen synthase: homologous enzymes catalyze glycogen synthesis and degradation. In *The EMBO journal* 23 (16), pp. 3196–3205. DOI: 10.1038/sj.emboj.7600324.

Cahill, George F. (2006): Fuel metabolism in starvation. In *Annual review of nutrition* 26, pp. 1–22. DOI: 10.1146/annurev.nutr.26.061505.111258.

Cardell, R. R.; Cardell, E. L. (1990): Heterogeneity of glycogen distribution in hepatocytes. In *Journal of electron microscopy technique* 14 (2), pp. 126–139. DOI: 10.1002/jemt.1060140206.

Castillo, Angelica; Nowak, Roberta; Littlefield, Kimberly P.; Fowler, Velia M.; Littlefield, Ryan S. (2009): A nebulin ruler does not dictate thin filament lengths. In *Biophysical journal* 96 (5), pp. 1856–1865. DOI: 10.1016/j.bpj.2008.10.053.

Chan, E. M.; Omer, S.; Ahmed, M.; Bridges, L. R.; Bennett, C.; Scherer, S. W.; Minassian, B. A. (2004): Progressive myoclonus epilepsy with polyglucosans (Lafora disease): evidence for a third locus. In *Neurology* 63 (3), pp. 565–567. DOI: 10.1212/01.wnl.0000133215.65836.03.

Cheng, Alan; Zhang, Mei; GENTRY, Matthew S.; Worby, Carolyn A.; Dixon, Jack E.; Saltiel, Alan R. (2007): A role for AGL ubiquitination in the glycogen storage disorders of Lafora and Cori's disease. In *Genes & development* 21 (19), pp. 2399–2409. DOI: 10.1101/gad.1553207.

Cheng, Alan; Zhang, Mei; Okubo, Minoru; Omichi, Kaoru; Saltiel, Alan R. (2009): Distinct mutations in the glycogen debranching enzyme found in glycogen storage disease type III lead to impairment in diverse cellular functions. In *Human molecular genetics* 18 (11), pp. 2045–2052. DOI: 10.1093/hmg/ddp128.

Chin, E. R.; Balnave, C. D.; Allen, D. G. (1997): Role of intracellular calcium and metabolites in low-frequency fatigue of mouse skeletal muscle. In *American Journal of Physiology-Legacy Content* 272 (2 Pt 1), C550-9. DOI: 10.1152/ajpcell.1997.272.2.C550.

Chomczynski, P.; Sacchi, N. (1987): Single-step method of RNA isolation by acid guanidinium thiocyanate-phenol-chloroform extraction. In *Analytical biochemistry* 162 (1), pp. 156–159. DOI: 10.1006/abio.1987.9999.

Christiansen, Camilla; Abou Hachem, Maher; Janecek, Stefan; Viksø-Nielsen, Anders; Blennow, Andreas; Svensson, Birte (2009a): The carbohydrate-binding module family 20--diversity, structure, and function. In *The FEBS journal* 276 (18), pp. 5006–5029. DOI: 10.1111/j.1742-4658.2009.07221.x.

Christiansen, Camilla; Hachem, Maher Abou; Glaring, Mikkel A.; Viksø-Nielsen, Anders; Sigurskjold, Bent W.; Svensson, Birte; Blennow, Andreas (2009b): A CBM20 low-affinity starch-binding domain from glucan, water dikinase. In *FEBS letters* 583 (7), pp. 1159–1163. DOI: 10.1016/j.febslet.2009.02.045.

References

Close, R. (1967): Properties of motor units in fast and slow skeletal muscles of the rat. In *The Journal of physiology* 193 (1), pp. 45–55. DOI: 10.1113/jphysiol.1967.sp008342.

Conlee, R. K.; Berg, T. L.; Han, D. H.; Kelly, K. P.; Barnett, D. W. (1989): Cocaine does not alter cardiac glycogen content at rest or during exercise. In *Metabolism: clinical and experimental* 38 (11), pp. 1039–1041. DOI: 10.1016/0026-0495(89)90037-1.

Cryer, Philip E. (2012): Minireview: Glucagon in the pathogenesis of hypoglycemia and hyperglycemia in diabetes. In *Endocrinology* 153 (3), pp. 1039–1048. DOI: 10.1210/en.2011-1499.

Delbridge, Lea M. D.; Mellor, Kimberley M.; Taylor, David J. R.; Gottlieb, Roberta A. (2015): Myocardial autophagic energy stress responses—macroautophagy, mitophagy, and glycophagy. In *American Journal of Physiology - Heart and Circulatory Physiology* 308 (10), H1194-204. DOI: 10.1152/ajpheart.00002.2015.

Demetriadou, Anthi; Morales-Sanfrutos, Julia; Nearchou, Marianna; Baba, Otto; Kyriacou, Kyriacos; Tate, Edward W. et al. (2017): Mouse Stbd1 is N-myristoylated and affects ER-mitochondria association and mitochondrial morphology. In *Journal of cell science* 130 (5), pp. 903–915. DOI: 10.1242/jcs.195263.

Díaz, Adelaida; Martínez-Pons, Carlos; Fita, Ignacio; Ferrer, Juan C.; Guinovart, Joan J. (2011): Processivity and subcellular localization of glycogen synthase depend on a non-catalytic high affinity glycogen-binding site. In *The Journal of biological chemistry* 286 (21), pp. 18505–18514. DOI: 10.1074/jbc.M111.236109.

DiNuzzo, Mauro; Schousboe, Arne (2019): Brain glycogen metabolism. Cham: Springer (Advances in neurobiology, v. 23).

Drochmans, P. (1962): Morphologie du glycogène. In *Journal of Ultrastructure Research* 6 (2), pp. 141–163. DOI: 10.1016/S0022-5320(62)90050-3.

DuBridge, R. B.; Tang, P.; Hsia, H. C.; Leong, P. M.; Miller, J. H.; Calos, M. P. (1987): Analysis of mutation in human cells by using an Epstein-Barr virus shuttle system. In *Molecular and cellular biology* 7 (1), pp. 379–387. DOI: 10.1128/MCB.7.1.379.

Ducommun, Serge; Deak, Maria; Zeigerer, Anja; Göransson, Olga; Seitz, Susanne; Collodet, Caterina et al. (2019): Chemical genetic screen identifies Gapex-5/GAPVD1 and STBD1 as novel AMPK substrates. In *Cellular signalling* 57, pp. 45–57. DOI: 10.1016/j.cellsig.2019.02.001.

Dukhande, Vikas V.; Rogers, Devin M.; Romá-Mateo, Carlos; Donderis, Jordi; Marina, Alberto; Taylor, Adam O. et al. (2011): Laforin, a dual specificity phosphatase involved in Lafora disease, is present mainly as monomeric form with full phosphatase activity. In *PloS one* 6 (8), e24040. DOI: 10.1371/journal.pone.0024040.

Dulhunty, A.; Carter, G.; Hinrichsen, C. (1984): The membrane capacity of mammalian skeletal muscle fibres. In *Journal of muscle research and cell motility* 5 (3), pp. 315–332. DOI: 10.1007/BF00713110.

Edström, L.; Kugelberg, E. (1968): Histochemical composition, distribution of fibres and fatiguability of single motor units. Anterior tibial muscle of the rat. In *Journal of Neurology, Neurosurgery, and Psychiatry* 31 (5), pp. 424–433.

ELRICK, H.; WITTEN, T. A.; ARAI, Y. (1958): Glucagon treatment of insulin reactions. In *The New England journal of medicine* 258 (10), pp. 476–480. DOI: 10.1056/NEJM195803062581005.

EMANUELLE, Shane; BREWER, M. Kathryn; MEEKINS, David A.; GENTRY, Matthew S. (2016): Unique carbohydrate binding platforms employed by the glucan phosphatases. In *Cellular and molecular life sciences : CMLS* 73 (14), pp. 2765–2778. DOI: 10.1007/s00018-016-2249-3.

References

Fernández-Sánchez, Maria Elena; Criado-García, Olga; Heath, Karen E.; García-Fojeda, Belén; Medraño-Fernández, Iria; Gomez-Garre, Pilar et al. (2003): Laforin, the dual-phosphatase responsible for Lafora disease, interacts with R5 (PTG), a regulatory subunit of protein phosphatase-1 that enhances glycogen accumulation. In *Human molecular genetics* 12 (23), pp. 3161–3171. DOI: 10.1093/hmg/ddg340.

Fisher, N. F. (1923): I. PREPARATION OF INSULIN. In *American Journal of Physiology-Legacy Content* 67 (1), pp. 57–64. DOI: 10.1152/ajplegacy.1923.67.1.57.

Fletterick, R. J.; Sygusch, J.; Semple, H.; Madsen, N. B. (1976): Structure of glycogen phosphorylase a at 3.0 A resolution and its ligand binding sites at 6 A. In *The Journal of biological chemistry* 251 (19), pp. 6142–6146.

Fogh, J.; Fogh, J. M.; Orfeo, T. (1977): One hundred and twenty-seven cultured human tumor cell lines producing tumors in nude mice. In *Journal of the National Cancer Institute* 59 (1), pp. 221–226. DOI: 10.1093/jnci/59.1.221.

FRAME, Sheelagh; COHEN, Philip (2001): GSK3 takes centre stage more than 20 years after its discovery. In *The Biochemical journal* 359 (1), pp. 1–16. DOI: 10.1042/bj3590001.

Ganesh, S.; Agarwala, K. L.; Ueda, K.; Akagi, T.; Shoda, K.; Usui, T. et al. (2000): Laforin, defective in the progressive myoclonus epilepsy of Lafora type, is a dual-specificity phosphatase associated with polyribosomes. In *Human molecular genetics* 9 (15), pp. 2251–2261. DOI: 10.1093/oxfordjournals.hmg.a018916.

Ganesh, Subramaniam; Delgado-Escueta, Antonio V.; Sakamoto, Toshiro; Avila, Maria Rosa; Machado-Salas, Jesus; Hoshii, Yoshinobu et al. (2002): Targeted disruption of the Epm2a gene causes formation of Lafora inclusion bodies, neurodegeneration, ataxia, myoclonus epilepsy and impaired behavioral response in mice. In *Human molecular genetics* 11 (11), pp. 1251–1262. DOI: 10.1093/hmg/11.11.1251.

Garetto, L. P.; Richter, E. A.; Goodman, M. N.; Ruderman, N. B. (1984): Enhanced muscle glucose metabolism after exercise in the rat: the two phases. In *The American journal of physiology* 246 (6 Pt 1), E471-5. DOI: 10.1152/ajpendo.1984.246.6.E471.

Garrett, Reginald H.; Grisham, Charles M. (2002): Principles of biochemistry. With a human focus. Fort Worth: Harcourt College Publishers.

Garyali, Punitee; Siwach, Pratibha; Singh, Pankaj Kumar; Puri, Rajat; Mittal, Shuchi; Sengupta, Sonali et al. (2009): The malin-laforin complex suppresses the cellular toxicity of misfolded proteins by promoting their degradation through the ubiquitin-proteasome system. In *Human molecular genetics* 18 (4), pp. 688–700. DOI: 10.1093/hmg/ddn398.

Gastaldelli, A.; Toschi, E.; Pettiti, M.; Frascerra, S.; Quiñones-Galvan, A.; Sironi, A. M. et al. (2001): Effect of physiological hyperinsulinemia on gluconeogenesis in nondiabetic subjects and in type 2 diabetic patients. In *Diabetes* 50 (8), pp. 1807–1812. DOI: 10.2337/diabetes.50.8.1807.

Gazdar, A. F.; Kurvari, V.; Virmani, A.; Gollahon, L.; Sakaguchi, M.; Westerfield, M. et al. (1998): Characterization of paired tumor and non-tumor cell lines established from patients with breast cancer. In *International journal of cancer* 78 (6), pp. 766–774. DOI: 10.1002/(sici)1097-0215(19981209)78:6<766::aid-ijc15>3.0.co;2-l.

GENTRY, Matthew S.; Dixon, Jack E.; Worby, Carolyn A. (2009): Lafora disease: insights into neurodegeneration from plant metabolism. In *Trends in biochemical sciences* 34 (12), pp. 628–639. DOI: 10.1016/j.tibs.2009.08.002.

References

Gerich, J. E.; Meyer, C.; Woerle, H. J.; Stumvoll, M. (2001): Renal gluconeogenesis: its importance in human glucose homeostasis. In *Diabetes care* 24 (2), pp. 382–391. DOI: 10.2337/diacare.24.2.382.

Giacometti, Luigi (1969): Paul Langerhans: A Tribute. In *Arch Dermatol* 100 (6), p. 770. DOI: 10.1001/archderm.1969.01610300120022.

Gibbons, Brian J.; Roach, Peter J.; Hurley, Thomas D. (2002): Crystal Structure of the Autocatalytic Initiator of Glycogen Biosynthesis, Glycogenin. In *Journal of molecular biology* 319 (2), pp. 463–477. DOI: 10.1016/S0022-2836(02)00305-4.

Gilbert, Harry J. (Ed.) (1999): Recent advances in carbohydrate bioengineering. The proceedings of the 3rd Carbohydrate Bioengineering Meeting held at the University of Newcastle upon Tyne on 11 - 14 April 1999. Carbohydrate Bioengineering Meeting. Cambridge: RSC Royal Society of Chemistry (Special publication / Royal Society of Chemistry, 246).

Gollnick, P. D.; Karlsson, J.; Piehl, K.; Saltin, B. (1974): Selective glycogen depletion in skeletal muscle fibres of man following sustained contractions. In *The Journal of physiology* 241 (1), pp. 59–67. DOI: 10.1113/jphysiol.1974.sp010640.

Gollnick, P. D.; Pernow, B.; Essen, Birgitta; Jansson, Eva; Saltin, B. (1981): Availability of glycogen and plasma FFA for substrate utilization in leg muscle of man during exercise. In *Clin Physiol* 1 (1), pp. 27–42. DOI: 10.1111/j.1475-097X.1981.tb00872.x.

Gollnick, P. D.; Piehl, K.; Saubert, C. W.; Armstrong, R. B.; Saltin, B. (1972): Diet, exercise, and glycogen changes in human muscle fibers. In *Journal of applied physiology (Bethesda, Md. : 1985)* 33 (4), pp. 421–425. DOI: 10.1152/jappl.1972.33.4.421.

Graham, T. E.; Yuan, Z.; Hill, A. K.; Wilson, R. J. (2010): The regulation of muscle glycogen: the granule and its proteins. In *Acta physiologica (Oxford, England)* 199 (4), pp. 489–498. DOI: 10.1111/j.1748-1716.2010.02131.x.

Greenhaff, P. L.; Söderlund, K.; Ren, J. M.; Hultman, E. (1993): Energy metabolism in single human muscle fibres during intermittent contraction with occluded circulation. In *The Journal of physiology* 460, pp. 443–453. DOI: 10.1113/jphysiol.1993.sp019480.

Guth, Lloyd; Samaha, Frederick J. (1969): Qualitative differences between actomyosin ATPase of slow and fast mammalian muscle. In *Experimental Neurology* 25 (1), pp. 138–152. DOI: 10.1016/0014-4886(69)90077-6.

Habegger, Kirk M.; Heppner, Kristy M.; Geary, Nori; Bartness, Timothy J.; DiMarchi, Richard; Tschöp, Matthias H. (2010): The metabolic actions of glucagon revisited. In *Nature reviews. Endocrinology* 6 (12), pp. 689–697. DOI: 10.1038/nrendo.2010.187.

Han, Hye-Sook; Kang, Geon; Kim, Jun Seok; Choi, Byeong Hoon; Koo, Seung-Hoi (2016): Regulation of glucose metabolism from a liver-centric perspective. In *Experimental & molecular medicine* 48, e218. DOI: 10.1038/emm.2015.122.

Han, J. W.; Thieleczek, R.; Varsányi, M.; Heilmeyer, L. M. (1992): Compartmentalized ATP synthesis in skeletal muscle triads. In *Biochemistry* 31 (2), pp. 377–384. DOI: 10.1021/bi00117a010.

Hargreaves, M.; McConell, G.; Proietto, J. (1995): Influence of muscle glycogen on glycogenolysis and glucose uptake during exercise in humans. In *Journal of applied physiology (Bethesda, Md. : 1985)* 78 (1), pp. 288–292. DOI: 10.1152/jappl.1995.78.1.288.

Hashimoto, Takao; Yang, Bo; Okazaki, Yuri; Yoshizawa, Ikumi; Kajihara, Kaori; Kato, Norihisa et al. (2016): Time Course Analysis of Skeletal Muscle Pathology of GDE5 Transgenic Mouse. In *PloS one* 11 (9), e0163299. DOI: 10.1371/journal.pone.0163299.

References

Hasty, P.; Bradley, A.; Morris, J. H.; Edmondson, D. G.; Venuti, J. M.; Olson, E. N.; Klein, W. H. (1993): Muscle deficiency and neonatal death in mice with a targeted mutation in the myogenin gene. In *Nature* 364 (6437), pp. 501–506. DOI: 10.1038/364501a0.

Hatting, Maximilian; Tavares, Clint D. J.; Sharabi, Kfir; Rines, Amy K.; Puigserver, Pere (2018): Insulin regulation of gluconeogenesis. In *Annals of the New York Academy of Sciences* 1411 (1), pp. 21–35. DOI: 10.1111/nyas.13435.

Helander, Ingrid; Westerblad, Håkan; Katz, Abram (2002): Effects of glucose on contractile function, Ca2+i, and glycogen in isolated mouse skeletal muscle. In *American journal of physiology. Cell physiology* 282 (6), C1306-12. DOI: 10.1152/ajpcell.00490.2001.

Hemmings, Brian A.; Restuccia, David F. (2012): PI3K-PKB/Akt pathway. In *Cold Spring Harbor perspectives in biology* 4 (9), a011189. DOI: 10.1101/cshperspect.a011189.

Higuchi, R.; Fockler, C.; Dollinger, G.; Watson, R. (1993): Kinetic PCR analysis: real-time monitoring of DNA amplification reactions. In *Bio/technology (Nature Publishing Company)* 11 (9), pp. 1026–1030. DOI: 10.1038/nbt0993-1026.

Hong, TingTing; Shaw, Robin M. (2017): Cardiac T-Tubule Microanatomy and Function. In *Physiological Reviews* 97 (1), pp. 227–252. DOI: 10.1152/physrev.00037.2015.

Horwitz, Kathryn B.; Mockus, Mary B.; Lessey, Bruce A. (1982): Variant T47D human breast cancer cells with high progesterone-receptor levels despite estrogen and antiestrogen resistance. In *Cell* 28 (3), pp. 633–642. DOI: 10.1016/0092-8674(82)90218-5.

Howald, H.; Hoppeler, H.; Claassen, H.; Mathieu, O.; Straub, R. (1985): Influences of endurance training on the ultrastructural composition of the different muscle fiber types in humans. In *Pflugers Archiv : European journal of physiology* 403 (4), pp. 369–376. DOI: 10.1007/BF00589248.

ILLINGWORTH, B.; LARNER, J.; CORI, G. T. (1952): Structure of glycogens and amylopectins. I. Enzymatic determination of chain length. In *The Journal of biological chemistry* 199 (2), pp. 631–640.

Irwin, Scot; Tecklin, Jan Stephen (2004): Cardiopulmonary physical therapy. 4th ed. St. Louis, Mo: Mosby; [Online]; Elsevier ScienceDirect Books.

Janah, Lina; Kjeldsen, Sasha; Galsgaard, Katrine D.; Winther-Sørensen, Marie; Stojanovska, Elena; Pedersen, Jens et al. (2019): Glucagon Receptor Signaling and Glucagon Resistance. In *International journal of molecular sciences* 20 (13). DOI: 10.3390/ijms20133314.

Janecek, S.; Sevcík, J. (1999): The evolution of starch-binding domain. In *FEBS letters* 456 (1), pp. 119–125. DOI: 10.1016/s0014-5793(99)00919-9.

Janecek, Stefan (2002): A motif of a microbial starch-binding domain found in human genethonin. In *Bioinformatics (Oxford, England)* 18 (11), pp. 1534–1537. DOI: 10.1093/bioinformatics/18.11.1534.

Janeček, Štefan; Svensson, Birte; MacGregor, E. Ann (2011): Structural and evolutionary aspects of two families of non-catalytic domains present in starch and glycogen binding proteins from microbes, plants and animals. In *Enzyme and microbial technology* 49 (5), pp. 429–440. DOI: 10.1016/j.enzmictec.2011.07.002.

Jiang, Sixin; Heller, Brigitte; Tagliabracci, Vincent S.; Zhai, Lanmin; Irimia, Jose M.; DePaoli-Roach, Anna A. et al. (2010): Starch binding domain-containing protein 1/genethonin 1 is a novel participant in glycogen metabolism. In *The Journal of biological chemistry* 285 (45), pp. 34960–34971. DOI: 10.1074/jbc.M110.150839.

Jiang, Sixin; Wells, Clark D.; Roach, Peter J. (2011): Starch-binding domain-containing protein 1 (Stbd1) and glycogen metabolism: Identification of the Atg8 family interacting motif (AIM) in Stbd1

required for interaction with GABARAPL1. In *Biochemical and biophysical research communications* 413 (3), pp. 420–425. DOI: 10.1016/j.bbrc.2011.08.106.

Kabbara, A. A.; Nguyen, L. T.; Stephenson, G. M.; Allen, D. G. (2000): Intracellular calcium during fatigue of cane toad skeletal muscle in the absence of glucose. In *Journal of muscle research and cell motility* 21 (5), pp. 481–489. DOI: 10.1023/a:1005650425513.

Khandelwal, R. L.; Zinman, S. M.; Knull, H. R. (1979): The effect of streptozotocin-induced diabetes on glycogen metabolism in rat kidney and its relationship to the liver system. In *Archives of biochemistry and biophysics* 197 (1), pp. 310–316. DOI: 10.1016/0003-9861(79)90250-9.

Knop, F. K.; Vilsbøll, T.; Madsbad, S.; Holst, J. J.; Krarup, T. (2007): Inappropriate suppression of glucagon during OGTT but not during isoglycaemic i.v. glucose infusion contributes to the reduced incretin effect in type 2 diabetes mellitus. In *Diabetologia* 50 (4), pp. 797–805. DOI: 10.1007/s00125-006-0566-z.

Kovacs, Erika; Le Xu; Pasek, Daniel A.; Liliom, Karoly; Meissner, Gerhard (2010): Regulation of ryanodine receptors by sphingosylphosphorylcholine: involvement of both calmodulin-dependent and -independent mechanisms. In *Biochemical and biophysical research communications* 401 (2), pp. 281–286. DOI: 10.1016/j.bbrc.2010.09.050.

Kuchtová, Andrea; GENTRY, Matthew S.; Janeček, Štefan (2018): The unique evolution of the carbohydrate-binding module CBM20 in laforin. In *FEBS letters* 592 (4), pp. 586–598. DOI: 10.1002/1873-3468.12994.

Kusunoki, Masataka; Tsutsumi, Kazuhiko; Hara, Tsutomu; Ogawa, Hitoshi; Nakamura, Takao; Miyata, Tetsuro et al. (2002): Correlation between lipid and glycogen contents in liver and insulin resistance in high-fat-fed rats treated with the lipoprotein lipase activator NO-1886. In *Metabolism: clinical and experimental* 51 (6), pp. 792–795. DOI: 10.1053/meta.2002.32732.

Lafora, Gonzalo R. (1911): Über das Vorkommen amyloider Körperchen im Innern der Ganglienzellen. In *Virchows Arch. path Anat.* 205 (2), pp. 295–303. DOI: 10.1007/BF01989438.

Lafora, Gonzalo R.; Glueck, Bernard (1911): Beitrag zur Histopathologie der myoklonischen Epilepsie. In *Z. f. d. g. Neur. u. Psych.* 6 (1), pp. 1–14. DOI: 10.1007/BF02863929.

LARNER, J.; ILLINGWORTH, B.; CORI, G. T.; CORI, C. F. (1952): Structure of glycogens and amylopectins. II. Analysis by stepwise enzymatic degradation. In *The Journal of biological chemistry* 199 (2), pp. 641–651.

Lasfargues, E. Y.; Coutinho, W. G.; Redfield, E. S. (1978): Isolation of two human tumor epithelial cell lines from solid breast carcinomas. In *Journal of the National Cancer Institute* 61 (4), pp. 967–978.

Lawson, C. L.; van Montfort, R.; Strokopytov, B.; Rozeboom, H. J.; Kalk, K. H.; Vries, G. E. de et al. (1994): Nucleotide sequence and X-ray structure of cyclodextrin glycosyltransferase from Bacillus circulans strain 251 in a maltose-dependent crystal form. In *Journal of molecular biology* 236 (2), pp. 590–600. DOI: 10.1006/jmbi.1994.1168.

Lazarow, A. (1942): PARTICULATE GLYCOGEN. In *Science (New York, N.Y.)* 95 (2454), p. 49. DOI: 10.1126/science.95.2454.49.

Lesjak, Michaela S.; Marchan, Rosemarie; Stewart, Joanna D.; Rempel, Eugen; Rahnenführer, Jörg; Hengstler, Jan G. (2014): EDI3 links choline metabolism to integrin expression, cell adhesion and spreading. In *Cell adhesion & migration* 8 (5), pp. 499–508. DOI: 10.4161/cam.29284.

Lin, Hua V.; Accili, Domenico (2011): Hormonal regulation of hepatic glucose production in health and disease. In *Cell metabolism* 14 (1), pp. 9–19. DOI: 10.1016/j.cmet.2011.06.003.

References

Lindl, Toni; Gstraunthaler, Gerhard (2008): Zell- und Gewebekultur. Von den Grundlagen zur Laborbank. 6. Aufl. Heidelberg: Spektrum, Akad. Verl.

Liu, Yan; Wang, Yin; Wu, Cindy; Liu, Yang; Zheng, Pan (2006): Dimerization of Laforin is required for its optimal phosphatase activity, regulation of GSK3beta phosphorylation, and Wnt signaling. In *The Journal of biological chemistry* 281 (46), pp. 34768–34774. DOI: 10.1074/jbc.M607778200.

Livak, K. J.; Schmittgen, T. D. (2001): Analysis of relative gene expression data using real-time quantitative PCR and the 2(-Delta Delta C(T)) Method. In *Methods (San Diego, Calif.)* 25 (4), pp. 402–408. DOI: 10.1006/meth.2001.1262.

Lizcano, Jose M.; Alessi, Dario R. (2002): The insulin signalling pathway. In *Current Biology* 12 (7), R236-R238. DOI: 10.1016/S0960-9822(02)00777-7.

Machovic, Martin; Janecek, Stefan (2006): The evolution of putative starch-binding domains. In *FEBS letters* 580 (27), pp. 6349–6356. DOI: 10.1016/j.febslet.2006.10.041.

Machovic, Martin; Svensson, Birte; MacGregor, E. Ann; Janecek, Stefan (2005): A new clan of CBM families based on bioinformatics of starch-binding domains from families CBM20 and CBM21. In *The FEBS journal* 272 (21), pp. 5497–5513. DOI: 10.1111/j.1742-4658.2005.04942.x.

Marchan, Rosemarie; Büttner, Bettina; Lambert, Jörg; Edlund, Karolina; Glaeser, Iris; Blaszkewicz, Meinolf et al. (2017): Glycerol-3-phosphate Acyltransferase 1 Promotes Tumor Cell Migration and Poor Survival in Ovarian Carcinoma. In *Cancer research* 77 (17), pp. 4589–4601. DOI: 10.1158/0008-5472.CAN-16-2065.

Marliss, E. B.; Aoki, T. T.; Unger, R. H.; Soeldner, J. S.; Cahill, G. F. (1970): Glucagon levels and metabolic effects in fasting man. In *The Journal of clinical investigation* 49 (12), pp. 2256–2270. DOI: 10.1172/JCI106445.

Massague, J.; Pilch, P. F.; Czech, M. P. (1980): Electrophoretic resolution of three major insulin receptor structures with unique subunit stoichiometries. In *Proceedings of the National Academy of Sciences of the United States of America* 77 (12), pp. 7137–7141. DOI: 10.1073/pnas.77.12.7137.

Meléndez, R.; Meléndez-Hevia, E.; Cascante, M. (1997): How did glycogen structure evolve to satisfy the requirement for rapid mobilization of glucose? A problem of physical constraints in structure building. In *Journal of molecular evolution* 45 (4), pp. 446–455. DOI: 10.1007/pl00006249.

Meléndez-Hevia, E.; Waddell, T. G.; Shelton, E. D. (1993): Optimization of molecular design in the evolution of metabolism: the glycogen molecule. In *The Biochemical journal* 295 (Pt 2), pp. 477–483. DOI: 10.1042/bj2950477.

Melkonian, Erica A.; Asuka, Edinen; Schury, Mark P. (2020): StatPearls. Physiology, Gluconeogenesis. Treasure Island (FL).

Mikami, B.; Adachi, M.; Kage, T.; Sarikaya, E.; Nanmori, T.; Shinke, R.; Utsumi, S. (1999): Structure of raw starch-digesting Bacillus cereus beta-amylase complexed with maltose. In *Biochemistry* 38 (22), pp. 7050–7061. DOI: 10.1021/bi9829377.

Minassian, B. A.; Lee, J. R.; Herbrick, J. A.; Huizenga, J.; Soder, S.; Mungall, A. J. et al. (1998): Mutations in a gene encoding a novel protein tyrosine phosphatase cause progressive myoclonus epilepsy. In *Nature genetics* 20 (2), pp. 171–174. DOI: 10.1038/2470.

Miyachi, Atsushi; Kobayashi, Masaki; Mieno, Eri; Goto, Moritaka; Furusawa, Kenichi; Inagaki, Takashi; Kitamura, Tadahiro (2017): Accurate analytical method for human plasma glucagon levels using liquid chromatography-high resolution mass spectrometry: comparison with commercially available

immunoassays. In *Analytical and bioanalytical chemistry* 409 (25), pp. 5911–5918. DOI: 10.1007/s00216-017-0534-0.

Moretti, Antimo; Paoletta, Marco; Liguori, Sara; Bertone, Matteo; Toro, Giuseppe; Iolascon, Giovanni (2020): Choline: An Essential Nutrient for Skeletal Muscle. In *Nutrients* 12 (7). DOI: 10.3390/nu12072144.

Mukund, Kavitha; Subramaniam, Shankar (2020): Skeletal muscle: A review of molecular structure and function, in health and disease. In *Wiley interdisciplinary reviews. Systems biology and medicine* 12 (1), e1462. DOI: 10.1002/wsbm.1462.

Nagase, T.; Kikuno, R.; Ishikawa, K. I.; Hirosawa, M.; Ohara, O. (2000): Prediction of the coding sequences of unidentified human genes. XVI. The complete sequences of 150 new cDNA clones from brain which code for large proteins in vitro. In *DNA research : an international journal for rapid publication of reports on genes and genomes* 7 (1), pp. 65–73. DOI: 10.1093/dnares/7.1.65.

Navarro, E.; Serrano-Heras, G.; Castaño, M. J.; Solera, J. (2015): Real-time PCR detection chemistry. In *Clinica chimica acta; international journal of clinical chemistry* 439, pp. 231–250. DOI: 10.1016/j.cca.2014.10.017.

Needham, Dorothy Moyle (1926): RED AND WHITE MUSCLE. In *Physiological Reviews* 6 (1), pp. 1–27. DOI: 10.1152/physrev.1926.6.1.1.

Needleman, Saul B.; Wunsch, Christian D. (1970): A general method applicable to the search for similarities in the amino acid sequence of two proteins. In *Journal of molecular biology* 48 (3), pp. 443–453. DOI: 10.1016/0022-2836(70)90057-4.

Nielsen, J.; Schrøder, H. D.; Rix, C. G.; Ørtenblad, N. (2009): Distinct effects of subcellular glycogen localization on tetanic relaxation time and endurance in mechanically skinned rat skeletal muscle fibres. In *The Journal of physiology* 587 (Pt 14), pp. 3679–3690. DOI: 10.1113/jphysiol.2009.174862.

Nielsen, Joachim; Ørtenblad, Niels (2013): Physiological aspects of the subcellular localization of glycogen in skeletal muscle. In *Applied physiology, nutrition, and metabolism = Physiologie appliquee, nutrition et metabolisme* 38 (2), pp. 91–99. DOI: 10.1139/apnm-2012-0184.

Nitschke, Felix; Ahonen, Saija J.; Nitschke, Silvia; Mitra, Sharmistha; Minassian, Berge A. (2018): Lafora disease - from pathogenesis to treatment strategies. In *Nature reviews. Neurology* 14 (10), pp. 606–617. DOI: 10.1038/s41582-018-0057-0.

Nordlie, R. C.; Foster, J. D.; Lange, A. J. (1999): Regulation of glucose production by the liver. In *Annual review of nutrition* 19, pp. 379–406. DOI: 10.1146/annurev.nutr.19.1.379.

Ohara, O.; Nagase, T.; Ishikawa, K.; Nakajima, D.; Ohira, M.; Seki, N.; Nomura, N. (1997): Construction and characterization of human brain cDNA libraries suitable for analysis of cDNA clones encoding relatively large proteins. In *DNA research : an international journal for rapid publication of reports on genes and genomes* 4 (1), pp. 53–59. DOI: 10.1093/dnares/4.1.53.

Okazaki, Yuri; Ohshima, Noriyasu; Yoshizawa, Ikumi; Kamei, Yasutomi; Mariggiò, Stefania; Okamoto, Keiko et al. (2010): A novel glycerophosphodiester phosphodiesterase, GDE5, controls skeletal muscle development via a non-enzymatic mechanism. In *The Journal of biological chemistry* 285 (36), pp. 27652–27663. DOI: 10.1074/jbc.M110.106708.

ORRELL, S. A.; BUEDING, E. (1964): A COMPARISON OF PRODUCTS OBTAINED BY VARIOUS PROCEDURES USED FOR THE EXTRACTION OF GLYCOGEN. In *The Journal of biological chemistry* 239, pp. 4021–4026.

References

Ørtenblad, Niels; Westerblad, Håkan; Nielsen, Joachim (2013): Muscle glycogen stores and fatigue. In *The Journal of physiology* 591 (Pt 18), pp. 4405–4413. DOI: 10.1113/jphysiol.2013.251629.

Owens, Jane; Moreira, Karen; Bain, Gerard (2013): Characterization of primary human skeletal muscle cells from multiple commercial sources. In *In Vitro Cellular & Developmental Biology. Animal* 49 (9), pp. 695–705. DOI: 10.1007/s11626-013-9655-8.

Park, J-T.; Park, H-S.; Kang, H-K.; Hong, J-S.; Cha, H.; Woo, E-J. et al. (2008): Oligomeric and functional properties of a debranching enzyme (TreX) from the archaeon Sulfolobus solfataricus P2. In *Biocatalysis and Biotransformation* 26 (1-2), pp. 76–85. DOI: 10.1080/10242420701806652.

Penninga, D.; van der Veen, B. A.; Knegtel, R. M.; van Hijum, S. A.; Rozeboom, H. J.; Kalk, K. H. et al. (1996): The raw starch binding domain of cyclodextrin glycosyltransferase from Bacillus circulans strain 251. In *The Journal of biological chemistry* 271 (51), pp. 32777–32784. DOI: 10.1074/jbc.271.51.32777.

Pernow, B.; Saltin, B. (1971): Availability of substrates and capacity for prolonged heavy exercise in man. In *Journal of applied physiology (Bethesda, Md. : 1985)* 31 (3), pp. 416–422. DOI: 10.1152/jappl.1971.31.3.416.

Peter, J. B.; Barnard, R. J.; Edgerton, V. R.; Gillespie, C. A.; Stempel, K. E. (1972): Metabolic profiles of three fiber types of skeletal muscle in guinea pigs and rabbits. In *Biochemistry* 11 (14), pp. 2627–2633. DOI: 10.1021/bi00764a013.

Petersen, Max C.; Vatner, Daniel F.; Shulman, Gerald I. (2017): Regulation of hepatic glucose metabolism in health and disease. In *Nature reviews. Endocrinology* 13 (10), pp. 572–587. DOI: 10.1038/nrendo.2017.80.

Prats, Clara; Graham, Terry E.; Shearer, Jane (2018): The dynamic life of the glycogen granule. In *The Journal of biological chemistry* 293 (19), pp. 7089–7098. DOI: 10.1074/jbc.R117.802843.

Ramnanan, C. J.; Edgerton, D. S.; Kraft, G.; Cherrington, A. D. (2011): Physiologic action of glucagon on liver glucose metabolism. In *Diabetes, obesity & metabolism* 13 Suppl 1, pp. 118–125. DOI: 10.1111/j.1463-1326.2011.01454.x.

Raththagala, Madushi; BREWER, M. Kathryn; Parker, Matthew W.; Sherwood, Amanda R.; Wong, Brian K.; Hsu, Simon et al. (2014): Structural Mechanism of Laforin Function in Glycogen Dephosphorylation and Lafora Disease. In *Molecular cell* 57 (2), pp. 261–272. DOI: 10.1016/j.molcel.2014.11.020.

Richardson, J. S. (1981): The anatomy and taxonomy of protein structure. In *Advances in protein chemistry* 34, pp. 167–339. DOI: 10.1016/s0065-3233(08)60520-3.

Roach, Peter J.; DePaoli-Roach, Anna A.; Hurley, Thomas D.; Tagliabracci, Vincent S. (2012): Glycogen and its metabolism: some new developments and old themes. In *The Biochemical journal* 441 (3), pp. 763–787. DOI: 10.1042/BJ20111416.

Romá-Mateo, Carlos; Solaz-Fuster, Maria del Carmen; Gimeno-Alcañiz, José Vicente; Dukhande, Vikas V.; Donderis, Jordi; Marina, Alberto et al. (2011): Laforin, a dual specificity protein phosphatase involved in Lafora disease, is phosphorylated at Ser25 by AMP-activated protein kinase. In *The Biochemical journal* 439 (2), pp. 265–275. DOI: 10.1042/BJ20110150.

Rowsell, E. V.; Snell, K.; Carnie, J. A.; Al-Tai, A. H. (1969): Liver-L-alanine-glyoxylate and L-serine-pyruvate aminotransferase activities: an apparent association with gluconeogenesis. In *The Biochemical journal* 115 (5), pp. 1071–1073. DOI: 10.1042/bj1151071.

References

Sanchez-Martin, Pablo; Lahuerta, Marcos; Viana, Rosa; Knecht, Erwin; Sanz, Pascual (2020): Regulation of the autophagic PI3KC3 complex by laforin/malin E3-ubiquitin ligase, two proteins involved in Lafora disease. In *Biochimica et biophysica acta. Molecular cell research* 1867 (2), p. 118613. DOI: 10.1016/j.bbamcr.2019.118613.

Sankhala, Rajeshwer S.; Koksal, Adem C.; Ho, Lan; Nitschke, Felix; Minassian, Berge A.; Cingolani, Gino (2015): Dimeric quaternary structure of human laforin. In *The Journal of biological chemistry* 290 (8), pp. 4552–4559. DOI: 10.1074/jbc.M114.627406.

Schade, David S.; Woodside, William; Eaton, R.Philip (1979): The role of glucagon in the regulation of plasma lipids. In *Metabolism* 28 (8), pp. 874–886. DOI: 10.1016/0026-0495(79)90215-4.

Schiaffino, S.; Ausoni, S.; Gorza, L.; Saggin, L.; Gundersen, K.; Lomo, T. (1988): Myosin heavy chain isoforms and velocity of shortening of type 2 skeletal muscle fibres. In *Acta physiologica Scandinavica* 134 (4), pp. 575–576. DOI: 10.1111/j.1748-1716.1998.tb08539.x.

Schiaffino, S.; Gorza, L.; Sartore, S.; Saggin, L.; Ausoni, S.; Vianello, M. et al. (1989): Three myosin heavy chain isoforms in type 2 skeletal muscle fibres. In *Journal of muscle research and cell motility* 10 (3), pp. 197–205. DOI: 10.1007/BF01739810.

Schiaffino, S.; Hanzlíková, V.; Pierobon, S. (1970): Relations between structure and function in rat skeletal muscle fibers. In *The Journal of cell biology* 47 (1), pp. 107–119. DOI: 10.1083/jcb.47.1.107.

Schiaffino, Stefano; Reggiani, Carlo (2011): Fiber types in mammalian skeletal muscles. In *Physiological Reviews* 91 (4), pp. 1447–1531. DOI: 10.1152/physrev.00031.2010.

Scott, R. V.; Bloom, S. R. (2018): Problem or solution: The strange story of glucagon. In *Peptides* 100, pp. 36–41. DOI: 10.1016/j.peptides.2017.11.013.

Seglen, P. O. (1976): Preparation of isolated rat liver cells. In *Methods in cell biology* 13, pp. 29–83. DOI: 10.1016/s0091-679x(08)61797-5.

Sengupta, Sonali; Badhwar, Ishima; Upadhyay, Mamta; Singh, Sweta; Ganesh, Subramaniam (2011): Malin and laforin are essential components of a protein complex that protects cells from thermal stress. In *Journal of cell science* 124 (Pt 13), pp. 2277–2286. DOI: 10.1242/jcs.082800.

Serratosa, J. M.; Gómez-Garre, P.; Gallardo, M. E.; Anta, B.; Bernabé, D. B. de; Lindhout, D. et al. (1999): A novel protein tyrosine phosphatase gene is mutated in progressive myoclonus epilepsy of the Lafora type (EPM2). In *Human molecular genetics* 8 (2), pp. 345–352. DOI: 10.1093/hmg/8.2.345.

Shi, Liang; Liu, Jun-Feng; An, Xiao-Min; Liang, Dong-Cai (2008): Crystal structure of glycerophosphodiester phosphodiesterase (GDPD) from Thermoanaerobacter tengcongensis, a metal ion-dependent enzyme: insight into the catalytic mechanism. In *Proteins* 72 (1), pp. 280–288. DOI: 10.1002/prot.21921.

Singh, Pankaj Kumar; Singh, Sweta; Ganesh, Subramaniam (2012): The laforin-malin complex negatively regulates glycogen synthesis by modulating cellular glucose uptake via glucose transporters. In *Molecular and cellular biology* 32 (3), pp. 652–663. DOI: 10.1128/MCB.06353-11.

Sjöström, M.; Angquist, K. A.; Bylund, A. C.; Fridén, J.; Gustavsson, L.; Scherstén, T. (1982): Morphometric analyses of human muscle fiber types. In *Muscle & nerve* 5 (7), pp. 538–553. DOI: 10.1002/mus.880050708.

Skurat, Alexander V.; Segvich, Dyann M.; DePaoli-Roach, Anna A.; Roach, Peter J. (2017): Novel method for detection of glycogen in cells. In *Glycobiology* 27 (5), pp. 416–424. DOI: 10.1093/glycob/cwx005.

References

Smith, T. F.; Waterman, M. S. (1981): Identification of common molecular subsequences. In *Journal of molecular biology* 147 (1), pp. 195–197. DOI: 10.1016/0022-2836(81)90087-5.

Solaz-Fuster, Maria Carmen; Gimeno-Alcañiz, José Vicente; Ros, Susana; Fernandez-Sanchez, Maria Elena; Garcia-Fojeda, Belen; Criado Garcia, Olga et al. (2008): Regulation of glycogen synthesis by the laforin-malin complex is modulated by the AMP-activated protein kinase pathway. In *Human molecular genetics* 17 (5), pp. 667–678. DOI: 10.1093/hmg/ddm339.

Song, Hyung-Nam; Jung, Tae-Yang; Park, Jong-Tae; Park, Byung-Chul; Myung, Pyung Keun; Boos, Winfried et al. (2010): Structural rationale for the short branched substrate specificity of the glycogen debranching enzyme GlgX. In *Proteins* 78 (8), pp. 1847–1855. DOI: 10.1002/prot.22697.

Sorimachi, K.; Le Gal-Coëffet, M. F.; Williamson, G.; Archer, D. B.; Williamson, M. P. (1997): Solution structure of the granular starch binding domain of Aspergillus niger glucoamylase bound to beta-cyclodextrin. In *Structure (London, England : 1993)* 5 (5), pp. 647–661. DOI: 10.1016/s0969-2126(97)00220-7.

Soule, H. D.; Vazguez, J.; Long, A.; Albert, S.; Brennan, M. (1973): A human cell line from a pleural effusion derived from a breast carcinoma. In *Journal of the National Cancer Institute* 51 (5), pp. 1409–1416. DOI: 10.1093/jnci/51.5.1409.

Spinazzola, Janelle M.; Gussoni, Emanuela (2017): Isolation of Primary Human Skeletal Muscle Cells. In *Bio-protocol* 7 (21). DOI: 10.21769/BioProtoc.2591.

Stapleton, David; Nelson, Chad; Parsawar, Krishna; McClain, Donald; Gilbert-Wilson, Ryan; Barker, Elizabeth et al. (2010): Analysis of hepatic glycogen-associated proteins. In *Proteomics* 10 (12), pp. 2320–2329. DOI: 10.1002/pmic.200900628.

Stephenson, D. G.; Nguyen, L. T.; Stephenson, G. M. (1999): Glycogen content and excitation-contraction coupling in mechanically skinned muscle fibres of the cane toad. In *The Journal of physiology* 519 Pt 1, pp. 177–187. DOI: 10.1111/j.1469-7793.1999.0177o.x.

Stewart, Joanna D.; Marchan, Rosemarie; Lesjak, Michaela S.; Lambert, Joerg; Hergenroeder, Roland; Ellis, James K. et al. (2012): Choline-releasing glycerophosphodiesterase EDI3 drives tumor cell migration and metastasis. In *Proceedings of the National Academy of Sciences of the United States of America* 109 (21), pp. 8155–8160. DOI: 10.1073/pnas.1117654109.

Tagliabracci, Vincent S.; Heiss, Christian; Karthik, Chandra; Contreras, Christopher J.; Glushka, John; Ishihara, Mayumi et al. (2011): Phosphate incorporation during glycogen synthesis and Lafora disease. In *Cell metabolism* 13 (3), pp. 274–282. DOI: 10.1016/j.cmet.2011.01.017.

Tagliabracci, Vincent S.; Turnbull, Julie; Wang, Wei; Girard, Jean-Marie; Zhao, Xiaochu; Skurat, Alexander V. et al. (2007): Laforin is a glycogen phosphatase, deficiency of which leads to elevated phosphorylation of glycogen in vivo. In *Proceedings of the National Academy of Sciences of the United States of America* 104 (49), pp. 19262–19266. DOI: 10.1073/pnas.0707952104.

Tan, Xinle; Sullivan, Mitchell A.; Nada, Sharif S.; Deng, Bin; Schulz, Benjamin L.; Gilbert, Robert G. (2018): Proteomic Investigation of the Binding Agent between Liver Glycogen β Particles. In *ACS Omega* 3 (4), pp. 3640–3645. DOI: 10.1021/acsomega.8b00119.

Temeles, G. L.; Ram, P. T.; Rothstein, J. L.; Schultz, R. M. (1994): Expression patterns of novel genes during mouse preimplantation embryogenesis. In *Molecular reproduction and development* 37 (2), pp. 121–129. DOI: 10.1002/mrd.1080370202.

References

Temeles, G. L.; Schultz, R. M. (1997): Transient polyadenylation of a maternal mRNA following fertilization of mouse eggs. In *Journal of reproduction and fertility* 109 (2), pp. 223–228. DOI: 10.1530/jrf.0.1090223.

Terjung, R. L.; Baldwin, K. M.; Winder, W. W.; Holloszy, J. O. (1974): Glycogen repletion in different types of muscle and in liver after exhausting exercise. In *American Journal of Physiology-Legacy Content* 226 (6), pp. 1387–1391. DOI: 10.1152/ajplegacy.1974.226.6.1387.

Tsubaki, Masaaki; Hiraiwa, Hitoshi (1971): Short Communications. In *Chemical engineering* 35 (3), 376-380,a1. DOI: 10.1252/kakoronbunshu1953.35.376.

Turnbull, J.; Girard, J-M; Pencea, N.; Zhao, X.; Graham, T. E.; Wang, P. et al. (2011): Lafora bodies in skeletal muscle are fiber type specific. In *Neurology* 76 (19), pp. 1674–1676. DOI: 10.1212/WNL.0b013e318219faf6.

Vernia, Santiago; Rubio, Teresa; Heredia, Miguel; Rodríguez de Córdoba, Santiago; Sanz, Pascual (2009): Increased endoplasmic reticulum stress and decreased proteasomal function in lafora disease models lacking the phosphatase laforin. In *PloS one* 4 (6), e5907. DOI: 10.1371/journal.pone.0005907.

Vilchez, David; Ros, Susana; Cifuentes, Daniel; Pujadas, Lluís; Vallès, Jordi; García-Fojeda, Belén et al. (2007): Mechanism suppressing glycogen synthesis in neurons and its demise in progressive myoclonus epilepsy. In *Nature neuroscience* 10 (11), pp. 1407–1413. DOI: 10.1038/nn1998.

Vissing, J.; Wallace, J. L.; Galbo, H. (1989): Effect of liver glycogen content on glucose production in running rats. In *Journal of applied physiology (Bethesda, Md. : 1985)* 66 (1), pp. 318–322. DOI: 10.1152/jappl.1989.66.1.318.

Voet, Donald; Voet, Judith G. (2004): Biochemistry. Biomolecules mechanisms of enzyme action, and metabolism. 3. ed.

Vøllestad, N. K.; Tabata, I.; Medbø, J. I. (1992): Glycogen breakdown in different human muscle fibre types during exhaustive exercise of short duration. In *Acta physiologica Scandinavica* 144 (2), pp. 135–141. DOI: 10.1111/j.1748-1716.1992.tb09278.x.

Vøllestad, N. K.; Vaage, O.; Hermansen, L. (1984): Muscle glycogen depletion patterns in type I and subgroups of type II fibres during prolonged severe exercise in man. In *Acta physiologica Scandinavica* 122 (4), pp. 433–441. DOI: 10.1111/j.1748-1716.1984.tb07531.x.

Wang, Jianyong; Stuckey, Jeanne A.; Wishart, Matthew J.; Dixon, Jack E. (2002): A unique carbohydrate binding domain targets the lafora disease phosphatase to glycogen. In *The Journal of biological chemistry* 277 (4), pp. 2377–2380. DOI: 10.1074/jbc.C100686200.

Wetlaufer, Donald B. (1973): Nucleation, Rapid Folding, and Globular Intrachain Regions in Proteins. In *Proceedings of the National Academy of Sciences of the United States of America* 70 (3), pp. 697–701.

Worby, Carolyn A.; GENTRY, Matthew S.; Dixon, Jack E. (2006): Laforin, a dual specificity phosphatase that dephosphorylates complex carbohydrates. In *The Journal of biological chemistry* 281 (41), pp. 30412–30418. DOI: 10.1074/jbc.M606117200.

Worby, Carolyn A.; GENTRY, Matthew S.; Dixon, Jack E. (2008): Malin decreases glycogen accumulation by promoting the degradation of protein targeting to glycogen (PTG). In *The Journal of biological chemistry* 283 (7), pp. 4069–4076. DOI: 10.1074/jbc.M708712200.

Yanaka, Noriyuki (2007): Mammalian glycerophosphodiester phosphodiesterases. In *Bioscience, biotechnology, and biochemistry* 71 (8), pp. 1811–1818. DOI: 10.1271/bbb.70062.

References

Yokoi, S.; Austin, J.; Witmer, F. (1967): Isolation and characterization of Lafora bodies in two cases of myoclonus epilepsy. In *Journal of neuropathology and experimental neurology* 26 (1), pp. 125–127.

Zhao, Hong; Tang, Mingzhu; Liu, Meiqing; Chen, Linxi (2018): Glycophagy: An emerging target in pathology. In *Clinica chimica acta; international journal of clinical chemistry* 484, pp. 298–303. DOI: 10.1016/j.cca.2018.06.014.

Zheng, Bin; Berrie, Christopher P.; Corda, Daniela; Farquhar, Marilyn G. (2003): GDE1/MIR16 is a glycerophosphoinositol phosphodiesterase regulated by stimulation of G protein-coupled receptors. In *Proceedings of the National Academy of Sciences of the United States of America* 100 (4), pp. 1745–1750. DOI: 10.1073/pnas.0337605100.

Zhou, Y.; Vitkup, D.; Karplus, M. (1999): Native proteins are surface-molten solids: application of the Lindemann criterion for the solid versus liquid state. In *Journal of molecular biology* 285 (4), pp. 1371–1375. DOI: 10.1006/JMBI.1998.2374.

Zhu, Yuanqi; Zhang, Mei; Kelly, Amber Renee; Cheng, Alan (2014): The carbohydrate-binding domain of overexpressed STBD1 is important for its stability and protein–protein interactions. In *Bioscience Reports* 34 (4). DOI: 10.1042/BSR20140053.

Zois, Christos E.; Favaro, Elena; Harris, Adrian L. (2014): Glycogen metabolism in cancer. In *Biochemical pharmacology* 92 (1), pp. 3–11. DOI: 10.1016/j.bcp.2014.09.001.

Zois, Christos E.; Harris, Adrian L. (2016): Glycogen metabolism has a key role in the cancer microenvironment and provides new targets for cancer therapy. In *Journal of molecular medicine (Berlin, Germany)* 94 (2), pp. 137–154. DOI: 10.1007/s00109-015-1377-9.

6. Supplementary data

6.1 Plasmid information

6.1.1 Whole Sequences

6.1.1.1 CMV-EDI3-3xHA

AATAAAATATCTTTATTTTCATTACATCTGTGTGTTGGTTTTTTGTGTGAATCGATAGTACTAACATACGCTCTCCATCAAAACAAAACGAAACAAAACAAACTAGCAAAATAGGCT
GTCCCCAGTGCAAGTGCAGGTGCCAGAACATTTCTCTATCGATAGGTACCGAGCTCTTACGCGTGCTAGCATCAACTTTGTATAGAAAAGTTGTAGTTATTAATAGTAATCAATTAC
GGGGTCATTAGTTCATAGCCCATATATGGAGTTCCGCGTTACATAACTTACGGTAAATGGCCCGCCTGGCTGACCGCCCAACGACCCCCGCCCATTGACGTCAATAATGACGTATG
TTCCCATAGTAACGCCAATAGGGACTTTCCATTGACGTCAATGGGTGGAGTATTTACGGTAAACTGCCCACTTGGCAGTACATCAAGTGTATCATATGCCAAGTACGCCCCCTATTG
ACGTCAATGACGGTAAATGGCCCGCCTGGCATTATGCCCAGTACATGACCTTATGGGACTTTCCTACTTGGCAGTACATCTACGTATTAGTCATCGCTATTACCATGGTGATGCGGT
TTTGGCAGTACATCAATGGGCGTGGATAGCGGTTTGACTCACGGGGATTTCCAAGTCTCCACCCCATTGACGTCAATGGGAGTTTGTTTTGGCACCAAAATCAACGGGACTTTCCA
AAATGTCGTAACAACTCCGCCCCATTGACGCAAATGGGCGGTAGGCGTGTACGGTGGGAGGTCTATATAAGCAGAGCTGGTTTAGTGAACCGTCAGATCCAAGTTTGTACAAAAA
AGCAGGCTGCCACCATGACACCTTCTCAGGTTGCCTTTGAAATAAGAGGAACTCTTTTACCAGGAGAAGTTTTTGCGATATGTGGAAGCTGTGATGCTTTGGGAAACTGGAATCCT
CAAAATGCTGTGGCTCTTCTTCCAGAGAATGACACAGGTGAAAGCATGCTATGGAAAGCAACCATTGTACTCAGTAGAGGAGTATCAGTTCAGTATCGCTACTTCAAAGGGTACTT
TTTAGAACCAAAGACTATCGGTGGTCCATGTCAAGTGATAGTTCACAAGTGGGAGACTCATCTACAACCACGATCAATAACCCCTTTAGAAAGCGAAATTATTATTGACGATGGAC
AATTTGGAATCCACAATGGTGTTGAAACTCTGGATTCTGGATGGCTGACATGTCAGACTGAAATAAGATTACGTTTGCATTATTCTGAAAAACCTCCTGTGTCAATAACCAAGAAA
AAATTAAAAAAATCTAGATTTAGGGTGAAGCTGACACTAGAAGGCCTGGAGGAAGATGACGATGATAGGGTATCTCCCACTGTACTCCACAAAATGTCCAATAGCTTGGAGATAT
CCTTAATAAGCGACAATGAGTTCAAGTGCAGGCATTCACAGCCGGAGTGTGGTTATGGCTTGCAGCCTGATCGTTGGACAGAGTACAGCATACAGACGATGGAACCAGATAACCT
GGAACTAATCTTTGATTTTTTCGAAGAAGATCTCAGTGAGCACGTAGTTCAGGGTGATGCCCTTCCTGGACATGTGGGTACAGCTTGTCTCTTATCATCCACCATTGCTGAGAGTGG
AAAGAGTGCTGGAATTCTTACTCTTCCCATCATGAGCAGAAATTCCCGGAAAACAATAGGCAAAGTGAGAGTTGACTATATAATTATTAAGCCATTACCAGGATACAGTTGTGACA
TGAAATCTTCATTTTCCAAGTATTGGAAGCCAAGAATACCATTGGATGTTGGCCATCGAGGTGCAGGAAACTCTACAACAACTGCCCAGCTGGCTAAAGTTCAAGAAAATACTATT
GCTTCTTTAAGAAATGCTGCTAGTCATGGTGCAGCCTTTGTAGAATTTGACGTACACCTTTCAAAGGACTTTGTGCCCGTGGTATATCATGATCTTACCTGTTGTTTGACTATGAAAA
AGAAATTTGATGCTGATCCAGTTGAATTATTTGAAATTCCAGTAAAAGAATTAACATTTGACCAACTCCAGTTGTTAAAGCTCACTCATGTGACTGCACTGAAATCTAAGGATCGGA
AAGAATCTGTGGTTCAGGAGGAAAATTCCTTTTCAGAAAATCAGCCATTTCCTTCTCTTAAGATGGTTTTAGAGTCTTTGCCAGAAGATGTAGGGTTTAACATTGAAATAAAATGG
ATCTGCCAGCAAAGGGATGGAATGTGGGATGGTAACTTATCAACATATTTTGACATGAATCTGTTTTTGGATATAATTTTAAAAACTGTTTTAGAAAATTCTGGGAAGAGGAGAAT
AGTGTTTTCTTCATTTGATGCAGATATTTGCACAATGGTTCGGCAAAAGCAGAACAAATATCCGATACTATTTTTAACTCAAGGAAAATCTGAGATTTATCCTGAACTCATGGACCT
CAGATCTCGGACAACCCCCATTGCAATGAGCTTTGCACAGTTTGAAAATCTACTGGGGATAAATGTACATACTGAAGACTTGCTCAGAAACCCATCCTATATTCAAGAGGCAAAAG
CTAAGGGACTAGTCATATTCTGCTGGGGTGATGATACCAATGATCCTGAAAACAGAAGGAAATTGAAGGAACTTGGAGTTAATGGTCTAATTTATGATAGGATATATGATTGGAT
GCCTGAACAACCAAATATATTCCAAGTGGAGCAATTGGAACGCCTGAAGCAGGAATTGCCAGAGCTTAAGAGCTGTTTGTGTCCCACTGTTAGCCGCTTTGTTCCCTCATCTTTGT
GTGGGGAGTCTGATATCCATGTGGATGCCAACGGCATTGATAACGTGGAGAATGCTTACCCATACGATGTTCCAGATTACGCTTACCCATACGATGTTCCAGATTACGCTTAGACCCAG
TACGATGTTCCAGATTACGCTTAGACCCAGCTTTCTTGTACAAAGTGGTGATGGCCGGCCGCTTCGAGCAGACATGATAAGATACATTGATGAGTTTGGACAAACCACAACTAGAA
TGCAGTGAAAAAAATGCTTTATTTGTGAAATTTGTGATGCTATTGCTTTATTTGTAACCATTATAAGCTGCAATAAACAAGTTAACAACAACAATTGCATTCATTTTATGTTTCAGGT
TCAGGGGGAGGTGTGGGAGGTTTTTTAAAGCAAGTAAAACCTCTACAAATGTGGTAAAATCGATAAGGATCCGTCGACCGATGCCCTTGAGAGCCTTCAACCCAGTCAGCTCCTT
CCGGTGGGCGCGGGGCATGACTATCGTCGCCGCACTTATGACTGTCTTCTTTATCATGCAACTCGTAGGACAGGTGCCGGCAGCGCTCTTCCGCTTCCTCGCTCACTGACTCGCTG
CGCTCGGTCGTTCGGCTGCGGCGAGCGGTATCAGCTCACTCAAAGGCGGTAATACGGTTATCCACAGAATCAGGGGATAACGCAGGAAAGAACATGTGAGCAAAAGGCCAGCA
AAAGGCCAGGAACCGTAAAAAGGCCGCGTTGCTGGCGTTTTTCCATAGGCTCCGCCCCCCTGACGAGCATCACAAAAATCGACGCTCAAGTCAGAGGTGGCGAAACCCGACAGG
ACTATAAAGATACCAGGCGTTTCCCCCTGGAAGCTCCCTCGTGCGCTCTCCTGTTCCGACCCTGCCGCTTACCGGATACCTGTCCGCCTTTCTCCCTTCGGGAAGCGTGGCGCTTTCT
CATAGCTCACGCTGTAGGTATCTCAGTTCGGTGTAGGTCGTTCGCTCCAAGCTGGGCTGTGTGCACGAACCCCCCGTTCAGCCCGACCGCTGCGCCTTATCCGGTAACTATCGTCTT
GAGTCCAACCCGGTAAGACACGACTTATCGCCACTGGCAGCAGCCACTGGTAACAGGATTAGCAGAGCGAGGTATGTAGGCGGTGCTACAGAGTTCTTGAAGTGGTGGCCTAAC
TACGGCTACACTAGAAGAACAGTATTTGGTATCTGCGCTCTGCTGAAGCCAGTTACCTTCGGAAAAAGAGTTGGTAGCTCTTGATCCGGCAAACAAACCACCGCTGGTAGCGGTG
GTTTTTTTGTTTGCAAGCAGCAGATTACGCGCAGAAAAAAAGGATCTCAAGAAGATCCTTTGATCTTTTCTACGGGGTCTGACGCTCAGTGGAACGAAAACTCACGTTAAGGGATT
TTGGTCATGAGATTATCAAAAAGGATCTTCACCTAGATCCTTTTAAATTAAAAATGAAGTTTTAAATCAATCTAAAGTATATATGAGTAAACTTGGTCTGACAGTTACCAATGCTTAA
TCAGTGAGGCACCTATCTCAGCGATCTGTCTATTTCGTTCATCCATAGTTGCCTGACTCCCCGTCGTGTAGATAACTACGATACGGGAGGGCTTACCATCTGGCCCCAGTGCTGCAA
TGATACCGCGAGACCCACGCTCACCGGCTCCAGATTTATCAGCAATAAACCAGCCAGCCGGAAGGGCCGAGCGCAGAAGTGGTCCTGCAACTTTATCCGCCTCCATCCAGTCTATT
AATTGTTGCCGGGAAGCTAGAGTAAGTAGTTCGCCAGTTAATAGTTTGCGCAACGTTGTTGCCATTGCTACAGGCATCGTGGTGTCACGCTCGTCGTTTGGTATGGCTTCATTCAG
CTCCGGTTCCCAACGATCAAGGCGAGTTACATGATCCCCCATGTTGTGCAAAAAAGCGGTTAGCTCCTTCGGTCCTCCGATCGTTGTCAGAAGTAAGTTGGCCGCAGTGTTATCAC
TCATGGTTATGGCAGCACTGCATAATTCTCTTACTGTCATGCCATCCGTAAGATGCTTTTCTGTGACTGGTGAGTACTCAACCAAGTCATTCTGAGAATAGTGTATGCGGCGACCGA
GTTGCTCTTGCCCGGCGTCAATACGGGATAATACCGCGCCACATAGCAGAACTTTAAAAGTGCTCATCATTGGAAAACGTTCTTCGGGGCGAAAACTCTCAAGGATCTTACCGCTG
TTGAGATCCAGTTCGATGTAACCCACTCGTGCACCCAACTGATCTTCAGCATCTTTTACTTTCACCAGCGTTTCTGGGTGAGCAAAAACAGGAAGGCAAAATGCCGCAAAAAAGGG
AATAAGGGCGACACGGAAATGTTGAATACTCATACTCTTCCTTTTTCAATATTATTGAAGCATTTATCAGGGTTATTGTCTCATGAGCGGATACATATTTGAATGTATTTAGAAAAA
TAAACAAATAGGGGTTCCGCGCACATTTCCCCGAAAAGTGCCACCTGACGCGCCCTGTAGCGGCGCATTAAGCGCGGCGGGTGTGGTGGTTACGCGCAGCGTGACCGCTACACT
TGCCAGCGCCCTAGCGCCCGCTCCTTTCGCTTTCTTCCCTTCCTTTCTCGCCACGTTCGCCGGCTTTCCCCGTCAAGCTCTAAATCGGGGGCTCCCTTTAGGGTTCCGATTTAGTGCTT
TACGGCACCTCGACCCCAAAAAACTTGATTAGGGTGATGGTTCACGTAGTGGGCCATCGCCCTGATAGACGGTTTTTCGCCCTTTGACGTTGGAGTCCACGTTCTTTAATAGTGGA
CTCTTGTTCCAAACTGGAACAACACTCAACCCTATCTCGGTCTATTCTTTTGATTTATAAGGGATTTTGCCGATTTCGGCCTATTGGTTAAAAAATGAGCTGATTTAACAAAAATTTA
ACGCGAATTTTAACAAAATATTAACGCTTACAATTTGCCATTCGCCATTCAGGCTGCGCAACTGTTGGGAAGGGCGATCGGTGCGGGCCTCTTCGCTATTACGCCAGCCCAAGCTA
CCATGATAAGTAAGTAATATTAAGGTACGGGAGGTACTTGGAGCGGCCGC

6.1.1.2 CMV-EDI3-W32A-3xHA

AATAAAATATCTTTATTTTCATTACATCTGTGTGTTGGTTTTTTGTGTGAATCGATAGTACTAACATACGCTCTCCATCAAAACAAAACGAAACAAAACAAACTAGCAAAATAGGCT
GTCCCCAGTGCAAGTGCAGGTGCCAGAACATTTCTCTATCGATAGGTACCGAGCTCTTACGCGTGCTAGCATCAACTTTGTATAGAAAAGTTGTAGTTATTAATAGTAATCAATTAC
GGGGTCATTAGTTCATAGCCCATATATGGAGTTCCGCGTTACATAACTTACGGTAAATGGCCCGCCTGGCTGACCGCCCAACGACCCCCGCCCATTGACGTCAATAATGACGTATG
TTCCCATAGTAACGCCAATAGGGACTTTCCATTGACGTCAATGGGTGGAGTATTTACGGTAAACTGCCCACTTGGCAGTACATCAAGTGTATCATATGCCAAGTACGCCCCCTATTG
ACGTCAATGACGGTAAATGGCCCGCCTGGCATTATGCCCAGTACATGACCTTATGGGACTTTCCTACTTGGCAGTACATCTACGTATTAGTCATCGCTATTACCATGGTGATGCGGT
TTTGGCAGTACATCAATGGGCGTGGATAGCGGTTTGACTCACGGGGATTTCCAAGTCTCCACCCCATTGACGTCAATGGGAGTTTGTTTTGGCACCAAAATCAACGGGACTTTCCA
AAATGTCGTAACAACTCCGCCCCATTGACGCAAATGGGCGGTAGGCGTGTACGGTGGGAGGTCTATATAAGCAGAGCTGGTTTAGTGAACCGTCAGATCCAAGTTTGTACAAAAA
AGCAGGCTGCCACCATGACACCTTCTCAGGTTGCCTTTGAAATAAGAGGAACTCTTTTACCAGGAGAAGTTTTTGCGATATGTGGAAGCTGTGATGCTTTGGGAAACGCGAATCCT
CAAAATGCTGTGGCTCTTCTTCCAGAGAATGACACAGGTGAAAGCATGCTATGGAAAGCAACCATTGTACTCAGTAGAGGAGTATCAGTTCAGTATCGCTACTTCAAAGGGTACTT
TTTAGAACCAAAGACTATCGGTGGTCCATGTCAAGTGATAGTTCACAAGTGGGAGACTCATCTACAACCACGATCAATAACCCCTTTAGAAAGCGAAATTATTATTGACGATGGAC
AATTTGGAATCCACAATGGTGTTGAAACTCTGGATTCTGGATGGCTGACATGTCAGACTGAAATAAGATTACGTTTGCATTATTCTGAAAAACCTCCTGTGTCAATAACCAAGAAA
AAATTAAAAAAATCTAGATTTAGGGTGAAGCTGACACTAGAAGGCCTGGAGGAAGATGACGATGATAGGGTATCTCCCACTGTACTCCACAAAATGTCCAATAGCTTGGAGATAT
CCTTAATAAGCGACAATGAGTTCAAGTGCAGGCATTCACAGCCGGAGTGTGGTTATGGCTTGCAGCCTGATCGTTGGACAGAGTACAGCATACAGACGATGGAACCAGATAACCT
GGAACTAATCTTTGATTTTTTCGAAGAAGATCTCAGTGAGCACGTAGTTCAGGGTGATGCCCTTCCTGGACATGTGGGTACAGCTTGTCTCTTATCATCCACCATTGCTGAGAGTGG
AAAGAGTGCTGGAATTCTTACTCTTCCCATCATGAGCAGAAATTCCCGGAAAACAATAGGCAAAGTGAGAGTTGACTATATAATTATTAAGCCATTACCAGGATACAGTTGTGACA
TGAAATCTTCATTTTCCAAGTATTGGAAGCCAAGAATACCATTGGATGTTGGCCATCGAGGTGCAGGAAACTCTACAACAACTGCCCAGCTGGCTAAAGTTCAAGAAAATACTATT
GCTTCTTTAAGAAATGCTGCTAGTCATGGTGCAGCCTTTGTAGAATTTGACGTACACCTTTCAAAGGACTTTGTGCCCGTGGTATATCATGATCTTACCTGTTGTTTGACTATGAAAA
AGAAATTTGATGCTGATCCAGTTGAATTATTTGAAATTCCAGTAAAAGAATTAACATTTGACCAACTCCAGTTGTTAAAGCTCACTCATGTGACTGCACTGAAATCTAAGGATCGGA
AAGAATCTGTGGTTCAGGAGGAAAATTCCTTTTCAGAAAATCAGCCATTTCCTTCTCTTAAGATGGTTTTAGAGTCTTTGCCAGAAGATGTAGGGTTTAACATTGAAATAAAATGG
ATCTGCCAGCAAAGGGATGGAATGTGGGATGGTAACTTATCAACATATTTTGACATGAATCTGTTTTTGGATATAATTTTAAAAACTGTTTTAGAAAATTCTGGGAAGAGGAGAAT
AGTGTTTTCTTCATTTGATGCAGATATTTGCACAATGGTTCGGCAAAAGCAGAACAAATATCCGATACTATTTTTAACTCAAGGAAAATCTGAGATTTATCCTGAACTCATGGACCT

6. Supplementary data

CAGATCTCGGACAACCCCCATTGCAATGAGCTTTGCACAGTTTGAAAATCTACTGGGGATAAATGTACATACTGAAGACTTGCTCAGAAACCCATCCTATATTCAAGAGGCAAAAG
CTAAGGGACTAGTCATATTCTGCTGGGGTGATGATACCAATGATCCTGAAAACAGAAGGAAATTGAAGGAACTTGGAGTTAATGGTCTAATTTATGATAGGATATATGATTGGAT
GCCTGAACAACCAAATATATTCCAAGTGGAGCAATTGGAACGCCTGAAGCAGGAATTGCCAGAGCTTAAGAGCTGTTTGTGTCCCACTGTTAGCCGCTTTGTTCCCTCATCTTTGT
GTGGGGAGTCTGATATCCATGTGGATGCCAACGGCATTGATAACGTGGAGAATGCTTACCCATACGATGTTCCAGATTACGCTTACCCATACGATGTTCCAGATTACGCTTACCCA
TACGATGTTCCAGATTACGCTTAGACCCAGCTTTCTTGTACAAAGTGGTGATGGCCGGCCGCTTCGAGCAGACATGATAAGATACATTGATGAGTTTGGACAAACCACAACTAGAA
TGCAGTGAAAAAAATGCTTTATTTGTGAAATTTGTGATGCTATTGCTTTATTTGTAACCATTATAAGCTGCAATAAACAAGTTAACAACAACAATTGCATTCATTTTATGTTTCAGGT
TCAGGGGGAGGTGTGGGAGGTTTTTTAAAGCAAGTAAAACCTCTACAAATGTGGTAAAATCGATAAGGATCCGTCGACCGATGCCCTTGAGAGCCTTCAACCCAGTCAGCTCCTT
CCGGTGGGCGCGGGGCATGACTATCGTCGCCGCACTTATGACTGTCTTCTTTATCATGCAACTCGTAGGACAGGTGCCGGCAGCGCTCTTCCGCTTCCTCGCTCACTGACTCGCTG
CGCTCGGTCGTTCGGCTGCGGCGAGCGGTATCAGCTCACTCAAAGGCGGTAATACGGTTATCCACAGAATCAGGGGATAACGCAGGAAAGAACATGTGAGCAAAAGGCCAGCA
AAAGGCCAGGAACCGTAAAAAGGCCGCGTTGCTGGCGTTTTTCCATAGGCTCCGCCCCCCTGACGAGCATCACAAAAATCGACGCTCAAGTCAGAGGTGGCGAAACCCGACAGG
ACTATAAAGATACCAGGCGTTTCCCCCTGGAAGCTCCCTCGTGCGCTCTCCTGTTCCGACCCTGCCGCTTACCGGATACCTGTCCGCCTTTCTCCCTTCGGGAAGCGTGGCGCTTTCT
CATAGCTCACGCTGTAGGTATCTCAGTTCGGTGTAGGTCGTTCGCTCCAAGCTGGGCTGTGTGCACGAACCCCCCGTTCAGCCCGACCGCTGCGCCTTATCCGGTAACTATCGTCTT
GAGTCCAACCCGGTAAGACACGACTTATCGCCACTGGCAGCAGCCACTGGTAACAGGATTAGCAGAGCGAGGTATGTAGGCGGTGCTACAGAGTTCTTGAAGTGGTGGCCTAAC
TACGGCTACACTAGAAGAACAGTATTTGGTATCTGCGCTCTGCTGAAGCCAGTTACCTTCGGAAAAAGAGTTGGTAGCTCTTGATCCGGCAAACAAACCACCGCTGGTAGCGGTG
GTTTTTTTGTTTGCAAGCAGCAGATTACGCGCAGAAAAAAAGGATCTCAAGAAGATCCTTTGATCTTTTCTACGGGGTCTGACGCTCAGTGGAACGAAAACTCACGTTAAGGGATT
TTGGTCATGAGATTATCAAAAAGGATCTTCACCTAGATCCTTTTAAATTAAAAATGAAGTTTTAAATCAATCTAAAGTATATATGAGTAAACTTGGTCTGACAGTTACCAATGCTTAA
TCAGTGAGGCACCTATCTCAGCGATCTGTCTATTTCGTTCATCCATAGTTGCCTGACTCCCCGTCGTGTAGATAACTACGATACGGGAGGGCTTACCATCTGGCCCCAGTGCTGCAA
TGATACCGCGAGACCCACGCTCACCGGCTCCAGATTTATCAGCAATAAACCAGCCAGCCGGAAGGGCCGAGCGCAGAAGTGGTCCTGCAACTTTATCCGCCTCCATCCAGTCTATT
AATTGTTGCCGGGAAGCTAGAGTAAGTAGTTCGCCAGTTAATAGTTTGCGCAACGTTGTTGCCATTGCTACAGGCATCGTGGTGTCACGCTCGTCGTTTGGTATGGCTTCATTCAG
CTCCGGTTCCCAACGATCAAGGCGAGTTACATGATCCCCCATGTTGTGCAAAAAAGCGGTTAGCTCCTTCGGTCCTCCGATCGTTGTCAGAAGTAAGTTGGCCGCAGTGTTATCAC
TCATGGTTATGGCAGCACTGCATAATTCTCTTACTGTCATGCCATCCGTAAGATGCTTTTCTGTGACTGGTGAGTACTCAACCAAGTCATTCTGAGAATAGTGTATGCGGCGACCGA
GTTGCTCTTGCCCGGCGTCAATACGGGATAATACCGCGCCACATAGCAGAACTTTAAAAGTGCTCATCATTGGAAAACGTTCTTCGGGGCGAAAACTCTCAAGGATCTTACCGCTG
TTGAGATCCAGTTCGATGTAACCCACTCGTGCACCCAACTGATCTTCAGCATCTTTTACTTTCACCAGCGTTTCTGGGTGAGCAAAAACAGGAAGGCAAAATGCCGCAAAAAAGGG
AATAAGGGCGACACGGAAATGTTGAATACTCATACTCTTCCTTTTTCAATATTATTGAAGCATTTATCAGGGTTATTGTCTCATGAGCGGATACATATTTGAATGTATTTAGAAAAA
TAAACAAATAGGGGTTCCGCGCACATTTCCCCGAAAAGTGCCACCTGACGCGCCCTGTAGCGGCGCATTAAGCGCGGCGGGTGTGGTGGTTACGCGCAGCGTGACCGCTACACT
TGCCAGCGCCCTAGCGCCCGCTCCTTTCGCTTTCTTCCCTTCCTTTCTCGCCACGTTCGCCGGCTTTCCCCGTCAAGCTCTAAATCGGGGGCTCCCTTTAGGGTTCCGATTTAGTGCTT
TACGGCACCTCGACCCCAAAAAACTTGATTAGGGTGATGGTTCACGTAGTGGGCCATCGCCCTGATAGACGGTTTTTCGCCCTTTGACGTTGGAGTCCACGTTCTTTAATAGTGGA
CTCTTGTTCCAAACTGGAACAACACTCAACCCTATCTCGGTCTATTCTTTTGATTTATAAGGGATTTTGCCGATTTCGGCCTATTGGTTAAAAAATGAGCTGATTTAACAAAAATTTA
ACGCGAATTTTAACAAAATATTAACGCTTACAATTTGCCATTCGCCATTCAGGCTGCGCAACTGTTGGGAAGGGCGATCGGTGCGGGCCTCTTCGCTATTACGCCAGCCCAAGCTA
CCATGATAAGTAAGTAATATTAAGGTACGGGAGGTACTTGGAGCGGCCGC

6.1.1.3 CMV-EDI3- ΔCBM20 -3xHA

CAACTTTGTATAGAAAAGTTGTAGTTATTAATAGTAATCAATTACGGGGTCATTAGTTCATAGCCCATATATGGAGTTCCGCGTTACATAACTTACGGTAAATGGCCCGCCTGGCTG
ACCGCCCAACGACCCCCGCCCATTGACGTCAATAATGACGTATGTTCCCATAGTAACGCCAATAGGGACTTTCCATTGACGTCAATGGGTGGAGTATTTACGGTAAACTGCCCACT
TGGCAGTACATCAAGTGTATCATATGCCAAGTACGCCCCCTATTGACGTCAATGACGGTAAATGGCCCGCCTGGCATTATGCCCAGTACATGACCTTATGGGACTTTCCTACTTGGC
AGTACATCTACGTATTAGTCATCGCTATTACCATGGTGATGCGGTTTTGGCAGTACATCAATGGGCGTGGATAGCGGTTTGACTCACGGGGATTTCCAAGTCTCCACCCCATTGAC
GTCAATGGGAGTTTGTTTTGGCACCAAAATCAACGGGACTTTCCAAAATGTCGTAACAACTCCGCCCCATTGACGCAAATGGGCGGTAGGCGTGTACGGTGGGAGGTCTATATAA
GCAGAGCTGGTTTAGTGAACCGTCAGATCCAAGTTTGTACAAAAAAGCAGGCTGCCACCATGACACCTAGGTGTCATGGTGGCAGCGTAAACGTATTCAGCATCAGGATTTTGAG
CGGCGGCTACGTGAGATGGTTGCCGAACGCAGAGCCCGTCTGGCGCGGGTGACCGATCTCGTGGAACAGCAAACGCTGCATCGTGAAGTGGAAGCCTATGAAGCGCGCCTGGC
ACGCTGCCACCATGACACCTACATGTCAGACTGAAATAAGATTACGTTTGCATTATTCTGAAAAACCTCCTGTGTCAATAACCAAGAAAAAATTAAAAAAATCTAGATTTAGGGTG
AAGCTGACACTAGAAGGCCTGGAGGAAGATGACGATGATAGGGTATCTCCCACTGTACTCCACAAAATGTCCAATAGCTTGGAGATATCCTTAATAAGCGACAATGAGTTCAAGT
GCAGGCATTCACAGCCGGAGTGTGGTTATGGCTTGCAGCCTGATCGTTGGACAGAGTACAGCATACAGACGATGGAACCAGATAACCTGGAACTAATCTTTGATTTTTTCGAAGA
AGATCTCAGTGAGCACGTAGTTCAGGGTGATGCCCTTCCTGGACATGTGGGTACAGCTTGTCTCTTATCATCCACCATTGCTGAGAGTGGAAAGAGTGCTGGAATTCTTACTCTTC
CCATCATGAGCAGAAATTCCCGGAAAACAATAGGCAAAGTGAGAGTTGACTATATAATTATTAAGCCATTACCAGGATACAGTTGTGACATGAAATCTTCATTTTCCAAGTATTGG
AAGCCAAGAATACCATTGGATGTTGGCCATCGAGGTGCAGGAAACTCTACAACAACTGCCCAGCTGGCTAAAGTTCAAGAAAATACTATTGCTTCTTTAAGAAATGCTGCTAGTCA
TGGTGCAGCCTTTGTAGAATTTGACGTACACCTTTCAAAGGACTTTGTGCCCGTGGTATATCATGATCTTACCTGTTGTTTGACTATGAAAAAGAAATTTGATGCTGATCCAGTTGA
ATTATTTGAAATTCCAGTAAAAGAATTAACATTTGACCAACTCCAGTTGTTAAAGCTCACTCATGTGACTGCACTGAAATCTAAGGATCGGAAAGAATCTGTGGTTCAGGAGGAAA
ATTCCTTTTCAGAAAATCAGCCATTTCCTTCTCTTAAGATGGTTTTAGAGTCTTTGCCAGAAGATGTAGGGTTTAACATTGAAATAAAATGGATCTGCCAGCAAAGGGATGGAATGT
GGGATGGTAACTTATCAACATATTTTGACATGAATCTGTTTTTGGATATAATTTTAAAAACTGTTTTAGAAAATTCTGGGAAGAGGAGAATAGTGTTTTCTTCATTTGATGCAGATA
TTTGCACAATGGTTCGGCAAAAGCAGAACAAATATCCGATACTATTTTTAACTCAAGGAAAATCTGAGATTTATCCTGAACTCATGGACCTCAGATCTCGGACAACCCCCATTGCAA
TGAGCTTTGCACAGTTTGAAAATCTACTGGGGATAAATGTACATACTGAAGACTTGCTCAGAAACCCATCCTATATTCAAGAGGCAAAAGCTAAGGGACTAGTCATATTCTGCTGG
GGTGATGATACCAATGATCCTGAAAACAGAAGGAAATTGAAGGAACTTGGAGTTAATGGTCTAATTTATGATAGGATATATGATTGGATGCCTGAACAACCAAATATATTCCAAG
TGGAGCAATTGGAACGCCTGAAGCAGGAATTGCCAGAGCTTAAGAGCTGTTTGTGTCCCACTGTTAGCCGCTTTGTTCCCTCATCTTTGTGTGGGGAGTCTGATATCCATGTGGAT
GCCAACGGCATTGATAACGTGGAGAATGCTTACCCATACGATGTTCCAGATTACGCTTACCCATACGATGTTCCAGATTACGCTTACCCATACGATGTTCCAGATTACGCTTAGACC
CAGCTTTCTTGTACAAAGTGGTGATGGCCGGCCGCTTCGAGCAGACATGATAAGATACATTGATGAGTTTGGACAAACCACAACTAGAATGCAGTGAAAAAAATGCTTTATTTGT
GAAATTTGTGATGCTATTGCTTTATTTGTAACCATTATAAGCTGCAATAAACAAGTTAACAACAACAATTGCATTCATTTTATGTTTCAGGTTCAGGGGGAGGTGTGGGAGGTTTTT
TAAAGCAAGTAAAACCTCTACAAATGTGGTAGCGGCCGCGGCGCTCTTCCGCTTCCTCGCTCACTGACTCGCTGCGCTCGGTCGTTCGGCTGCGGCGAGCGGTATCAGCTCACTCA
AAGGCGGTAATACGGTTATCCACAGAATCAGGGGATAACGCAGGAAAGAACATGTGAGCAAAAGGCCAGCAAAAGGCCAGGAACCGTAAAAAGGCCGCGTTGCTGGCGTTTTT
CCATAGGCTCCGCCCCCCTGACGAGCATCACAAAAATCGACGCTCAAGTCAGAGGTGGCGAAACCCGACAGGACTATAAAGATACCAGGCGTTTCCCCCTGGAAGCTCCCTCGTG
CGCTCTCCTGTTCCGACCCTGCCGCTTACCGGATACCTGTCCGCCTTTCTCTCTTCGGGAAGCGTGGCGCTTTCTCATAGCTCACGCTGTAGGTATCTCAGTTCGGTGTAGGTCGTTC
GCTCCAAGCTGGGCTGTGTGCACGAACCCCCCGTTCAGCCCGACCGCTGCGCCTTATCCGGTAACTATCGTCTTGAGTCCAACCCGGTAAGACACGACTTATCGCCACTGGCAGCA
GCCACTGGTAACAGGATTAGCAGAGCGAGGTATGTAGGCGGTGCTACAGAGTTCTTGAAGTGGTGGCCTAACTACGGCTACACTAGAAGAACAGTATTTGGTATCTGCGCTCTGC
TGAAGCCAGTTACCTTCGGAAAAAGAGTTGGTAGCTCTTGATCCGGCAAACAAACCACCGCTGGTAGCGGTGGTTTTTTTGTTTGCAAGCAGCAGATTACGCGCAGAAAAAAAGG
ATCTCAAGAAGATCCTTTGATCTTTTCTACGGGGTCTGACGCTCAGTGGAACGAAAACTCACGTTAAGGGATTTTGGTCATGAGATTATCAAAAAGGATCTTCACCTAGATCCTTTT
AAATTAAAAATGAAGTTTTAAATCAATCTAAAGTATATATGAGTAAACTTGGTCTGACAGTTACCAATGCTTAATCAGTGAGGCACCTATCTCAGCGATCTGTCTATTTCGTTCATCC
ATAGTTGCCTGACTCCCCGTCGTGTAGATAACTACGATACGGGAGGGCTTACCATCTGGCCCCAGTGCTGCAATGATACCGCGAGACCCACGCTCACCGGCTCCAGATTTATCAGC
AATAAACCAGCCAGCCGGAAGGGCCGAGCGCAGAAGTGGTCCTGCAACTTTATCCGCCTCCATCCAGTCTATTAATTGTTGCCGGGAAGCTAGAGTAAGTAGTTCGCCAGTTAAT
AGTTTGCGCAACGTTGTTGCCATTGCTACAGGCATCGTGGTGTCACGCTCGTCGTTTGGTATGGCTTCATTCAGCTCCGGTTCCCAACGATCAAGGCGAGTTACATGATCCCCCATG
TTGTGCAAAAAAGCGGTTAGCTCCTTCGGTCCTCCGATCGTTGTCAGAAGTAAGTTGGCCGCAGTGTTATCACTCATGGTTATGGCAGCACTGCATAATTCTCTTACTGTCATGCCA
TCCGTAAGATGCTTTTCTGTGACTGGTGAGTACTCAACCAAGTCATTCTGAGAATAGTGTATGCGGCGACCGAGTTGCTCTTGCCCGGCGTCAATACGGGATAATACCGCGCCACA
TAGCAGAACTTTAAAAGTGCTCATCATTGGAAAACGTTCTTCGGGGCGAAAACTCTCAAGGATCTTACCGCTGTTGAGATCCAGTTCGATGTAACCCACTCGTGCACCCAACTGAT
CTTCAGCATCTTTTACTTTCACCAGCGTTTCTGGGTGAGCAAAAACAGGAAGGCAAAATGCCGCAAAAAAGGGAATAAGGGCGACACGGAAATGTTGAATACTCATACTCTTCCTT
TTTCAATATTATTGAAGCATTTATCAGGGTTATTGTCTCATGAGCGGATACATATTTGAATGTATTTAGAAAAATAAACAAATAGGGGTTCCGCGCACATTTCCCCGAAAAGTGCCA
CCTGACGTCTAAGAAACCATTATTATCATGACATTAACCTATAAAAATAGGCGTATCACGAGGCCCTTTCGTCGGCGCGCCGCGGCCGC

6.1.1.4 CAG-EDI3-turboRFP

CAACTTTGTATAGAAAAGTTGCTCGACATTGATTATTGACTAGTTATTAATAGTAATCAATTACGGGGTCATTAGTTCATAGCCCATATATGGAGTTCCGCGTTACATAACTTACGG
TAAATGGCCCGCCTGGCTGACCGCCCAACGACCCCCGCCCATTGACGTCAATAATGACGTATGTTCCCATAGTAACGCCAATAGGGACTTTCCATTGACGTCAATGGGTGGAGTAT
TTACGGTAAACTGCCCACTTGGCAGTACATCAAGTGTATCATATGCCAAGTACGCCCCCTATTGACGTCAATGACGGTAAATGGCCCGCCTGGCATTATGCCCAGTACATGACCTT
ATGGGACTTTCCTACTTGGCAGTACATCTACGTATTAGTCATCGCTATTACCATGGTCGAGGTGAGCCCCACGTTCTGCTTCACTCTCCCCATCTCCCCCCCCTCCCCACCCCCAATTT

6. Supplementary data

TGTATTTATTTATTTTTTAATTATTTTGTGCAGCGATGGGGGCGGGGGGGGGGGGGGGCGCGCGCCAGGCGGGGCGGGGCGGGGCGAGGGGCGGGGCGGGGCGAGGCGGA
GAGGTGCGGCGGCAGCCAATCAGAGCGGCGCGCTCCGAAAGTTTCCTTTTATGGCGAGGCGGCGGCGGCGGCGGCCCTATAAAAAGCGAAGCGCGCGGCGGGCGGGAGTCGC
TGCGCGCTGCCTTCGCCCCGTGCCCCGCTCCGCCGCCGCCTCGCGCCGCCCGCCCCGGCTCTGACTGACCGCGTTACTCCCACAGGTGAGCGGGCGGGACGGCCCTTCTCCTCCGG
GCTGTAATTAGCGCTTGGTTTAATGACGGCTTGTTTCTTTTCTGTGGCTGCGTGAAAGCCTTGAGGGGCTCCGGGAGGGCCCTTTGTGCGGGGGGAGCGGCTCGGGGGGTGCGT
GCGTGTGTGTGTGCGTGGGGAGCGCCGCGTGCGGCTCCGCGCTGCCCGGCGGCTGTGAGCGCTGCGGGCGCGGCGCGGGGCTTTGTGCGCTCCGCAGTGTGCGCGAGGGGAG
CGCGGCCGGGGGCGGTGCCCCGCGGTGCGGGGGGGGCTGCGAGGGGAACAAAGGCTGCGTGCGGGGTGTGTGCGTGGGGGGGTGAGCAGGGGGTGTGGGCGCGTCGGTCG
GGCTGCAACCCCCCCCTGCACCCCCCTCCCCGAGTTGCTGAGCACGGCCCGGCTTCGGGTGCGGGGCTCCGTACGGGGCGTGGCGCGGGGCTCGCCGTGCCGGGCGGGGGGTGG
CGGCAGGTGGGGGTGCCGGGCGGGGCGGGGCCGCCTCGGGCCGGGGAGGGCTCGGGGGAGGGGCGCGGCGGCCCCCGGAGCGCCGGCGGCTGTCGAGGCGCGGCGAGCC
GCAGCCATTGCCTTTTATGGTAATCGTGCGAGAGGGCGCAGGGACTTCCTTTGTCCCAAATCTGTGCGGAGCCGAAATCTGGGAGGCGCCGCCGCACCCCCTCTAGCGGGCGCG
GGGCGAAGCGGTGCGGCGCCGGCAGGAAGGAAATGGGCGGGGAGGGCCTTCGTGCGTCGCCGCGCCGCCGTCCCCTTCTCCCTCTCCAGCCTCGGGGCTGTCCGCGGGGGGAC
GGCTGCCTTCGGGGGGGACGGGGCAGGGCGGGGTTCGGCTTCTGGCGTGTGACCGGCGGCTCTAGAGCCTCTGCTAACCATGTTCATGCCTTCTTCTTTTTCCTACAGCTCCTGG
GCAACGTGCTGGTTATTGTGCTGTCTCATCATTTTGGCAAAGAATTGCAAGTTTGTACAAAAAAGCAGGCTGCCACCATGACACCTTCTCAGGTTGCCTTTGAAATAAGAGGAACT
CTTTTACCAGGAGAAGTTTTTGCGATATGTGGAAGCTGTGATGCTTTGGGAAACTGGAATCCTCAAAATGCTGTGGCTCTTCTTCCAGAGAATGACACAGGTGAAAGCATGCTATG
GAAAGCAACCATTGTACTCAGTAGAGGAGTATCAGTTCAGTATCGCTACTTCAAAGGGTACTTTTTAGAACCAAAGACTATCGGTGGTCCATGTCAAGTGATAGTTCACAAGTGGG
AGACTCATCTACAACCACGATCAATAACCCCTTTAGAAAGCGAAATTATTATTGACGATGGACAATTTGGAATCCACAATGGTGTTGAAACTCTGGATTCTGGATGGCTGACATGT
CAGACTGAAATAAGATTACGTTTGCATTATTCTGAAAAACCTCCTGTGTCAATAACCAAGAAAAAATTAAAAAAATCTAGATTTAGGGTGAAGCTGACACTAGAAGGCCTGGAGG
AAGATGACGATGATAGGGTATCTCCCACTGTACTCCACAAAATGTCCAATAGCTTGGAGATATCCTTAATAAGCGACAATGAGTTCAAGTGCAGGCATTCACAGCCGGAGTGTGG
TTATGGCTTGCAGCCTGATCGTTGGACAGAGTACAGCATACAGACGATGGAACCAGATAACCTGGAACTAATCTTTGATTTTTTCGAAGAAGATCTCAGTGAGCACGTAGTTCAG
GGTGATGCCCTTCCTGGACATGTGGGTACAGCTTGTCTCTTATCATCCACCATTGCTGAGAGTGGAAAGAGTGCTGGAATTCTTACTCTTCCCATCATGAGCAGAAATTCCCGGAA
AACAATAGGCAAAGTGAGAGTTGACTATATAATTATTAAGCCATTACCAGGATACAGTTGTGACATGAAATCTTCATTTTCCAAGTATTGGAAGCCAAGAATACCATTGGATGTTG
GCCATCGAGGTGCAGGAAACTCTACAACAACTGCCCAGCTGGCTAAAGTTCAAGAAAATACTATTGCTTCTTTAAGAAATGCTGCTAGTCATGGTGCAGCCTTTGTAGAATTTGAC
GTACACCTTTCAAAGGACTTTGTGCCCGTGGTATATCATGATCTTACCTGTTGTTTGACTATGAAAAAGAAATTTGATGCTGATCCAGTTGAATTATTTGAAATTCCAGTAAAAGAA
TTAACATTTGACCAACTCCAGTTGTTAAAGCTCACTCATGTGACTGCACTGAAATCTAAGGATCGGAAAGAATCTGTGGTTCAGGAGGAAAATTCCTTTTCAGAAAATCAGCCATTT
CCTTCTCTTAAGATGGTTTTAGAGTCTTTGCCAGAAGATGTAGGGTTTAACATTGAAATAAAATGGATCTGCCAGCAAAGGGATGGAATGTGGGATGGTAACTTATCAACATATTT
TGACATGAATCTGTTTTTGGATATAATTTTAAAAACTGTTTTAGAAAATTCTGGGAAGAGGAGAATAGTGTTTTCTTCATTTGATGCAGATATTTGCACAATGGTTCGGCAAAAGCA
GAACAAATATCCGATACTATTTTTAACTCAAGGAAAATCTGAGATTTATCCTGAACTCATGGACCTCAGATCTCGGACAACCCCCATTGCAATGAGCTTTGCACAGTTTGAAAATCT
ACTGGGGATAAATGTACATACTGAAGACTTGCTCAGAAACCCATCCTATATTCAAGAGGCAAAAGCTAAGGGACTAGTCATATTCTGCTGGGGTGATGATACCAATGATCCTGAA
AACAGAAGGAAATTGAAGGAACTTGGAGTTAATGGTCTAATTTATGATAGGATATATGATTGGATGCCTGAACAACCAAATATATTCCAAGTGGAGCAATTGGAACGCCTGAAGC
AGGAATTGCCAGAGCTTAAGAGCTGTTTGTGTCCCACTGTTAGCCGCTTTGTTCCCTCATCTTTGTGTGGGGAGTCTGATATCCATGTGGATGCCAACGGCATTGATAACGTGGAG
AATGCTTCTGGTGGCGGAGGCTCGGGCGGAGGTGGGTCGGGTGGCGGCGGATCAATGAGCGAGCTGATCAAGGAGAACATGCACATGAAGCTGTACATGGAGGGCACCGTGA
ACAACCACCACTTCAAGTGCACATCCGAGGGCGAAGGCAAGCCCTACGAGGGCACCCAGACCATGAAGATCAAGGTGGTCGAGGGCGGCCCTCTCCCCTTCGCCTTCGACATCCT
GGCTACCAGCTTCATGTACGGCAGCAAAGCCTTCATCAACCACACCCAGGGCATCCCCGACTTCTTTAAGCAGTCCTTCCCTGAGGGCTTCACATGGGAGAGAATCACCACATACG
AAGACGGGGGCGTGCTGACCGCTACCCAGGACACCAGCTTCCAGAACGGCTGCATCATCTACAACGTCAAGATCAACGGGGTGAACTTCCCATCCAACGGCCCTGTGATGCAGA
AGAAAACACGCGGCTGGGAGGCCAACACCGAGATGCTGTACCCCGCTGACGGCGGCCTGAGAGGCCACAGCCAGATGGCCCTGAAGCTCGTGGGCGGGGGCTACCTGCACTGC
TCCTTCAAGACCACATACAGATCCAAGAAACCCGCTAAGAACCTCAAGATGCCCGGCTTCCACTTCGTGGACCACAGACTGGAAAGAATCAAGGAGGCCGACAAAGAGACCTACG
TCGAGCAGCACGAGATGGCTGTGGCCAAGTACTGCGACCTCCCTAGCAAACTGGGGCACAGATGAACCCAGCTTTCTTGTACAAAGTGGTGATGGCCGGCCGCTTCGAGCAGAC
ATGATAAGATACATTGATGAGTTTGGACAAACCACAACTAGAATGCAGTGAAAAAAATGCTTTATTTGTGAAATTTGTGATGCTATTGCTTTATTTGTAACCATTATAAGCTGCAAT
AAACAAGTTAACAACAACAATTGCATTCATTTTATGTTTCAGGTTCAGGGGGAGGTGTGGGAGGTTTTTTAAAGCAAGTAAAACCTCTACAAATGTGGTACGCGTTGACATTGATT
ATTGACTAGTTATTAATAGTAATCAATTACGGGGTCATTAGTTCATAGCCCATATATGGAGTTCCGCGTTACATAACTTACGGTAAATGGCCCGCCTGGCTGACCGCCCAACGACCC
CCGCCCATTGACGTCAATAATGACGTATGTTCCCATAGTAACGCCAATAGGGACTTTCCATTGACGTCAATGGGTGGAGTATTTACGGTAAACTGCCCACTTGGCAGTACATCAAG
TGTATCATATGCCAAGTACGCCCCCTATTGACGTCAATGACGGTAAATGGCCCGCCTGGCATTATGCCCAGTACATGACCTTATGGGACTTTCCTACTTGGCAGTACATCTACGTAT
TAGTCATCGCTATTACCATGGTGATGCGGTTTTGGCAGTACATCAATGGGCGTGGATAGCGGTTTGACTCACGGGGATTTCCAAGTCTCCACCCCATTGACGTCAATGGGAGTTTG
TTTTGGCACCAAAATCAACGGGACTTTCCAAAATGTCGTAACAACTCCGCCCCATTGACGCAAATGGGCGGTAGGCGTGTACGGTGGGAGGTCTATATAAGCAGAGCTCTCTGGC
TAACTAGAGAACCCACTGCGCCACCATGATTGAACAAGATGGATTGCACGCAGGTTCTCCGGCCGCTTGGGTGGAGAGGCTATTCGGCTATGACTGGGCACAACAGACAATCGG
CTGCTCTGATGCCGCCGTGTTCCGGCTGTCAGCGCAGGGGCGCCCGGTTCTTTTTGTCAAGACCGACCTGTCCGGTGCCCTGAATGAACTGCAAGACGAGGCAGCGCGGCTATCG
TGGCTGGCCACGACGGGCGTTCCTTGCGCAGCTGTGCTCGACGTTGTCACTGAAGCGGGAAGGGACTGGCTGCTATTGGGCGAAGTGCCGGGGCAGGATCTCCTGTCATCTCAC
CTTGCTCCTGCCGAGAAAGTATCCATCATGGCTGATGCAATGCGGCGGCTGCATACGCTTGATCCGGCTACCTGCCCATTCGACCACCAAGCGAAACATCGCATCGAGCGAGCAC
GTACTCGGATGGAAGCCGGTCTTGTCGATCAGGATGATCTGGACGAAGAGCATCAGGGGCTCGCGCCAGCCGAACTGTTCGCCAGGCTCAAGGCGAGCATGCCCGACGGCGAG
GATCTCGTCGTGACCCATGGCGATGCCTGCTTGCCGAATATCATGGTGGAAAATGGCCGCTTTTCTGGATTCATCGACTGTGGCCGGCTGGGTGTGGCGGACCGCTATCAGGACA
TAGCGTTGGCTACCCGTGATATTGCTGAAGAGCTTGGCGGCGAATGGGCTGACCGCTTCCTCGTGCTTTACGGTATCGCCGCTCCCGATTCGCAGCGCATCGCCTTCTATCGCCTTC
TTGACGAGTTCTTCTGACTCGAGTCTAGAGGGCCCGTTTAAACCCGCTGATCAGCCTCGACTGTGCCTTCTAGTTGCCAGCCATCTGTTGTTTGCCCCTCCCCCGTGCCTTCCTTGAC
CCTGGAAGGTGCCACTCCCACTGTCCTTTCCTAATAAAATGAGGAAATTGCATCGCATTGTCTGAGTAGGTGTCATTCTATTCTGGGGGGTGGGGTGGGGCAGGACAGCAAGGG
GGAGGATTGGGAAGACAATAGCAGGCATGCTGGGGATGCGGTGGGCTCTATGGGCGGCCGCGGCGCTCTTCCGCTTCCTCGCTCACTGACTCGCTGCGCTCGGTCGTTCGGCTG
CGGCGAGCGGTATCAGCTCACTCAAAGGCGGTAATACGGTTATCCACAGAATCAGGGGATAACGCAGGAAAGAACATGTGAGCAAAAGGCCAGCAAAAGGCCAGGAACCGTAA
AAAGGCCGCGTTGCTGGCGTTTTTCCATAGGCTCCGCCCCCCTGACGAGCATCACAAAAATCGACGCTCAAGTCAGAGGTGGCGAAACCCGACAGGACTATAAAGATACCAGGC
GTTTCCCCCTGGAAGCTCCCTCGTGCGCTCTCCTGTTCCGACCCTGCCGCTTACCGGATACCTGTCCGCCTTTCTCTCTTCGGGAAGCGTGGCGCTTTCTCATAGCTCACGCTGTAGG
TATCTCAGTTCGGTGTAGGTCGTTCGCTCCAAGCTGGGCTGTGTGCACGAACCCCCCGTTCAGCCCGACCGCTGCGCCTTATCCGGTAACTATCGTCTTGAGTCCAACCCGGTAAG
ACACGACTTATCGCCACTGGCAGCAGCCACTGGTAACAGGATTAGCAGAGCGAGGTATGTAGGCGGTGCTACAGAGTTCTTGAAGTGGTGGCCTAACTACGGCTACACTAGAAG
AACAGTATTTGGTATCTGCGCTCTGCTGAAGCCAGTTACCTTCGGAAAAAGAGTTGGTAGCTCTTGATCCGGCAAACAAACCACCGCTGGTAGCGGTGGTTTTTTTGTTTGCAAGC
AGCAGATTACGCGCAGAAAAAAAGGATCTCAAGAAGATCCTTTGATCTTTTCTACGGGGTCTGACGCTCAGTGGAACGAAAACTCACGTTAAGGGATTTTGGTCATGAGATTATC
AAAAAGGATCTTCACCTAGATCCTTTTAAATTAAAAATGAAGTTTTAAATCAATCTAAAGTATATATGAGTAAACTTGGTCTGACAGTTACCAATGCTTAATCAGTGAGGCACCTAT
CTCAGCGATCTGTCTATTTCGTTCATCCATAGTTGCCTGACTCCCCGTCGTGTAGATAACTACGATACGGGAGGGCTTACCATCTGGCCCCAGTGCTGCAATGATACCGCGAGACCC
ACGCTCACCGGCTCCAGATTTATCAGCAATAAACCAGCCAGCCGGAAGGGCCGAGCGCAGAAGTGGTCCTGCAACTTTATCCGCCTCCATCCAGTCTATTAATTGTTGCCGGGAA
GCTAGAGTAAGTAGTTCGCCAGTTAATAGTTTGCGCAACGTTGTTGCCATTGCTACAGGCATCGTGGTGTCACGCTCGTCGTTTGGTATGGCTTCATTCAGCTCCGGTTCCCAACGA
TCAAGGCGAGTTACATGATCCCCCATGTTGTGCAAAAAAGCGGTTAGCTCCTTCGGTCCTCCGATCGTTGTCAGAAGTAAGTTGGCCGCAGTGTTATCACTCATGGTTATGGCAGC
ACTGCATAATTCTCTTACTGTCATGCCATCCGTAAGATGCTTTTCTGTGACTGGTGAGTACTCAACCAAGTCATTCTGAGAATAGTGTATGCGGCGACCGAGTTGCTCTTGCCCGGC
GTCAATACGGGATAATACCGCGCCACATAGCAGAACTTTAAAAGTGCTCATCATTGGAAAACGTTCTTCGGGGCGAAAACTCTCAAGGATCTTACCGCTGTTGAGATCCAGTTCGA
TGTAACCCACTCGTGCACCCAACTGATCTTCAGCATCTTTTACTTTCACCAGCGTTTCTGGGTGAGCAAAAACAGGAAGGCAAAATGCCGCAAAAAAGGGAATAAGGGCGACACG
GAAATGTTGAATACTCATACTCTTCCTTTTTCAATATTATTGAAGCATTTATCAGGGTTATTGTCTCATGAGCGGATACATATTTGAATGTATTTAGAAAAATAAACAAATAGGGGTT
CCGCGCACATTTCCCCGAAAAGTGCCACCTGACGTCTAAGAAACCATTATTATCATGACATTAACCTATAAAAATAGGCGTATCACGAGGCCCTTTCGTCGGCGCGCCGCGGCCGC

6.1.1.5 CMV-EDI3-GFP

AACAAAATATTAACGCTTACAATTTCCATTCGCCATTCAGGCTGCGCAACTGTTGGGAAGGGCGATCGGTGCGGGCCTCTTCGCTATTACGCCAGCTGGCGAAAGGGGGATGTGC
TGCAAGGCGATTAAGTTGGGTAACGCCAGGGTTTTCCCAGTCACGACGTTGTAAAACGACGGCCAGTGCCAAGCTGATCTATACATTGAATCAATATTGGCAATTAGCCATATTAG
TCATTGGTTATATAGCATAAATCAATATTGGCTATTGGCCATTGCATACGTTGTATCTATATCATAATATGTACATTTATATTGGCTCATGTCCAATATGACCGCCATGTTGACATTG
ATTATTGACTAGTTATTAATAGTAATCAATTACGGGGTCATTAGTTCATAGCCCATATATGGAGTTCCGCGTTACATAACTTACGGTAAATGGCCCGCCTGGCTGACCGCCCAACGA
CCCCCGCCCATTGACGTCAATAATGACGTATGTTCCCATAGTAACGCCAATAGGGACTTTCCATTGACGTCAATGGGTGGAGTATTTACGGTAAACTGCCCACTTGGCAGTACATC
AAGTGTATCATATGCCAAGTCCGCCCCCTATTGACGTCAATGACGGTAAATGGCCCGCCTGGCATTATGCCCAGTACATGACCTTACGGGACTTTCCTACTTGGCAGTACATCTACG
TATTAGTCATCGCTATTACCATGGTGATGCGGTTTTGGCAGTACACCAATGGGCGTGGATAGCGGTTTGACTCACGGGGATTTCCAAGTCTCCACCCCATTGACGTCAATGGGAGT
TTGTTTTGGCACCAAAATCAACGGGACTTTCCAAAATGTCGTAATAACCCCGCCCCGTTGACGCAAATGGGCGGTAGGCGTGTACGGTGGGAGGTCTATATAAGCAGAGCTCGTT
TAGTGAACCGTCAGAATTTTGTAATACGACTCACTATAGGGCGGCCGGGAATTCGTCGACTGGATCCGGTACCGAGGAGATCTGCCGCCGCGATCGCCATGACACCTTCTCAGGT
TGCCTTTGAAATAAGAGGAACTCTTTACCAGGAGAAGTTTTTGCGATATGTGGAAGCTGTGATGCTTTGGGAAACTGGAATCCTCAAAATGCTGTGGCTCTTCTTCCAGAGAATG
ACACAGGTGAAAGCATGCTATGGAAAGCAACCATTGTACTCAGTAGAGGAGTATCAGTTCAGTATCGCTACTTCAAAGGGTACTTTTTAGAACCAAAGACTATCGGTGGTCCATGT

6. Supplementary data

CAAGTGATAGTTCACAAGTGGGAGACTCATCTACAACCACGATCAATAACCCCTTTAGAAAGCGAAATTATTATTGACGATGGACAATTTGGAATCCACAATGGTGTTGAAACTCT
GGATTCTGGATGGCTGACATGTCAGACTGAAATAAGATTACGTTTGCATTATTCTGAAAAACCTCCTGTGTCAATAACCAAGAAAAAATTAAAAAAATCTAGATTTAGGGTGAAGC
TGACACTAGAAGGCCTGGAGGAAGATGACGATGATAGGGTATCTCCCACTGTACTCCACAAAATGTCCAATAGCTTGGAGATATCCTTAATAAGCGACAATGAGTTCAAGTGCAG
GCATTCACAGCCGGAGTGTGGTTATGGCTTGCAGCCTGATCGTTGGACAGAGTACAGCATACAGACGATGGAACCAGATAACCTGGAACTAATCTTTGATTTTTTCGAAGAAGAT
CTCAGTGAGCACGTAGTTCAGGGTGATGCCCTTCCTGGACATGTGGGTACAGCTTGTCTCTTATCATCCACCATTGCTGAGAGTGGAAAGAGTGCTGGAATTCTTACTCTTCCCATC
ATGAGCAGAAATTCCCGGAAAACAATAGGCAAAGTGAGAGTTGACTATATAATTATTAAGCCATTACCAGGATACAGTTGTGACATGAAATCTTCATTTTCCAAGTATTGGAAGCC
AAGAATACCATTGGATGTTGGCCATCGAGGTGCAGGAAACTCTACAACAACTGCCCAGCTGGCTAAAGTTCAAGAAAATACTATTGCTTCTTTAAGAAATGCTGCTAGTCATGGTG
CAGCCTTTGTAGAATTTGACGTACACCTTTCAAAGGACTTTGTGCCCGTGGTATATCATGATCTTACCTGTTGTTTGACTATGAAAAAGAAATTTGATGCTGATCCAGTTGAATTATT
TGAAATTCCAGTAAAAGAATTAACATTTGACCAACTCCAGTTGTTAAAGCTCACTCATGTGACTGCACTGAAATCTAAGGATCGGAAAGAATCTGTGGTTCAGGAGGAAAATTCCT
TTTCAGAAAATCAGCCATTTCCTTCTCTTAAGATGGTTTTAGAGTCTTTGCCAGAAGATGTAGGGTTTAACATTGAAATAAAATGGATCTGCCAGCAAAGGGATGGAATGTGGGAT
GGTAACTTATCAACATATTTTGACATGAATCTGTTTTTGGATATAATTTTAAAAACTGTTTTAGAAAATTCTGGGAAGAGGAGAATAGTGTTTTCTTCATTTGATGCAGATATTTGCA
CAATGGTTCGGCAAAAGCAGAACAAATATCCGATACTATTTTTAACTCAAGGAAAATCTGAGATTTATCCTGAACTCATGGACCTCAGATCTCGGACAACCCCCATTGCAATGAGC
TTTGCACAGTTTGAAAATCTACTGGGGATAAATGTACATACTGAAGACTTGCTCAGAAACCCATCCTATATTCAAGAGGCAAAAGCTAAGGGACTAGTCATATTCTGCTGGGGTGA
TGATACCAATGATCCTGAAAACAGAAGGAAATTGAAGGAACTTGGAGTTAATGGTCTAATTTATGATAGGATATATGATTGGATGCCTGAACAACCAAATATATTCCAAGTGGAG
CAATTGGAACGCCTGAAGCAGGAATTGCCAGAGCTTAAGAGCTGTTTGTGTCCCACTGTTAGCCGCTTTGTTCCCTCATCTTTGTGTGGGGAGTCTGATATCCATGTGGATGCCAA
CGGCATTGATAACGTGGAGAATGCTACGCGTACGCGGCCGCTCGAGATGGAGAGCGACGAGAGCGGCCTGCCCGCCATGGAGATCGAGTGCCGCATCACCGGCACCCTGAACG
GCGTGGAGTTCGAGCTGGTGGGCGGCGGAGAGGGCACCCCCGAGCAGGGCCGCATGACCAACAAGATGAAGAGCACCAAAGGCGCCCTGACCTTCAGCCCCTACCTGCTGAGC
CACGTGATGGGCTACGGCTTCTACCACTTCGGCACCTACCCCAGCGGCTACGAGAACCCCTTCCTGCACGCCATCAACAACGGCGGCTACACCAACACCCGCATCGAGAAGTACG
AGGACGGCGGCGTGCTGCACGTGAGCTTCAGCTACCGCTACGAGGCCGGCCGCGTGATCGGCGACTTCAAGGTGATGGGCACCGGCTTCCCCGAGGACAGCGTGATCTTCACCG
ACAAGATCATCCGCAGCAACGCCACCGTGGAGCACCTGCACCCCATGGGCGATAACGATCTGGATGGCAGCTTCACCCGCACCTTCAGCCTGCGCGACGGCGGCTACTACAGCTC
CGTGGTGGACAGCCACATGCACTTCAAGAGCGCCATCCACCCCAGCATCCTGCAGAACGGGGGCCCCATGTTCGCCTTCCGCCGCGTGGAGGAGGATCACAGCAACACCGAGCT
GGGCATCGTGGAGTACCAGCACGCCTTCAAGACCCCGGATGCAGATCCGGTGAAGAAAGAGTTTAAACGGCCGGCCGCGGTCATAGCTGTTTCCTGAACAGATCCCGGGTGGC
ATCCCTGTGACCCCTCCCCAGTGCCTCTCCTGGCCCTGGAAGTTGCCACTCCAGTGCCCACCAGCCTTGTCCTAATAAAATTAAGTTGCATCATTTTGTCTGACTAGGTGTCCTTCTA
TAATATTATGGGGTGGAGGGGGGTGGTATGGAGCAAGGGGCAAGTTGGGAAGACAACCTGTAGGGCCTGCGGGGTCTATTGGGAACCAAGCTGGAGTGCAGTGGCACAATCT
TGGCTCACTGCAATCTCCGCCTCCTGGGTTCAAGCGATTCTCCTGCCTCAGCCTCCCGAGTTGTTGGGATTCCAGGCATGCATGACCAGGCTCAGCTAATTTTTGTTTTTTTGGTAGA
GACGGGGTTTCACCATATTGGCCAGGCTGGTCTCCAACTCCTAATCTCAGGTGATCTACCCACCTTGGCCTCCCAAATTGCTGGGATTACAGGCGTGAACCACTGCTCCCTTCCCTG
TCCTTCTGATTTTAAAATAACTATACCAGCAGGAGGACGTCCAGACACAGCATAGGCTACCTGGCCATGCCCAACCGGTGGGACATTTGAGTTGCTTGCTTGGCACTGTCCTCTCAT
GCGTTGGGTCCACTCAGTAGATGCCTGTTGAATTGGGTACGCGGCCAGCTTGGCTGTGGAATGTGTGTCAGTTAGGGTGTGGAAAGTCCCCAGGCTCCCCAGCAGGCAGAAGTA
TGCAAAGCATGCATCTCAATTAGTCAGCAACCAGGTGTGGAAAGTCCCCAGGCTCCCCAGCAGGCAGAAGTATGCAAAGCATGCATCTCAATTAGTCAGCAACCATAGTCCCGCC
CCTAACTCCGCCCATCCCGCCCCTAACTCCGCCCAGTTCCGCCCATTCTCCGCCCCATGGCTGACTAATTTTTTTTATTTATGCAGAGGCCGAGGCCGCCTCGGCCTCTGAGCTATTC
CAGAAGTAGTGAGGAGGCTTTTTTGGAGGCCTAGGCTTTTGCAAAAAGCTCCCGGGAGCTTGTATATCCATTTTCGGATCTGATCAAGAGACAGGATGAGGATCGTTTCGCATGA
TTGAACAAGATGGATTGCACGCAGGTTCTCCGGCCGCTTGGGTGGAGAGGCTATTCGGCTATGACTGGGCACAACAGACAATCGGCTGCTCTGATGCCGCCGTGTTCCGGCTGTC
AGCGCAGGGGCGCCCGGTTCTTTTTGTCAAGACCCGACCTGTCCGGTGCCCTGAATGAACTGCAGGACGAGGCAGCGCGGCTATCGTGGCTGGCCACGACGGGCGTTCCTTGCGC
AGCTGTGCTCGACGTTGTCACTGAAGCGGGAAGGGACTGGCTGCTATTGGGCGAAGTGCCGGGGCAGGATCTCCTGTCATCTCACCTTGCTCCTGCCGAGAAAGTATCCATCATG
GCTGATGCAATGCGGCGGCTGCATACGCTTGATCCGGCTACCTGCCCATTCGACCACCAAGCGAAACATCGCATCGAGCGAGCACGTACTCGGATGGAAGCCGGTCTTGTCGATC
AGGATGATCTGGACGAAGAGCATCAGGGGCTCGCGCCAGCCGAACTGTTCGCCAGGCTCAAGGCGCGCATGCCCGACGGCGAGGATCTCGTCGTGACCCATGGCGATGCCTGCT
TGCCGAATATCATGGTGGAAAATGGCCGCTTTTCTGGATTCATCGACTGTGGCCGGCTGGGTGTGGCCGACCGCTATCAGGACATAGCGTTGGCTACCCGTGATATTGCTGAAGA
GCTTGGCGGCGAATGGGCTGACCGCTTCCTCGTGCTTTACGGTATCGCCGCTCCCGATTCGCAGCGCATCGCCTTCTATCGCCTTCTTGACGAGTTCTTCTGAGCGGGACTCTGGG
GTTCGAAATGACCGACCAAGCGACGCCCAACCTGCCATCACGAGATTTCGATTCCACCGCCGCCTTCTATGAAAGGTTGGGCTTCGGAATCGTTTTCCGGGACGCCGGCTGGATG
ATCCTCCAGCGCGGGGATCTCATGCTGGAGTTCTTCGCCCACCCCAACTTGTTTATTGCAGCTTATAATGGTTACAAATAAAGCAATAGCATCACAAATTTCACAAATAAAGCATTT
TTTTCACTGCATTCTAGTTGTGGTTTGTCCAAACTCATCAATGTATCTTATCATGTCTGTATACCGTCGACCTCTAGCTAGAGCTTGGCGTAATCATGGTCATAGCTGTTTCCTGTGTG
AAATTGTTATCCGCTCACAATTCCACACAACATACGAGCCGGAAGCATAAAGTGTAAAGCCTGGGGTGCCTAATGAGTGAGCTAACTCACATTAATTGCGTTGCGCTCACTGCCCG
CTTTCCAGTCGGGAAACCTGTCGTGCCAGCTGCATTAATGAATCGGCCAACGCGCGGGGAGAGGCGGTTTGCGTATTGGGCGCTCTTCCGCTTCCTCGCTCACTGACTCGCTGCGC
TCGGTCGTTCGGCTGCGGCGAGCGGTATCAGCTCACTCAAAGGCGGTAATACGGTTATCCACAGAATCAGGGGATAACGCAGGAAAGAACATGTGAGCAAAAGGCCAGCAAAA
GGCCAGGAACCGTAAAAAGGCCGCGTTGCTGGCGTTTTTCCATAGGCTCCGCCCCCCTGACGAGCATCACAAAAATCGACGCTCAAGTCAGAGGTGGCGAAACCCGACAGGACT
ATAAAGATACCAGGCGTTTCCCCCTGGAAGCTCCCTCGTGCGCTCTCCTGTTCCGACCCTGCCGCTTACCGGATACCTGTCCGCCTTTCTCCCTTCGGGAAGCGTGGCGCTTTCTCAT
AGCTCACGCTGTAGGTATCTCAGTTCGGTGTAGGTCGTTCGCTCCAAGCTGGGCTGTGTGCACGAACCCCCCGTTCAGCCCGACCGCTGCGCCTTATCCGGTAACTATCGTCTTGA
GTCCAACCCGGTAAGACACGACTTATCGCCACTGGCAGCAGCCACTGGTAACAGGATTAGCAGAGCGAGGTATGTAGGCGGTGCTACAGAGTTCTTGAAGTGGTGGCCTAACTA
CGGCTACACTAGAAGAACAGTATTTGGTATCTGCGCTCTGCTGAAGCCAGTTACCTTCGGAAAAAGAGTTGGTAGCTCTTGATCCGGCAAACAAACCACCGCTGGTAGCGGTTTTT
TTGTTTGCAAGCAGCAGATTACGCGCAGAAAAAAAGGATCTCAAGAAGATCCTTTGATCTTTTCTACGGGGTCTGACGCTCAGTGGAACGAAAACTCACGTTAAGGGATTTTGGT
CATGAGATTATCAAAAAGGATCTTCACCTAGATCCTTTTAAATTAAAAATGAAGTTTTAAATCAATCTAAAGTATATATGAGTAAACTTGGTCTGACAGTTACCAATGCTTAATCAGT
GAGGCACCTATCTCAGCGATCTGTCTATTTCGTTCATCCATAGTTGCCTGACTCCCCGTCGTGTAGATAACTACGATACGGGAGGGCTTACCATCTGGCCCCAGTGCTGCAATGATA
CCGCGAGACCCACGCTCACCGGCTCCAGATTTATCAGCAATAAACCAGCCAGCCGGAAGGGCCGAGCGCAGAAGTGGTCCTGCAACTTTATCCGCCTCCATCCAGTCTATTAATTG
TTGCCGGGAAGCTAGAGTAAGTAGTTCGCCAGTTAATAGTTTGCGCAACGTTGTTGCCATTGCTACAGGCATCGTGGTGTCACGCTCGTCGTTTGGTATGGCTTCATTCAGCTCCG
GTTCCCAACGATCAAGGCGAGTTACATGATCCCCCATGTTGTGCAAAAAAGCGGTTAGCTCCTTCGGTCCTCCGATCGTTGTCAGAAGTAAGTTGGCCGCAGTGTTATCACTCATG
GTTATGGCAGCACTGCATAATTCTCTTACTGTCATGCCATCCGTAAGATGCTTTTCTGTGACTGGTGAGTACTCAACCAAGTCATTCTGAGAATAGTGTATGCGGCGACCGAGTTGC
TCTTGCCCGGCGTCAATACGGGATAATACCGCGCCACATAGCAGAACTTTAAAAGTGCTCATCATTGGAAAACGTTCTTCGGGGCGAAAACTCTCAAGGATCTTACCGCTGTTGAG
ATCCAGTTCGATGTAACCCACTCGTGCACCCAACTGATCTTCAGCATCTTTTACTTTCACCAGCGTTTCTGGGTGAGCAAAAACAGGAAGGCAAAATGCCGCAAAAAAGGGAATAA
GGGCGACACGGAAATGTTGAATACTCATACTCTTCCTTTTTCAATATTATTGAAGCATTTATCAGGGTTATTGTCTCATGAGCGGATACATATTTGAATGTATTTAGAAAAATAAAC
AAATAGGGGTTCCGCGCACATTTCCCCGAAAAGTGCCACCTGACGCGCCCTGTAGCGGCGCATTAAGCGCGGCGGGTGTGGTGGTTACGCGCAGCGTGACCGCTACACTTGCCA
GCGCCCTAGCGCCCGCTCCTTTCGCTTTCTTCCCTTCCTTTCTCGCCACGTTCGCCGGCTTTCCCCGTCAAGCTCTAAATCGGGGGCTCCCTTTAGGGTTCCGATTTAGTGCTTTACGG
CACCTCGACCCCAAAAAACTTGATTAGGGTGATGGTTCACGTAGTGGGCCATCGCCCTGATAGACGGTTTTTCGCCCTTTGACGTTGGAGTCCACGTTCTTTAATAGTGGACTCTTG
TTCCAAACTGGAACAACACTCAACCCTATCTCGGTCTATTCTTTTGATTTATAAGGGATTTTGCCGATTTCGGCCTATTGGTTAAAAAATGAGCTGATTTAACAAAAATTTAACGCGA
ATTTT

6.1.1.6 CMV-STBD1-3xFLAG-EGFP

CAACTTTGTATAGAAAAGTTGTAGTTATTAATAGTAATCAATTACGGGGTCATTAGTTCATAGCCCATATATGGAGTTCCGCGTTACATAACTTACGGTAAATGGCCCGCCTGGCTG
ACCGCCCAACGACCCCCGCCCATTGACGTCAATAATGACGTATGTTCCCATAGTAACGCCAATAGGGACTTTCCATTGACGTCAATGGGTGGAGTATTTACGGTAAACTGCCCACT
TGGCAGTACATCAAGTGTATCATATGCCAAGTACGCCCCCTATTGACGTCAATGACGGTAAATGGCCCGCCTGGCATTATGCCCAGTACATGACCTTATGGGACTTTCCTACTTGGC
AGTACATCTACGTATTAGTCATCGCTATTACCATGGTGATGCGGTTTTGGCAGTACATCAATGGGCGTGGATAGCGGTTTGACTCACGGGGATTTCCAAGTCTCCACCCCATTGAC
GTCAATGGGAGTTTGTTTTGGCACCAAAATCAACGGGACTTTCCAAAATGTCGTAACAACTCCGCCCCATTGACGCAAATGGGCGGTAGGCGTGTACGGTGGGAGGTCTATATAA
GCAGAGCTGGTTTAGTGAACCGTCAGATCCAAGTTTGTACAAAAAAGCAGGCTGCCACCATGGGCGCCGTCTGGTCCGCCCTGCTGGTTGGAGGGGGTCTGGCCGGAGCACTTT
TCGTTTGGCTGCTGCGGGGCGGCCCTGGCGACACCGGGAAGGACGGGGATGCGGAGCAGGAGAAAGACGCCCCTCTTGGGGGAGCTGCGATTCCGGGAGGCCATCAGAGTGG
CAGCAGCGGACTGAGCCCTGGACCTTCCGGGCAGGAGCTGGTCACCAAACCAGAGCATCTTCAAGAAAGCAATGGACATTTGATTTCTAAGACCAAAGACCTTGGTAAACTGCAA
GCAGCATCATGGAGATTGCAGAATCCTTCCAGGGAAGTCTGTGACAATTCAAGAGAACATGTTCCTTCTGGACAGTTTCCAGACACAGAAGCTCCAGCTACCTCTGAGACCAGTAA
CTCTAGGAGTTACTCTGAAGTTTCAAGAAATGAAAGCCTTGAATCTCCTATGGGAGAATGGGGATTCCAAAAAGGACAAGAGATATCTGCTAAAGCAGCTACATGTTTTGCAGAG
AAGTTGCCTTCTAGCAACCTGCTCAAGAACAGAGCTAAAGAAGAAATGAGCCTCTCTGATTTGAACAGTCAGGACCGGGTTGACCACGAGGAGTGGGAAATGGTGCCTAGGCAC
TCATCTTGGGGGGATGTTGGTGTGGGTGGCAGTCTTAAGGCTCCAGTGTTAAACCTAAACCAGGGAATGGACAATGGAAGAAGCACTTTGGTGGAAGCAAGAGGTCAGCAAGT
GCATGGGAAAATGGAAAGGGTAGCAGTGATGCCTGCAGGGTCTCAGCAAGTTAGTGTCAGGTTCCAGGTCCATTATGTCACAAGCACTGATGTGCAATTCATTGCAGTAACTGG
AGACCATGAGTGTCTTGGGAGATGGAACACTTACATCCCACTCCACTATAACAAGGATGGGTTCTGGTCTCATTCCATTTTCCTGCCTGCAGATACAGTGGTGGAGTGGAAGTTTG
TGTTGGTAGAGAATGGGGGAGTTACCCGCTGGGAAGAATGCAGCAATAGATTCCTAGAAACTGGCCATGAGGATAAAGTGGTTCACGCATGGTGGGGGATTCACGACTACAAA
GACCATGACGGTGATTATAAAGATCATGATATCGATTACAAGGATGACGATGACAAGTCTGGTGGCGGAGGCTCGGGCGGAGGTGGGTCGGGTGGCGGCGGATCAATGGTGA
GCAAGGGCGAGGAGCTGTTCACCGGGGTGGTGCCCATCCTGGTCGAGCTGGACGGCGACGTAAACGGCCACAAGTTCAGCGTGTCCGGCGAGGGCGAGGGCGATGCCACCTAC

6. Supplementary data

GGCAAGCTGACCCTGAAGTTCATCTGCACCACCGGCAAGCTGCCCGTGCCCTGGCCCACCCTCGTGACCACCCTGACCTACGGCGTGCAGTGCTTCAGCCGCTACCCCGACCACAT
GAAGCAGCACGACTTCTTCAAGTCCGCCATGCCCGAAGGCTACGTCCAGGAGCGCACCATCTTCTTCAAGGACGACGGCAACTACAAGACCCGCGCCGAGGTGAAGTTCGAGGG
CGACACCCTGGTGAACCGCATCGAGCTGAAGGGCATCGACTTCAAGGAGGACGGCAACATCCTGGGGCACAAGCTGGAGTACAACTACAACAGCCACAACGTCTATATCATGGC
CGACAAGCAGAAGAACGGCATCAAGGTGAACTTCAAGATCCGCCACAACATCGAGGACGGCAGCGTGCAGCTCGCCGACCACTACCAGCAGAACACCCCCATCGGCGACGGCCC
CGTGCTGCTGCCCGACAACCACTACCTGAGCACCCAGTCCGCCCTGAGCAAAGACCCCAACGAGAAGCGCGATCACATGGTCCTGCTGGAGTTCGTGACCGCCGCCGGGATCACT
CTCGGCATGGACGAGCTGTACAAGTAAACCCAGCTTTCTTGTACAAAGTGGTGATGGCCGGCCGCTTCGAGCAGACATGATAAGATACATTGATGAGTTTGGACAAACCACAACT
AGAATGCAGTGAAAAAAATGCTTTATTTGTGAAATTTGTGATGCTATTGCTTTATTTGTAACCATTATAAGCTGCAATAAACAAGTTAACAACAACAATTGCATTCATTTTATGTTTC
AGGTTCAGGGGGAGGTGTGGGAGGTTTTTTAAAGCAAGTAAAACCTCTACAAATGTGGTAGCGGCCGCGGCGCTCTTCCGCTTCCTCGCTCACTGACTCGCTGCGCTCGGTCGTT
CGGCTGCGGCGAGCGGTATCAGCTCACTCAAAGGCGGTAATACGGTTATCCACAGAATCAGGGGATAACGCAGGAAAGAACATGTGAGCAAAAGGCCAGCAAAAGGCCAGGAA
CCGTAAAAAGGCCGCGTTGCTGGCGTTTTTCCATAGGCTCCGCCCCCCTGACGAGCATCACAAAAATCGACGCTCAAGTCAGAGGTGGCGAAACCCGACAGGACTATAAAGATAC
CAGGCGTTTCCCCCTGGAAGCTCCCTCGTGCGCTCTCCTGTTCCGACCCTGCCGCTTACCGGATACCTGTCCGCCTTTCTCTCTTCGGGAAGCGTGGCGCTTTCTCATAGCTCACGCT
GTAGGTATCTCAGTTCGGTGTAGGTCGTTCGCTCCAAGCTGGGCTGTGTGCACGAACCCCCCGTTCAGCCCGACCGCTGCGCCTTATCCGGTAACTATCGTCTTGAGTCCAACCCG
GTAAGACACGACTTATCGCCACTGGCAGCAGCCACTGGTAACAGGATTAGCAGAGCGAGGTATGTAGGCGGTGCTACAGAGTTCTTGAAGTGGTGGCCTAACTACGGCTACACT
AGAAGAACAGTATTTGGTATCTGCGCTCTGCTGAAGCCAGTTACCTTCGGAAAAAGAGTTGGTAGCTCTTGATCCGGCAAACAAACCACCGCTGGTAGCGGTGGTTTTTTTGTTTG
CAAGCAGCAGATTACGCGCAGAAAAAAAGGATCTCAAGAAGATCCTTTGATCTTTTCTACGGGGTCTGACGCTCAGTGGAACGAAAACTCACGTTAAGGGATTTTGGTCATGAGA
TTATCAAAAAGGATCTTCACCTAGATCCTTTTAAATTAAAAATGAAGTTTTAAATCAATCTAAAGTATATATGAGTAAACTTGGTCTGACAGTTACCAATGCTTAATCAGTGAGGCA
CCTATCTCAGCGATCTGTCTATTTCGTTCATCCATAGTTGCCTGACTCCCCGTCGTGTAGATAACTACGATACGGGAGGGCTTACCATCTGGCCCCAGTGCTGCAATGATACCGCGA
GACCCACGCTCACCGGCTCCAGATTTATCAGCAATAAACCAGCCAGCCGGAAGGGCCGAGCGCAGAAGTGGTCCTGCAACTTTATCCGCCTCCATCCAGTCTATTAATTGTTGCCG
GGAAGCTAGAGTAAGTAGTTCGCCAGTTAATAGTTTGCGCAACGTTGTTGCCATTGCTACAGGCATCGTGGTGTCACGCTCGTCGTTTGGTATGGCTTCATTCAGCTCCGGTTCCC
AACGATCAAGGCGAGTTACATGATCCCCCATGTTGTGCAAAAAAGCGGTTAGCTCCTTCGGTCCTCCGATCGTTGTCAGAAGTAAGTTGGCCGCAGTGTTATCACTCATGGTTATG
GCAGCACTGCATAATTCTCTTACTGTCATGCCATCCGTAAGATGCTTTTCTGTGACTGGTGAGTACTCAACCAAGTCATTCTGAGAATAGTGTATGCGGCGACCGAGTTGCTCTTGC
CCGGCGTCAATACGGGATAATACCGCGCCACATAGCAGAACTTTAAAAGTGCTCATCATTGGAAAACGTTCTTCGGGGCGAAAACTCTCAAGGATCTTACCGCTGTTGAGATCCA
GTTCGATGTAACCCACTCGTGCACCCAACTGATCTTCAGCATCTTTTACTTTCACCAGCGTTTCTGGGTGAGCAAAAACAGGAAGGCAAAATGCCGCAAAAAAGGGAATAAGGGC
GACACGGAAATGTTGAATACTCATACTCTTCCTTTTTCAATATTATTGAAGCATTTATCAGGGTTATTGTCTCATGAGCGGATACATATTTGAATGTATTTAGAAAAATAAACAAATA
GGGGTTCCGCGCACATTTCCCCGAAAAGTGCCACCTGACGTCTAAGAAACCATTATTATCATGACATTAACCTATAAAAATAGGCGTATCACGAGGCCCTTTCGTCGGCGCGCCGC
GGCCGC

6.1.1.7 CMV-Neo (empty vector)

AACAAAATATTAACGCTTACAATTTCCATTCGCCATTCAGGCTGCGCAACTGTTGGGAAGGGCGATCGGTGCGGGCCTCTTCGCTATTACGCCAGCTGGCGAAAGGGGGATGTGC
TGCAAGGCGATTAAGTTGGGTAACGCCAGGGTTTTCCCAGTCACGACGTTGTAAAACGACGGCCAGTGCCAAGCTGATCTATACATTGAATCAATATTGGCAATTAGCCATATTAG
TCATTGGTTATATAGCATAAATCAATATTGGCTATTGGCCATTGCATACGTTGTATCTATATCATAATATGTACATTTATATTGGCTCATGTCCAATATGACCGCCATGTTGACATTG
ATTATTGACTAGTTATTAATAGTAATCAATTACGGGGTCATTAGTTCATAGCCCATATATGGAGTTCCGCGTTACATAACTTACGGTAAATGGCCCGCCTGGCTGACCGCCCAACGA
CCCCCGCCCATTGACGTCAATAATGACGTATGTTCCCATAGTAACGCCAATAGGGACTTTCCATTGACGTCAATGGGTGGAGTATTTACGGTAAACTGCCCACTTGGCAGTACATC
AAGTGTATCATATGCCAAGTCCGCCCCCTATTGACGTCAATGACGGTAAATGGCCCGCCTGGCATTATGCCCAGTACATGACCTTACGGGACTTTCCTACTTGGCAGTACATCTACG
TATTAGTCATCGCTATTACCATGGTGATGCGGTTTTGGCAGTACACCAATGGGCGTGGATAGCGGTTTGACTCACGGGGATTTCCAAGTCTCCACCCCATTGACGTCAATGGGAGT
TTGTTTTGGCACCAAAATCAACGGGACTTTCCAAAATGTCGTAATAACCCCGCCCCGTTGACGCAAATGGGCGGTAGGCGTGTACGGTGGGAGGTCTATATAAGCAGAGCTCGTT
TAGTGAACCGTCAGAATTTTGTAATACGACTCACTATAGGGCGGCCGCGAATTCAGATCTGGTACCGATATCAAGCTTGTCGACTCTAGATTGCGGCCGCGGTCATAGCTGTTTCC
TGAACATGTGATCCCGGGTGGCATCCCTGTGACCCCTCCCCAGTGCCTCTCCTGGCCCTGGAAGTTGCCACTCCAGTGCCCACCAGCCTTGTCCTAATAAAATTAAGTTGCATCATT
TTGTCTGACTAGGTGTCCTTCTATAATATTATGGGGTGGAGGGGGGTGGTATGGAGCAAGGGGCAAGTTGGGAAGACAACCTGTAGGGCCTGCGGGGTCTATTGGGAACCAAG
CTGGAGTGCAGTGGCACAATCTTGGCTCACTGCAATCTCCGCCTCCTGGGTTCAAGCGATTCTCCTGCCTCAGCCTCCCGAGTTGTTGGGATTCCAGGCATGCATGACCAGGCTCA
GCTAATTTTTGTTTTTTTGGTAGAGACGGGGTTTCACCATATTGGCCAGGCTGGTCTCCAACTCCTAATCTCAGGTGATCTACCCACCTTGGCCTCCCAAATTGCTGGGATTACAGG
CGTGAACCACTGCTCCCTTCCCTGTCCTTCTGATTTTAAAATAACTATACCAGCAGGAGGACGTCCAGACACAGCATAGGCTACCTGGCCATGCCCAACCGGTGGGACATTTGAGT
TGCTTGCTTGGCACTGTCCTCTCATGCGTTGGGTCCACTCAGTAGATGCCTGTTGAATTGGGTACGCGGCCAGCTTGGCTGTGGAATGTGTGTCAGTTAGGGTGTGGAAAGTCCCC
AGGCTCCCCAGCAGGCAGAAGTATGCAAAGCATGCATCTCAATTAGTCAGCAACCAGGTGTGGAAAGTCCCCAGGCTCCCCAGCAGGCAGAAGTATGCAAAGCATGCATCTCAA
TTAGTCAGCAACCATAGTCCCGCCCCTAACTCCGCCCATCCCGCCCCTAACTCCGCCCAGTTCCGCCCATTCTCCGCCCCATGGCTGACTAATTTTTTTTATTTATGCAGAGGCCGAG
GCCGCCTCGGCCTCTGAGCTATTCCAGAAGTAGTGAGGAGGCTTTTTTGGAGGCCTAGGCTTTTGCAAAAAGCTCCCGGGAGCTTGTATATCCATTTTCGGATCTGATCAAGAGAC
AGGATGAGGATCGTTTCGCATGATTGAACAAGATGGATTGCACGCAGGTTCTCCGGCCGCTTGGGTGGAGAGGCTATTCGGCTATGACTGGGCACAACAGACAATCGGCTGCTC
TGATGCCGCCGTGTTCCGGCTGTCAGCGCAGGGGCGCCCGGTTCTTTTTGTCAAGACCGACCTGTCCGGTGCCCTGAATGAACTGCAGGACGAGGCAGCGCGGCTATCGTGGCT
GGCCACGACGGGCGTTCCTTGCGCAGCTGTGCTCGACGTTGTCACTGAAGCGGGAAGGGACTGGCTGCTATTGGGCGAAGTGCCGGGGCAGGATCTCCTGTCATCTCACCTTGC
TCCTGCCGAGAAAGTATCCATCATGGCTGATGCAATGCGGCGGCTGCATACGCTTGATCCGGCTACCTGCCCATTCGACCACCAAGCGAAACATCGCATCGAGCGAGCACGTACT
CGGATGGAAGCCGGTCTTGTCGATCAGGATGATCTGGACGAAGAGCATCAGGGGCTCGCGCCAGCCGAACTGTTCGCCAGGCTCAAGGCGCGCATGCCCGACGGCGAGGATCT
CGTCGTGACCCATGGCGATGCCTGCTTGCCGAATATCATGGTGGAAAATGGCCGCTTTTCTGGATTCATCGACTGTGGCCGGCTGGGTGTGGCGGACCGCTATCAGGACATAGCG
TTGGCTACCCGTGATATTGCTGAAGAGCTTGGCGGCGAATGGGCTGACCGCTTCCTCGTGCTTTACGGTATCGCCGCTCCCGATTCGCAGCGCATCGCCTTCTATCGCCTTCTTGAC
GAGTTCTTCTGAGCGGGACTCTGGGGTTCGAAATGACCGACCAAGCGACGCCCAACCTGCCATCACGAGATTTCGATTCCACCGCCGCCTTCTATGAAAGGTTGGGCTTCGGAAT
CGTTTTCCGGGACGCCGGCTGGATGATCCTCCAGCGCGGGGATCTCATGCTGGAGTTCTTCGCCCACCCCAACTTGTTTATTGCAGCTTATAATGGTTACAAATAAAGCAATAGCA
TCACAAATTTCACAAATAAAGCATTTTTTTCACTGCATTCTAGTTGTGGTTTGTCCAAACTCATCAATGTATCTTATCATGTCTGTATACCGTCGACCTCTAGCTAGAGCTTGGCGTAA
TCATGGTCATAGCTGTTTCCTGTGTGAAATTGTTATCCGCTCACAATTCCACACAACATACGAGCCGGAAGCATAAAGTGTAAAGCCTGGGGTGCCTAATGAGTGAGCTAACTCAC
ATTAATTGCGTTGCGCTCACTGCCCGCTTTCCAGTCGGGAAACCTGTCGTGCCAGCTGCATTAATGAATCGGCCAACGCGCGGGGAGAGGCGGTTTGCGTATTGGGCGCTCTTCC
GCTTCCTCGCTCACTGACTCGCTGCGCTCGGTCGTTCGGCTGCGGCGAGCGGTATCAGCTCACTCAAAGGCGGTAATACGGTTATCCACAGAATCAGGGGATAACGCAGGAAAGA
ACATGTGAGCAAAAGGCCAGCAAAAGGCCAGGAACCGTAAAAAGGCCGCGTTGCTGGCGTTTTTCCATAGGCTCCGCCCCCCTGACGAGCATCACAAAAATCGACGCTCAAGTC
AGAGGTGGCGAAACCCGACAGGACTATAAAGATACCAGGCGTTTCCCCCTGGAAGCTCCCTCGTGCGCTCTCCTGTTCCGACCCTGCCGCTTACCGGATACCTGTCCGCCTTTCTCC
CTTCGGGAAGCGTGGCGCTTTCTCATAGCTCACGCTGTAGGTATCTCAGTTCGGTGTAGGTCGTTCGCTCCAAGCTGGGCTGTGTGCACGAACCCCCCGTTCAGCCCGACCGCTGC
GCCTTATCCGGTAACTATCGTCTTGAGTCCAACCCGGTAAGACACGACTTATCGCCACTGGCAGCAGCCACTGGTAACAGGATTAGCAGAGCGAGGTATGTAGGCGGTGCTACAG
AGTTCTTGAAGTGGTGGCCTAACTACGGCTACACTAGAAGAACAGTATTTGGTATCTGCGCTCTGCTGAAGCCAGTTACCTTCGGAAAAAGAGTTGGTAGCTCTTGATCCGGCAAA
CAAACCACCGCTGGTAGCGGTTTTTTTGTTTGCAAGCAGCAGATTACGCGCAGAAAAAAAGGATCTCAAGAAGATCCTTTGATCTTTTCTACGGGGTCTGACGCTCAGTGGAACGA
AAACTCACGTTAAGGGATTTTGGTCATGAGATTATCAAAAAGGATCTTCACCTAGATCCTTTTAAATTAAAAATGAAGTTTTAAATCAATCTAAAGTATATATGAGTAAACTTGGTC
TGACAGTTACCAATGCTTAATCAGTGAGGCACCTATCTCAGCGATCTGTCTATTTCGTTCATCCATAGTTGCCTGACTCCCCGTCGTGTAGATAACTACGATACGGGAGGGCTTACC
ATCTGGCCCCAGTGCTGCAATGATACCGCGAGACCCACGCTCACCGGCTCCAGATTTATCAGCAATAAACCAGCCAGCCGGAAGGGCCGAGCGCAGAAGTGGTCCTGCAACTTTA
TCCGCCTCCATCCAGTCTATTAATTGTTGCCGGGAAGCTAGAGTAAGTAGTTCGCCAGTTAATAGTTTGCGCAACGTTGTTGCCATTGCTACAGGCATCGTGGTGTCACGCTCGTCG
TTTGGTATGGCTTCATTCAGCTCCGGTTCCCAACGATCAAGGCGAGTTACATGATCCCCCATGTTGTGCAAAAAAGCGGTTAGCTCCTTCGGTCCTCCGATCGTTGTCAGAAGTAAG
TTGGCCGCAGTGTTATCACTCATGGTTATGGCAGCACTGCATAATTCTCTTACTGTCATGCCATCCGTAAGATGCTTTTCTGTGACTGGTGAGTACTCAACCAAGTCATTCTGAGAAT
AGTGTATGCGGCGACCGAGTTGCTCTTGCCCGGCGTCAATACGGGATAATACCGCGCCACATAGCAGAACTTTAAAAGTGCTCATCATTGGAAAACGTTCTTCGGGGCGAAAACT
CTCAAGGATCTTACCGCTGTTGAGATCCAGTTCGATGTAACCCACTCGTGCACCCAACTGATCTTCAGCATCTTTTACTTTCACCAGCGTTTCTGGGTGAGCAAAAACAGGAAGGCA
AAATGCCGCAAAAAAGGGAATAAGGGCGACACGGAAATGTTGAATACTCATACTCTTCCTTTTTCAATATTATTGAAGCATTTATCAGGGTTATTGTCTCATGAGCGGATACATATT
TGAATGTATTTAGAAAAATAAACAAATAGGGGTTCCGCGCACATTTCCCCGAAAAGTGCCACCTGACGCGCCCTGTAGCGGCGCATTAAGCGCGGCGGGTGTGGTGGTTACGCG
CAGCGTGACCGCTACACTTGCCAGCGCCCTAGCGCCCGCTCCTTTCGCTTTCTTCCCTTCCTTTCTCGCCACGTTCGCCGGCTTTCCCCGTCAAGCTCTAAATCGGGGGCTCCCTTTA
GGGTTCCGATTTAGTGCTTTACGGCACCTCGACCCCAAAAAACTTGATTAGGGTGATGGTTCACGTAGTGGGCCATCGCCCTGATAGACGGTTTTTCGCCCTTTGACGTTGGAGTC
CACGTTCTTTAATAGTGGACTCTTGTTCCAAACTGGAACAACACTCAACCCTATCTCGGTCTATTCTTTTGATTTATAAGGGATTTTGCCGATTTCGGCCTATTGGTTAAAAAATGAG
CTGATTTAACAAAAATTTAACGCGAATTTTAACAAAATATT

6.1.2 Sequencing results from SeqLab

6.1.2.1 CMV-EDI3-3xHA

Primer Sequence: CMV-fwd: CGCAAATGGGCGGTAGGCGTG

CCGTCAGATCCAAGTTTGTACAAAAAAGCAGGCTGCCACCATGACACCTTCTCAGGTTGCCTTTGAAATAAGAGGAACTCTTTTACCAGGAGAAGTTTTTGCGATATGTGGAAGCT
GTGATGCTTTGGGAAACTGGAATCCTCAAAATGCTGTGGCTCTTCTTCCAGAGAATGACACAGGTGAAAGCATGCTATGGAAAGCAACCATTGTACTCAGTAGAGGAGTATCAGT
TCAGTATCGCTACTTCAAAGGGTACTTTTTAGAACCAAAGACTATCGGTGGTCCATGTCAAGTGATAGTTCACAAGTGGGAGACTCATCTACAACCACGATCAATAACCCCTTTAGA
AAGCGAAATTATTATTGACGATGGACAATTTGGAATCCACAATGGTGTTGAAACTCTGGATTCTGGATGGCTGACATGTCAGACTGAAATAAGATTACGTTTGCATTATTCTGAAA
AACCTCCTGTGTCAATAACCAAGAAAAAATTAAAAAAATCTAGATTTAGGGTGAAGCTGACACTAGAAGGCCTGGAGGAAGATGACGATGATAGGGTATCTCCCACTGTACTCCA
CAAAATGTCCAATAGCTTGGAGATATCCTTAATAAGCGACAATGAGTTCAAGTGCAGGCATTCACAGCCGGAGTGTGGTTATGGCTTGCAGCCTGATCGTTGGACAGAGTACAGC
ATACAGACGATGGAACCAGATAACCTGGAACTAATCTTTGATTTTTTCGAAGAAGATCTCAGTGAGCACGTAGTTCAGGGTGATGCCCTTCCTGGACATGTGGGTACAGCTTGTCT
CTTATCATCCACCATTGCTGAGAGTGGAAAGAGTGCTGGAATTCTTACTCTTCCCATCATGAGCAGAAATTCCCGGAAAACAATAGGCAAAGTGAGAGTTGACTATATAATTATTA
AGCCATTACCAGGATACAGTTGTGACATGAAATCTTCATTTTCCAAGTATTGGAAGCCAAGA

Primer Sequence: EDI3-Seq2:

ATGTGGATGCCAACGGCATTGATAACGTGGAGAATGCTTACCCATACGATGTTCCAGATTACGCTTACCCATACGATGTTCCAGATTACGCTTACCCATACGATGTTCCAGATTACG
CTTAGACCCAGCTTTCTTGTACAAAGTGGTGATGGCCGGCCGCTTCGAGCAGACATGATAAGATACATTGATGAGTTTGGACAAACCACAACTAGAATGCAGTGAAAAAAATGCT
TTATTTGTGAAATTTGTGATGCTATTGCTTTATTTGTAACCATTATAAGCTGCAATAAACAAGTTAACAACAACAATTGCATTCATTTTATGTTTCAGGTTCAGGGGGAGGTGTGGG
AGGTTTTTTAAAGCAAGTAAAACCTCTACAAATGTGGTAAAATCGATAAGGATCCGTCGACCGATGCCCTTGAGAGCCTTCAACCCAGTCAGCTCCTTCCGGTGGGCGCGGGGCA
TGACTATCGTCGCCGCACTTATGACTGTCTTCTTTATCATGCAACTCGTAGGACAGGTGCCGGCAGCGCTCTTCCGCTTCCTCGCTCACTGACTCGCTGCGCTCGGTCGTTCGGCTG
CGGCGAGCGGTATCAGCTCACTCAAAGGCGGTAATACGGTTATCCACAGAATCAGGGGATAACGCAGGAAAGAACATGTGAGCAAAAGGCCAGCAAAAGGCCAGGAACCGTAA
AAAGGCCGCGTTGCTGGCGTTTTTCCATAGGCTCCGCCCCCCTGACGAGCATCACAAAAATCGACGCTCAAGTCAGAGGTGGCGAAACCCGACAGGACTATAAAGATACCAGGC
GTTTCCCCCTGGAAGCTCCCTCGTGCGCTCTCCTGTTCCGACCCTGCCGCTTACCGGATACCTGTCCGCCTTTCTCCCTTCGGGAAGCGTGGCGCTTTCTCATAGCTCACGCTGTAGG
TATCTCAGTTCGGTGTAGGTCGTTCGCTCCAAGCTGGGCTGTGTGCACGAACCCCCCGTTCAGCCCGACCGCTGCGCCTTATCCGGTAACTATCGTCTTGAGTCCAACCCGGTAAG
ACACGACTTATCGCCACTGGCAGCAGCCACTGGTAACAGGATTAGCAGAGCGAGGTATGTAGGCGGTGCTACAGAGTTCTTGAAGTGGTGGCCTAACTACGGCTA

6.1.2.2 CMV-EDI3-W32A-3xHA

Primer Sequence: CMV-fwd: CGCAAATGGGCGGTAGGCGTG

ACCGTCAGATCCAAGTTTGTACAAAAAAGCAGGCTGCCACCATGACACCTTCTCAGGTTGCCTTTGAAATAAGAGGAACTCTTTTACCAGGAGAAGTTTTTGCGATATGTGGAAGC
TGTGATGCTTTGGGAAACGCG*AATCCTCAAAATGCTGTGGCTCTTCTTCCAGAGAATGACACAGGTGAAAGCATGCTATGGAAAGCAACCATTGTACTCAGTAGAGGAGTATCA
GTTCAGTATCGCTACTTCAAAGGGTACTTTTTAGAACCAAAGACTATCGGTGGTCCATGTCAAGTGATAGTTCACAAGTGGGAGACTCATCTACAACCACGATCAATAACCCCTTTA
GAAAGCGAAATTATTATTGACGATGGACAATTTGGAATCCACAATGGTGTTGAAACTCTGGATTCTGGATGGCTGACATGTCAGACTGAAATAAGATTACGTTTGCATTATTCTGA
AAAACCTCCTGTGTCAATAACCAAGAAAAAATTAAAAAAATCTAGATTTAGGGTGAAGCTGACACTAGAAGGCCTGGAGGAAGATGACGATGATAGGGTATCTCCCACTGTACTC
CACAAAATGTCCAATAGCTTGGAGATATCCTTAATAAGCGACAATGAGTTCAAGTGCAGGCATTCACAGCCGGAGTGTGGTTATGGCTTGCAGCCTGATCGTTGGACAGAGTACA
GCATACAGACGATGGAACCAGATAACCTGGAACTAATCTTTGATTTTTTCGAAGAAGATCTCAGTGAGCACGTAGTTCAGGGTGATGCCCTTCCTGGACATGTGGGTACAGCTTGT
CTCTTATCATCCACCATTGCTGAGAGTGGAAAGAGTGCTGGAATTCTTACTCTTCCCATCATGAGCAGAAATTCCCGGAAAACAATAGGCAAAGTGAGAGTTGACTATATAATTAT
TAAGCCATTACCAGGATACAGTTGTGACATGAAATCTTCATTTTCCAAGTATTGGAAGCCAAGAATACCATTGGATGTTGGCCATCGAGGTGCAGGAAACTCTACAACAACTGCCC
AGCTGGCTAAAGTTCAAGAA

*Point mutation

Primer Sequence: EDI3-Seq2:

TGATATCCATGTGGATGCCAACGGCATTGATAACGTGGAGAATGCTTACCCATACGATGTTCCAGATTACGCTTACCCATACGATGTTCCAGATTACGCTTACCCATACGATGTTCC
AGATTACGCTTAGACCCAGCTTTCTTGTACAAAGTGGTGATGGCCGGCCGCTTCGAGCAGACATGATAAGATACATTGATGAGTTTGGACAAACCACAACTAGAATGCAGTGAAA
AAAATGCTTTATTTGTGAAATTTGTGATGCTATTGCTTTATTTGTAACCATTATAAGCTGCAATAAACAAGTTAACAACAACAATTGCATTCATTTTATGTTTCAGGTTCAGGGGGAG
GTGTGGGAGGTTTTTTAAAGCAAGTAAAACCTCTACAAATGTGGTAAAATCGATAAGGATCCGTCGACCGATGCCCTTGAGAGCCTTCAACCCAGTCAGCTCCTTCCGGTGGGCG
CGGGGCATGACTATCGTCGCCGCACTTATGACTGTCTTCTTTATCATGCAACTCGTAGGACAGGTGCCGGCAGCGCTCTTCCGCTTCCTCGCTCACTGACTCGCTGCGCTCGGTCGT
TCGGCTGCGGCGAGCGGTATCAGCTCACTCAAAGGCGGTAATACGGTTATCCACAGAATCAGGGGATAACGCAGGAAAGAACATGTGAGCAAAAGGCCAGCAAAAGGCCAGGA
ACCGTAAAAAGGCCGCGTTGCTGGCGTTTTTCCATAGGCTCCGCCCCCCTGACGAGCATCACAAAAATCGACGCTCAAGTCAGAGGTGGCGAAACCCGACAGGACTATAAAGATA
CCAGGCGTTTCCCCCTGGAAGCTCCCTCGTGCGCTCTCCTGTTCCGACCCTGCCGCTTACCGGATACCTGTCCGCCTTTCTCCCTTCGGGAAGCGTGGCGCTTTCTCATAGCTCACGC
TGTAGGTATCTCAGTTCGGTGTAGGTCGTTCGCTCCAAGCTGGGCTGTGTGCACGAACCCCCCGTTCAGCCCGACCGCTGCGCCTTA

6.1.2.3 CMV-EDI3-ΔCBM20-3xHA

Primer Sequence: CMV-fwd: CGCAAATGGGCGGTAGGCGTG

[ATGACACCTAGGTGTCATGGTGGCAGCGTAAACGTATTCAGCATCAGGATTTTGAGCGGCGGCTACGTGAGATGGTTGCCGAACGCAGAGCCCGTCTGGCGCGGGTGA**]***CCGA
TCTCGTGGAACAGCAAACGCTGCATCGTGAAGTGGAAGCCTATGAAGCGCGCCTGGCACGCTGCCACCATGACACCT**ACATGTCAGACTGAAATAAGATTACGTTTGCATTATT
CTGAAAAACCTCCTGTGTCAATAACCAAGAAAAAATTAAAAAAATCTAGATTTAGGGTGAAGCTGACACTAGAAGGCCTGGAGGAAGATGACGATGATAGGGTATCTCCCACTGT
ACTCCACAAAATGTCCAATAGCTTGGAGATATCCTTAATAAGCGACAATGAGTTCAAGTGCAGGCATTCACAGCCGGAGTGTGGTTATGGCTTGCAGCCTGATCGTTGGACAGAG
TACAGCATACAGACGATGGAACCAGATAACCTGGAACTAATCTTTGATTTTTTCGAAGAAGATCTCAGTGAGCACGTAGTTCAGGGTGATGCCCTTCCTGGACATGTGGGTACAG
CTTGTCTCTTATCATCCACCATTGCTGAGAGTGGAAAGAGTGCTGGAATTCTTACTCTTCCCATCATGAGCAGAAATTCCCGGAAAACAATAGGCAAAGTGAGAGTTGACTATATA
ATTATTAAGCCATTACCAGGATACAGTTGTGACATGAAATCTTCATTTTCCAAGTATTGGAAGCCAAGAATACCATTGGATGTTGGCCATCGAGGTGCAGGAAACTCTACAACAAC
TGCCCAGCTGGCTAAAGTTCAAGAAAATACTATTGCTTCTTTAAGAAATGCTGCTAGTCATGGTGCAGCCTTTGTAGAATTTGACGTACACCTTTCAAAGGACTTTGTGCCCGTGGT
ATATCATGATCTTACCTGTTGTTTGACTATGAAAAAGAAATTTGATGCTGATCCAGTTGAATTATTTGAAATTCCAGTAAAAGAATTAACATTTGACCAACTCCAGTTGTTAAAGCTC
ACTCATGTGACTGCACTGAAATCTAAGGATCGGAAAGAATCTGTGGTTCAGGAGGAAAATTCCTTTTCAGAA

***Nonsense Sequence **Domain deletion**

Primer Sequence: EDI3-Seq2:

GTGGATGCCAACGGCATTGATAACGTGGAGAATGCTTACCCATACGATGTTCCAGATTACGCTTACCCATACGATGTTCCAGATTACGCTTACCCATACGATGTTCCAGATTACGCT
TAGACCCAGCTTTCTTGTACAAAGTGGTGATGGCCGGCCGCTTCGAGCAGACATGATAAGATACATTGATGAGTTTGGACAAACCACAACTAGAATGCAGTGAAAAAAATGCTTT
ATTTGTGAAATTTGTGATGCTATTGCTTTATTTGTAACCATTATAAGCTGCAATAAACAAGTTAACAACAACAATTGCATTCATTTTATGTTTCAGGTTCAGGGGGAGGTGTGGGAG
GTTTTTTAAAGCAAGTAAAACCTCTACAAATGTGGTAAAATCGATAAGGATCCGTCGACCGATGCCCTTGAGAGCCTTCAACCCAGTCAGCTCCTTCCGGTGGGCGCGGGGCATG
ACTATCGTCGCCGCACTTATGACTGTCTTCTTTATCATGCAACTCGTAGGACAGGTGCCGGCAGCGCTCTTCCGCTTCCTCGCTCACTGACTCGCTGCGCTCGGTCGTTCGGCTGCG
GCGAGCGGTATCAGCTCACTCAAAGGCGGTAATACGGTTATCCACAGAATCAGGGGATAACGCAGGAAAGAACATGTGAGCAAAAGGCCAGCAAAAGGCCAGGAACCGTAAAA
AGGCCGCGTTGCTGGCGTTTTTCCATAGGCTCCGCCCCCCTGACGAGCATCACAAAAATCGACGCTCAAGTCAGAGGTGGCGAAACCCGACAGGACTATAAAGATACCAGGCGTT
TCCCCCTGGAAGCTCCCTCGTGCGCTCTCCTGTTCCGACCCTGCCGCTTACCGGATACCTGTCCGCCTTTCTCCCTTCGGGAAGCGTGGCGCTTTCTCATAGCTCACGCTGTAGGTAT
CTCAGTTCGGTGTAGGTCGTTCGCTCCAAGCTGGGCTGTGTGCACGAACCCCCCGTTCAGCCCGACCGCTGCGCCTTATCCGGTAAC

6.1.2.4 CAG-EDI3-turboRFP

Primer Sequence: EDI3-Seq1: GTAGCGATACTGAAC

GTGTCATTCTCTGGAAGAAGAGCCACAGCATTTTGAGGATTCCAGTTTCCCAAAGCATCACAGCTTCCACATATCGCAAAAACTTCTCCTGGTAAAAGAGTTCCTCTTATTTCAAAG
GCAACCTGAGAAGGTGTCATGGTGGCAGCCTGCTTTTTTGTACAAACTTGCAATTCTTTGCCAAAATGATGAGACAGCACAATAACCAGCACGTTGCCCAGGAGCTGTAGGAAAA
AGAAGAAGGCATGAACATGGTTAGCAGAGGCTCTAGAGCCGCCGGTCACACGCCAGAAGCCGAACCCCGCCCTGCCCCGTCCCCCCCGAAGGCAGCCGTCCCCCCGCGGACAGC
CCCGAGGCTGGAGAGGGAGAAGGGGACGGCGGCGCGGCGACGCACGAAGGCCCTCCCCGCCCATTTCCTTCCTGCCGGCGCCGCACCGCTTCGCCCCGCGCCCGCTAGAGGGG
GTGCGGCGGCGCCTCCCAGATTTCGGCTCCGCACAGATTTGGGACAAAGGAAGTCCCTGCGCCCTCTCGCACGATTACCATAAAAGGCAATGGCTGCGGCTCGCCGCGCCTCGAC
AGCCGCCGGCGCTCCGGGGGCCGCCGCGCCCCTCCCCCGAGCCCTCCCCGGCCCGAGGCGGCCCCGCCCCGCCCGGCACCCCCACCTGC

Primer Sequence: EDI3-Seq2: CCCACTGTTAGCCGC

ATCCATGTGGATGCCAACGGCATTGATAACGTGGAGAATGCTTCTGGTGGCGGAGGCTCGGGCGGAGGTGGGTCGGGTGGCGGCGGATCAATGAGCGAGCTGATCAAGGAGA
ACATGCACATGAAGCTGTACATGGAGGGCACCGTGAACAACCACCACTTCAAGTGCACATCCGAGGGCGAAGGCAAGCCCTACGAGGGCACCCAGACCATGAAGATCAAGGTG
GTCGAGGGCGGCCCTCTCCCCTTCGCCTTCGACATCCTGGCTACCAGCTTCATGTACGGCAGCAAAGCCTTCATCAACCACACCCAGGGCATCCCCGACTTCTTTAAGCAGTCCTTC
CCTGAGGGCTTCACATGGGAGAGAATCACCACATACGAAGACGGGGGCGTGCTGACCGCTACCCAGGACACCAGCTTCCAGAACGGCTGCATCATCTACAACGTCAAGATCAAC
GGGGTGAACTTCCCATCCAACGGCCCTGTGATGCAGAAGAAAACACGCGGCTGGGAGGCCAACACCGAGATGCTGTACCCCGCTGACGGCGGCCTGAGAGGCCACAGCCAGAT
GGCCCTGAAGCTCGTGGGCGGGGGCTACCTGCACTGCTCCTTCAAGACCACATACAGATCCAAGAAACCCGCTAAGAACCTCAAGATGCCCGGCTTCCACTTCGTGGACCACAGA
CTGGAAAGAATCAAGGAGGCCGACAAAGAGACCTACGTCGAGCAGCACGAGATGGCTGTGGCCAAGTACTGCGACCTCCCTAGCAAACTGGGGCACAGATGAACCCAGCTTTCT
TGTACAAAGTGGTGATGGCCGGCCGCTTCGAGCAGACATGATAAGATACATTGATGAGTTTGGACAAACCACAACTAGAATGCAGTGAAAAAAATGCTTTATTTGTGAAATTTGT
GATGCTATTGCTTTATTTGTAACCATTATAAGCTGCAATAAACAAGTTAACAACAACAATTGCATTCATTTTATGTTTCAGGTTCAGGGGGAG

Primer Sequence: CMV-fwd: CGCAAATGGGCGGTAGGCGTG

GGCTAACTAGAGAACCCACTGCGCCACCATGATTGAACAAGATGGATTGCACGCAGGTTCTCCGGCCGCTTGGGTGGAGAGGCTATTCGGCTATGACTGGGCACAACAGACAAT
CGGCTGCTCTGATGCCGCCGTGTTCCGGCTGTCAGCGCAGGGGCGCCCGGTTCTTTTTGTCAAGACCGACCTGTCCGGTGCCCTGAATGAACTGCAAGACGAGGCAGCGCGGCTA
TCGTGGCTGGCCACGACGGGCGTTCCTTGCGCAGCTGTGCTCGACGTTGTCACTGAAGCGGGAAGGGACTGGCTGCTATTGGGCGAAGTGCCGGGGCAGGATCTCCTGTCATCT
CACCTTGCTCCTGCCGAGAAAGTATCCATCATGGCTGATGCAATGCGGCGGCTGCATACGCTTGATCCGGCTACCTGCCCATTCGACCACCAAGCGAAACATCGCATCGAGCGAG
CACGTACTCGGATGGAAGCCGGTCTTGTCGATCAGGATGATCTGGACGAAGAGCATCAGGGGCTCGCGCCAGCCGAACTGTTCGCCAGGCTCAAGGCGAGCATGCCCGACGGC
GAGGATCTCGTCGTGACCCATGGCGATGCCTGCTTGCCGAATATCATGGTGGAAAATGGCCGCTTTTCTGGATTCATCGACTGTGGCCGGCTGGGTGTGGCGGACCGCTATCAGG
ACATAGCGTTGGCTACCCGTGATATTGCTGAAGAGCTTGGCGGCGAATGGGCTGACCGCTTCCTCGTGCTTTACGGTATCGCCGCTCCCGATTCGCAGCGCATCGCCTTCTATCGC
CTTCTTGACGAGTTCTTCTGACTCGAGTCTAGAGGGCCCGTTTAAACCCGCTGATCAGCCTCGACTGTGCCTTCTAGTTGCCAGCCATCTGTTGTTTGCCCCTCCCCCGTGCCTTCCT
TGACCCTGGAAGGTGCCACTCCCACTGTCCTTTCCTAATAAAATGAGGAAATTGCATCGCATTGTCTGAGTAGGTGTC

6.1.2.5 CMV-EDI3-GFP

Primer Sequence: CMV-fwd: CGCAAATGGGCGGTAGGCGTG

AGATCTGCCGCCGCGATCGCCATGACACCTTCTCANGTTGCCTTTGAAATAAGAGGAACTCTTTTACCAGGAGAANTTTTTGCNATATGTGGAANCTGTGATGCTTTGGGAAACTG
GAATCCTCAAAATGCTGTGGCTCTTCTTCCANAGAATGACACAGGTGAAAGCNTGCTATGGAAAGCAACCATTGTACTCAGTAGAGGAGTATCAGTTCANTATCGCTACTTCAAA
GGGTACTTTTTAGAACCAAANACTATCGGTGGTCCATGTCAAGTGATAGTTCACAAGTGGGAGACTCATCTACAACCACGATCAATAACCCCTTTAGAAAGCNAAATTATTATTGA
CGATGGACAATTTGGAATCCACAATGGTGTTGAAACTCNGGATTCTGGATGGCTGACNTGTCAGACTGAAATAAGATTACGTTTGCATTATTCTGAAAAACCTCCTGTGTCAATAA
CCANGAAAAAATTAAAAAAATCTANATTTAGGNTGAAGCTGACACTAGAAGGCCTGNAGGAAGANGACGATGATAGAGTATCTCCCACTGTACTCCACAAAATGTC

Primer Sequence: EDI3-Seq2:

CGACGAGAGCGGCCTGCCCGCCATGGAGATCGAGTGCCGCATCACCGGCACCCTGAACGGCGTGGAGTTCGAGCTGGTGGGCGGCGGAGAGGGCACCCCCGAGCAGGGCCGC
ATGACCAACAAGATGAAGAGCACCAAAGGCGCCCTGACCTTCAGCCCCTACCTGCTGAGCCACGTGATGGGCTACGGCTTCTACCACTTCGGCACCTACCCCAGCGGCTACGAGA
ACCCCTTCCTGCACGCCATCAACAACGGCGGCTACACCAACACCCGCATCGAGAAGTACGAGGACGGCGGCGTGCTGCACGTGAGCTTCAGCTACCGCTACGAGGCCGGCCGCG
TGATCGGCGACTTCAAGGTGATGGGCACCGGCTTCCCCGAGGACAGCGTGATCTTCACCGACAAGATCATCCGCAGCAACGCCACCGTGGAGCACCTGCACCCCATGGGCGATA
ACGATCTGGATGGCAGCTTCACCCGCACCTTCAGCCTGCGCGACGGCGGCTACTACAGCTCCGTGGTGGACAGCCACATGCACTTCAAGAGCGCCATCCACCCCAGCATCCTGCA
GAACGGGGGCCCCATGTTCGCCTTCCGCCGCGTGGAGGAGGATCACAGCAACACCGAGCTGGGCATCGTGGAGTACCAGCACGCCTTCAAGACCCCGGATGCAGATGCCGGTG
AAGAAAGAGTTTAAACGGCCGGCCGCGGTCATAGCTGTTTCCTGAACAGATCCCGGGTGGCATCCCTGTGACCCCTCCCCAGTGCCTCTCCTGG

6.1.2.6 CMV-STBD1-3xFLAG-EGFP

Primer Sequence: CMV-fwd: CGCAAATGGGCGGTAGGCGTG

CAAAAAAGCAGGCTGCCACCATGGGCGCCGTCTGGTCCGCCCTGCTGGTTGGAGGGGGTCTGGCCGGAGCACTTTTCGTTTGGCTGCTGCGGGGCGGCCCTGGCGACACCGGGA
AGGACGGGGATGCGGAGCAGGAGAAAGACGCCCCTCTTGGGGGAGCTGCGATTCCGGGAGGCCATCAGAGTGGCAGCAGCGGACTGAGCCCTGGACCTTCCGGGCAGGAGCT
GGTCACCAAACCAGAGCATCTTCAAGAAAGCAATGGACATTTGATTTCTAAGACCAAAGACCTTGGTAAACTGCAAGCAGCATCATGGAGATTGCAGAATCCTTCCAGGGAAGTC
TGTGACAATTCAAGAGAACATGTTCCTTCTGGACAGTTTCCAGACACAGAAGCTCCAGCTACCTCTGAGACCAGTAACTCTAGGAGTTACTCTGAAGTTTCAAGAAATGAAAGCCT
TGAATCTCCTATGGGAGAATGGGGATTCCAAAAAGGACAAGAGATATCTGCTAAAGCAGCTACATGTTTTGCAGAGAAGTTGCCTTCTAGCAACCTGCTCAAGAACAGAGCTAAA
GAAGAAATGAGCCTCTCTGATTTGAACAGTCAGGACCGGGTTGACCACGAGGAGTGGGAAATGGTGCCTAGGCACTCATCTTGGGGGGATGTTGGTGTGGGTGGCAGTCTTAA

GGCTCCAGTGTTAAACCTAAACCAGGGAATGGACAATGGAAGAAGCACTTTGGTGGAAGCAAGAGGTCAGCAAGTGCATGGGAAAATGGAAAGGGTAGCAGTGATGCCTGCA
GGGTCTCAGCAAGTTAGTGTCAGGTTCCAGGTCCATTAT

Primer Sequence: EGFP-N-rev: GCTTGCCGTAGGTGGCATC

GCTCGACCAGGATGGGCACCACCCCGGTGAACAGCTCCTCGCCCTTGCTCACCATTGATCCGCCGCCACCCGACCCACCTCCGCCCGAGCCTCCGCCACCAGACTTGTCATCGTCAT
CCTTGTAATCGATATCATGATCTTTATAATCACCGTCATGGTCTTTGTAGTCGTGAATCCCCCACCATGCGTGAACCACTTTATCCTCATGGCCAGTTTCTAGGAATCTATTGCTGCAT
TCTTCCCAGCGGGTAACTCCCCCATTCTCTACCAACACAAACTTCCACTCCACCACTGTATCTGCAGGCAGGAAAATGGAATGAGACCAGAACCCATCCTTGTTATAGTGGAGTGG
GATGTAAGTGTTCCATCTCCCAAGACACTCATGGTCTCCAGTTACTGCAATGAATTGCACATCAGTGCTTGTGACATAATGGACCTGGAACCTGACACTAACTTGCTGAGACCCTGC
AGGCATCACTGCTACCCTTTCCATTTTCCCATGCACTTGCTGACCTCTTGCTTCCACCAAAGTGCTTCTTCCATTGTCCATTCCCTGGTTTAGGTTTAACACTGGAGCCTTAAGACTGC
CACCCACACCAACATCCCCCCAAGATGAGTGCCTAGGCACCATTTCCCACTCCTCGTGGTCAACCCGGTCCTGACTGTTCAAATCAGAGAGGCTCATTTCTTCTTTAGCTCTGTTCTT
GAGCAGGTTGCTAGAAGGCAACTTCTCTGCAAAACATGTAGCTGCTTTAGCAGATATCTCTTGTCCTTTTTGGAATCCCCATTCTCCCATAGGAGATTCAAGGCTTTCATTTCTTGAA
ACTTCAGAGTAACTCCTAGAGTTACTGGTCTCAGAGGTAGCTGGAGCTTCTGTGTCTGGAAACTGTCCAGAAGGAACATGTTCTCTTGAATTGTCACAGACTTCCCTGGAAGGATT
CTGCAATCTCCATGATGCTGCTTGCAGTTTACCAAGGTCTTTGGTCTTAGAAATCAAATGTCCATTGCTTTCTTGAAGATGCTCTGGTTTGGTGACCAGCTCCTGCCCGGAAGGTCC
AGGGCTCAGTCCGCTGCTGCCACTCTGATGGCCTCCCGGAATCGCAGCTCCCCCAAGAGGGGCGTCTTTCTC

Primer Sequence: EGFP-c-rev: GCTTGCCGTAGGTGGCATC

GGTTCAGGGGGAGGTGTGGGAGGTTTTTTAAAGCAAGTAAAACCTCTACAAATGTGGTAGCGGCCGCGGCGCTCTTCCGCTTCCTCGCTCACTGACTCGCTGCGCTCGGTCGTTC
GGCTGCGGCGAGCGGTATCAGCTCACTCAAAGGCGGTAATACGGTTATCCACAGAATCAGGGGATAACGCAGGAAAGAACATGTGAGCAAAAGGCCAGCAAAAGGCCAGGAAC
CGTAAAAAGGCCGCGTTGCTGGCGTTTTTCCATAGGCTCCGCCCCCCTGACGAGCATCACAAAAATCGACGCTCAAGTCAGAGGTGGCGAAACCCGACAGGACTATAAAGATACC
AGGCGTTTCCCCCTGGAAGCTCCCTCGTGCGCTCTCCTGTTCCGACCCTGCCGCTTACCGGATACCTGTCCGCCTTTCTCTCTTCGGGAAGCGTGGCGCTTTCTCATAGCTCACGCTG
TAGGTATCTCAGTTCGGTGTAGGTCGTTCGCTCCAAGCTGGGCTGTGTGCACGAACCCCCCGTTCAGCCCGACCGCTGCGCCTTATCCGGTAACTATCGTCTTGAGTCCAACCCGG
TAAGACACGACTTATCGCCACTGGCAGCAGCCACTGGTAACAGGATTAGCAGAGCGAGGTATGTAGGCGGTGCTACAGAGTTCTTGAAGTGGTGGCCTAACTACGGCTACACTA
GAAGAACAGTATTTGGTATCTGCGCTCTGCTGAAGCCAGTTACCTTCGGAAAAAGAGTTGGTAGCTCTTGATCCGGCAAACAAACCACCGCTGGTAGCGGTGGTTTTTTTGTTTGC
AAGCAGCAGATTACGCGCAGAAAAAAAGGATCTCAAGAAGATCCTTTGATCTTTTCTACGGGGTCTGACGCTCAGTGGAACGAAAACTCACGTTAAGGGATTTTGGTCATGAGAT
TATCAAAAAGGATCTTCACCTAGATCCTTTTAAATTAAAAATGAAGTTTTAAATCAATCTAAAGTATATATGAGTAAACTTGGTCTGACAG

6.2 Donor information

6.2.1 Primary human hepatocytes

All primary human hepatocytes were stored cryopreserved until they were cultivated.

Donor ID	Age	Race	Gender	Body Mass Index (BMI)	Supplier
GID	58	African-American	Male	34.4	Bio IVT
IAN	48	Caucasian	Male	22.1	Bio IVT
4229	61	caucasian	Female	31,8	Lonza
4108	42	African-American	Female	35	Lonza

6.2.2. Human liver donor

Donor ID	Age	Gender	Body Mass Index (BMI)
A918691	60-69	Male	31
Spender 1	Unknown	Unknown	Unknown

6.2.3 Skeletal muscle Donor

Donor ID	Age	Gender	Anatomical site	Supplier
Donor 1	87	Male	Skeletal muscle*	AMSbio
Donor 2	29	Male	Skeletal muscle*	AMSbio
Donor 3	45	Female	Skeletal muscle*	AMSbio
Donor 4	49	Male	Gastrocnemius	AMSbio
Donor 5	66	Female	Skeletal muscle*	BioCat
Donor 6	81	Male	tigh	UK-Bochum

*specific muscle not known

6.2.4 Myocardium Donor

Donor ID	Age	Gender	Anatomical site	Supplier
CU141218	55	Male	Heart, Myocardium (LV)	AMSbio

6.2.5 Antibody validaition

Muscle

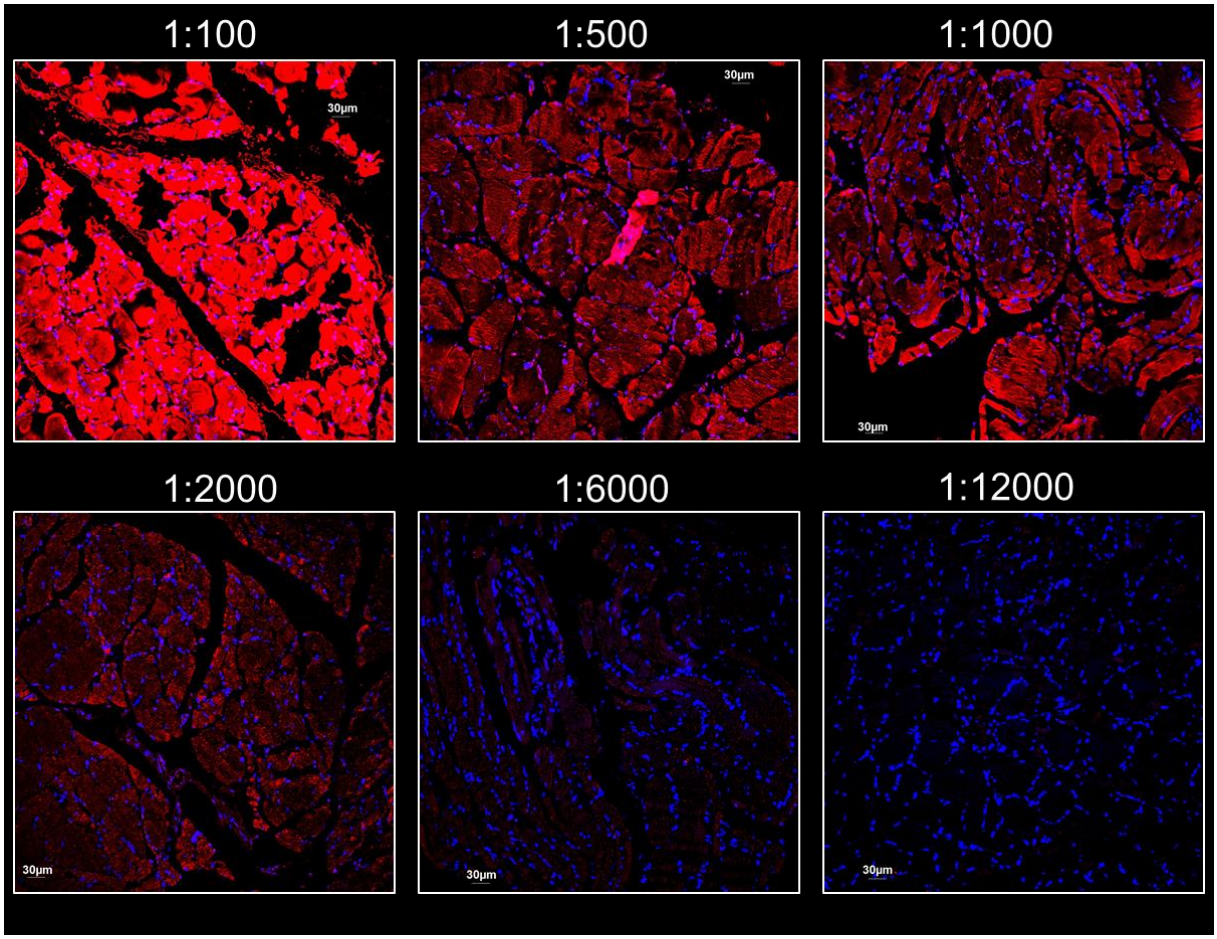

Figure 6..1 **Antibody titration of EDI3.** Titration of the custom made EDI3 antibody 3B8G3 in human skeletal muscle in a range from 1:100 to 1:12000 in Donor 1

6. Supplementary data

7. Appendix

7.1 Publication bibliography

Marchan, Rosemarie; Büttner, Bettina; Lambert, Jörg; Edlund, Karolina; Glaeser, Iris; Blaszkewicz, Meinolf Leonhardt, Gregor et al. (2017): **Glycerol-3-phosphate Acyltransferase 1 Promotes Tumor Cell Migration and Poor Survival in Ovarian Carcinoma**. In *Cancer research* 77 (17), pp. 4589–4601 DOI: 10.1158/0008-5472.CAN-16-2065.

Bukhari, Hassan; Glotzbach, Annika; Kolbe, Katharina; Leonhardt, Gregor; Loosse, Christina; Müller, Thorsten (2017): **Small things matter: Implications of APP intracellular domain AICD nuclear signaling in the progression and pathogenesis of Alzheimer's disease**. In *Progress in neurobiology* 156, pp. 189 213. DOI: 10.1016/j.pneurobio.2017.05.005.

Bukhari, Hassan; Kolbe, Katharina; Leonhardt, Gregor; Loosse, Christina; Schröder, Elisabeth; Knauer, Shirley et al. (2016**): Membrane tethering of APP c-terminal fragments is a prerequisite for T668 phosphorylation preventing nuclear sphere generation**. In *Cellular signalling* 28 (11), pp. 1725 1734. DOI: 10.1016/j.cellsig.2016.08.007.

Kolbe, Katharina; Bukhari, Hassan; Loosse, Christina; Leonhardt, Gregor; Glotzbach, Annika; Pawlas, Magdalena et al. (2016): **Extensive nuclear sphere generation in the human Alzheimer's brain**. In *Neurobiology of aging* 48, pp. 103–113. DOI: 10.1016/j.neurobiolaging.2016.08.016.

7.2 Contribution on congresses

2017:
Poster: **Characterization of the glycerophosphodiesterase EDI3,** Gregor M. Leonhardt, Michaela S. Lesjak, Bettina Büttner, Olga Orishkevich, Jörg Lambert, Lisa Marienhoff, Joanna D. Stewart, Karolina Edlund,Jan G. Hengstler, Cristina Cadenas, Rosemarie Marchan. GBM Fall conference 2017 24–27.09.2017 (Bochum)

2018:
Poster: **A role of glycerophosphodiesterase EDI3 in glycogen metabolism,** Gregor M. Leonhardt, Adelina Jashari, Annika Glotzbach, Michaela S. Lesjak, Bettina Büttner, Jan G. Hengstler, Cristina Cadenas, Rosemarie Marchan. Mechanisms to Therapies Inovations in Cancer Metabolism (EACR 2018) 09-11.10.2018 (Bilbao)

2019:
Poster: **Gycerophosphodiesterase1 (EDI3) - A new player in glycogen metabolism,** Gregor M. Leonhardt, Adelina Jashari, Annika Glotzbach, Brigitte Begher-Tibbe, Michaela S. Lesjak, Karolina Edlund, Jan G. Hengstler, Cristina Cadenas, Rosemarie Marchan. GBM/DGZ Fall conference 2019 25-27.09.2019 (Tübingen)

7. Appendix

7.3 Eidesstattliche Versicherung (Affidavit)

Name, Vorname
(Surname, first name)

Matrikel-Nr.
(Enrolment number)

Belehrung:

Wer vorsätzlich gegen eine die Täuschung über Prüfungsleistungen betreffende Regelung einer Hochschulprüfungsordnung verstößt, handelt ordnungswidrig. Die Ordnungswidrigkeit kann mit einer Geldbuße von bis zu 50.000,00 € geahndet werden. Zuständige Verwaltungsbehörde für die Verfolgung und Ahndung von Ordnungswidrigkeiten ist der Kanzler/die Kanzlerin der Technischen Universität Dortmund. Im Falle eines mehrfachen oder sonstigen schwerwiegenden Täuschungsversuches kann der Prüfling zudem exmatrikuliert werden, § 63 Abs. 5 Hochschulgesetz NRW.

Die Abgabe einer falschen Versicherung an Eides statt ist strafbar.

Wer vorsätzlich eine falsche Versicherung an Eides statt abgibt, kann mit einer Freiheitsstrafe bis zu drei Jahren oder mit Geldstrafe bestraft werden, § 156 StGB. Die fahrlässige Abgabe einer falschen Versicherung an Eides statt kann mit einer Freiheitsstrafe bis zu einem Jahr oder Geldstrafe bestraft werden, § 161 StGB.

Die oben stehende Belehrung habe ich zur Kenntnis genommen:

Official notification:

Any person who intentionally breaches any regulation of university examination regulations relating to deception in examination performance is acting improperly. This offence can be punished with a fine of up to EUR 50,000.00. The competent administrative authority for the pursuit and prosecution of offences of this type is the chancellor of the TU Dortmund University. In the case of multiple or other serious attempts at deception, the candidate can also be unenrolled, Section 63, paragraph 5 of the Universities Act of North Rhine-Westphalia.

The submission of a false affidavit is punishable.

Any person who intentionally submits a false affidavit can be punished with a prison sentence of up to three years or a fine, Section 156 of the Criminal Code. The negligent submission of a false affidavit can be punished with a prison sentence of up to one year or a fine, Section 161 of the Criminal Code.

I have taken note of the above official notification.

Ort, Datum
(Place, date)

Unterschrift
(Signature)

Titel der Dissertation:
(Title of the thesis):

Ich versichere hiermit an Eides statt, dass ich die vorliegende Dissertation mit dem Titel selbstständig und ohne unzulässige fremde Hilfe angefertigt habe. Ich habe keine anderen als die angegebenen Quellen und Hilfsmittel benutzt sowie wörtliche und sinngemäße Zitate kenntlich gemacht.
Die Arbeit hat in gegenwärtiger oder in einer anderen Fassung weder der TU Dortmund noch einer anderen Hochschule im Zusammenhang mit einer staatlichen oder akademischen Prüfung vorgelegen.

I hereby swear that I have completed the present dissertation independently and without inadmissible external support. I have not used any sources or tools other than those indicated and have identified literal and analogous quotations.

The thesis in its current version or another version has not been presented to the TU Dortmund University or another university in connection with a state or academic examination.*

*Please be aware that solely the German version of the affidavit ("Eidesstattliche Versicherung") for the PhD thesis is the official and legally binding version.

Ort, Datum
(Place, date)

Unterschrift
(Signature)

7. Appendix

7.4 Acknowledgement

Diese Arbeit wäre ohne die Mithilfe vieler engagierter Menschen nicht vervollständigt worden. An erster Stelle gilt mein Dank meinen beiden Supervisoren **Prof. Dr. Jan G. Hengstler** und **Dr. Rosemarie Marchan**.

Lieber Herr Professor, Sie haben es mir ermöglicht, meine Promotion unter ihrer Leitung bei Ihnen am Leibniz-Institut für Arbeitsforschung durchzuführen. Hierbei hatten Sie trotz eines immensen Arbeitspensums immer eine offene Tür und Zeit sich mit meiner Forschung zu befassen. Sie haben die nötigen kritischen Fragen gestellt aber immer auch weiterführende Ideen gehabt. Weiterhin boten sie mir durch die exzellente Infrastruktur ein optimales Umfeld für mein Dissertationsvorhaben. Vielen herzlichen Dank.

Dear Rosie, I am extremely grateful that you have been my supervisor. You motivated me when the results did not meet my expectations, you always had smart ideas, a good sense of humour, and you never lost your laugh. It was always fun working with you. Thank you very much, I have learned a lot from you.

Weiterhin gilt meine Dankbarkeit **Brigitte Begher-Tibbe**, die mich ganz besonders bei den immunhistochemischen Färbungen unterstützt hat. Auch von dir habe ich viel gelernt und ohne dich wären viele Färbungen nur halb so schön geworden. Ich möchte mich auch bei **Kathy Belgasmi** und **Georgia Günther** für die Leberperfusionen und bei **Wiebke Albrecht** und **Tim Brecklinghaus** für die primären humanen Hepatozyten bedanken. **Adelina Jashari** und **Cristina Cadenas** danke ich für die enge Zusammenarbeit während der Glukagon-Experimenten, **Lena Zak** für die Zusammenarbeit bei der Durchführung der Glykogen Assays Experimente in den Brustkrebszelllinen und **Prof. Dr. med. Andrea Tannapfel** für die humanen Muskelschnitte. **Annika Glotzbach, Michaela Lesjak** und **Moritz Anft** möchte ich dafür danken, dass ich die Zelllinen die sie produziert haben verwenden durfte. Weiterhin möchte ich meiner (erweiterten) Arbeitsgruppe: **Lena Zak, Lisa Marienhoff, Annika Glotzbach, Simon Schäfers, Katharina Rohlf, Anastasia Oprisko, Darius Kaszta, Dr. Karolina Edlund, Katharina Grgas** und **Rosemarie Marchan** für den kollegialen Umgang und gegenseitige Unterstützung im Labor bedanken. Auch bei vielen Mitarbeitern des Fachbereichs Toxikologie am IfADo möchte ich mich bedanken, mit allen habe ich positive Erinnerungen.

Mein größter Dank gilt meiner Ehefrau **Anne Leonhardt**, die mir die vielen Stunden im Labor ermöglicht hat und mich nach einem langen Labortag immer wieder aufgebaut hat. Lukas und Paul, ihr seid immer in meinem Herzen. Dank gilt auch meinen Eltern Malte und Claudia Leonhardt, sowie meinen Schwiegereltern Ellen und Klaus Dabringhausen die mich im Hintergrund viel unterstützt haben.